

Meso – and Neoarchean tectonic evolution  
of the northwestern Superior Province:  
Insights from a U-Pb geochronology, Nd  
isotope, and geochemistry study of the  
Island Lake greenstone belt, Northeastern  
Manitoba

by

Jennifer E. Parks

A thesis  
presented to the University of Waterloo  
in fulfillment of the  
thesis requirement for the degree of  
Doctor of Philosophy  
in  
Earth Sciences

Waterloo, Ontario, Canada, 2011

©Jennifer E. Parks 2011

## **Author's Declaration**

I hereby declare that I am the sole author of this thesis. This is a true copy of the thesis, including any required final revisions, as accepted by my examiners.

I understand that my thesis may be made electronically available to the public.

## Abstract

What tectonic processes were operating in the Archean, and whether they were similar to the “modern-style” plate tectonics seen operating today, is a fundamental question about Archean geology. The Superior Province is the largest piece of preserved Archean crust on Earth. As such it provides an excellent opportunity to study Archean tectonic processes. Much work has been completed in the southern part of the Superior Province. A well-documented series of discrete, southward younging orogenies related to a series of northward dipping subduction zones, has been proposed for amalgamating this part of the Superior Province. The tectonic evolution in the northwestern Superior Province is much less constrained, and it is unclear if it is related to the series of subduction zones in the southern part of the Superior Province, or if it is related to an entirely different process. Such ideas need to be tested in order to develop a concise model for the Meso – and Neoarchean tectonic evolution of the northwestern Superior Province.

To this end, a field mapping, U-Pb geochronology, Nd isotope, and lithogeochemistry study was undertaken in the Island Lake greenstone belt. This granite-greenstone belt is part of the northern margin of the North Caribou terrane, a larger reworked Mesoarchean crustal block located in the northwestern Superior Province. U-Pb TIMS zircon geochronology data shows that the Island Lake greenstone belt experienced a long and complex geological history that included the deposition of three distinct volcanic assemblages at ca. 2897 Ma, 2852 Ma, and 2744 Ma, as well as a younger clastic sedimentary group, the Island Lake group. All of these volcanic assemblages include felsic and mafic volcanic rocks, as well as a suite of contemporaneous plutonic rocks. The U-Pb data set shows that the Savage Island shear zone, a regional fault structure that transects the Island Lake greenstone belt, is not a terrane-bounding feature as correlative supracrustal assemblages are observed on both sides of it. The Nd isotope data shows that the volcanic assemblages and contemporaneous plutons

have been variably contaminated by an older ca. 3.0 Ga crustal source. The mafic volcanic rocks in the assemblages have two distinct geochemical signatures, and show a pattern of decreasing crustal contamination with decreasing age. Together these data suggests that the Meso – and Neoproterozoic volcanic assemblages are part of an intact primary volcanic stratigraphy that were built on the same ca. 3.0 Ga basement and have autochthonous relationships with each other. This basement is the North Caribou terrane.

The youngest sedimentary group in the belt, the Island Lake group, was deposited between 2712 Ma and 2699 Ma. It consists of “Timiskaming-type” sedimentary rocks, and is the youngest clastic sedimentary package in the belt. A detailed study of detrital zircons in units from the stratigraphic bottom to the top of the sedimentary group indicates an age pattern of detrital zircons that is most consistent with a scenario in which sediments were deposited in inter-diapiric basins created by diapirism and sagduction (i.e., vertical tectonic) processes. During the diapiric ascent of the felsic material, inter-diapiric basins were formed in the synclines between adjacent domes, into which sediments were deposited.

U-Pb zircon TIMS geochronology identified two ages of deformation in the Island Lake greenstone belt. Two dykes that crosscut an older, D<sub>1</sub> foliation place a minimum age of ca. 2723 Ma on the D<sub>1</sub> deformation, and two syn-kinematic dykes date movement along two transpressional shear zones to 2700 Ma.

Together all these data indicate that the tectonic evolution in the Island Lake greenstone belt and in the northwestern Superior Province took place in three main stages. The first two stages involved the generation of Meso – and Neoproterozoic volcanic assemblages and contemporaneous plutonic rocks due to southward dipping subduction under the North Caribou micro-continent. The third stage involved the deposition of late “Timiskaming-type” sediments during vertical tectonic processes in

conjunction with horizontal tectonic movement along late transpressional shear zones at ca. 2.70 Ga. At the end of this process the North Superior superterrane was terminally docked to the North Caribou terrane along the North Kenyon fault. This study shows that while a version of horizontal or “modern” style plate tectonics were operating in the Archean, vertical tectonic processes were also occurring and that these processes operated synchronously in the Neoproterozoic.

## Acknowledgements

I would like to thank the following organizations for financial support for this project: LITHOPROBE, NSERC and NSERC discovery grants to Shoufa Lin and Larry Heman, the Northern Scientific Training Program, the University of Waterloo, the Ontario Graduate Scholarships, and the Ontario Graduate Scholarships Science and Technology program.

The Manitoba Geological Survey has played an important part of Ph. D. project. They provided financial, logistical, and technical support. In particular I'd like to thank Ric Syme for access to samples he collected in the field and for use of his field notes. I'd like to thank Tim Corkery for helping me make sense of things in the field, and for his moral support and his infectious enthusiasm when talking about rocks in the northwestern Superior Province.

The second chapter of this thesis is a modified version of the publication: Parks, J., Lin, S., Davis, D., and Corkery, M.T., 2006: New high-precision U-Pb ages for the Island Lake greenstone belt, northwestern Superior Province: implications for regional stratigraphy and the extent of the North Caribou Terrane. *Canadian Journal of Earth Sciences*. v 43, p.789-803 The version presented here includes minor modifications and editorial changes. Appendix A is 40 x 26 inch geological map which is included in a pocket at the back of the thesis in printed copies. The map has been published by the Manitoba Geological Survey. Neither the map nor chapter two require written permission to reproduce.

Many people have assisted me in different stages of research during my PhD. I'd like to thank Shoufa for his advice and being patient, as well as the rest of my committee for helping me in different stages of this processes. Scott Snider, Matt Chalaturnyk and Daniel Martin are thanked for assistance in the field, and Neill Brandson is thanked for logistical support during the field season. I would like to thank Don Davis, John Ketchum, Kim Kwok, Sandra Kamo, and Tom Pestaj for assistance with geochronology at the Jack Satterly Laboratory, and Larry Heman, Antony Simonetti,

Rob Creaser, Judy Shultz and Kendra Siemens and the rest of the staff at the Radiogenic Isotope Facility at the University of Alberta. As well, thanks to Kirsty Tomlinson for assistance in the field and with preliminary Nd isotope and geochemical data interpretation. Greg Stott and Gary Beakhouse are thanked for providing comments and suggestions on an early version of Chapter three.

At the University of Waterloo I'd like to thank Sue Fisher for helping me to navigate the bureaucracy of being a graduate student at UW, and for always providing helpful advice and a supportive shoulder. I would not have learned or enjoyed myself as much over the past few years without the support of the Shoufa Squad. Thanks to Edith, Andy, Sandra, A.J., Paul, Justin, Matt, Yvette, Nathan and Ben as well as other fellow graduate students at UW and the University of Alberta. Outside of school I need to thank the following people for helping me keep my sanity: my Toronto friends (Heather and Jenever- thanks for letting me crash), the 2006 Edmonton Oilers, the Melrose Crew, Mathryn, Randrea, too many roommates to count, and anyone I ever shared a beer with at Ethels.

Last but not least I need to thank my family for always being supportive and only asking me a few times why it was taking me so long to finish my thesis. Super thanks BP.

## **Dedication**

Thanks Mom

For N.A.P.

## Table of Contents

Author's Declaration .....	ii
Abstract .....	iii
Acknowledgements .....	vi
Dedication .....	viii
Table of Contents .....	ix
List of Figures .....	xii
List of Tables .....	xvii
Chapter 1 .....	1
Introduction .....	1
1.1 The Archean .....	1
1.2 The Island Lake greenstone belt .....	3
1.2.1 Location and previous work .....	3
1.3 Thesis objectives .....	4
1.4 Organization of Thesis .....	5
Chapter 2 .....	9
New high-precision U-Pb ages for the Island Lake greenstone belt, northwestern Superior Province: implications for regional stratigraphy and the extent of the North Caribou Terrane <sup>1</sup> .....	9
2.1 Summary .....	9
2.2 Introduction .....	10
2.2.1 Regional Geological Setting .....	11
2.3 Results of geological and geochronological investigations .....	12
2.3.1 Supracrustal rocks (samples 859, 839, 425, 289, 105, 02) .....	13
2.3.2 Plutonic Rocks (samples 04, 176, 067, 899) .....	19
2.4 Discussion .....	21
2.4.1 Composition and history of the Island Lake greenstone belt .....	21
2.4.2 Regional correlations .....	26
2.5 Conclusions .....	30
Chapter 3 Meso – and Neoproterozoic evolution of the Northwestern Superior Province: evidence from lithochemistry and Nd isotope data of volcanic and plutonic rocks and U-Pb dyke ages from the Island Lake greenstone belt .....	45
3.1 Introduction .....	45

3.2 Geological setting .....	47
3.2.1 Regional Geology .....	47
3.2.2 Geology of the Island Lake greenstone belt .....	49
3.2.3 Deformation.....	50
3.3 Nature of Volcanic Assemblages and contemporaneous plutonic rocks: Litho-geochemistry and Nd isotope results .....	51
3.3.1 Mesoarchean rocks .....	52
3.3.2 Neoproterozoic rocks .....	55
3.4 Timing of Deformation in the Island Lake greenstone belt: U-Pb Dyke Dating .....	57
3.4.1 Sample Description .....	57
3.4.2 Results .....	58
3.5 Discussion .....	60
3.5.1 Litho-geochemical signatures .....	60
3.5.2 Nd isotopic signatures .....	62
3.5.3 Timing of deformation .....	63
3.5.4 Regional Implications.....	64
3.6 Tectonic synthesis .....	69
3.6.1 Mesoarchean Events.....	69
3.6.2 Neoproterozoic Events .....	70
3.7 Conclusions .....	72
Chapter 4 Archean tectonics and basin formation: Constraints from U- Pb detrital zircon dating by LA-MC-ICP-MS in a “Timiskaming-type” sedimentary group in the Superior craton .....	114
4.1 Introduction .....	114
4.2 Geological Setting .....	115
4.2.1 The Superior Province and Timiskaming-type sedimentary sequences .....	115
4.2.2 Geology of the Island Lake greenstone belt .....	117
4.3 Results .....	119
4.4 Discussion .....	121
4.5 Synchronous Vertical and Horizontal Processes in the Neoproterozoic .....	123
4.6 Conclusions .....	125
Chapter 5 Summary of Conclusions.....	147
5.1 Summary of Findings .....	147

5.2 Tectonic evolution of the northwestern Superior Province .....	149
5.3 Scientific Contributions.....	150
5.4 Future Studies.....	150
References.....	152
Appendix A Geological Map – Geology of the western portion of Island Lake (NTS 53E15) .....	166
Appendix B Analytical Methods - Chapter 2 .....	167
U/Pb Geochronology .....	167
Appendix C Analytical Techniques – Chapter 3.....	168
Lithochemical analysis .....	168
Nd isotopic analysis.....	170
U-Pb geochronology.....	170
Appendix D Analytical Techniques – Chapter 4.....	177
U-Pb LA-MC-ICP-MS .....	177

## List of Figures

- Figure 1.1 Precambrian tectonic domains for North America. Location of the Island Lake greenstone belt is indicated by the red box. Abbreviations: QMB: Quebec Minto Block; EAO: East Alberta orogen; MRV: Minnesota River valley gneiss; Mak-Ket: Makkovik-Ketilidean. CB: Cumberland batholith; GF: Great Falls Tectonic Zone; GS: Great Slave Lake shear zone; NQ: New Quebec orogen; STZ: Snowbird Tectonic zone; TO: Torngat orogen. Modified from Hoffman 1989) and Percival et al. (2004).....7
- Figure 1.2 Map of the Superior Province in Manitoba and Ontario showing the location of basins, domains, terranes and superterranes. The location of the Island Lake greenstone belt and other belts mentioned in the text are indicated. Map modified from Stott (2009).....8
- Figure 2.1 Regional terrane map of the northwestern Superior Province. The proposed extent of the North Caribou terrane, its northern margin, southern margin and core are shown (Percival et al. 2006; Stott 2009; this study). Locations of the greenstone belts cited in text and relevant terrane boundaries are shown. Boxed area is the location of the map shown in Figure 2.2. Abbreviations for faults: NKF, North Kenyon fault; GSWF, Gods Lake Narrows-Stull Lake-Wunnummin Lake fault zone; SISZ, Savage Island shear zone; SSF, Sydney Lake, St. Joseph fault. Abbreviations for greenstone belts: IL, Island Lake; RL, Red Lake; GL, Gods Lake; SL, Stull-Edmund Lake; HL, Hornby Lake; ML, McInnes Lake; FL, Favourable Lake. Modified from Thurston et al. (1991); Stott (1997); Percival et al. (2004); Parks et at. (2006); and Stott (2009). ..... 32
- Figure 2.2 Simplified geology of the Island Lake greenstone belt. Locations of samples analyzed in this study are shown. Abbreviations used for shear zones: HISZ, Harper Island shear zone; WCSZ, Whiteway Channel shear zone; CBSZ, Chapin Bay shear zone. U-Pb ages from Turek et al. (1986), Stevenson and Turek (1992), and Corfu and Lin (2000). Map modified from Lin et al. (1998). ..... 34
- Figure 2.3 Composite schematic cross section showing the fold geometry and stratigraphy of the Jubilee assemblage, south of the Garden Hill area. See text for more details. .... 35
- Figure 2.4 Concordia diagrams showing zircon data for samples in the Island Lake greenstone belt. The unshaded datum for sample 859 is not included in the average  $^{207}\text{Pb}/^{206}\text{Pb}$  age calculation. .... 36

Figure 2.5 Photograph of the dacitic lapilli tuff in the Loonfoot assemblage. The dacite is interlayered with the basalt and in places it contains rounded clasts of felsic volcanic material, as well as locally derived basalt detritus. Camera lens for scale. ....	37
Figure 2.6 Photograph of the contact between the Bella Lake pluton and the Island Lake group (dashed lines). Locally derived clasts of the Bella Lake pluton infill paleo-topographic depressions on the pluton surface. Pen for scale .....	38
Figure 2.7 Concordia diagrams showing zircon data for samples from plutonic rocks in the Island Lake greenstone belt. The unshaded datum for sample 067 is not included in the average $^{207}\text{Pb}/^{206}\text{Pb}$ age calculation. ....	39
Figure 2.8. Proposed original stratigraphy of the volcanic assemblages and intrusive rocks in the Island Lake greenstone belt. The uneven surface of the intrusive suite accounts for the contact relationships observed in the Island Lake greenstone belt. ....	40
Figure 2.9 Timeline showing age relationships of volcanic, plutonic and sedimentary rocks in the Island Lake greenstone belt, as well as other relevant volcanic and plutonic ages in the northwestern and western Superior Province. See text for discussion. Abbreviations: OSD, Oxford Stull domain; MLT, Munro Lake terrane; ILB, Island Lake greenstone belt; NCT, North Caribou terrane; RLB, Red Lake greenstone belt. Ages from Corfu and Ayres (1991), Corfu et al. (1998) and references there in, Sanborn-Barrie et al. (2000), Skulski et al. (2000), Lin et al. (2006) and references there in.....	41
Figure 3.1 Map of the Superior Province showing the location of basins, domains, terranes and superterrane. The location of the Island Lake greenstone belt and other belts mentioned in the text are indicated. Abbreviations for places names and greenstone belts mentioned in text: SLEL - Stull Lake-Edmund Lake greenstone belt; OL - Oxford Lake greenstone belt; KnL - Knee Lake greenstone belt; GL - Gods Lake greenstone belt; KL - Kasabonika Lake; PLSL - Ponask Lake–Sachigo Lake greenstone belt; ML - McFaulds Lake; NC - North Caribou greenstone belt; CL - Cross Lake. Map modified from Stott (2009).....	73
Figure 3.2 Map of the Island Lake greenstone belt. Dashed rectangle indicates area shown in Figure 3.3. Abbreviations: HISZ - Harper Island shear zone; WCSZ - Whiteway Channel shear zone; SISZ - Savage Island shear zone. ....	74
Figure 3.3 Map of the eastern portion of the Island Lake greenstone belt. The location of shear zones and U-Pb samples are indicated. Abbreviations: HISZ - Harper Island shear zone; WCSZ - Whiteway Channel shear zone; SISZ - Savage Island shear zone.....	75

Figure 3.4 Transposition of an older foliation ( $S_1$ – solid line) into the orientation of the foliation associated with the Savage Island shear zone ( $S_2$ – dashed line). Camera lens for scale.	76
Figure 3.5 Classification diagrams for the mafic volcanic rocks in the different assemblages in the Island Lake greenstone belt. Fields on the Zr/TiO <sub>2</sub> vs. Nb/Y plot after Pearce (1996) and AFM diagram after Irving and Baragar (1971). Fields on the Zr/Y plot are from Barrett and MacLean (1999).	77
Figure 3.6 Primitive mantle normalized multi element diagrams of mafic volcanic rocks in the Island Lake greenstone belt. Values from Sun and McDonough (1989).	78
Figure 3.7 $\epsilon$ Nd diagram for rocks in the Island Lake greenstone belt. DM - depleted mantle curve from DePaolo (1981). CHUR – chondritic uniform reservoir.	79
Figure 3.8 Classification diagrams for the felsic intrusive and extrusive rocks in the Island Lake greenstone belt. Fields on the AFM diagram after Irving and Baragar (1971).	80
Figure 3.9 Primitive mantle normalized multi element diagrams of felsic intrusive and extrusive rocks in the Island Lake greenstone belt. Values from Sun and McDonough (1989).	81
Figure 3.10 Field photos showing field setting of U-Pb samples. A - Sample 684, a post kinematic dyke that cross cuts an early foliation ( $S_1$ indicated by dashed line) and contains a xenolith of foliated mafic country rock. Camera lens for scale. B - Sample 06 from the Savage Island shear zone, a post-tectonic quartz porphyry dyke running from the top to the bottom of the photo, cross cutting foliation in the mafic host rock ( $S_1$ indicated by dashed line). Hammer for scale. C – Sample 103, a pre-to early syn-kinematic quartz porphyry dike that is strongly internally sheared and folded with the sheared mafic country rock ( $S_2$ indicated by dashed line). D – Sample 106 from the Savage Island shear zone, a post- to late syn-kinematic quartz porphyry dyke that cuts $S_2$ , indicated by dashed line. Contact between dyke and country rock indicated by solid line. Hammer and feet at top of photo for scale.	82
Figure 3.11 Unabraded zircon populations from each dyke. 200 $\mu$ m scale bar on each photo.	83
Figure 3.12 Concordia diagrams showing zircon data for dyke samples in the Island Lake greenstone belt. Inset histogram on sample 06, <sup>206/207</sup> Pb Laser ablation ages.	84
Figure 3.13 Nb/Th vs. La/Sm plot for all of the mafic volcanic rocks in the Island Lake greenstone belt. The data falls on an array from N-MORB through Primitive mantle to a proposed composition of Archean upper crust, and falls below the E-MORB and OIB data points. Values for N-MORB, E-MORB, OIB, and primitive mantle from Sun and McDonough (1989). Value for Archean upper crust from Condie (1993).	85

Figure 3.14 Tectonic discrimination diagram for the felsic intrusive and extrusive rocks in the Island Lake greenstone belt. Fields on diagram after Pearce et al. 1984. ....	86
Figure 3.15 A timeline showing age relationships of volcanic and plutonic rocks in the northern part of the northwestern Superior Province. Ages from Stevenson and Turek (1992); Corfu and Lin (2000); Corkery et al. (2000); Skulski et al. (2000); Rayner and Stott (2005); and Lin et al. (2006). ....	87
Figure 3.16 A model for the tectonic evolution of the northwestern Superior Province in the Meso and Neoproterozoic. Abbreviations: NCT - North Caribou terrane; NSS - Northern Superior superterrane; ILGB - Island Lake greenstone belt, OSD - Oxford Stull domain, SISZ - Savage Island shear zone; GSWF - Gods Lake Narrows-Stull Lake-Wunnummin Lake fault zone; NKF - North Kenyon fault.....	88
Figure 4.1 Location of the Island Lake greenstone belt and distribution of “Timiskaming” type groups in the northwestern Superior Province. All of the greenstone belts in the that have a “Timiskaming” type group are shown. Box in inset map shows location within the larger Superior Province. The relative positions of the Northern Superior superterrane, the North Caribou terrane, and the location of the North Kenyon Fault (dashed line) are shown. The dome and keel structure is evident across the whole North Caribou terrane, and is particularly well developed in the Oxford and Gods Lake area as well as the Muskrat Dam and North Caribou lake area. Abbreviations of greenstone belts: IL - Island Lake; CL - Cross Lake; CR - Carrot River; OL - Oxford Lake, KL - Knee Lake; GL - God's Lake; ST - Stull Lake; ML - Muskrat Dam Lake; NC - North Caribou Lake; FL - Favourable Lake; NST - North Spirit Lake; NTL - North Trout Lake. Ages from Corkery et al. 1992; Corfu et al. 1998; Skulski et al. 2000; Corkery et al. 2000; Corfu and Lin 2000; Lin et al. 2006. Modified after Stott (2009). ....	126
Figure 4.2. Detailed map of the Island Lake Group with reversals in younging directions that show an overall synclinal fold geometry. Data from this study and Lin et al. (1998). ....	127
Figure 4.3 Schematic stratigraphic column for the Island Lake greenstone belt. The sample locations within the Island Lake Group are noted. ....	128
Figure 4.4 Photographs of units in the Island Lake Group. A - Lower mixed sandstone/shale unit (sample I), pen at bottom of picture for scale. B- Interbedded sandstone –polymictic conglomerate unit (sample II), pen at bottom of picture for scale. C- Massive sandstone unit (sample III), pen at bottom of picture for scale. D- Upper mixed sandstone/shale unit (sample IV), pen at top right of picture for scale. ....	129

Figure 4.5 Photographs of representative zircon populations from each sample.....130

Figure 4.6  $^{207}\text{Pb}/^{206}\text{Pb}$  age frequency- probability histograms for four samples from the Island Lake Group. “n” indicates the number of analysis used to construct each histogram. Analysis that were more than +/-10% discordant, showed evidence of “mixed ages” during runs, or had anomalously high  $^{204}\text{Pb}$  counts during analysis are not included in the final data...131

Figure 4.7 Cartoon diagrams of the stages of evolution of an inter-diapiric basin. Stage A - original stratigraphy of greenstone belt, stage B though D - progressive stages of basin development. In stages B and C, the supracrustal pile is eroded from top to bottom, and is the major supply of detritus to the basin until a time at which they are either completely eroded away, or they lie below the “erosional surface”, represented by the dashed line. In stage D, the underlying plutons and youngest porphyries and dykes are eroded and supply detritus to the basin.....132

Figure 4.8 A summary of age/space (craton)/tectonic regime operating in the Archean. Position of dashed arrow on time line indicates when evidence for regime being active has been documented. Data from this study; Calvert et al. 1995; Choukroune et al. 1997; Bedard et al. 2003; Van Kranendonk et al. 2004; Wang et al. 2004; Lin 2005; Percival et al. 2006; Van Kranendonk et al. 2007.....133

## List of Tables

Table 2-1 U-Pb data .....	42
Table 3-1 Lithogeochemical results .....	89
Table 3-2 Nd isotope data summary.....	111
Table 3-3 U-Pb dyke data.....	112
Table 4-1 LA-ICP-MS U-Pb data.....	134

# Chapter 1

## Introduction

### 1.1 The Archean

Many aspects of Archean geology are not well understood, even though much research has been focused on this time period in the Earth's history. Many issues remain unresolved regarding what geological and tectonic processes were operating during the Archean. Current issues in Archean geology range from broad scale questions about the nature of the Earth (e.g. Was the Earth hotter at the time?) to map scale questions about the primary relationships between rocks that have since been altered (e.g. Do units have allochthonous or autochthonous relationships with each other?). One of the most fundamental questions concerning the Archean is what style of tectonic processes were occurring at the time. Were the same tectonic processes occurring as we see on the Earth today ("modern" plate tectonics) or were they different?

Approximately 30 Archean cratons exist worldwide (Condie 2005). The largest and best-exposed is the Superior Province, and as such it provides a natural laboratory in which to study geological and tectonic processes in the Archean. The Superior province forms the nucleus of the Canadian Shield, in which younger orogens were subsequently built on or sandwiched against (Figure 1.1). The Superior Province was originally divided into roughly E-W trending subprovinces based on distinct geological and tectonic characteristics (Stockwell 1982; Card and Ciesielski 1986). This concept has been refined and now instead of subprovinces, the Superior Province is divided into domains, terranes and superterranes (Figure 1.2). By definition, domains are rocks that have different geological histories from rocks in adjacent domains, but have (para) autochthonous relationships with adjacent domains. Terranes are fault-bounded units of rocks that have a common tectonic history that is different from adjacent terranes, and superterranes are tectonic packages that formed by the juxtaposition of different terranes prior to amalgamation of the Superior Province as a whole (Thurston et al. 1991b; Percival et

al. 2006). A dominant feature in the northwestern part of the Superior Province is the North Caribou terrane (NCT), a ca. 3.0 Ga crustal block, which terranes to the south and north were either built on or juxtaposed against during final tectonic amalgamation. Granite-greenstone terranes and domains proximal to the NCT have geological histories that include Meso – and Neoproterozoic volcano-plutonic events and commonly show geochemical and/or isotopic evidence of recycling of an older crustal component (e.g. the Island Lake greenstone belt; Stevenson and Turek 1992). Terranes and domains distal to the North Caribou terrane have individual histories, some of which include the involvement of unique, older crustal components (e.g. the Winnipeg River terrane; Tomlinson and Percival 2000), and some that have younger Neoproterozoic volcano-plutonic histories and are isotopically juvenile in nature (e.g. the Wawa-Abitibi terrane; Stott 1997; Ayer et al. 2002).

The domains/terranes/superterranes of the Superior Province were amalgamated during a sequence of Neoproterozoic orogenies, which juxtaposed the tectonic elements to the south of the 3.0 Ga North Caribou terrane via a series of northward-dipping, southward-younging subduction zones (termed phases of the Kenoran orogeny by Stott (1997), now considered discrete orogenies by Percival et al. (2006). This sequence of subduction and accretion is well documented to the south and on the southern margin of the North Caribou terrane (Sanborn-Barrie 2000; Young et al. 2006; Percival et al. 2006 and references within). The tectonic evolution along the northern margin of the North Caribou terrane is much less constrained. Recent studies have suggested that rocks in this area were generated and/or amalgamated via southward-dipping subduction zones that were situated north of the northern margin (Percival 2006; Parks et al. 2006), or by a northward-dipping subduction zone parallel to that along the southern margin situated along the North Kenyon Fault (Greg Stott pers. comm. 2010). These ideas need to be tested in order to develop a concise model of the tectonic evolution along the northern margin of the North Caribou terrane.

## **1.2 The Island Lake greenstone belt**

Greenstone belts are characteristic of the Archean, and as such are well suited to study when investigating geological and tectonic processes during this time. Over the past 30 years models of greenstone belt development have ranged from “modern” plate tectonic models that are mobilistic/subduction based (Langford and Morin 1976; Kusky and Polat 1999), to models that require coeval and interacting arc/plume systems (Hollings et al. 1999; Wyman et al. 2002), to models that are driven by “catalytic” crustal delamination (Bedard 2006) and do not require horizontal plate movement.

The Island Lake greenstone belt is one of the best-exposed greenstone belts in the northwestern Superior Province (Figure 1.1) and records close to 300 Ma of crustal inheritance, plutonism, volcanism, sedimentation and deformation (Turek et al. 1985; Stevenson and Turek 1992; Corfu and Lin 2000; Parks et al. 2006). The Island Lake greenstone belt’s location within the Superior Province makes it ideal to study both belt - and regional - scale questions about the nature of rocks and the mechanisms of greenstone belt assembly in the northwestern Superior Province. This information will help in determining the overall tectonic evolution of the area, and the results of this work can then be extrapolated to answer larger questions about the Archean Earth, and may shed light on what style of tectonic processes were occurring during this time.

### **1.2.1 Location and previous work**

The Island Lake greenstone belt is located in northeastern Manitoba (Figure 1.1, and Figure 1.2, map sheets NTS 53E15 and 16). The greenstone belt underlies approximately two 1:50,000 scale map sheets. The area is accessible only by aircraft and winter roads, and the three native reserves in the area (Garden Hill, St. Theresa Point and Waasagomach) and one town (Island Lake) are fly-in communities.

The Island Lake greenstone belt was mapped at the scale of 1:63 360 by Godard (1963 a, b) and at a scale of 1:20 000 by Neale (1981), Neale and Weber (1981), McGregor and Weber (1982), Neale et al.(1982), Weber et al. (1982a,b), Gilbert et al. (1982, 1983), and Gilbert (1984 a, 1985 a, b). Lin et al. (1998) studied the high strain zones in the belt. An Nd and Rb-Sr isotope study was carried out by Stevenson and Turek (1992), and U-Pb geochronology studies were done by Turek et al. (1985), Stevenson and Turek (1992), and Corfu and Lin (2000). The geology of mineral occurrences have been described by Theyer (1998), Lin and Cameron, (1997) and Lin and Corfu (2002).

### **1.3 Thesis objectives**

The research objectives and associated research questions of this thesis have been designed to investigate the nature of the supracrustal and intrusive rocks in the belt and how they formed, the mechanisms of greenstone belt assembly in this area, as well as this area's importance with respect to the tectonic evolution of the surrounding terranes in the northwestern Superior Province. These objectives may shed light on larger issues about what tectonic processes were operating in the Archean. Specifically, the main objectives of this thesis are to investigate:

1. the ages of volcano-plutonic events in the greenstone belt.
  - Are the volcanic rocks part of the same or multiple assemblages? What are the ages of plutonic rocks in the belt? What are the implications of these results for the tectonic evolution of the greenstone belt and surrounding terranes?
2. the nature of the volcanic assemblage and correlative plutons.
  - What are the geochemical and Sm-Nd isotopic signatures of the volcanic rocks in the belt and what do these signatures tell us about their geodynamic setting?
  - What are the implications of the above to the tectonic evolution of the Island Lake greenstone belt and other belts along the north margin of the North Caribou terrane?

3. the ages of deformation events and shear zone activity in the belt.
  - Can the ages of syn-tectonic dykes place temporal constraints on the tectonic evolution of the Island Lake greenstone belt and terminal collision in northwestern Superior Province?
4. the distribution of ages of detrital zircons from the stratigraphic top to the bottom of the Island Lake group.
  - What do these data tell us about what tectonic processes were responsible for opening the basin in which these sediments were deposited?
  - What implication does this tectonic setting have on the overall tectonic evolution of the Island Lake greenstone belt and the northwestern Superior Province?

To achieve these objectives, approximately 6 months of geological field work were completed in the Island Lake greenstone belt over the course of four summers. During this work, samples were collected for geochemical, isotopic and geochronological analysis, and key areas were mapped to better understand the stratigraphy of the volcanic assemblages. This work also resulted in a 1: 50, 000 map sheet published with the Manitoba Geological Survey (Appendix A).

## **1.4 Organization of Thesis**

This thesis is presented as a series of three journal articles. The thesis is divided into three main chapters (Chapters 2-4), each of which addresses one or two of the objectives discussed above. These chapters are intended to be stand-alone journal papers. Each chapter is written in a format that includes an introduction to the topic, presentation of data, and then a discussion of the results and a conclusion. Some repetition occurs between the chapters, in particular in the introduction material and where the regional and local geology are discussed. The chapters are presented in a particular order so that the main ideas and conclusions build on previous chapters, and that no data or ideas are

referred to that have not already been presented. References and appendices for all of the chapters are presented at the end of the thesis.

The second chapter addresses the first objective and presents U-Pb geochronology data that address the age of the different volcanic assemblages, as well as key intrusive rocks. The results show that the volcanic assemblages are chronologically unique and not structurally bound. The third chapter addresses the 2<sup>nd</sup> and 3<sup>rd</sup> objectives, and presents whole rock lithochemical and  $\epsilon$ Nd data from the volcanic assemblages and contemporaneous plutons in the Island Lake greenstone belt as well as geochronological results for four dykes that bracket the age of shear zone deformation in the belt. These data are used to develop a tectonic model for the generation of these volcanic rocks, and for the terminal collision of this part of the Superior Province. The fourth chapter addresses the 4<sup>th</sup> objective and presents U-Pb detrital zircon ages from the youngest stratigraphic group in the greenstone belt, the Island Lake Group. The detrital zircons show a distinct distribution pattern from the stratigraphic bottom to the top of the group. The implications of this pattern on the tectonic processes that created the basin in which the sediments were deposited are discussed. Finally, the fifth chapter is an integration of conclusions from all of the previous chapters.

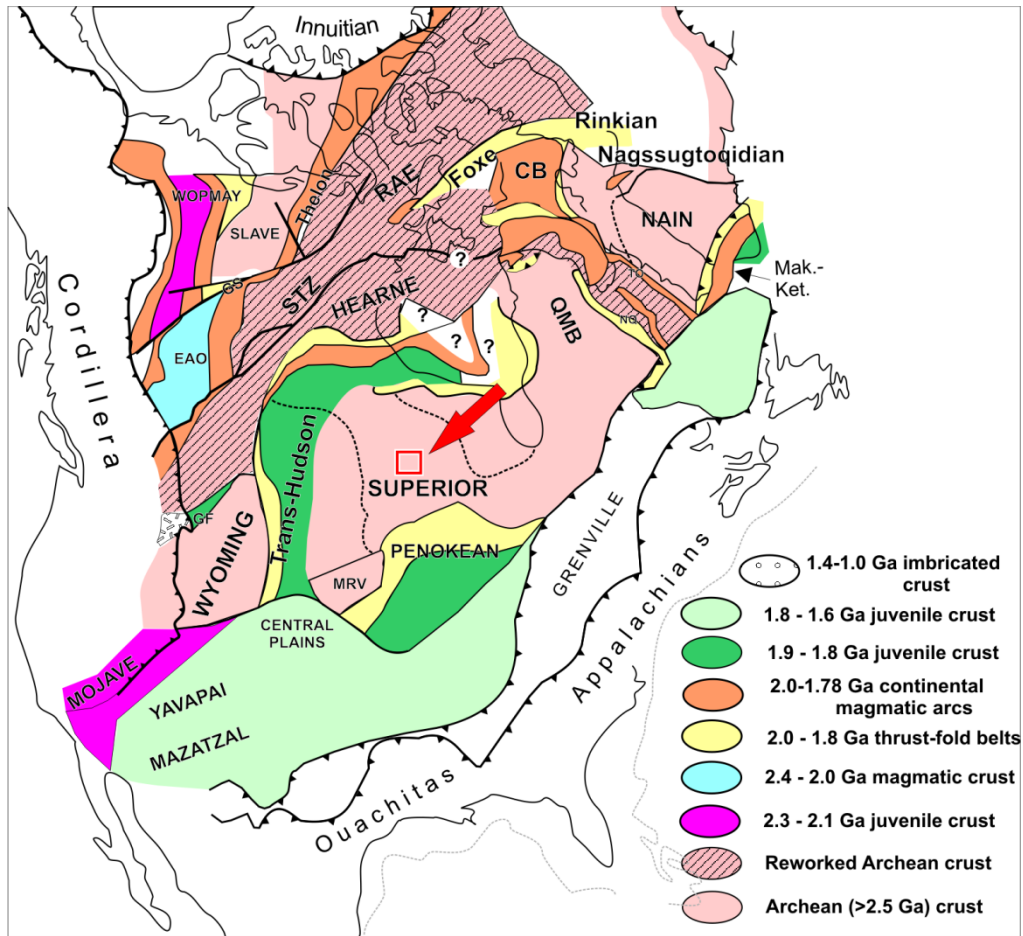


**Figure 1.1** Precambrian tectonic domains for North America. Location of the Island Lake greenstone belt is indicated by the red box. Abbreviations: QMB: Quebec Minto Block; EAO: East Alberta orogen; MRV: Minnesota River valley gneiss; Mak-Ket: Makkovik-Ketilidean. CB: Cumberland batholith; GF: Great Falls Tectonic Zone; GS: Great Slave Lake shear zone; NQ: New Quebec orogen; STZ: Snowbird Tectonic zone; TO: Torngat orogen. Modified from Hoffman 1989) and Percival et al. (2004).

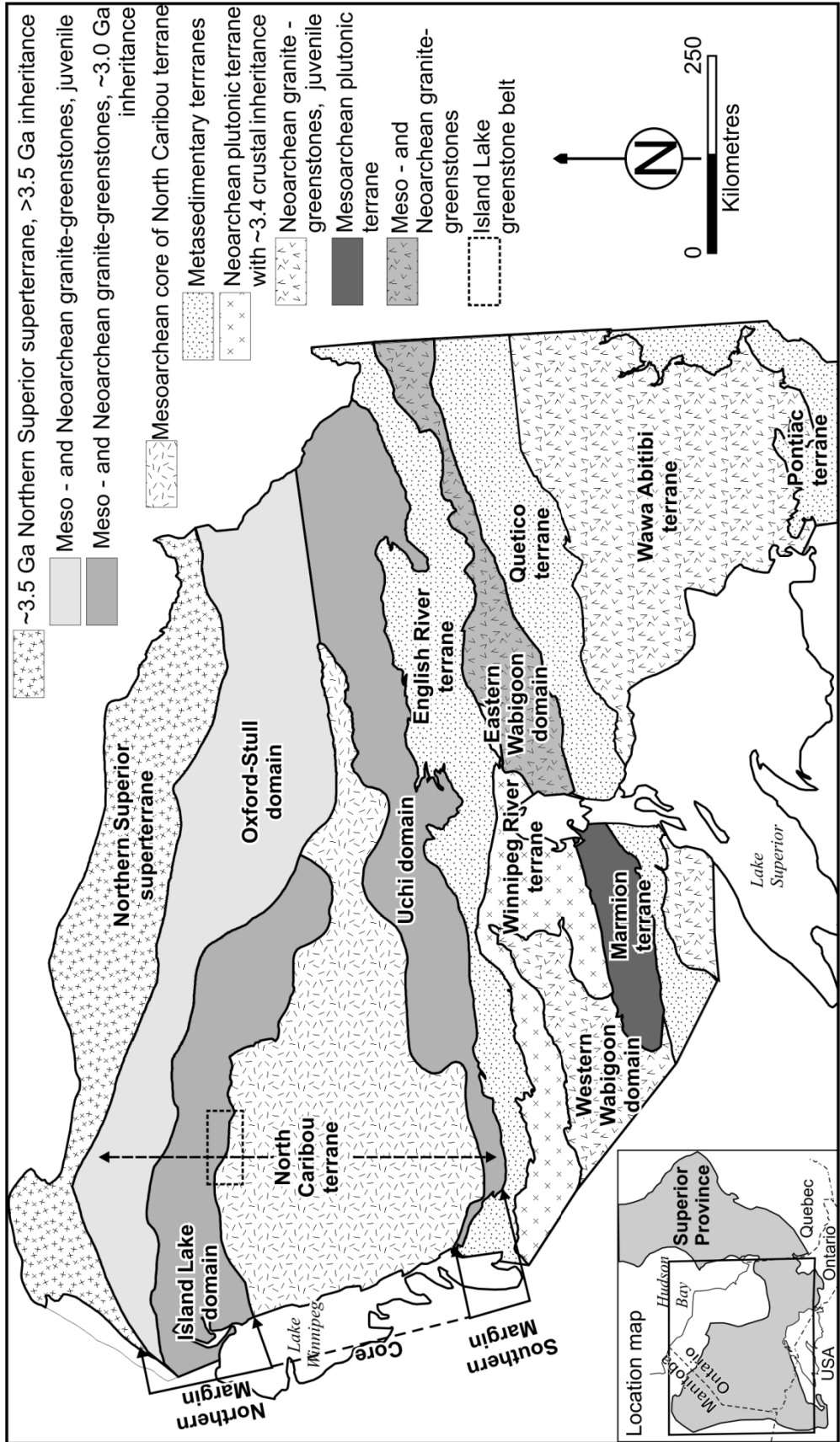


**Figure 1.2** Map of the Superior Province in Manitoba and Ontario showing the location of basins, domains, terranes and superterrane. The location of the Island Lake greenstone belt and other belts mentioned in the text are indicated. Map modified from Stott (2009).

## Chapter 2

### **New high-precision U-Pb ages for the Island Lake greenstone belt, northwestern Superior Province: implications for regional stratigraphy and the extent of the North Caribou Terrane<sup>1</sup>**

#### **2.1 Summary**

A combined U-Pb and field mapping study of the Island Lake greenstone belt has led to the recognition of three distinct supracrustal assemblages. These assemblages record magmatic episodes at 2897 Ma, 2852 Ma, and 2744 Ma. Voluminous plutonic rocks within the belt range in age from 2894 Ma to 2730 Ma, with a concentration at 2744 Ma. U-Pb data also show that a regional fault that transects the belt, the Savage Island shear zone, is not a terrane-bounding structure. The youngest sedimentary group in the belt, the Island Lake Group, has an unconformable relationship with older plutons. Sedimentation in this group is bracketed between 2712 Ma and 2699 Ma. This group and others similar to it in the northwestern Superior Province are akin to Timiskaming-type sedimentary groups found throughout the Superior Province and in other Archean cratons. These data confirm that this belt experienced a complex geological history that spanned at least 200 m.y., which is typical of greenstone belts in this area. Age correlations between the Island Lake belt and other belts in the northwest Superior Province, in combination with Nd isotopic data, indicate that the Oxford-Stull and Island Lake domains and the North Caribou terrane may have been part of a much larger reworked Mesoproterozoic crustal block. The block has a core region bounded by northern and southern margins. It appears that the Superior Province was assembled by accretion of such large independent crustal blocks, whose individual histories involved extended periods of autochthonous development.

---

<sup>1</sup> Published as: Parks, J., Lin, S., Davis, D., and Corkery, M.T., 2006: New high-precision U-Pb ages for the Island Lake greenstone belt, northwestern Superior Province: implications for regional stratigraphy and the extent of the North Caribou Terrane. *Canadian Journal of Earth Sciences*. v 43, p.789-803 The version presented here includes some minor modifications and editorial changes.

## 2.2 Introduction

The Superior Province consists of linear to curved fragments of bimodal volcanic rocks that have been built on, or sandwiched between, older continental crustal blocks. This pattern is seen on both the belt and regional scales. The northwestern Superior Province is a relatively inaccessible and poorly understood area compared to the southern Superior Province. It has been divided into various domains, terranes and superterranes (Figure 2.1; see below; Thurston et al. 1999b; Stott 1997; Skulski et al. 2000; Percival et al. 2004; Percival et al. 2006; Stott 2009). Many of the original subdivisions into domains, terranes and superterranes were proposed based on limited data available at the time (Thurston et al. 1999b). Understanding the geological evolution of each of the domains, terranes or superterranes and the relationships between them can help to test if they are true domains, terranes or superterranes, a first-order question concerning this part of the Superior Province. By definition, domains are packages of rocks that have different geological histories from rocks in adjacent domains, but have (para) autochthonous relationships with adjacent domains. Terranes are fault-bounded packages of rocks that have a common tectonic history that is different from adjacent terranes, and superterranes are tectonic packages that formed by the juxtaposition of different terranes prior to amalgamation of the Superior Province as a whole (Thurston et al. 1999b; Percival et al. 2006).

This chapter reports on the results of a field mapping and geochronological study of the Island Lake greenstone belt in the northwestern Superior Province, focusing on detailed dating of supracrustal rocks. The greenstone belt is well exposed and is situated across the Savage Island shear zone, the boundary between the Island Lake domain and the North Caribou terrane (Figure 2.1; Thurston et al. 1999b). Our results show that the belt has a long and complex history that can be correlated with volcanic events in adjacent domains and terranes. In combination with Nd isotope

data, the results indicate that these domains and terranes were part of a single crustal entity and the Savage Island shear zone is thus not a terrane-bounding structure. While not giving definitive evidence on the nature of Archean tectonic processes, this study helps to define the extent and composition of some of the fundamental tectonic building blocks of the Superior Province.

### **2.2.1 Regional Geological Setting**

Terranes and domains in the northwestern Superior Province (Figure 2.1), from north to south, are the Northern Superior superterrane (NSS, Skulski et al. 2000), the Oxford-Stull domain (OSD; Thurston et al. 1991b; Stott 1997; Stott 2009), the Island Lake domain (ILD; Thurston et al. 1991b; Percival et al. 2007; Stott 2009) and the North Caribou terrane (NCT, Thurston et al. 1991b). The last is part of the larger North Caribou -La Grande-Goudalie superterrane that extends into northern Quebec (Stott 1997; Corfu and Stone 1998; Percival et al. 2001; Percival et al. 2004 and references therein). Together these comprise the Sachigo and Berens subprovinces formerly defined by Card and Ciesielski (1986), as well as part of the Minto block (Percival et al. 2001) in northern Quebec.

The Northern Superior superterrane consist of ancient, ca. >3.5 Ga granitic rocks that have been strongly overprinted by later metamorphic, magmatic, and deformational events (Skulski et al. 2000, Bohm et al. 2000, Bohm et al. 2003, and Percival et al. 2006). The North Kenyon fault separates the North Superior superterrane from the Oxford-Stull domain to the south (Skulski et al. 2000). The Oxford-Stull domain consists of ca. 2.84 Ga oceanic (Syme et al. 1999; Corkery et al. 2000) volcanic rocks, which show only a few instance of Nd inheritance (Rayner and Stott 2005). The Island Lake domain lies south of the Oxford-Stull domain, and consists of the previously defined Munro Lake and Island Lake terranes of Thurston et al. (1991, for the location of the original Island Lake terrane and the Munro Lake terrane, see Figure 1 of Parks et al. 2006). Since this division, work has shown that both the Island Lake terrane and Munro Lake terrane have both been influenced by an older crustal

source (Stevenson and Turek 1992; Corfu and Lin 2000; Skulski et al. 2000; Parks et al. 2006). It has been suggested that this crust is the northern extension of the North Caribou terrane (Skulski et al. 2000; Sanborn-Barrie et al. 2001). As such, the terms Island Lake and Munro Lake domain were introduced (Percival et al. 2006; Percival and Easton 2007). More recent work by Stott (2009) groups both of these domains into one, the Island Lake domain, and refines the boundaries of both the Island Lake domain and Oxford-Stull domain (Figure 2.1). This idea needs to be tested, as it is possible that the Savage Island shear zone is indeed a terrane bounding fault as originally suggested by Thurston et al. (1991) that juxtaposes the North Caribou terrane with an entirely different ~3.0 Ga crustal block on which the Island Lake domain could have been built (the extent, geometry, and kinematics are discussed more in section 3.2.3). The North Caribou terrane itself is interpreted to be an old proto-continental nucleus that acted as a stable platform onto which other terranes were accreted during terminal collision of the Superior Province in Neoproterozoic time (Thurston et al. 1991b; Skulski et al. 2000).

### **2.3 Results of geological and geochronological investigations**

What follows is a description of geological relationships, including both previous age data and new results. Sample locations are shown on Figure 2.2. Analytical data are given in Table 2.1 and Concordia diagrams are shown on Figures 2.4 and 2.7. Analytical methods are given in Appendix B.

The geology of rocks in the belt are discussed below, and further details can be found in Parks et al. (2001) Parks et al. (2002) and Parks et al. (2003). The rocks in the Island Lake greenstone belt are variably metamorphosed from lower greenschist to lower amphibolite facies. Supracrustal rocks in the belt are either intruded by, or have unconformable relationships with, various plutonic bodies in the belt and have experienced multiple deformation events. Late shear zone deformation has produced at least four spatially distinct shear zones and overprinted much of the early deformation fabrics (see

Lin et al. 1998 for details on structure in the belt and the kinematics of shear zones). The shear zones are shown in Figure 2.2. From south to north they are the Savage Island shear zone, the Harper Island shear zone, the Whiteway Channel shear zone and the Chapin Bay shear zone.

### **2.3.1 Supracrustal rocks (samples 859, 839, 425, 289, 105, 02)**

Supracrustal rocks in the region have traditionally been divided into the older volcanic and volcanogenic rocks of the Hayes River Group (HRG), and the unconformably overlying younger sedimentary rocks of the Island Lake Group (ILG). The term “Hayes River Group” has been applied to all volcanic and volcanogenic rocks below the unconformity in the Island Lake greenstone belt (Wright 1928) and more broadly within the northwest Superior Province in northern Manitoba. Lin et al. (1998) and Corfu and Lin (2000) suggested that the rocks of the HRG in the Island Lake greenstone belt could be subdivided into dissimilar, shear-bounded packages. This suggestion was based on lithological differences seen in the basalts and the presence of high strain zones that separate these packages into distinct shear zone-bounded panels. However, this study has observed that the contacts between the panels are not observed directly in the field. These contact relationships are discussed more in section 2.4.2. The HRG is sub-divided here into the Whiteway, Jubilee and Loonfoot assemblages (Figure 2.2).

#### **2.3.1.1 Whiteway assemblage**

The Whiteway assemblage is located in the east – central part of the map area (Figure 2.2). This assemblage consists predominantly of mafic volcanic rocks, large gabbroic intrusions and rare lenses of volcanogenic sedimentary rocks. The basaltic rocks of the Whiteway assemblage are aphyric and pillowed, the latter having thin selvages and commonly exhibiting rusty (iron sulphide?) alteration. They are metamorphosed to greenschist facies and are strongly deformed in the Harper Island and

Whiteway Channel shear zones. Away from the shear zones, they are only weakly deformed and primary structures are locally well preserved. The gabbro that intrudes the basaltic package gave a U-Pb zircon age of  $2807 \pm 1$  Ma (Corfu and Lin 2000), providing a minimum age constraint on volcanism and sedimentation in the Whiteway assemblage.

Detrital zircons were dated from a sample of a volcanogenic sedimentary rock in this assemblage (sample 859). The detrital zircon population in this sample consists of grains that are elongate to acicular prisms, or broken fragments of larger prismatic crystals. The grains are light brown to colourless, clear and commonly contain clear inclusions in the larger broken fragments. All grains show little effects of natural mechanical abrasion suggesting they were not transported a long distance and may have been only locally reworked. Five zircons were analyzed all of which gave slightly discordant data but with quite similar  $^{207}\text{Pb}/^{206}\text{Pb}$  ages. The  $^{207}\text{Pb}/^{206}\text{Pb}$  age of the youngest grain gives a maximum age for sedimentation at  $2896.2 \pm 2.9$  Ma (Figure 2.4A; Table 2.1). This is indistinguishable from the average age of four overlapping data,  $2897.0 \pm 1.4$  Ma, while the fifth zircon was only slightly older (unfilled ellipse, not used in average  $^{207}\text{Pb}/^{206}\text{Pb}$  age calculation). This probably represents the age of the principal source. While this age strictly represents a maximum age of sedimentation in the Whiteway assemblage, lack of evidence of rounding by transport in the zircons and the uniform aged provenance could indicate a time of proximal felsic volcanism at ca. 2897 Ma. The interpretation of the age of these sediments is discussed further below.

The rocks found north of the Whiteway Channel shear zone are mafic and ultramafic volcanic rocks that are metamorphosed to amphibolite facies and strongly deformed. It is unclear if these rocks are higher grade equivalents of the basalt south of the shear zone, or whether they represent a distinct assemblage. Accordingly, they are not differentiated here (Figure 2.2).

### 2.3.1.2 Jubilee assemblage

The Jubilee assemblage is located in the south to southwest portion of the Island Lake greenstone belt. A main aim of the fieldwork completed during this study was to determine the stratigraphy and fold geometry of the area, and this work resulted in a schematic cross section (Figure 2.3). South of Garden Hill a continuous supracrustal sequence of basalt (oldest) to felsic and sedimentary rocks (youngest) is observed (between the two northmost sheared contacts in Figure 2.3). The basalt is both pillowed and massive, has thin pillow selvages, and is aphyric. Locally there are well-preserved primary structures such as well-rounded pillows with cusps and flow top breccias that define reliable younging directions. A felsic volcanic unit overlies the basalts, and consists of tuffaceous beds as well as quartz-feldspar phyrlic flows. Stratigraphically overlying this unit is a sedimentary unit that grades from argillite through sandstone to conglomerate. The sequence of units is repeated by folding in this area (Figure 2.3). South of this sequence is another package of metasedimentary rocks, which is bound on its north and south margins by high-strain zones. This package contains greywacke, siltstone and argillitic rocks. Further to the south (south of the southernmost sheared contact in Figure 2.3) a continuous sequence of basalt (older) to felsic volcanics (younger) is observed. The basalt here is pillowed, aphyric and contains epidote and quartz-carbonate veining. The felsic volcanic unit overlying the basalt is composed primarily of tuffaceous beds that have 1-2 mm rounded quartz and feldspar crystals set in a buff to grey fine grained felsic matrix. The unit is generally well foliated with pervasive chlorite alteration along foliation planes. This package is also repeated by folding (Figure 2.3). Based on lithological similarities seen in the field, the volcanic units in the northern part of the section appear to correlate with those in the southern part of the section shown in Figure 2.3. This correlation needs to be tested (see Chapter 3).

Felsic volcanic rocks (termed felsic volcanic unit in Figure 2.3) in the Jubilee assemblage were previously dated at  $2852 \pm 1.5$  Ma (Corfu and Lin 2000) and  $2861 \pm 12$  Ma (Turek et al. 1986). Corfu and Lin (2000) found that detrital zircons from the volcanogenic sedimentary rocks (termed middle sedimentary unit in Figure 2.3) in this assemblage show a tight range in  $^{207}\text{Pb}/^{206}\text{Pb}$  ages of 2858 - 2847 Ma, consistent with a provenance from the nearby felsic volcanic rocks. One felsic volcanic sample from the northwest portion of the map area (samples 839) and another felsic volcanic sample from north of the Savage Island shear zone (sample 425) were dated to test whether they could be correlated with the Jubilee assemblage which is predominately observed to outcrop in the southeast and south of the Savage Island shear zone.

The zircon population in sample 839 consists of abundant short, squat doubly terminated prisms that are brown in colour, clear and have rod and round shaped inclusions. Three zircon grains were analyzed, and gave slightly discordant data with overlapping  $^{207}\text{Pb}/^{206}\text{Pb}$  ages giving an average of  $2852.5 \pm 1.0$  Ma (Figure 2.4B; Table 2.1). This is the most likely age of eruption.

The zircon population in sample 425 (Figure 2.4C) consists of elongate to squat euhedral prismatic grains that are brown in colour and clear. Two concordant and one slightly discordant data points have overlapping  $^{207}\text{Pb}/^{206}\text{Pb}$  ages with an average of  $2854.5 \pm 1.0$  Ma, the probable age of eruption. The  $2852.5 \pm 1.0$  Ma age from sample 839 (Figure 2.4B; Table 2.1) and the  $2854.5 \pm 1.0$  Ma age from sample 425 (Figure 2.4C; Table 2.1) are essentially identical to the other ages of volcanism in the Jubilee assemblage. This confirms that the volcanic rocks within and on both sides of the Savage Island shear zone are all part of the same assemblage.

A tonalitic intrusion (sample 289) that is observed locally to dyke into and cut the basaltic rocks was also dated. The zircon population in this sample consists of euhedral prismatic grains that are clear, brown to light brown in colour, exhibit a high lustre and occasionally contain small clear

inclusions. Three zircons were analyzed from this sample (Figure 2.4D). One datum is lightly discordant, and one is slightly reversely discordant, possibly because of incomplete dissolution. The average of  $^{207}\text{Pb}/^{206}\text{Pb}$  ages is  $2851.0 \pm 0.9$  Ma but the data scatter slightly outside of error. The  $2852 \pm 2$  Ma age of the concordant datum gives the best estimate for the age of emplacement. It is identical to the volcanic ages and indicates that the intrusion is subvolcanic and could have acted as a feeder for the Jubilee assemblage felsic volcanism.

### 2.3.1.3 Loonfoot assemblage

The Loonfoot assemblage is located in the east portion of the map area. This assemblage contains voluminous massive basalt and minor amounts of dacitic lapilli tuff. This assemblage is metamorphosed to greenschist facies. The basalt is light green to grey, pillowed or massive and aphyric. The dacitic lapilli tuff is interlayered with the basalt. In places it contains rounded clasts of felsic volcanic material, as well as locally derived basalt detritus (Figure 2.5). A sample was taken from the tuff to constrain the age of volcanism in the assemblage (sample 105). The zircon population in this sample consists of euhedral prisms and fragments of larger grains that are pink to brown in colour and clear. Two concordant and one slightly discordant data have overlapping  $^{207}\text{Pb}/^{206}\text{Pb}$  ages with an average of  $2744.0 \pm 1.3$  Ma (Figure 2.4E; Table 2.1). This is likely the age of volcanism and shows that the Loonfoot assemblage is significantly younger than the Jubilee assemblage that outcrops to the south.

### 2.3.1.4 Island Lake Group

The Island Lake Group (ILG) is the youngest supracrustal package in the Island Lake greenstone belt. It has an unconformable relationship with the underlying HRG (Lin et al 1998, this study), however in many places this relationship is overprinted and the contact is marked by a high strain

zone (the Savage Island shear zone). The lowest unit exposed in the Island Lake Group north of this high strain zone is a thin, blue quartz bearing mixed sandstone/shale unit that grades into an extensive sandstone and polymictic conglomerate unit that marks the base of the Island Lake Group in most other locations. The group then grades into a cross bedded sandstone unit, which in turn grades into the upper greenish mixed sandstone/mudstone unit (Lin et al. 1998; Corfu and Lin 2000; this study). The group as a whole is weakly to moderately deformed and metamorphosed to greenschist grade. Well-preserved primary features such as graded bedding, cross bedding, and flame structures define younging directions, from which reversal infer macroscopic folds (Lin et al. 1998). Clasts in the polymictic conglomerate are locally derived and some are observed to contain a tectonic (including mylonitic) fabric, indicating that the belt had experienced at least one deformational event before the deposition of the Island Lake Group (Lin et al. 1998; Corfu and Lin 2000).

The ILG outcrops in both the eastern and western portion of the map area and is spatially separated by the Bella Lake Pluton (Figure 2.2). Detrital zircon dating by Corfu and Lin (2000) on samples from the upper mixed sandstone/shale sequences in the east and west part of the belt show similar age distributions. Detrital zircons analyzed in the eastern mixed sandstone/shale (n=10) range in age from 2920 Ma to 2712 Ma, whereas those analyzed from the western mixed sandstone/shale (n=8) range in age from 2938 Ma to 2722 Ma. The blue quartz bearing mixed sandstone/shale from the base of the ILG in the east part of the belt was also analyzed by Corfu and Lin (2000). Detrital zircons from this unit (n=8) range in age from 2896 Ma to 2821 Ma, a very different age pattern from that of the younger mixed sandstone/shale.

These data, and the interpretation of previous workers that the 2744 Ma Bella Lake pluton intruded the lower part of the ILG (Turek et al. 1986; Lin et al. 1998; Corfu and Lin 2000), suggest that the ILG was deposited over an extended period of time (at least 30 m.y.). During this study, a critical

outcrop showing the contact relationship between the Bella Lake pluton and the sandstone and polymictic conglomerate unit of the ILG was cleaned and re-examined. The contact, previously interpreted as intrusive, is seen to be an unconformity where locally derived clasts of the Bella Lake pluton have filled in paleo-topographic depressions on the pluton surface (Figure 2.6). Three detrital zircon grains from a sandy layer above the contact at the cleaned outcrop (sample 02) range from well preserved multifaceted elongate prisms to well rounded, mechanically abraded and pitted zircons. The zircons are slightly brown to colourless, clear and contain small clear inclusions. Near-concordant data from three detrital zircon grains give  $^{207}\text{Pb}/^{206}\text{Pb}$  ages of  $3015 \pm 2$  Ma,  $2934 \pm 2$  Ma and  $2717 \pm 2$  Ma (Figure 2.4F; Table 2.1). The youngest age is an older limit on deposition at the base of the ILG and confirms the unconformable relationship observed in the field between the Island Lake Group and the Bella Lake pluton.

### **2.3.2 Plutonic Rocks (samples 04, 176, 067, 899)**

Batholiths surround the supracrustal rocks in the Island Lake greenstone belt and range in age from 2894 Ma to 2699 Ma (Turek et al. 1986; Stevenson and Turek 1992; Corfu and Lin 2000; this study). In the Cochrane Bay area a leucotonalite and a foliated diorite are exposed. The diorite contains mafic xenoliths and is locally seen to be the source of large (>30 cm) clasts in the ILG. The leucotonalite gave a previous age of  $2886 \pm 12$  Ma (Turek et al. 1986). A sample was collected from the diorite for this study (sample 04). The zircon population in this sample consists of equant euhedral grains with double terminated prisms that are orange to pale brown in colour, clear, and contain minor clear and opaque inclusions. Three zircon grains were analyzed from this sample and gave overlapping near-concordant data with an average  $^{207}\text{Pb}/^{206}\text{Pb}$  age of  $2894.1 \pm 1.0$  Ma (Figure 2.7A; Table 2.1). This age is interpreted as the time of crystallization for the diorite and is the oldest intrusive U-Pb age yet recorded in the Island Lake greenstone belt.

A batholith south of the belt has an age of  $2825 \pm 2$  Ma (Corfu and Lin 2000), while plutons in the northwest portion of the belt have younger ages of  $2778 \pm 5$  Ma (Wassagomach Tonalite, Stevenson and Turek 1992), and  $2748 \pm 3$  Ma (Chapin Bay Tonalite, Stevenson and Turek 1992). A deformed tonalite with S/C fabric and rotated porphyroblasts outcrops in Chapin Bay and was dated as part of this study (sample 176). The zircons in this sample are euhedral, short, stubby, doubly terminated prismatic grains that are pink to brown in colour and internally clear. Inclusions and fractures are common in most grains, and were avoided during picking. Three zircons gave overlapping near-concordant data with an average  $^{207}\text{Pb}/^{206}\text{Pb}$  age of  $2747.2 \pm 1.2$  Ma (Figure 2.7B; Table 2.1). This is the likely crystallization age of the tonalite, which agrees with the previous age on the Chapin Bay tonalite sampled to the north and places a maximum age on the deformational fabric developed in the tonalite.

The Bella Lake pluton outcrops in the middle of the Island Lake greenstone belt. The eastern part of the Bella Lake pluton was dated at  $2744 \pm 2$  Ma by Corfu and Lin (2000), who suggested, along with others, that this pluton could be traced westward to the Cochrane Bay area. Sample (067) was taken to test this, and the zircon population in this sample consists of equant and elongate euhedral prisms and broken tips of larger prisms that are light to dark brown in colour. Larger grains tend to be more heavily fractured, and small clear inclusions are rare in all grains. Three zircon grains gave concordant or near-concordant data with variable precision. The three define an average  $^{207}\text{Pb}/^{206}\text{Pb}$  age of  $2741 \pm 1.0$  Ma but the most precise datum is slightly older than the others (unfilled ellipse, not used in average  $^{207}\text{Pb}/^{206}\text{Pb}$  age calculation). A very discordant datum (63%) not shown in Figure 2.7C is listed in Table 2.1, and also shows evidence of a slightly older age. These zircons define an age for the pluton of  $2741 \pm 1.0$  Ma (Figure 2.7C; Table 2.1), which is essentially identical to the age of the Bella Lake Pluton.

In the Pipe Point Island area (near sample location 899), Turek et al. (1986) reported ages of porphyry intrusion at  $2729 \pm 2$  Ma, however the discordia line that defines this age gave a negative lower intercept. A high-level quartzofeldspathic porphyry (sample 899) that cuts volcanics of the Jubilee assemblage contains a zircon population that consists of euhedral elongate prisms and broken tips of larger grains. The zircons range in colour from orangey-pink to colorless and rarely contain clear inclusions. Five zircons gave overlapping concordant data with an average  $^{207}\text{Pb}/^{206}\text{Pb}$  age of  $2729.6 \pm 1.0$  Ma (Figure 2.7D; Table 2.1). This age is the best estimate for crystallization of the porphyry. A younger 2699 Ma porphyry crosscuts the ILG (Turek et al. 1986). This represents the youngest known age of magmatic activity in the belt and puts a younger age limit on deposition of the ILG.

## **2.4 Discussion**

### **2.4.1 Composition and history of the Island Lake greenstone belt**

Stevenson and Turek (1992) carried out an Nd isotopic study in the western portion of the Island Lake greenstone belt. Dacite tuffs in the 2852 Ma Jubilee assemblage and granites associated with the 2744 Ma Loonfoot assemblage (located north of the Savage Island shear zone) have negative (enriched)  $\epsilon\text{Nd}$  values ( $t=2.85$  Ga and 2.74 Ga, respectively) that range from  $-2.0$  to  $-0.4$  and Nd model ages that range from 2.97 Ga to over 3.0 Ga, suggesting involvement of a Mesoproterozoic crustal component in both of these volcanic assemblages. This evidence and the presence of 3.0 Ga age detrital zircon in the ILG suggests that there was continual involvement of an older crustal component throughout the development of the greenstone belt.

Strictly speaking, the 2897 Ma age of detrital zircons in the Whiteway assemblage (sample 859) represents a maximum age for sedimentation in this assemblage but, as suggested above, the age

could record felsic volcanism and deposition in the assemblage. The second interpretation is favored here for several reasons. First, the rocks in this assemblage are lithologically distinct from other volcanic assemblages in the belt (Lin et al. 1998; this study). Second, the presence of volcanic material associated with 2.9 Ga plutons has been previously documented in the belt. In the Cochrane Bay area, a  $2886 \pm 12$  Ma (Turek et al. 1986) leucotonalite (similar in age to the diorite, sample 04, dated in this study), cuts a mafic to intermediate fragmental volcanic rock (Corfu and Lin 2000; Turek et al. 1986). Thirdly, in the Jubilee assemblage, the age of detrital zircons reflects the age of felsic volcanism in the assemblage. Detrital zircons (n=6) dated by Corfu and Lin (2000) give near concordant  $^{207}\text{Pb}/^{206}\text{Pb}$  ages that form a tight cluster of ages in the range 2858-2847 Ma. These ages are similar to the four ages of felsic volcanism of ca. 2852 Ma obtained in the assemblage (Corfu and Lin 2000; this study). This pattern supports the suggestion of Corfu et al. (1998) that the absence of younger components in volcanogenic sediments can be taken as an indication that deposition predated the younger periods of volcanism, and that the ages of detrital zircons are likely close to that of deposition of the unit. All these observations suggest that the 2897 Ma detrital zircon in sample 859 reflects the age of volcanism and deposition in the assemblage. If so, the Whiteway assemblage is the oldest dated felsic volcanic unit in the Island Lake greenstone belt. The age of 2894 Ma for the diorite from Cochrane Bay (sample 04) is quite similar and suggests that the Cochrane Bay diorite represents an intrusive component of the Whiteway assemblage.

The Jubilee assemblage preserves the most voluminous volcanism in the belt. The data from this study and others indicate that the assemblage is continuous along strike in the belt and records a ca. 2852 Ma period of bimodal volcanism and associated plutonism that lasted only a few million years.

The Loonfoot assemblage represents a previously unknown period of 2744 Ma volcanism that was coeval with emplacement of major plutons around Bella Lake and Chapin Bay. Except for

volumetrically minor porphyries, this appears to be the youngest significant period of volcanic and plutonic activity. Although only minor exposures of supracrustal rocks from this assemblage are preserved in the area, the assemblage contains the largest exposures of subvolcanic intrusions.

#### 2.4.1.1 Contact relationships between the volcanic assemblages

The new geochronology presented in this paper confirms the sub-division of rocks of the HRG into three distinct volcanic assemblages with ages of 2897 Ma, 2852 Ma, and 2744 Ma (Lin et al., 1998; Corfu and Lin, 2000; this study). This study, however, questions the significance of faults between the assemblages. In several places the assemblages were thought to be bound by later shear zones (Lin et al., 1998, Corfu and Lin, 2000), however identically aged rocks are present on both sides of the shear zones (e.g. in the Jubilee assemblage, samples 425 and 839). This leads to the conclusion that the original contact relationships between the volcanic assemblages of the HRG are not the fault structures, and as such the contacts are not directly observed in the field. It is clear that these assemblages are not fault-bounded panels as described by Lin et al. (1998) and Corfu and Lin (2000).

Given that the contacts are not directly observed in the field, nor are they tectonic as previously interpreted, they can only be inferred from other field observations and the currently available U-Pb ages and Nd isotope data. All three of the volcanic assemblages are observed in the field to be intruded by plutons that are close in age to that of the volcanic assemblage in which they intrude. The Whiteway assemblage is intruded by the York Lake granodiorite (Parks et al., 2003), which has not been directly dated, but is inferred to be the eastern extension of the 2894Ma Cochrane Bay Diorite (sample 04, this study). The Jubilee assemblage is intruded by the 2851 Ma Jubilee Tonalite (sample 289, this study), as well as the younger southern tonalite gneiss (Corfu and Lin, 2000). The Loonfoot assemblage is intruded by the Loonfoot pluton, which is currently not dated, however it is interpreted to have a similar age as the 2.744 Ga Bella Lake pluton.

The limited Nd isotope data set of Stevenson and Turek (1992) summarized above indicate that two of the volcanic assemblages (the Jubilee and Loonfoot assemblages) have been influenced by an older ~3.0 Ga crustal source. If the Whiteway assemblage has also been influenced by an older crustal source, it is possible that the ages of the plutons observed in the field to be in contact with each volcanic assemblage represent local, (pene) contemporaneous reworking of older Mesoarchean crust. In such a scenario, the volcanic assemblages could have autochthonous relationships with each other. A possible stratigraphic reconstruction that would account for the intrusive contacts observed in the field is presented in Figure 2.8. In this reconstruction, an “uneven” intrusive surface that is not at the same stratigraphic level within all three of the volcanic assemblages would produce the contact relationships seen in the field. This original geometry was subsequently modified by folding and late shear zones, and the whole stratigraphic section was eroded to result in the outcrop pattern observed today. This proposed original stratigraphy needs to be tested by further Nd and geochemical work (see chapter 3).

Regardless of their original geometry with respect to each other, the volcanic rocks in the Island Lake greenstone belt include lithologically distinct assemblages that have discrete ages spanning nearly 200 m.y. Therefore they cannot all be considered as part of a single “Hayes River Group”. Chronological divisions of the HRG are also being made in other greenstone belts in the Northwestern Superior Province in Manitoba (such as in the Oxford Lake-Knee Lake-Gods Lake greenstone belt; Corkery et al. 2000; Lin et al., 2006). It is clear that the use of this term in the northwestern Superior Province needs to be re-evaluated and that the term “Hayes River Group” be abandoned.

#### 2.4.1.2 Contact relationships between the Island Lake group and plutons in the Island Lake greenstone belt

U-Pb data confirm new field observations that the relationship between the ILG and Bella Lake Pluton is unconformable (Figure 2.6). Based on available data, the age of deposition of the Island Lake Group is bracketed between 2712 Ma (the age of the youngest detrital zircon dated, Corfu and Lin 2000) and ca. 2699 Ma (the age of a crosscutting intrusion, Turek et al. 1986). This group is similar in geological character and age of deposition to sedimentary sequences that occur in the Stull Lake ( $<2713 \pm 5$  Ma, Skulski et al. 2000), Gods Lake ( $<2711 \pm 2$  Ma, Lin et al. 2006), Cross Lake ( $<2709$  Ma, Corkery et al. 1992), Knee Lake ( $<2707 \pm 9$  Ma, Corkery et al. 2000), and Oxford Lake ( $2705 \pm 2$  Ma, Lin et al. 2006) greenstone belts. Moreover, these groups in the northwestern Superior Province are similar in geological character to groups deposited in late orogenic basins in the southern part of the Superior Province, such as the Timiskaming Group in the Abitibi greenstone belt. The groups in the northwest Superior occupy similar stratigraphic positions within their respective belts, have similar lithologies and contact relationships with underlying rocks, and are also spatially related to late faults and mineralization. Such similarities may also indicate similar tectonic environments of their deposition. The groups in the northwest Superior, however, show a contribution of deep water sediments, and are distinctly older than those in the southern Superior Province, which were deposited in the period 2.68-2.67 Ga (Corfu et al. 1991; Davis 2002). Despite these two differences, the interpretation that these groups are akin to Timiskaming type groups and were deposited in late orogenic basins is supported by recent proposals that collision occurred ca. 20-40 m.y. earlier in the northwestern Superior Province. (i.e. Figs. 10 and 11 of Percival et al. 2004; Percival et al. 2006; Lin et al. 2006). The tectonic significance of these basins are discussed in detail in Chapter 4.

## 2.4.2 Regional correlations

The Island Lake terrane (now the Island Lake domain) was originally considered distinct from the North Caribou terrane to the south due to the presence of the Savage Island shear zone. Thurston et al. (1991b) interpreted this structure to be responsible for juxtaposing the Island Lake “terrane” to the 3.0 Ga North Caribou terrane. However, more recent work has shown that the Island Lake greenstone belt was built on ca. 3.0 Ga crust (Stevenson and Turek 1992; Corfu and Lin 2000), as was the once subdivided Munroe Lake domain to the north (Skulski et al. 2000). As a result, the northern margin of the North Caribou terrane has been drawn in different locations by different authors (Thurston et al. 1991b; Stott 1997; Skulski et al. 2000; Beaumont-Smith et al. 2003; Percival et al. 2004). The true location of this boundary, and the importance of the Savage Island shear zone as a terrane bounding fault have never been tested.

A goal of this study was to determine where the North Caribou terrane boundary should be drawn, and to determine the affinity of the Island Lake domain. New field mapping and geochronology show the continuity of supracrustal assemblages across the Savage Island shear zone, and clearly indicates that this structure is not a regionally important feature that juxtaposed geologically distinct terranes. This evidence, and the ca. 3.0 Ga Nd model ages of Stevenson and Turek (1991) on either side of the shear zone leads to the conclusion that the old crustal source in the Island Lake greenstone belt is in fact the North Caribou terrane.

In the once subdivided Munro Lake domain to the north, U-Pb ages of  $2855 \pm 5$  Ma and  $2848 \pm 7$  Ma and ca. 3.0 Ga Nd model ages were reported for tonalite gneisses by Skulski et al. (2000). These are similar to ages of volcanism and plutonism in the Jubilee assemblage, and have led to the Munro Lake domain now being considered as part of the Island Lake domain (Stott 2009). A rifted margin sequence at Ponask Lake in the once subdivided Munro Lake domain is not yet directly dated, but its

detrital zircons gave a uniform age of 2865 Ma, while a porphyry intruded into basalts gave  $2857 \pm 2$  Ma (D. W. Davis and M. Moore, Geochronology in the western Superior Province, unpublished report, Royal Ontario Museum 1991, with interpretations by Skulski et al. 2000).

The Oxford-Stull domain consists of ca. 2.84 Ga oceanic (Syme et al. 1999, Corkery et al. 2000) volcanic rocks, which show local Nd inheritance and contains detrital zircons as old as 2.94 Ga in a sedimentary group that is unconformable on the volcanic rocks (Stott, pers comm. 2006). These ages are close, although not identical, to the age of the Jubilee assemblage in the Island Lake greenstone belt. North of this domain, no other events of similar ages or geological environment are found, with the exception of an age of  $2846 \pm 5$  Ma measured for a granitoid pluton in the Northern Superior superterrane (Skulski et al. 2000). This has a Nd mantle extraction age of 3.57 Ga (op. cit) and therefore formed by melting of much older crust than that beneath the Island Lake domain or North Caribou terranes.

Volcanic rocks similar in age to those at Island Lake can also be found in areas to the south of Island Lake. The most striking age correlations are with volcanic sequences in the Red Lake greenstone belt in the Uchi domain on the southern margin of the North Caribou terrane (Figure 2.9, Red Lake ages summarized by Sanborn-Barrie et al. 2001). The Red Lake belt is dominated by 2.99-2.92 Ga volcanics of the Balmer and Ball assemblages (Corfu and Wallace 1986; Corfu and Andrews 1987). The Balmer assemblage is disconformably overlain by a thin sequence of intermediate volcanoclastic rocks and overlying sediments called the Bruce Channel assemblage, which gave two identical ages of 2894 Ma for felsic tuffs (Corfu and Wallace 1986; Corfu and Andrews 1987). These are close to the age from the Whiteway assemblage. The Trout Bay assemblage is in tectonic contact with the Ball assemblage. It contains a lower sequence of basalt overlain by clastic, intermediate volcanic rocks and chert-magnetite iron formation. Zircon from an intermediate tuff gave an age of

2853 ± 1 Ma (Sanborn-Barrie et al. 2001). Both the age and general stratigraphy are similar to the Jubilee assemblage. The calc-alkalic McNeely volcanic sequence of the Confederation Lake assemblage lies with an angular unconformity over the Balmer assemblage and gives ages of 2745-2742 Ma, similar to the Loonfoot assemblage.

This continuity is also supported by ages of small greenstone belts in the Berens River subprovince (the area now termed the North Caribou terrane core), situated in the middle of the North Caribou terrane (Corfu et al. 1998; Sanborn-Barrie et al. 2001). The Favourable Lake, Hornby Lake and McInnes Lake belts are the largest of a series of north-south trending greenstone slivers extending northward from the Red Lake belt (Figure 2.1). Felsic volcanics from the Hornby Lake belt gave an age of 2901 ± 2 Ma (Corfu et al. 1998), close to ages from the Whiteway and Bruce Channel assemblages, while three volcanic units from the McInnes Lake belt gave ages ranging from 2974 Ma to 2928 Ma (Corfu et al. 1998), a range similar to that of the Balmer and Ball assemblages at Red Lake. A felsic tuff from the Favourable Lake belt gave an age of 2858 ± 5/-4 Ma (Corfu and Ayers 1991), an almost identical age to the Jubilee and Trout Bay assemblages.

The similarity of ages for all three periods of magmatism in the Island Lake belt with greenstone belts to the south suggests that the region from Red Lake to Island Lake may have acted as a continuous crustal block over distances of at least 400 km, a scenario previously proposed by Corfu et al. (1998) and Sanborn-Barrie et al. (2001). The two new volcanic ages of 2897 Ma and 2744 Ma reported here extend the duration of this continuity to at least ca. 200 m.y., and provide evidence for continuity at times younger than those proposed by other workers. The age correlations among all these belts suggest the existence of a regionally important and paraconformable volcanic “megasequence” (Figure 2.9) (Corfu et al. 1998; Sanborn-Barrie et al. 2001; this study). The term “megasequence” is used here to mean a volcanic package that is continuous, volumetrically large, and

includes more than one assemblage. The Red Lake belt apparently preserves all of the volcanic episodes of this megasequence, whereas the Hornby Lake and McInnes Lake belts contain remnants of the lower volcanic units, and the Island Lake greenstone belt, remnants of the upper volcanic units.

The distribution of this volcanic megasequence, as well as the evidence presented above, shows a clear commonality across the entire width of the North Caribou terrane and into the areas originally differentiated as the Munro Lake terrane and the Island Lake terrane (now the Island Lake domain), and possibly as far north as the Oxford-Stull domain (Percival et al. 2006). The North Caribou terrane is now used to describe all areas in the northwestern Superior Province that show evidence of reworked ca. 3.0 Ga Mesoarchean crust. This would make the North Caribou terrane a continuous reworked crustal block that extends from at least the Gods Lake Narrows-Stull Lake-Wunnummin Lake fault zone (which separates the Oxford-Stull domain from the Island Lake domain), to possibly as far north as the North Kenyon Fault (which separates the Northern Superior superterrane from the Oxford-Stull) domain over 400 km southward (Percival et al. 2006). The crustal block is divided into 3 components, a northern margin which consists of the Island Lake domain and possibly the Oxford-Stull domain, a core region occupies the area originally defined by Thruston et al. (1991) as the North Caribou terrane, and the southern margin which consists of the Uchi domain (Figure 2.1; Stott 2009). The southern boundary of this terrane is proposed to be the southern boundary of the Red Lake greenstone belt. It may extend as far south as the Sydney Lake-St. Joseph Fault, which separates the Uchi domain and English River subprovince (Figure 2.1; Thurston et al. 1991b; Stott 1997; Percival et al. 2004 and references therein).

The Berens subprovince (the area now termed the North Caribou terrane core) greenstone belts are now engulfed by younger 2750-2680 Ma granitoid plutons. These plutons extensively reworked the lower crust in what is interpreted to be an Andean-type margin developed during Neoproterozoic

subduction of oceanic crust along the southern margin of the North Caribou terrane (Stott and Corfu 1991; Corfu and Stone 1998; Sanborn-Barrie et al. 2001). This interpretation is supported by seismic data (White et al. 2003), where north dipping seismic reflectors are interpreted to be a product of northward subduction of parautochthonous terrane(s) that have subsequently been telescoped (Percival et al. 2004). The age correlations presented above may indicate that similar tectonic processes were occurring on the north margin of the North Caribou terrane. South dipping seismic reflectors are observed near the north margin of the North Caribou terrane (White et al. 2003), as well as north vergent structures such as the Savage Island shear zone in this area (Lin et al. 1998) and the Gods Lake Narrows shear zone in the OSD (Lin et al. 2006). These data, along with the geometry and kinematics of shear zones led Lin et al. (2006) to suggest the existence of a southward dipping subduction zone on this margin. The true nature of the northern margin of the North Caribou terrane and the Island Lake greenstone belt can only be decided after more extensive geochemical, isotopic and structural study. In any case, geochronology supports the notion that the Superior Province was assembled by accretion of large independent crustal blocks, even though the individual histories of these blocks involved extended periods of autochthonous greenstone development.

## **2.5 Conclusions**

The Island Lake greenstone belt experienced a long and complex geological history. Three distinct ages of volcanism are observed at ca. 2897 Ma, 2852 Ma, and 2744 Ma. These ages occur in what was previously considered as one supracrustal group, the Hayes River Group. This study and others, which are also showing new chronological subdivisions, indicate that the term “Hayes River Group” should no longer be used for all volcanic rocks in the northwestern Superior Province. The youngest supracrustal group in the belt, the Island Lake Group, unconformably overlies the 2744 Ma old Bella Lake Pluton. Sedimentation in the ILG is bracketed between 2712 Ma and 2699 Ma, similar to the

ages of sedimentation found in other late sedimentary packages in the northwestern Superior Province. These groups in the northwestern Superior Province are analogous to the late orogenic Timiskaming groups located in the southern Superior Province.

The Savage Island shear zone, a regional fault structure that transects the Island Lake greenstone belt, is not a terrane-bounding feature as correlative supracrustal assemblages are observed on both sides of it. Igneous rocks of all ages within the Island Lake greenstone belt were influenced by Mesoarchean crust whose source is likely to have been the North Caribou terrane. The volcanic sequences at Island Lake can be correlated on the basis of age with rocks in the adjacent Munro Lake and North Caribou terranes, and possibly in the Oxford-Stull domain, as well. Similar ages of volcanism are also found in the Favourable Lake, McInnes Lake, Hornby Lake, and in particular the Red Lake greenstone belts, suggesting the presence of a large volcanic megasequence. Based on these data, the Island Lake domain, and North Caribou terranes, and possibly the Oxford-Stull domain, are suggested to be part of a larger reworked Mesoarchean crustal block.

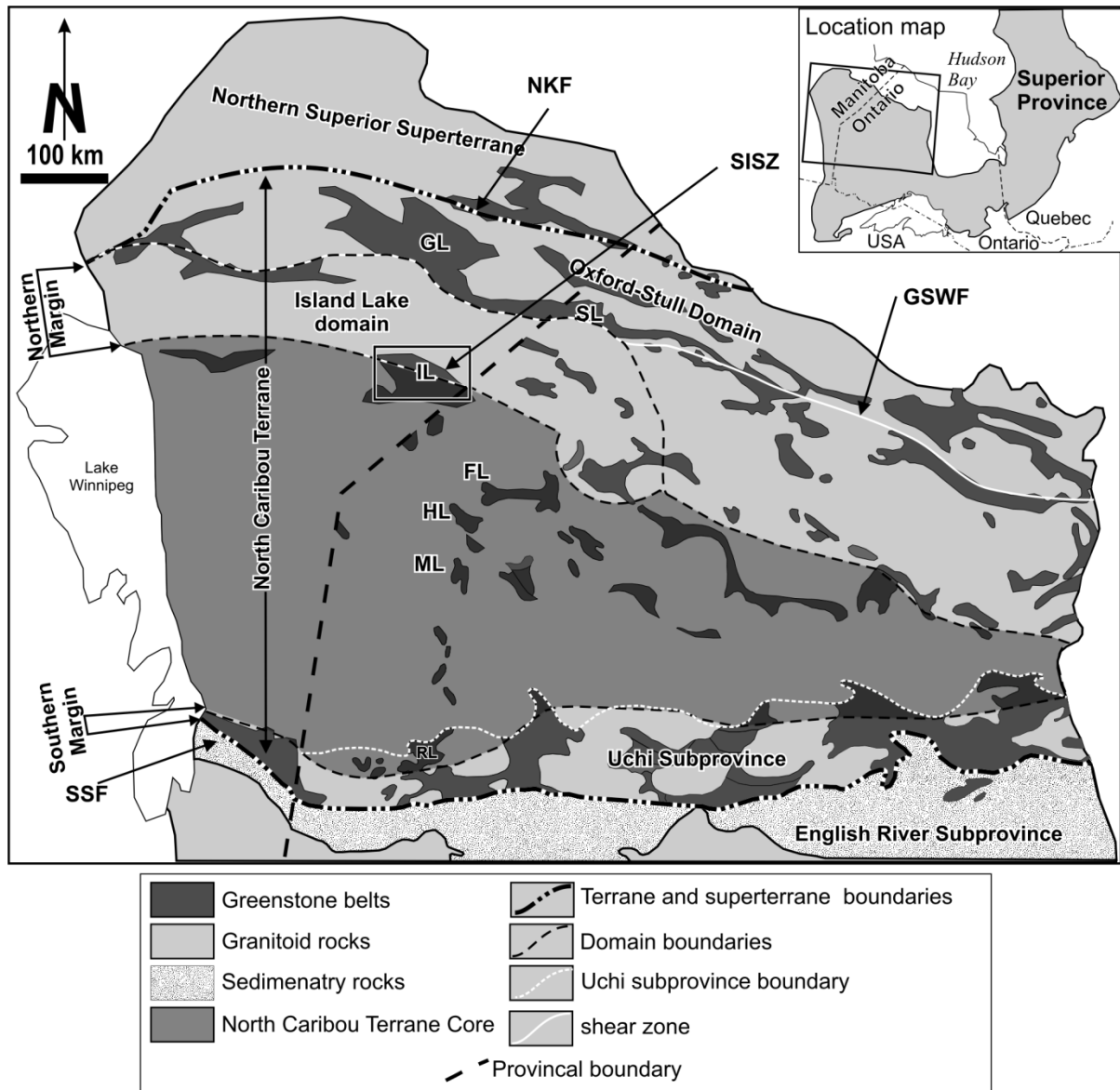
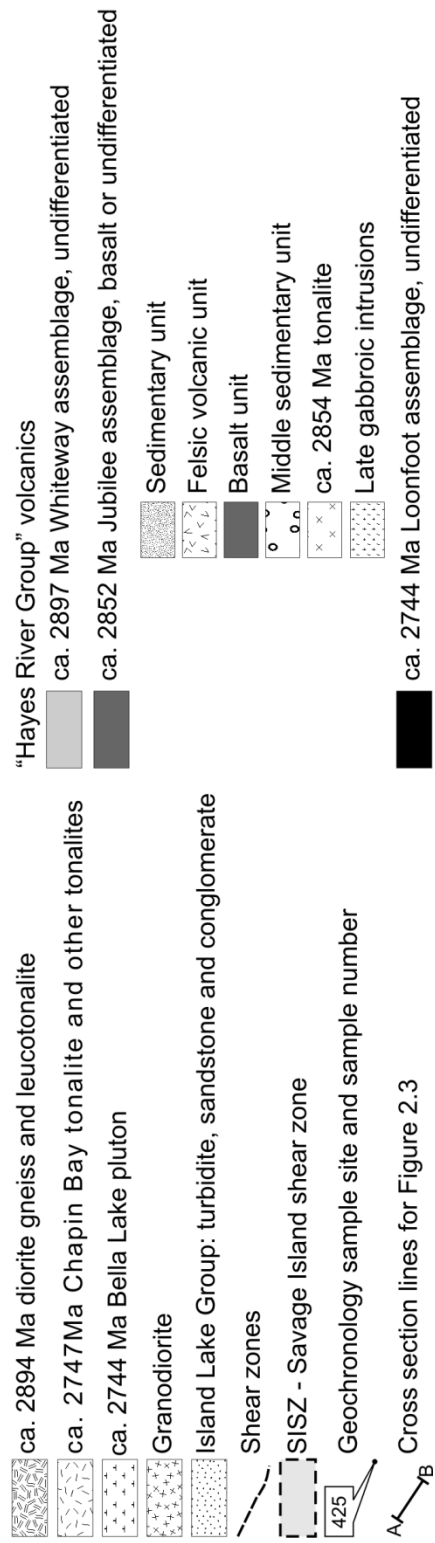


**Figure 2.1** Regional terrane map of the northwestern Superior Province. The proposed extent of the North Caribou terrane, its northern margin, southern margin and core are shown (Percival et al. 2006; Stott 2009; this study). Locations of the greenstone belts cited in text and relevant terrane boundaries are shown. Boxed area is the location of the map shown in Figure 2.2. Abbreviations for faults: NKF, North Kenyon fault; GSWF, Gods Lake Narrows-Stull Lake-Wunnummin Lake fault zone; SISZ, Savage Island shear zone; SSF, Sydney Lake, St. Joseph fault. Abbreviations for greenstone belts: IL, Island Lake; RL, Red Lake; GL, Gods Lake; SL, Stull-Edmund Lake; HL, Hornby Lake; ML, McInnes Lake; FL, Favourable Lake. Modified from Thurston et al. (1991); Stott (1997); Percival et al. (2004); Parks et al. (2006); and Stott (2009).



**Legend for Figure 2.2**

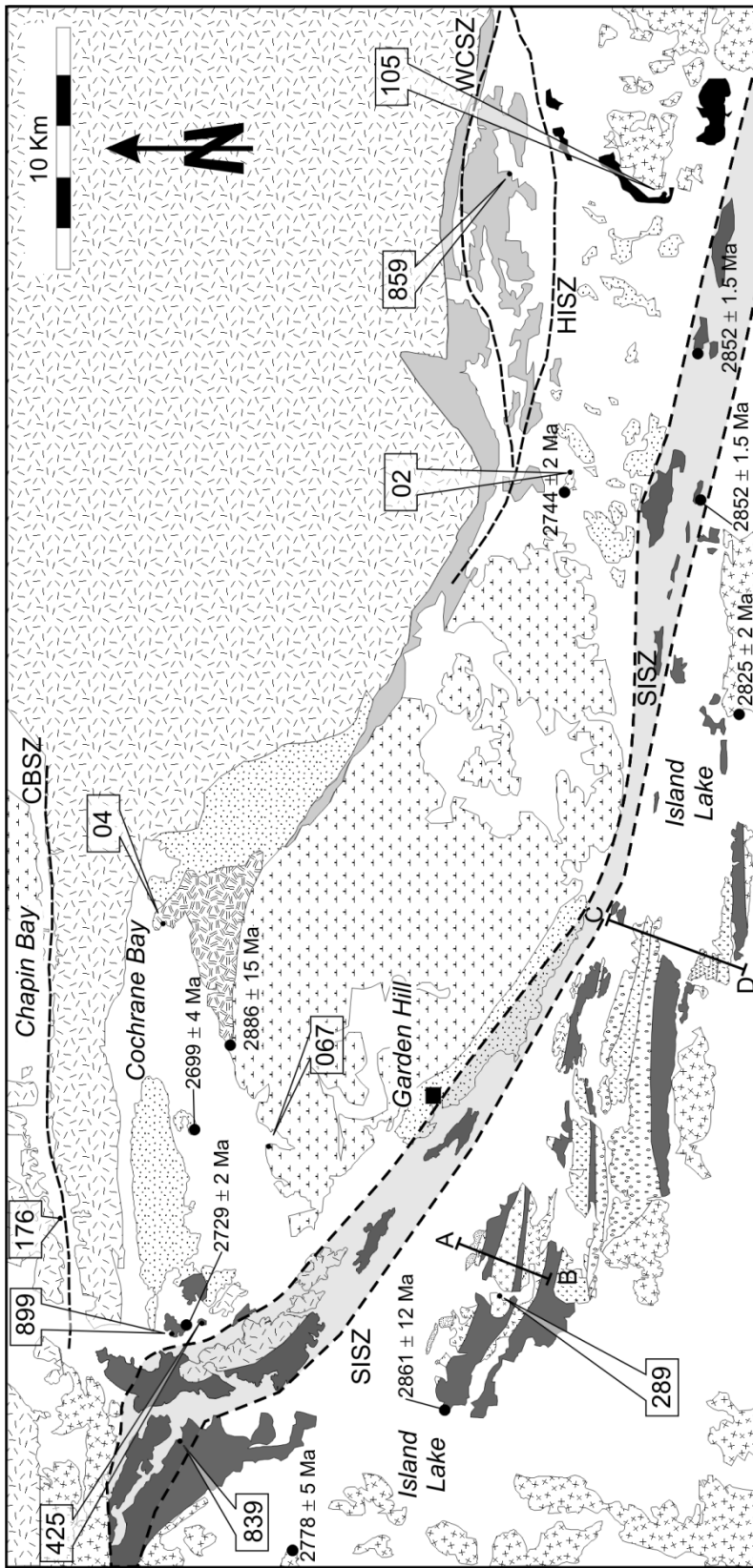


**Figure 2.2** Simplified geology of the Island Lake greenstone belt. Locations of samples analyzed in this study are shown. Abbreviations used for shear zones: HISZ, Harper Island shear zone; WCSZ, Whiteway Channel shear zone; CBSZ, Chapin Bay shear zone. U-Pb ages from Turek et al. (1986), Stevenson and Turek (1992), and Corfu and Lin (2000). Map modified from Lin et al. (1998).

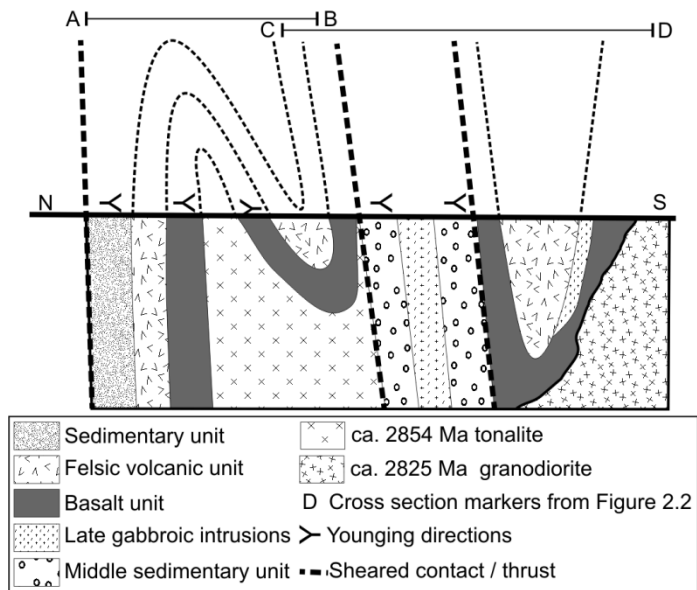


**Figure 2.3** Composite schematic cross section showing the fold geometry and stratigraphy of the Jubilee assemblage, south of the Garden Hill area. See text for more details.

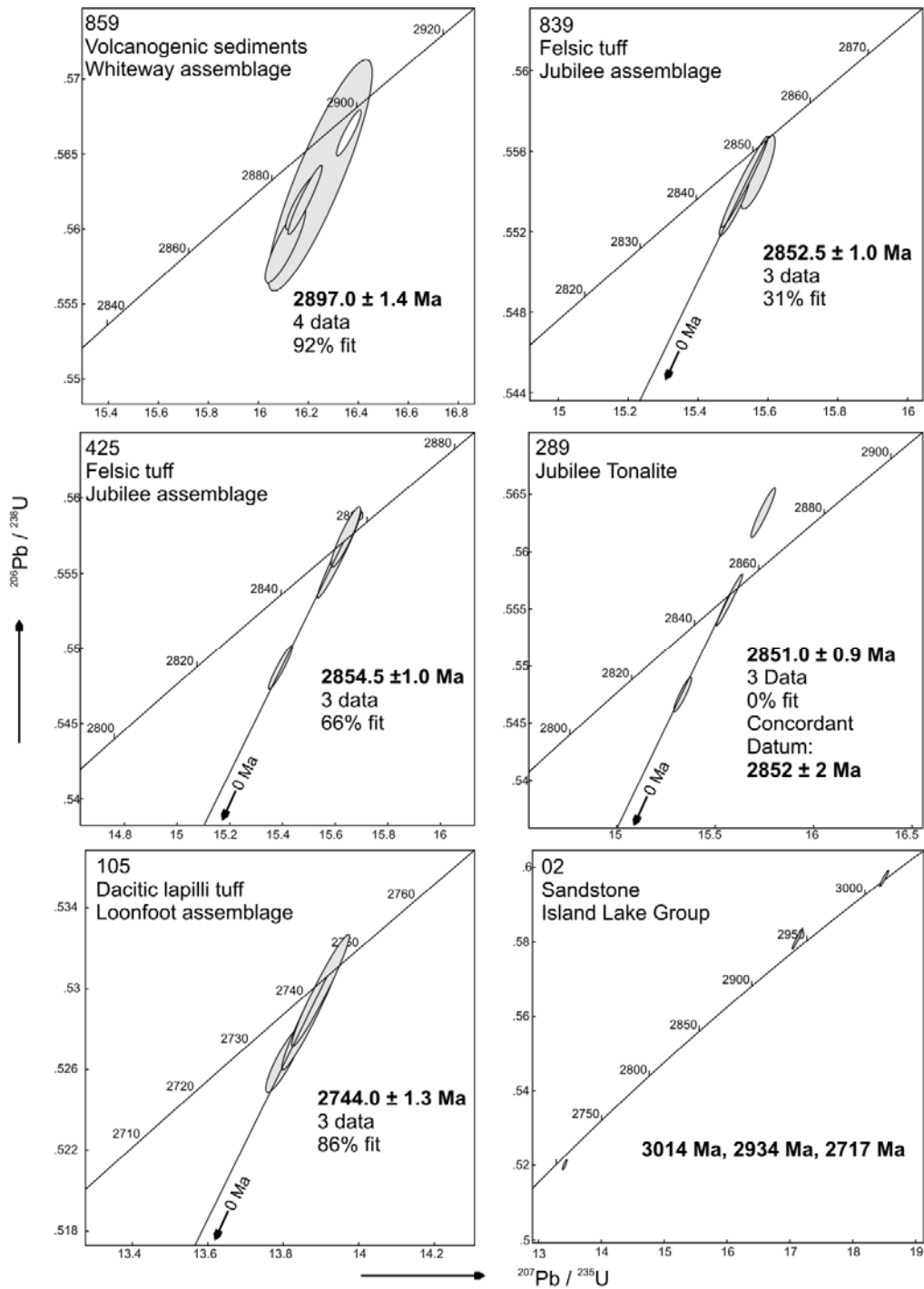


**Figure 2.4** Concordia diagrams showing zircon data for samples in the Island Lake greenstone belt. The unshaded datum for sample 859 is not included in the average  $^{207}\text{Pb}/^{206}\text{Pb}$  age calculation.



**Figure 2.5** Photograph of the dacitic lapilli tuff in the Loonfoot assemblage. The dacite is interlayered with the basalt and in places it contains rounded clasts of felsic volcanic material, as well as locally derived basalt detritus. Camera lens for scale.

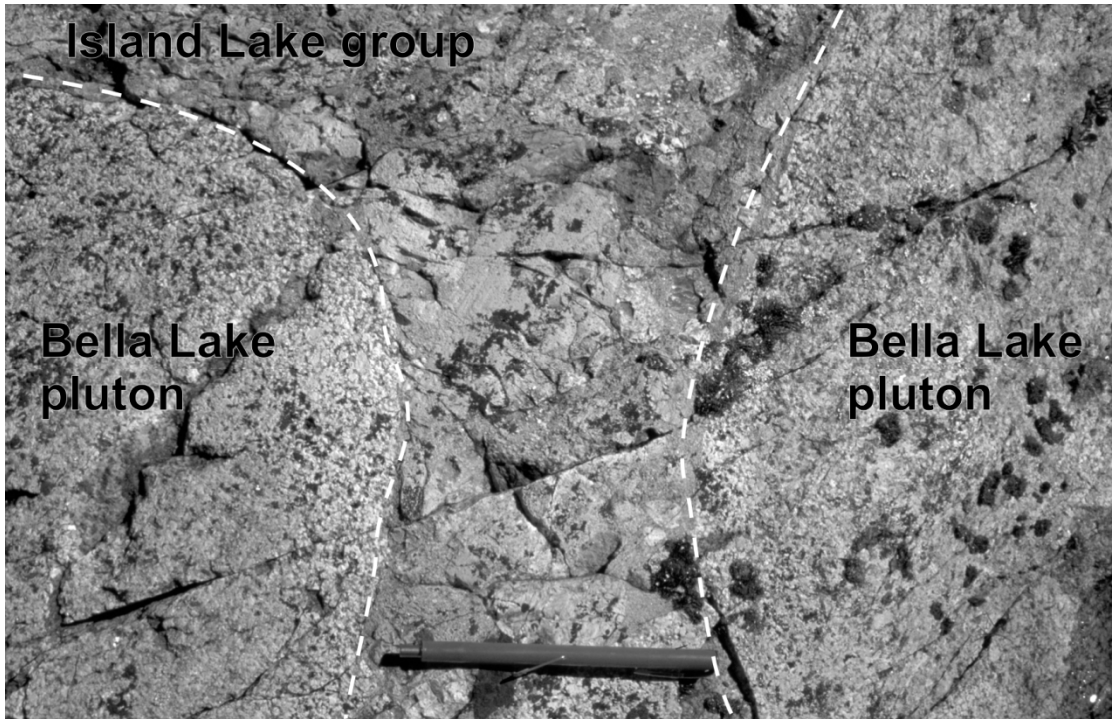


**Figure 2.6** Photograph of the contact between the Bella Lake pluton and the Island Lake group (dashed lines). Locally derived clasts of the Bella Lake pluton infill paleo-topographic depressions on the pluton surface. Pen for scale

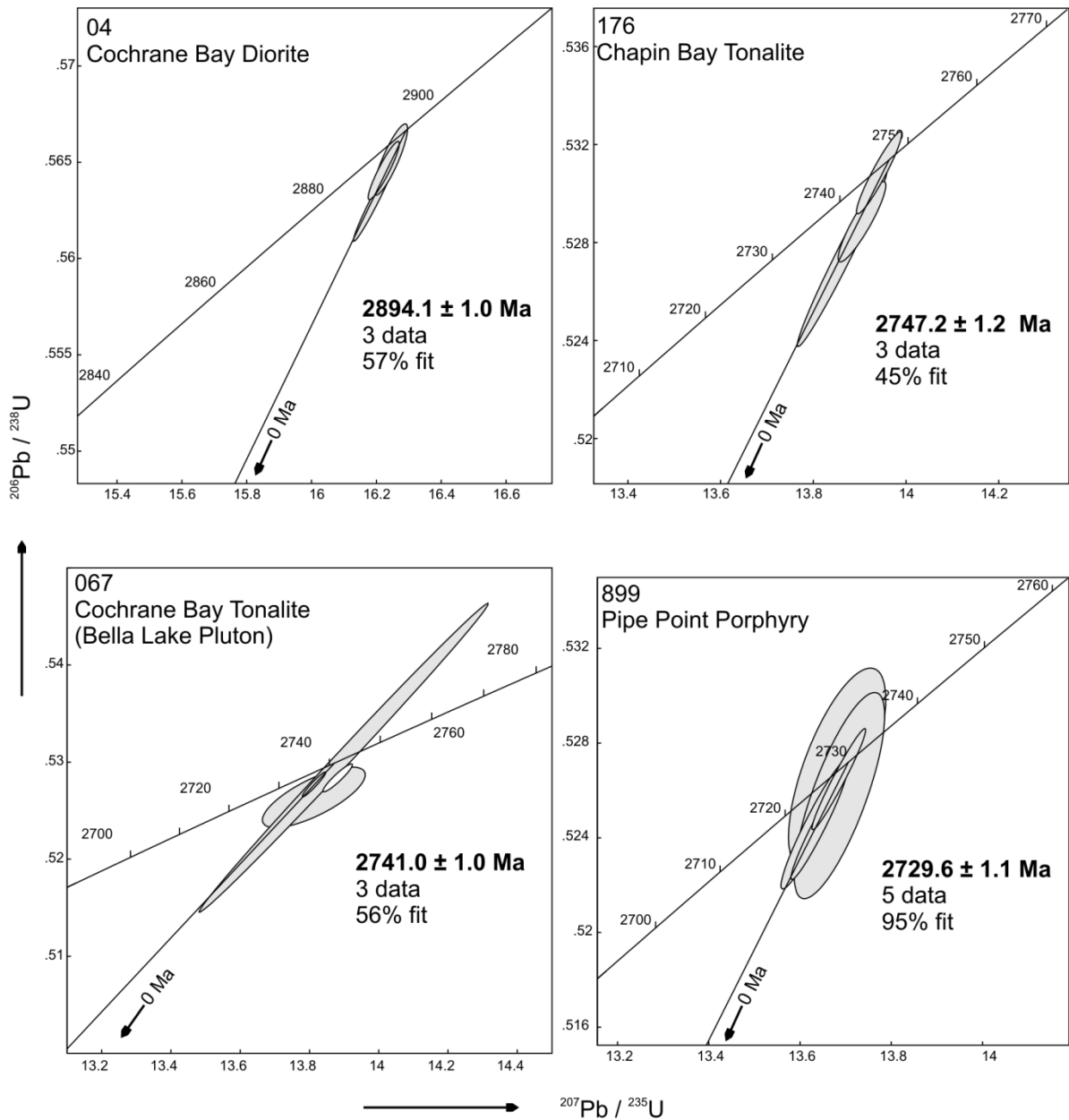


**Figure 2.7** Concordia diagrams showing zircon data for samples from plutonic rocks in the Island Lake greenstone belt. The unshaded datum for sample 067 is not included in the average  $^{207}\text{Pb}/^{206}\text{Pb}$  age calculation.

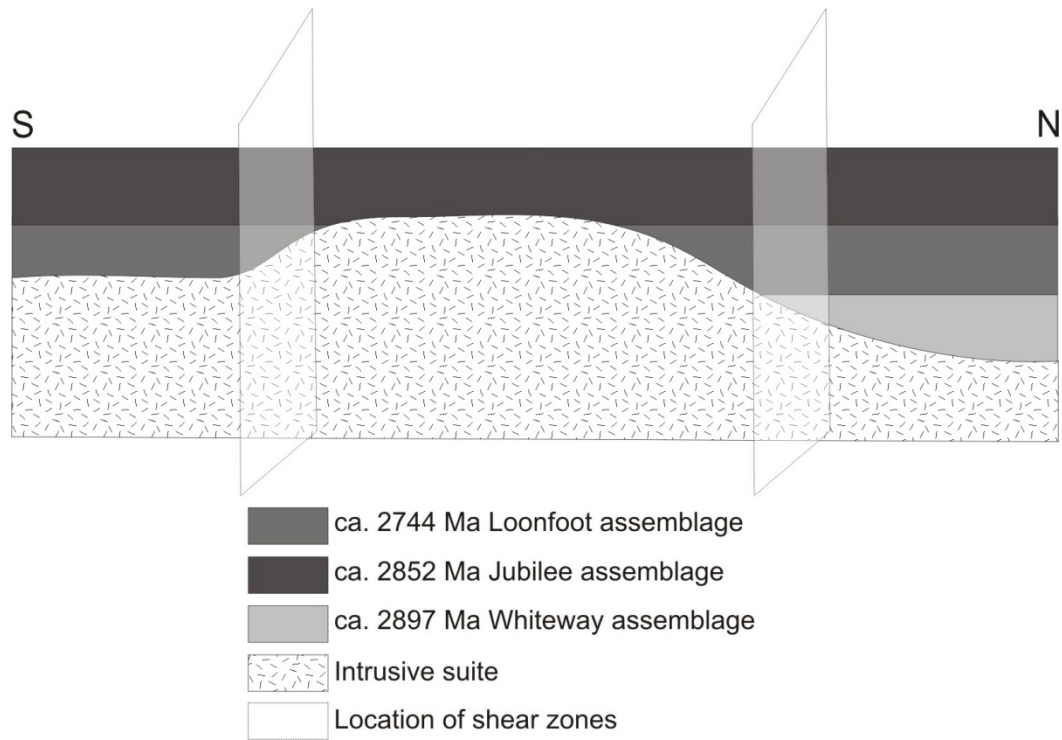


**Figure 2 8.** Proposed original stratigraphy of the volcanic assemblages and intrusive rocks in the Island Lake greenstone belt. The uneven surface of the intrusive suite accounts for the contact relationships observed in the Island Lake greenstone belt.

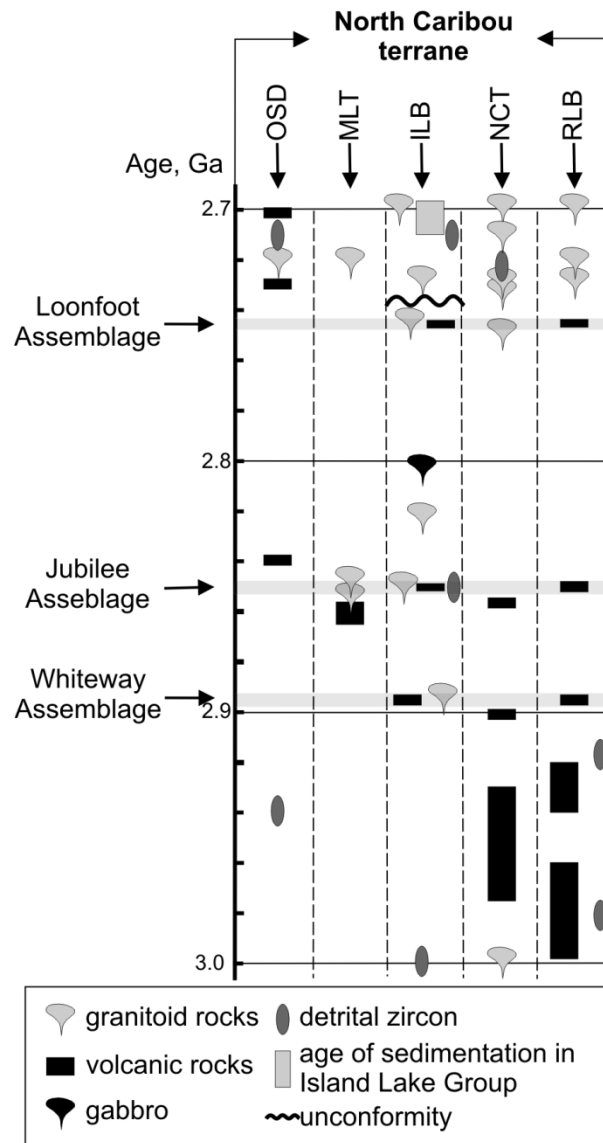


**Figure 2.9** Timeline showing age relationships of volcanic, plutonic and sedimentary rocks in the Island Lake greenstone belt, as well as other relevant volcanic and plutonic ages in the northwestern and western Superior Province. See text for discussion. Abbreviations: OSD, Oxford Stull domain; MLT, Munro Lake terrane; ILB, Island Lake greenstone belt; NCT, North Caribou terrane; RLB, Red Lake greenstone belt. Ages from Corfu and Ayres (1991), Corfu et al. (1998) and references there in, Sanborn-Barrie et al. (2000), Skulski et al. (2000), Lin et al. (2006) and references there in.

**Table 2-1 U-Pb data**

Sample Description	Wt. (mg)	U (ppm)	Th/U	PbCom (pg)	<sup>207</sup> Pb / <sup>204</sup> Pb	<sup>206</sup> Pb / <sup>238</sup> U	2 sig	<sup>207</sup> Pb / <sup>235</sup> U	2 sig	Age (Ma)	2 sig	Disc. %	Error Corr.	Lab No.
<b>859: Volcanogenic sediments in the Whiteway Assemblage (UTM coordinates: 5966294N, 424849E)</b>														
1 Ab zr, pale brn	0.002	61	0.46	2.81	342.1	0.5618	0.0018	16.173	0.063	2896.2	2.9	1.0	0.8881	dwd3693
1 Ab zr, eq, pale brn	0.001	133	0.50	0.72	1398	0.5619	0.0023	16.187	0.068	2897.1	2.1	1.0	0.9501	dwd3695
1 Ab zr	0.002	58	0.49	2.70	341.7	0.5636	0.0077	16.247	0.209	2898.4	10.5	0.7	0.8832	dwd3694
1 Ab zr, md, inc, brn	0.0007	127	0.58	0.82	834.2	0.5664	0.0015	16.362	0.049	2901.7	2.0	0.4	0.9155	dwd3921
1 Ab zr, md, inc, brn	0.0005	70	0.60	0.96	289.4	0.5590	0.0026	16.108	0.081	2897.8	4.2	1.5	0.8608	dwd3922
<b>839: Felsic tuff in the Jubilee Assemblage (UTM coordinates: 5978878N, 379818E)</b>														
1 Ab zr, incl, brn	0.008	55	0.47	0.42	7587	0.5550	0.0018	15.572	0.049	2854.5	3.0	0.4	0.8346	dwd3564
1 Ab zr, incl, brn	0.004	58	0.50	0.54	3110	0.5532	0.0014	15.503	0.043	2852.5	1.7	0.6	0.9295	dwd3565
1 Ab zr, incl, brn	0.002	72	0.46	0.46	2265	0.5545	0.0023	15.533	0.067	2851.9	1.5	0.4	0.9773	dwd3566
<b>425: Felsic tuff in the Jubilee Assemblage (UTM coordinates: 5977554N, 383881E)</b>														
1 Ab zr, eq, incl, brn	0.002	183	0.43	1.57	1686	0.5487	0.0015	15.392	0.045	2854.1	1.6	1.5	0.9438	dwd4335
1 Ab zr, incl	0.002	175	0.48	1.22	2095	0.5563	0.0029	15.616	0.083	2855.3	2.0	0.2	0.9723	dwd4336
1 Ab zr, incl	0.002	201	0.44	1.19	2473	0.5574	0.0020	15.641	0.056	2854.5	2.4	-0.1	0.9136	dwd4337
<b>289: Jubilee Tonalite (UTM coordinates: 5967142N, 385602E)</b>														
1 Ab zr, eq, brn	0.001	260	0.51	0.71	2649	0.5558	0.0023	15.573	0.067	2852.2	1.5	0.1	0.9765	dwd4332
1 Ab zr, brn	0.001	198	0.50	0.84	1688	0.5475	0.0015	15.335	0.045	2851.7	1.9	1.6	0.9175	dwd4333
1 Ab zr, brn	0.0008	185	0.49	0.49	2212	0.5634	0.0022	15.744	0.062	2847.9	2.2	-1.4	0.9426	dwd4334
<b>105: Extrusive felsic volcanic rock in the Loonfoot Assemblage (UTM coordinates: 5961134N, 425563E)</b>														
1 Ab zr, eq	0.0019	89	0.74	2.57	439.1	0.5265	0.0016	13.803	0.050	2743.4	2.7	0.7	0.8909	dwd3876
1 Ab zr, euh	0.0007	134	0.88	0.89	693.0	0.5289	0.0029	13.874	0.078	2744.3	2.5	0.3	0.9629	dwd3878

1 Ab zr	0.001	135	0.75	1.62	551.5	0.5299	0.0028	13.899	0.077	2744.1	2.3	0.1	0.9664	dwd3877
<u>Sample</u> Description	<u>Wt.</u> (mg)	<u>U</u> (ppm)	<u>Th/U</u>	<u>Pb/Com</u> (pg)	$\frac{^{207}\text{Pb}}{^{204}\text{Pb}}$	$\frac{^{206}\text{Pb}}{^{238}\text{U}}$	$\frac{^{207}\text{Pb}}{^{235}\text{U}}$	<u>2 sig</u>	$\frac{^{207}\text{Pb}}{^{206}\text{Pb}}$	$\frac{^{207}\text{Pb}}{^{206}\text{Pb}}$	<u>2 sig</u>	<u>Disc.</u> %	<u>Error</u> Coeff.	<u>Lab No.</u>
<b>02: Sandstone in the Island Lake Group (UTM coordinates: 5965440N, 414401E)</b>														
1 Ab zr, incl, pnk	0.008	26	0.97	0.78	1681	0.5201	0.0013	13.419	0.037	2716.9	2.2	0.8	0.8800	dwd3507
1 Ab zr, incl, pnk	0.003	25	0.65	0.37	1617	0.5809	0.0028	17.121	0.084	2934.3	2.0	-0.8	0.9670	dwd3508
1 Ab zr, incl, brn	0.003	19	0.40	0.37	1315	0.5971	0.0022	18.500	0.072	3014.8	1.8	-0.1	0.9586	dwd3509
<b>04: Chapin Bay Diorite Gneiss (UTM coordinates: 5979790N, 398318E)</b>														
1 Ab zr, pale brn	0.003	83	0.55	0.75	2528	0.5630	0.0021	16.194	0.065	2894.8	1.4	0.7	0.9767	dwd3696
1 ab zr, eq, pale brn	0.001	118	0.56	0.70	1276	0.5646	0.0015	16.223	0.048	2893.2	1.8	0.3	0.9241	dwd3698
1 ab zr, pale brn	0.0035	103	0.55	1.22	2258	0.5651	0.0019	16.244	0.053	2893.6	2.8	0.2	0.8643	dwd4046
<b>176: Chapin Bay Tonalite (Bella Lake Pluton) (UTM coordinates: 5982855N, 387261E)</b>														
1 Ab zr	0.0013	204	0.90	4.48	399.0	0.5288	0.0016	13.905	0.052	2748.2	2.6	0.5	0.9043	dwd3882
1 Ab zr	0.001	126	0.77	0.91	905.9	0.5274	0.0036	13.862	0.097	2747.7	2.2	0.8	0.9816	dwd3883
1 Ab zr	0.0005	210	0.62	0.93	752.3	0.5308	0.0017	13.942	0.049	2746.3	1.9	0.1	0.9428	dwd3884
<b>067: Cochrane Bay Tonalite (UTM coordinates: 5975736N, 390580E)</b>														
+1 Ab zr, eq, incl, light brn	0.001	281	0.52	1.94	953.3	0.5284	0.0014	13.881	0.042	2746.8	1.8	0.5	0.9353	dwd4376
1 Ab zr, eq, light brn	0.001	203	0.80	0.91	1462	0.5304	0.0159	13.899	0.418	2742.5	3.6	0.0	0.9974	dwd4377
1 Ab zr, eq, light brn	0.0008	174	0.62	12.53	86.78	0.5264	0.0031	13.813	0.149	2744.9	12.2	0.8	0.7498	dwd4378
*1 Ab zr, eq, incl, brn	0.008	88	0.73	4.97	900.8	0.5277	0.0146	13.813	0.015	2740.8	0.4	0.4	0.9585	JP01-067-A
*+1 Ab zr, eq, incl, brn	0.002	60	0.37	5.74	66.66	0.1973	0.1537	5.203	0.396	2753.3	50.4	63.0	0.7302	JP01-067-B

<u>Sample</u> Description	<u>Wt.</u> (mg)	<u>U</u> (ppm)	<u>Th/U</u>	<u>PbCom</u> (pg)	$\frac{207\text{Pb}}{204\text{Pb}}$	$\frac{206\text{Pb}}{238\text{U}}$	$\frac{2\text{ sig}}$	$\frac{207\text{Pb}}{235\text{U}}$	$\frac{2\text{ sig}}$	$\frac{207\text{Pb}}{206\text{Pb}}$	$\frac{2\text{ sig}}$	$\frac{2}{\text{sig}}$	<u>Disc.</u> %	<u>Error</u> <u>Coef.</u>	<u>Lab No.</u>
<b>899: Pipe Point Porphyry (UTM coordinates: 5979444N, 383615E)</b>															
1 Ab zr, eq	0.002	44	0.14	2.78	216.9	0.5269	0.0042	13.681	0.107	2727.5	10.3	0.0	0.0	0.6852	dwd3690
1 Ab zr	0.002	71	0.08	4.45	219.6	0.5277	0.0046	13.755	0.123	2733.9	9.2	0.1	0.1	0.7959	dwd3691
1 Ab zr, pnk	0.0028	39	0.14	0.44	1594	0.5245	0.0022	13.640	0.060	2730.2	2.0	0.5	0.5	0.9626	dwd3918
1 Ab zr, pnk	0.002	38	0.11	1.07	464.3	0.5246	0.0028	13.634	0.076	2729.0	2.9	0.5	0.5	0.9487	dwd3919
1 Ab zr, rnd, pnk	0.0029	48	0.15	0.95	956.3	0.5265	0.0021	13.685	0.059	2729.3	1.7	0.1	0.1	0.9701	dwd3920

FOOTNOTES TO TABLE

zr - zircon grain; Ab - abraded; eq - equant; euh - euhedral; rnd - rounded; incl - inclusions; brn - brownish, pnk - pink

Pbcom is total measured common Pb assuming the isotopic composition of laboratory blank:

206/204 - 18.221; 207/204 - 15.612; 208/204 - 39.360 (1 sigma errors of 2%).

Th/U calculated from radiogenic 208Pb/206Pb ratio and 207Pb/206Pb age assuming concordance.

Disc - per cent discordance for the given 207Pb/206Pb age

Uranium decay constants are from Jaffey et al. (1971).

Fractions with \* were analyzed at the Radiogenic Isotope Facility, University of Alberta

+ Analysis not used in age determination

## Chapter 3

# Meso – and Neoproterozoic evolution of the Northwestern Superior Province: evidence from litho-geochemistry and Nd isotope data of volcanic and plutonic rocks and U-Pb dyke ages from the Island Lake greenstone belt

### 3.1 Introduction

The Superior Province covers 1,572,000 km<sup>2</sup> (Goodwin 1991) and is the largest piece of preserved Archean crust on Earth. Work here in the past few decades has involved using a multi-disciplinary approach including field mapping, U-Pb geochronology, Nd isotopes, litho-geochemistry and structural studies to refine the subdivisions of rocks within the Superior Province, as well as to generate regional tectonic models for the Superior Province. Recent models for the generation of greenstone belts and the tectonic evolution of different regions in the Superior Province have included step-wise northward dipping subduction-based models for the western and southern part of the Superior Province (Percival et al. 2006 and references within), and models that are driven by catalytic crustal delamination for the north eastern part of the Superior Province in Quebec (Bedard 2006).

The Superior Province is divided into distinct superterrane, terrane and domains that all have different geological histories (Figure 3.1, Card and Ciesielski 1986; Card 1990; Stott 1997; Percival et al. 2006; Stott 2009). The granite-greenstone elements in the northwestern Superior Province consist of the North Caribou terrane, which is composed of a 3.0 Ga core region, and a northern and southern margin (Figure 3.1). Magmatism in greenstone belts in these areas include both Mesoarchean and Neoproterozoic events, and most volcanic rocks show geochemical and isotopic evidence of recycling of

an older crustal component (Thurston and Chivers 1990; Stott 1997; Percival et al. 2006; Parks et al. 2006 and references within).

The southern part of the Superior Province contains the Abitibi greenstone belt (Figure 3.1), which is the most continuous and arguably the most studied belt in the Superior Province. In contrast to the northwestern Superior Province, volcanism in the Abitibi is restricted to juvenile oceanic Neoproterozoic events (2760-2670 Ma, Stott 1997; Ayer et al 2002), and is interpreted to represent island arc or oceanic plateau sequences (Stott 1997; Ayer et al 2002). Tectonic amalgamation south of the North Caribou terrane core region occurred via a series of northward dipping, southward younging, subduction zones that accreted the domains, terranes and basins to the south of the North Caribou terrane; a processes that ended with the accretion of the Wawa-Abitibi terrane and the Minnesota River Valley (Thurston et al. 1991; Stott 1997; Percival et al. 2006 and references within).

In contrast, detailed models for the generation of volcanic assemblages and tectonic amalgamation along the northern margin of the North Caribou terrane are not as well documented. It is not clear if the northern margin is also related to a northward dipping subduction zone and is potentially the first and oldest event in this step-wise model (Stott 1997), or if it is related to subduction with opposite (southward) polarity as suggested by recent work (Lin et al. 2006; Parks et al. 2006; Percival et al. 2006).

The Island Lake greenstone belt is located on the northern margin of the North Caribou terrane, and as such is well situated to investigate the tectonic affinity of the northern margin. Three chronologically distinct volcanic assemblages have been identified in the belt, and the contacts between the assemblages are proposed to be unconformable/autochthonous in nature (Chapter 2; Figure 2.8; Parks et al. 2006). Nd isotope studies by Stevenson and Turek (1992) suggest that the belt

has been variably influenced by an older crustal source, however the newly identified volcanic assemblages were not sampled in this previous study, and the Nd isotope data set needs to be expanded to test if an older crustal source is seen to influence all of the volcanic assemblages. This chapter investigates the geochemical and isotopic nature of packages of Mesoarchean and Neoarchean volcanic rocks, as well as the timing of deformation events in the Island Lake greenstone belt in Northern Manitoba. The lithochemical and Nd isotopic characteristics of the Mesoarchean and Neoarchean volcanic assemblages and contemporaneous plutons in the belt are examined in order to determine the geodynamic settings in which these rocks formed and to test if the contacts between them truly juxtapose autochthonous terranes. The timing of movement along two regionally important shear zones is also investigated in order to place timing constraints on deformation and tectonic amalgamation in this part of the Superior Province. These data are considered in a regional context and a tectonic setting in which these volcanic rocks were generated is proposed. Together with timing constraints from shear zones, Meso – and Neoarchean episodes of southward dipping subduction along the northern margin of the North Caribou terrane are proposed for the tectonic evolution of this part of the northwestern Superior Province.

## **3.2 Geological setting**

### **3.2.1 Regional Geology**

As discussed above, the Superior Province is divided into roughly E-W trending domains, terranes and superterranes with distinct geological and tectonic characteristics (Figure 3.1, Card and Ciesielski 1986; Card 1990; Stott 1997; Stott 2009). In the northwestern Superior Province, the terranes and domains are separated by regionally continuous fault structures and the last episode(s) of movement

on these faults, and structures that parallel them, are related to the last stages of terminal collision (the  $D_2$  structures discussed in section 3.2.3, Thurston et al. 1991). The most recent update to the subdivision of terranes in the Superior Province is that by Stott (2009; Figure 3.1). The divisions in the northwestern Superior Province (Figure 3.1) include the Northern Superior superterrane (NSS), a ca. 3.7 Ga crustal block that is bound to the south by the northern margin of the North Caribou terrane via the North Kenyon fault (Skulski et al. 2000; Percival et al. 2006). The northern margin of the North Caribou terrane consists of the Oxford-Stull domain (OSD) and the Island Lake domain (ILD). The OSD is a granite-greenstone domain of isotopically juvenile affinity (Skulski et al. 2000), however new data suggests evidence of an older crustal component (e.g. 2.92 Ga tonalities and negative  $\epsilon_{\text{Nd}}$  data of Rayner and Stott (2005)). The OSD is separated from the Island Lake domain (ILD) via the Gods Narrows-Stull -Wunnummin fault zone (GSWF, Lin et al. 2006). The ILD consists of greenstone belts of dominantly continental affinity (eg. the Island Lake greenstone belt, Stevenson and Turek. 1992; Corfu and Lin 2000; Parks et al. 2006; the Ponask Lake – Sachigo Lake greenstone belt, Skulski et al. 2000), and includes the previously recognized Munro Lake domain (Stott 2009). South of the northern margin is the core region of the North Caribou terrane, which contains the 3.0 Ga cratonic block in the centre of the North Caribou terrane (Figure 3.1, Stott 2009; Thurston et al. 1991). The Uchi domain sits on the southern margin of the North Caribou terrane (Stott 2009; Percival et al. 2006). The North Caribou terrane as a whole is the oldest stable craton onto which the Northern Superior superterrane and the southern part of the Superior Province were juxtaposed during terminal collision (Thurston 1991; Stott 1997; Percival et al. 2006).

### **3.2.2 Geology of the Island Lake greenstone belt**

The Island Lake greenstone belt is composed of volcanic, plutonic and sedimentary rocks that range in age from 2.900 to 2.699 Ga (Figure 3.2; Turek et al. 1986; Corfu and Lin 2000; Parks et al. 2006). The rocks in the belt are divided into three broad packages; (1) Mesoarchean and (2) Neoarchean packages of volcanic and plutonic rocks; and (3) a 2.71-2.70 Ga clastic sedimentary group. All of these rocks have been variably metamorphosed to either greenschist or lower amphibolite facies, and the prefix “meta” is implied for most of the rock names in the Island Lake greenstone belt.

The Mesoarchean package includes two episodes of volcanism and associated sedimentation and plutonism in the belt (Figure 3.2, the 2.897 Ga Whiteway assemblage and 2.852 Ga Jubilee assemblage of Parks et al. 2006), as well as a younger 2.825 Ga gneiss (Corfu and Lin 2000). The Neoarchean package includes the 2.744 Ga Loonfoot assemblage and related intrusive suite, and a suite of 2.73 Ga and 2.70 Ga volumetrically small porphyries (Turek et al. 1986; Parks et al. 2006). The lithologies of these packages are described in detail in Chapter 2, and discussed briefly below. Although not directly observed in the field, recent work (this study; Parks et al. 2006) shows that the contacts between the volcanic assemblages are most likely unconformable and are not the shear zones found in the belt as originally described by Lin et al. (1998). The third and youngest package in the belt is the sedimentary Island Lake group. It consists of fluvial-alluvial conglomerates, sandstones and turbidites that were deposited between 2.712 Ga and 2.699 Ga (described in more detail in Chapter 4, Corfu and Lin 2000; Parks et al. 2006). This group has unconformable relationships with the older volcanic assemblages and the older plutonic rocks in the belt (Parks et al. 2006; Chapter 2)

### 3.2.3 Deformation

The Island Lake greenstone belt has experienced at least two distinct episodes of deformation. The first event ( $D_1$ ) produced a foliation ( $S_1$ ) in the belt, which is most likely related to large scale folds in the volcanic and volcanogenic assemblages, and a second, younger event ( $D_2$ ), related to late movement along the shear zones in the belt and terminal collision (Figure 3.2; Figure 3.3). The older  $D_1$  event(s) in the belt is best expressed in the 2.852 Ga Jubilee assemblage, where it occurs as a set of upright tight to isoclinal folds that have an axial planar foliation ( $S_1$ ) that strikes roughly east-west and dips near vertically or steeply to the south (Chapter 2; Parks et al. 2006).

The second event ( $D_2$ ) is related to movement along the shear zones located in the belt and terminal collision in the NW Superior Province. The most prominent structure in the belt is the Savage Island shear zone (SISZ), a  $D_2$  fault structure which extends for >65 km within the belt and is observed to continue further to the east and west on regional scale maps. The SISZ is a wide, 1-3 km wide zone of intensely deformed rocks that trends east-south-east, and in the eastern part of the belt is parallel to sub-parallel to two smaller shear zones, the Harper Island and Whiteway Channel shear zones (HISZ and WCSZ respectively) (Figure 3.2; Figure 3.3). The HISZ and WCSZ are both discrete, narrow zones that are intensely deformed and are not observed to be continuous on regional scale maps (Percival et al. 2006; Stott 2009).

Detailed kinematic work on all three of these shear zones was completed by Lin et al. (1998), and the western portion of the SISZ is described in more detail in Parks et al. (2001). The rocks in the SISZ contain a well developed foliation ( $S_2$ ) that strikes east to south-east and dips steeply with lineations that plunge steeply eastward. The  $S_2$  foliation in the SISZ is seen to transpose an older  $S_1$  foliation thought to have been produced by the  $D_1$  folding events in the volcanic assemblages to the

south of the SISZ (Figure 3. 4; this study; Lin et al. 1998). Shear sense indicators show evidence for south-over-north dip slip and dextral strike slip movement (Lin et al. 1998). This shear sense is similar to other major shear zones to the north of the Island Lake greenstone belt, including the Southern Knee Lake shear zone (Lin and Jiang 2001) and the Gods Lake Narrows shear zone (Lin et al. 2006). Rocks in the Harper Island shear zone contain a well developed foliation that strikes easterly and dips steeply. Lineations plunge steeply and shear sense indicators show evidence of dextral movement on horizontal surfaces (Lin et al. 1998). The Whiteway Channel shear zone outcrops north of the HISZ. Lineations plunge steeply and shear indicators show north-over-south dip slip (Lin et al. 1998).

### **3.3 Nature of Volcanic Assemblages and contemporaneous plutonic rocks: Litho-geochemistry and Nd isotope results**

The lithological, geochemical and Nd isotopic characteristics of the Meso – and Neoproterozoic volcanic and plutonic rocks are discussed below. Geochemical analysis was performed on extrusive mafic and felsic volcanic rocks from each volcanic assemblage as well as contemporaneous plutons to help classify them and to investigate their tectonic origin. Nd isotopic analysis was completed on selected samples of mafic and felsic volcanic rocks as well as plutonic rocks that are contemporaneous with the volcanic assemblages to investigate the influence or lack of influence of an older crustal source in their origin. Below, these data are presented for each of the different ages of rocks, and then the implications of each data set are discussed. Nd model ages quoted are calculated based on the depleted mantle values of DePaolo (1981). Details of the analytical techniques are outlined in Appendix C.

### 3.3.1 Mesoarchean rocks

#### 3.3.1.1 - 2.89 Ga Whiteway assemblage and contemporaneous plutonic rocks

The volcanic rocks in this assemblage consist primarily of pillowed flows, with rare occurrences of volcanogenic sediments and gabbroic intrusions. Based on similar geochemical patterns, it is observed to outcrop on either side of the Harper Island shear zone in the eastern part of the belt. The mafic volcanics plot in the basalt field on a Zr/TiO<sub>2</sub> vs Nb/Y diagram and as tholeiites on AFM and Zr vs. Y diagrams (Figure 3.5). The basaltic tholeiites have SiO<sub>2</sub> contents ranging from 48-58 wt.%, MgO of 3-10 wt.%, Fe<sub>2</sub>O<sub>3</sub> of 9-15 wt.%, and Mg #'s of 33-63. (Table 3.1). On a multi-element diagram normalized to primitive mantle of Sun and McDonough (1989, Figure 3.6), this assemblage shows a strong enrichment in Th ((Nb/Th)<sub>PM</sub>=0.13-0.36) and light REE ((La/Sm)<sub>PM</sub>=1.3-2.6) with a flat to slightly depleted heavy REE profile ((Gd/Yb)<sub>PM</sub>=1.09-1.38). The rocks have strong negative Nb and Ta anomalies and moderately negative Ti anomalies (Figure 3.6). Two basalts have positive εNd<sup>2.89 Ga</sup> values of 0.58 & 0.86 (Table 3.2 & A.1, Figure 3.7).

This volcanic assemblage is contemporaneous with the oldest plutonic rocks in the belt, the 2.894 Ga Cochrane Bay diorite (Chapter 2; Parks et al. 2006) and 2.886 Ga Cochrane Bay leucotonalite (Turek et al. 1986). These plutons plot in the calc-alkaline field on an AFM diagram, and have SiO<sub>2</sub> contents ranging from 72 to 76 wt.%, Mg#'s of 23-32, and a on multi element diagram normalized to primitive mantle (Sun and McDonough 1989), show positive Hf and Zr, and negative Nb, Ti and Eu anomalies (Table 3.1; Figure 3.9). These rocks are strongly light REE enriched ((La/Sm)<sub>PM</sub>=4.3-5.6), have slight heavy REE fractionation ((Gd/Yb)<sub>PM</sub>=1.11-1.19), and show moderate overall REE fractionation ((La/Yb)<sub>PM</sub>=6-8) (Table 3.1; Figure 3.9). Both of the old plutons have T<sub>DM</sub> ages over 3.1 Ga, and εNd<sup>2.89 Ga</sup> values of -0.63 & 0.39 (Table 3.2 & A.1, Figure 3.7).

### 3.3.1.2 - 2.85 Ga Jubilee assemblage and contemporaneous plutonic rocks

The supracrustal rocks in the Jubilee assemblage include units of volcanogenic sediments, felsic volcanic layers and mafic volcanic flow. An original stratigraphy for this group has been proposed in Chapter 2 and by Parks et al. (2006), and two basaltic suites have been identified: a northern and a southern suite. Both suites have identical ages (Chapter 2; Parks et al. 2006), while the lithochemistry presented here shows that they have different chemical signatures.

The volcanic rocks in the southern suite consist of pillowed flows that plot in the basalt field on a Zr/TiO<sub>2</sub> vs Nb/Y diagram and as tholeiites on AFM and Zr vs. Y diagrams (Figure 3.5). The basaltic tholeiites have contents of SiO<sub>2</sub> ranging from 49-54 wt.%, MgO of 5-10 wt.%, Fe<sub>2</sub>O<sub>3</sub> of 10-14 wt. %, and Mg #'s of 35-46 (Table 3.1). On a multi-element diagram normalized to primitive mantle of Sun and McDonough (1989, Figure 3.6), the suite shows moderate to strong Th and LREE enrichment ((La/Sm)<sub>PM</sub>= 1.01-2.77), and negative Nb and Ti anomalies. La and Ce are enriched relatively compared to the middle REE, and the heavy REE are slightly depleted ((La/Yb)<sub>PM</sub>= 1.11-4.04). Two basalts from the southern suite have εNd<sup>2.85 Ga</sup> values of -1.17 & -0.29 (Table 3.2; Table A.1; Figure 3.7).

Two intermediate tuffs in the southern suite plot in the calc-alkaline field on an AFM diagram and have SiO<sub>2</sub> contents ranging from 63-65 wt.% and Mg #'s of 60 and 53 (Table 3.1; Figure 3.8). On a multi element diagram normalized to primitive mantle of Sun and McDonough (1989), they show Nb and Ti anomalies and lack a Eu anomaly (Figure 3.9). The tuffs are enriched in light REE ((La/Sm)<sub>PM</sub>=3.14-3.28), and show moderate heavy REE fractionation ((Gd/Yb)<sub>PM</sub>=1.67-2.15) and overall REE fractionation ((La/Yb)<sub>PM</sub>=8-10) (Table 3.1; Figure 3.9).

The mafic volcanic rocks in the northern suite consist of both pillowed and massive flows that plot in the basalt field on a Zr/TiO<sub>2</sub> vs Nb/Y diagram and as tholeiites on AFM and Zr vs. Y diagrams (Figure 3.5). The basaltic tholeiites have contents of SiO<sub>2</sub> of 49-53 wt.%, MgO of 7-10 wt.%, Fe<sub>2</sub>O<sub>3</sub> of 8-11 wt. %, and Mg #'s of 60-65 (Table 3.1) . On a multi element diagram normalized to primitive mantle (Figure 3.6, Sun and McDonough, 1989), the suite has a low total REE abundance at 2 to 3 times primitive mantle, two distinctly different Nb signatures and erratic light REE and middle REE profiles. The erratic profiles and Nb anomalies do not follow any other chemical, isotopic, lithological, stratigraphic or structural trends. Four basalts from the northern suite have a wide range of  $\epsilon\text{Nd}^{2.85\text{ Ga}}$  values from -1.83 to 0.91 (Table 3.2; Table A.1; Figure 3.7).

Eight extrusive felsic volcanic samples from the northern suite plot in the calc-alkaline field on an AFM diagram and have SiO<sub>2</sub> contents of 64-74 wt.%, and Mg #'s of 23 to 67 (Table 3.1; Figure 3.8). On a multi element diagram normalized to primitive mantle of Sun and McDonough (1989), they show positive Zr and Hf anomalies, negative Nb and Ti anomalies, and lack an Eu anomaly (Figure 3.9). The tuffs are light REE enriched ((La/Sm)<sub>PM</sub>=3.63-6.34), moderately heavy REE fractionated ((Gd/Yb)<sub>PM</sub>=1.68-3.34), and are slightly to heavily fractionated in overall REE ((La/Yb)<sub>PM</sub>=9-42) (Table 3.1, Figure 3.9). Five tuffs and one dacite in the supracrustal assemblage have negative to positive  $\epsilon\text{Nd}^{2.85\text{ Ga}}$  values close to zero and range from (-0.72 to 0.14), and T<sub>DM</sub> ages of 3.1 Ga.

A contemporaneous 2.852 Ga granodiorite (Parks et al. 2006) plots in the calc-alkaline field on an AFM diagram, has an SiO<sub>2</sub> content of 69 wt. % and Mg # of 45 (Table 3.1, Figure 3.8). On a multi element diagram normalized to primitive mantle of Sun and McDonough (1989), it has just positive Zr and Hf anomalies, negative Nb and Ti anomalies, and lacks an Eu anomaly (Figure 3.9). The sample is light REE enriched ((La/Sm)<sub>PM</sub>=5.69) and shows moderate overall and heavy REE

fractionation ((La/Yb)<sub>PM</sub>=24, and (Gd/Yb)<sub>PM</sub>=2.59) (Table 3.1; Figure 3.9). The granodiorite has an  $\epsilon\text{Nd}^{2.85\text{ Ga}}$  of -0.75 and  $T_{\text{DM}}$  of 3.19 Ga (Table 3.2; Table A.1; Figure 3.7).

### 3.3.1.3 - 2.825 Ga Plutons

Two samples from a 2.825 Ga tonalite gneiss (Corfu and Lin 2000) with a pre- shear zone foliation plot in the calc-alkaline field on an AFM diagram, have SiO<sub>2</sub> contents of 73-75wt%, and Mg # of 36 to 51 (Table 3.1; Figure 3.8). On a multi element diagram normalized to primitive mantle of Sun and McDonough (1989), the tonalites have negative Nb and Ti anomalies, and lack an Eu anomaly. They are light REE enriched ((La/Sm)<sub>PM</sub>=5.72-7.23) and show moderate overall and heavy REE fractionation ((La/Yb)<sub>PM</sub>=21-34 and (Gd/Yb)<sub>PM</sub>=1.93-2.65) (Figure 3.9).

## 3.3.2 Neoproterozoic rocks

### 3.3.2.1 - 2.74 Ga Loonfoot assemblage and contemporaneous plutonic rocks

The volcanic rocks of this assemblage consist of voluminous basalt flows and a subordinate amount of dacitic tuff. The mafic volcanics are both pillowed and massive, and they plot in the basalt field on a Zr/TiO<sub>2</sub> vs Nb/Y diagram and as tholeiites on an AFM diagram and a plot of Zr vs. Y (Figure 3.5). The basaltic tholeiites have contents of SiO<sub>2</sub> of 50-58 wt.%, MgO of 4-16 wt.%, Fe<sub>2</sub>O<sub>3</sub> of 8-15 wt. % and Mg #'s of 38-72 (Table 3.1). The basalt chemistry shows a relatively flat profile on a multi-element diagram normalized to primitive mantle (Figure 3.6, Sun and McDonough, 1989), with minor depletion in the heavy REE ((La/Yb)<sub>PM</sub>= 0.83-1.63)). A basalt from this assemblage has a  $\epsilon\text{Nd}^{2.74\text{ Ga}}$  of 2.08 (Table 3.2; Table A.1; Figure 3.7).

The felsic rocks in this assemblage include a rare tuff and a voluminous plutonic suite that is dominantly tonalite. Three samples from the suite plot in the calc-alkaline field on an AFM diagram

and have SiO<sub>2</sub> contents of 68-71 wt.% and Mg #'s of 35-48 (Table 3.1; Figure 3.8). On a multi element diagram normalized to primitive mantle of Sun and McDonough (1989), they have negative Nb and Ti anomalies, strong light REE enrichment ((La/Sm)<sub>PM</sub>=5.32-10.82), and moderate to high overall and heavy REE fractionation ((Gd/Yb)<sub>PM</sub>=1.97-2.57 and (La/Yb)<sub>PM</sub>=24-59) (Table 3.1; Figure 3.9). The tuff also plots in the calc-alkaline field on an AFM diagram and has an SiO<sub>2</sub> content of 71 wt % and an Mg # of 43 (Table 3.1; Figure 3.8). On a multi element diagram, the tuff is light REE enriched ((La/Sm)<sub>PM</sub>=5.92), has negative Nb and Ti anomalies, and shows moderate overall and heavy REE fractionation ((Gd/Yb)<sub>PM</sub>=1.80 and (La/Yb)<sub>PM</sub>=20) (Table 3.1; Figure 3.9). Six plutons and the tuff have negative εNd<sup>2.74 Ga</sup> values ranging from -1.80 to -0.48, with T<sub>DM</sub> model ages that range from 3.17 Ga to 3.01 Ga (Table 3.2; Table A.1; Figure 3.7).

### 3.3.2.2 –Younger porphyries

The young plutons in the belt are dominated by quartz feldspar porphyries, and are either 2.730 Ga or 2.699 Ga in age and all plot in the calc-alkaline field on an AFM diagram (Figure 3.8; Turek et al. 1986; Parks et al. 2006). A 2.730 Ga porphyry has an SiO<sub>2</sub> content of 66 wt. % and an Mg # of 49 (Table 3.1). On a multi element diagram normalized to primitive mantle of Sun and McDonough (1989), the porphyry shows negative Nb and Ti anomalies, only moderate light REE enrichment ((La/Sm)<sub>PM</sub>=2.17), negative Nb and Ti anomalies, and slight to moderate overall and heavy REE fractionation ((La/Yb)<sub>PM</sub>=10.30 and (Gd/Yb)<sub>PM</sub>=2.79) (Table 3.1; Figure 3.9). Two 2.700 Ga porphyries have SiO<sub>2</sub> contents of 71-72 wt % and Mg #s of 34-38 (Table 3.1). On a multi element diagram, the samples have negative Nb and Ti anomalies, are enriched in light REE ((La/Sm)<sub>PM</sub>=6.43-6.93), highly REE fractionated ((La/Yb)<sub>PM</sub>=47-30) and show moderate heavy REE fractionation ((Gd/Yb)<sub>PM</sub>=2.07-2.11) (Table 3.1, Figure 3.9). Four of five young porphyries in the belt

have  $\epsilon\text{Nd}^{2.73\text{ Ga}-2.70\text{ Ga}}$  values of 0.68 to 2.06, while one has a  $\epsilon\text{Nd}^{2.73\text{ Ga}}$  of -1.35. The  $T_{\text{DM}}$  ages range from 2.91 to 3.09 Ga (Table 3.2; Table A.1; Figure 3.7).

### **3.4 Timing of Deformation in the Island Lake greenstone belt: U-Pb Dyke Dating**

#### **3.4.1 Sample Description**

Four dykes were sampled in the field to provide constraints on the timing of  $D_1$  and  $D_2$  in the Island Lake greenstone belt. Two samples (sample 684 and 06, Figure 3.3) place timing constraints on the early pre-shear zone foliation ( $S_1$ ) in the belt, while samples taken from two prominent shear zones in the southeastern part of the belt will place timing constraints on the movement of these young  $D_2$  shear zones (sample 103 and sample 106, Figure 3.3). All analytical methods are described in Appendix C.

##### **3.4.1.1 Post- $D_1$ , Pre- $D_2$ samples**

Sample 684 is from a post  $D_1$  aplite dyke in the Harper Island shear zone. The presence of a xenolith of foliated mafic host rock in the dyke indicates the dyke was emplaced after the event that caused the  $S_1$  foliation in the mafic country rock (Figure 3.10A). The dyke itself contains a weak internal foliation most likely attributed to the  $D_2$  event (Figure 3.10A). The age of this sample places a minimum age on the  $D_1$  event.

Sample 06 is from a post  $D_1$  quartzo-feldspathic porphyry dyke that crosscuts a pre-shear zone foliation ( $S_1$ ) in a mafic mylonite (Figure 3.10B). This sample was dated in order to obtain a minimum age on the deformation event that caused the  $D_1$  foliation cut by this dyke.

#### 3.4.1.2 D<sub>2</sub> Shear zone samples

Sample 103 is from a pre- or early syn-kinematic aplite dyke in the Harper Island shear zone. The dyke is folded within the sheared mafic rocks it intrudes (Figure 3.10C). The age of this sample will constrain the timing of shear zone movement on the Harper Island shear zone.

Sample 106 is from a weakly boundinaged post or late syn-kinematic quartz-feldspar porphyry dyke that crosscuts the foliation (S<sub>2</sub>) developed in the Savage Island shear zone (Figure 3.10D). The age of this sample will constrain the timing of shear zone movement on the Savage Island shear zone.

### 3.4.2 Results

#### 3.4.2.1 Post-D<sub>1</sub>, Pre- D<sub>2</sub> samples

The zircons in sample 684 are of one morphology and are doubly terminated 2:1 to 4:1 prismatic grains that are clear and colourless to slightly orange in colour (Figure 3.11A). Some larger grains contain fractures that are parallel to the crystal faces and some have small clear or opaque inclusions. Sample 684 produced three overlapping near concordant analyses that define an average <sup>207</sup>Pb/<sup>206</sup>Pb age of 2722 ± 1.3 Ma (Figure 3.12; Table 3.3). This age is interpreted as the age of the post D<sub>1</sub> aplite dyke.

There are two zircon populations in sample 06 (Figure 3.11B). The first population consists of small (~100-200 μm) clear, colourless, subhedral, elongate 2:1 to 5:1, doubly terminated prismatic zircons. Some of these grains contain clear round inclusions, and internal fractures. The second, less dominant population in this sample consists of large (> 300 μm) rounded to stubby, multi-faceted brown to pink zircons. Some of the latter contained clear and orange inclusions and some show heavy internal fracturing. Six TIMS analyses yielded three different age populations in this sample (Figure

3.12; Table 3.3), which have no correlation with the different zircon morphologies. Three analyses give near identical and concordant  $^{207}\text{Pb}/^{206}\text{Pb}$  ages of  $2749 \pm 2$  Ma,  $2747 \pm 2$  Ma,  $2741 \pm 3$  Ma, while one analysis gave a  $^{207}\text{Pb}/^{206}\text{Pb}$  age of  $2734 \pm 2$  Ma, and two slightly younger concordant or near concordant grains gave near identical  $^{207}\text{Pb}/^{206}\text{Pb}$  ages of  $2725 \pm 5$  Ma and  $2723 \pm 3$  Ma. Seven zircons analyzed by LA-MC-ICP-MS yielded discordant  $^{207}\text{Pb}/^{206}\text{Pb}$  ages between 2893 and 2728 Ma, none of which are younger than the youngest, concordant TIMS ages of  $2725 \pm 5$  Ma &  $2723 \pm 3$  Ma (Figure 3.12; Table 3.3). Two interpretations are possible to explain these data; 1) the two youngest, essentially identical TIMS ages at ca.  $\sim 2723$  Ma represent the true crystallization age of the post D<sub>1</sub> quartz-feldspathic porphyry dyke, or 2) all of the zircon grains in the dyke are inherited, and instead this age represent the maximum age of the dyke. Given that the age of sample 684 is essentially identical to the age of the sample 06, the preferred interpretation here is that this age is in fact a crystallization age for sample 06.

#### 3.4.2.2 D<sub>2</sub> Shear zone samples

Sample 103 from the Harper Island shear zone contained zircons that are euhedral 2:1 to 3:1 multi-faceted sharply and doubly terminated prisms that are clear and brown in colour (Figure 3.11C). Most grains contain clear or orange coloured inclusions. One near concordant analysis and three overlapping, less concordant analyses together define an average  $^{207}\text{Pb}/^{206}\text{Pb}$  age of  $2701 \pm 1.7$  Ma (Figure 3.12; Table 3.3). This age is interpreted to represent the age of this pre- or early syn D<sub>2</sub> aplite dyke.

Sample 106 was taken from the Savage Island shear zone. The zircons in this sample are thin, acicular, needle like prisms and fragments of larger prisms (Figure 3.11D). Some zircons have opaque inclusions and fractures parallel to crystal faces. The smaller prisms are colourless to brown in colour,

and the larger fragments are often browner in colour and are internally turbid. Two overlapping analyses and one less concordant zircon analysis together give an average  $^{207}\text{Pb}/^{206}\text{Pb}$  age of  $2700 \pm 1.9$  Ma (Figure 3.12; Table 3.3). This date is interpreted to represent the age of this post or late syn  $D_2$  dyke.

## **3.5 Discussion**

### **3.5.1 Lithogeochemical signatures**

#### **3.5.1.1 Mafic volcanic rocks**

The major element geochemistry of all of the volcanic assemblages in the Island Lake greenstone belt are similar; however, the multi-element diagrams presented above show a large variation in the trace element composition of the assemblages. In general, both the Whiteway assemblage and the southern suite of the Jubilee assemblage are enriched in Th and LREE and have negative Nb, Ta, Ti anomalies. The mafic volcanic rocks in these two packages are here termed Th-LREE-enriched tholeiitic basalts (TLT basalts). These rocks have markedly different signatures from the northern suite of the Jubilee assemblage and the Loonfoot assemblage which show broadly flat REE patterns. The latter rocks are here termed flat profile tholeiitic basalts (FPT basalts).

On a plot of Nb/Th vs. La/Sm (Figure 3.13, Piercy 2002; Macdonald 2005) the TLT basalts and the FPT basalts plot in different areas. Values for N-MORB, E-MORB, OIB, and primitive mantle on the diagram are from Sun and McDonough (1989), and values for Archean upper crust are from Condie (1993). The data as a whole falls on a array from N-MORB that trends through primitive mantle and to a proposed composition of Archean Upper Crust (AUC), and falls below the E-MORB and OIB data points. The FPT basalts plot near N-MORB and primitive mantle data points, whereas the TLT

basalts plot away from these points, closer to the proposed composition of AUC. This pattern and the overall Th-LREE-Nb systematics of the TLT basalts indicate they have been contaminated to a higher degree by a crustal source, whereas the FPT are relatively less contaminated or uncontaminated. This transition from most to least contaminated in the basalt geochemistry correlates with the age of the basalts from the older TLT basalts that are part of the 2.89 Ga Whiteway assemblage, to the youngest FPT basalts that are part of the 2.74 Ga Loonfoot assemblage. The 2.85 Ga Jubilee assemblage appears to be a transitional assemblage, where the basalts in the southern suite have the TLT pattern, and the basalts from northern suite have the FPT pattern. Overall, this pattern shows decreasing contamination with decreasing age.

This transition from a contaminated to uncontaminated signature with decreasing age can be explained by 1) progressive trace element depletion of the continental basement underneath the volcanic complexes, reducing its effect of contamination over time; 2) the same magma conduits being exploited by subsequent volcanic eruptions, and over time the conduits developed chilled margins and became “sealed” which prevented any further wall/rock interaction and contamination (Hollings and Kerrich 1999; and Leshner and Arndt 1995); 3) extension in the basement, resulting in the magma travelling through a crust that is becoming thinned over time, reducing the amount of contact between the magma and crust, resulting in reduced contamination or 4) or a combination of these factors. In any case, given that the transition in basaltic geochemistry from TLT to FPT shows a correlation with age and the lack of any observed tectonic contacts between the volcanic assemblages in the field (Chapter 2; Parks et al. 2006), it is possible that the volcanic assemblages represent a (relatively) intact primary volcanic stratigraphy (see Figure 2.8).

### 3.5.1.2 Felsic extrusive and intrusive rocks

The felsic extrusive and intrusive rocks have broadly similar trace element patterns on multi-element diagrams with variable amounts of Th-LREE enrichment, and negative Nb and Ti anomalies (Figure 3.9), all which are characteristics of subduction related magmatism. The samples also all plot in the volcanic arc granite field on a plot of Y+Nb vs. Rb (Figure 3.14).

### 3.5.2 Nd isotopic signatures

Two patterns of particular interest are observed in the Nd isotopic data. First is a trend in the felsic rocks in the Meso – and Neoproterozoic volcanic assemblages and contemporaneous intrusive rocks that shows a transition from positive to negative  $\epsilon\text{Nd}$  values with decreasing age. Two of three felsic rocks associated with the 2.89 Ga Whiteway assemblage have slightly positive  $\epsilon\text{Nd}^{2.89\text{Ga}}$  values (0.47 & 0.39, Table 3.2; Table A.1), and the third is slightly negative (-0.63, Table 3.2; Table A.1). All of these rocks have Nd model ages over 3.14 Ga. In the younger 2.85 Ga Jubilee assemblage, tuffs and plutons have both positive and negative  $\epsilon\text{Nd}^{2.85\text{Ga}}$  values, however the majority of values (6 of 8 values, Table 3.2; Table A.1) are negative, and all of the felsic rocks have Nd model ages between 3.13 Ga to 3.18 Ga. In the 2.74 Ga Loonfoot assemblage, one tuff and six contemporaneous plutons all have negative  $\epsilon\text{Nd}^{2.74\text{Ga}}$  values and >3.01 Ga model ages (Table 3.2; Table A.1). In addition, all data except one (of 20) cluster around or fall below an evolution line for a sample with a 3.0 Ga model age and  $\epsilon\text{Nd}^{2.74\text{Ga}}$  of -0.48 (Figure 3.7). These data show that all of the chronologically and geochemically distinct volcanic assemblages in the Island Lake greenstone belt were sourced from a ca. 3.0 Ga crustal source (this study; Stevenson and Turek 1992). The most likely candidate for this source is the 3.0 Ga crust of the core region of the North Caribou terrane (this study; Stevenson and Turek 1992). Together with the lack of observed tectonic contacts, and the geochemical data above, it appears that the Meso -

and Neoproterozoic volcanic assemblages represent an original stratigraphy, as suggested in chapter 2 (Figure 2.8), which was built on the same basement and have autochthonous relationships with each other.

A second pattern observed in the data is from the youngest porphyry intrusions in the belt. Three young, volumetrically small porphyries have model ages of 2.9 Ga, and four of the five  $\epsilon\text{Nd}$  values are positive. The change from  $> 3.0$  Ga model ages observed in the Meso – and Neoproterozoic rocks to the 2.9 Ga model ages and positive  $\epsilon\text{Nd}$  values reflects that these young plutons were not as strongly influenced by the Neoproterozoic crust of the North Caribou terrane as the older rocks in the belt were, or they were extracted from a more depleted mantle source. This signature could be related to the changing geochemical signatures seen in the basaltic geochemistry.

### **3.5.3 Timing of deformation**

The age of the post  $D_1$  aplite dyke (sample 684) places a minimum age constraint of  $2722 \pm 1.3$  Ma on the deformation event that caused the foliation in the xenoliths contained in the dyke. The age of ca. 2.723 Ga for the post  $D_1$  quartzo-feldspathic porphyry dyke (sample 06) represents either a crystallization age or a maximum age of the dyke. As discussed above, the preferred interpretation here is that this age is in fact a crystallization age for sample 06, and the age places a minimum age constraint on the event that created the foliation that the dyke crosscuts. Together both of these dates confirm that at least one episode of deformation occurred in the Island Lake greenstone belt before ca. 2.722 Ga.

The ages of sample 103, a pre- or early syn-kinematic dyke, and sample 106, a post or late syn-kinematic dyke concisely bracket an episode of deformation to between  $2701 \pm 1.7$  Ma and  $2700 \pm 1.9$  Ma. Thus, two ages of deformation have been identified in this belt; a  $D_1$  event, most likely

related to folding in the supracrustal rocks that produced an early foliation at ca. 2.722 Ga, and a D<sub>2</sub> event related to the last stages of shear zone movement and terminal collision at 2.700 Ga.

### **3.5.4 Regional Implications**

The new data from this study is here discussed together with data from other areas in the northern margin of the North Caribou terrane, in order to put forward a spatial and temporal tectonic model for this part of the northwestern Superior Province. To this end, three areas will be discussed; 1) The northern extent of the 3.0 Ga North Caribou crust as basement in the northwestern Superior Province, 2) regional correlations of Meso – and Neoproterozoic events in the northern part of the northwestern Superior Province, and 3) regional timing constraints on deformation.

#### **3.5.4.1 Northern extent of 3.0 Ga North Caribou crust as basement in the northwestern Superior Province**

The North Caribou terrane has long been considered as a ca 3.0 Ga continental cratonic block onto which greenstone belts and domains to the north and south were built (Thurston et al. 1991). The  $\epsilon_{Nd}$  and geochemical data from this study agrees with previous work in the area and supports the conclusion that the Island Lake greenstone belt has been variably influenced by ca. 3.0 Ga North Caribou crust during the generation of the Meso – and Neoproterozoic volcanic assemblages (Chapter 2; Stevenson and Turek 1992; Corfu and Lin 2000; Parks et al. 2006). While the Island Lake greenstone belt contains ample evidence of being built on an older continental basement, evidence that the Oxford-Stull domain to the north should be included in this terrane has been inconclusive. The Oxford-Stull domain contains dominantly juvenile Nd signatures and was proposed to have developed on either a very thin continental margin or in an oceanic setting (Skulski et al. 2000). More recent work shows evidence of older crust in the Oxford-Stull domain with inherited zircon ages of >2.9 Ga

on gneisses that have negative  $\epsilon\text{Nd}$  values (e.g. location 9 of Rayner and Stott 2005). Given this new data, the interpretation that the Oxford-Stull domain was developed on a thin continental margin, and that this continental margin was that of the ca 3.0 Ga North Caribou crust is preferred here. The ca. 3.0 Ga North Caribou crust acted as basement to both the Island Lake and Oxford- Stull domains, and the northern limit of the 3.0 Ga North Caribou crust in the northwestern Superior Province is the northern limit of the Oxford- Stull domain, the North Kenyon Fault (Figure 3.1).

#### 3.5.4.2 Regional correlation of Mesoarchean and Neoarchean events in the northern margin of the North Caribou terrane, northwestern Superior Province.

Greenstone belts in the northwestern Superior Province contain both Mesoarchean and Neoarchean magmatic events (Figure 3.1; Figure 3.15) and in order to successfully reconstruct a tectonic history for the area, it is instructive to first review high precision U-Pb ages of intrusive and volcanic rocks in the area. The locations of the greenstone belts discussed below are show in Figure 3.1.

In the Mesoarchean, the oldest observed event in the Island Lake domain is the volcanism and plutonism in the 2.894 Ga Whiteway assemblage in the Island Lake greenstone belt (Figure 3. 15; Parks et al. 2006; Chapter 2). Two younger tonalites have ages of 2.855 Ga and 2.848 Ga south of the Stull Lake-Edmund Lake greenstone belt (located in the Island Lake domain, Skulski et al. 2000), which are identical to the age of volcanism in the Jubilee assemblage in the Island Lake greenstone belt. Farther north in the Oxford-Stull domain, three dacitic tuffs in the Knee Lake greenstone belt indicate a period of volcanism at 2.832 Ga (Corkery et al. 2000). The youngest Mesoarchean granitoid ages in the Island Lake domain are a 2.825 Ga gneiss (in the Island Lake greenstone belt, Corfu and Lin 2000), while the youngest age in the Oxford-Stull domain is a 2.813 Ga granodiorite

gneiss near Kasabonika Lake (Rayner and Stott 2005). The youngest mafic intrusive in the domain is a  $2.807 \pm 1$  Ga gabbro in the Island Lake greenstone belt (Corfu and Lin, 2000).

In the Neoproterozoic, again the oldest events are observed in the Island Lake greenstone belt (Island Lake domain; Figure 3.15). These oldest Neoproterozoic events are the eruption of the Loonfoot assemblage volcanics and emplacement of a voluminous plutonic suite at 2.750 Ga -2.740 Ga (Stevenson and Turek 1992; Corfu and Lin 2000; Parks et al. 2006). In the Oxford-Stull domain to the northeast, the oldest Neoproterozoic age observed to date is a 2.737 Ga intermediate volcanic rock in the McFaulds Lake area (Rayner and Stott 2005). In the Island Lake domain, two younger quartz-feldspar porphyries were emplaced at 2.730 Ga in the Island Lake greenstone belt, which are similar in age to a 2.732 Ga granodiorite dated in the Ponask Lake – Sachigo Lake greenstone belt to the east (Skulski et al 2000). In the Oxford-Stull domain, a younger 2.728 Ga granodiorite has also been dated in McFaulds Lake, which has an essentially identical age to a 2.727 Ga granodiorite at Kasabonika Lake (Rayner and Stott 2005). The next youngest event in the Oxford-Stull domain is a period of volcanism which is defined by two essentially identical ages of dacitic tuffs in the Knee Lake greenstone belt at  $2722 \pm 3$  Ma (Corkery et al. 2000), and in the Gods Lake greenstone belt at  $2719 \pm 1.4$  Ma (Lin et al. 2006). A contemporaneous tonalite has been dated at  $2721 \pm 1.2$  Ma in the Gods Lake greenstone belt (Lin et al. 2006). The youngest Neoproterozoic intrusive unit recognized in the Island Lake domain is a 2.699 Ga porphyry in the Island Lake greenstone belt (Stevenson and Turek 1992). A range of younger Neoproterozoic intrusive ages are observed in the Oxford-Stull domain from 2.715-2.683 Ga (Figure 3.15; Lin et al. 2006 and Rayner and Stott 2005).

Of particular interest in the regional geochronology data set presented above is that in both the Meso - and Neoproterozoic, a pattern of northeastward younging of volcanic and plutonic ages from the

Island Lake domain into the Oxford-Stull domain is observed. In each domain and during both eras, a predictable sequence of volcano-plutonic events is observed. The start of the sequence (ie. the oldest component) is marked by the eruption of volcanic rocks which may be accompanied by plutonism (Figure 3.15). In some areas this initial sequence is followed by other extrusive and/or intrusive sequences. The last stage of the sequence (i.e. the youngest component) is marked by the emplacement of the youngest plutonic suite, which has a characteristic lack of an extrusive volcanic component (Figure 3.15). This sequence of events begins first in the Island Lake domain in both the Meso – and Neoarchean, and the last stage is always observed last in the Oxford-Stull domain (Figure 3.15).

This sequence of events and the trend of the oldest sequences occurring in the Island Lake domain most likely reflects the movement of an active volcanic front towards the northeast in both the Meso – and Neoarchean. The location of the active front is marked by the presence of volcanic rocks, and as volcanism ceases and the front moves northeast ward, plutons are emplaced where the active volcanic front previously was.

#### 3.5.4.3 Regional timing constraints on deformation

Few ages of deformation exist for the northwestern Superior Province, although there is little doubt that the greenstone belts there have experienced multiple episodes of deformation over their evolution from ca 3.0 Ga to 2.7 Ga. The older episodes of deformation are commonly overprinted by younger events making them difficult to identify in the field, and generally impossible to precisely date. The oldest ages in the area are based on the age of intrusions which cross cut pre-existing foliations. These dates broadly bracket deformation events and place minimum age constraints on the deformation event that created these foliations. These ages include pre-2.87 Ga deformation in the North Caribou

greenstone belt (Thurston et al. 1991), a pre- 2.76 Ga G1 foliation in the Cross Lake greenstone belt (Parmenter et al. 2006), and pre- 2.73 Ga tectonism in the Stull Lake - Edmond lake greenstone belt (Skulski et al. 2000). It is unknown if these ages support three distinct episodes of deformation, or if the two younger plutons are also dating the pre-2.87 Ga event.

Evidence for pre-2.700 Ga deformation is the age of a 2.721 Ga dyke in the Gods Lake greenstone belt that is interpreted to be contemporaneous with early folds and shearing in the belt (Lin et al. 2006). This age agrees with the ages of the “pre D<sub>2</sub>-shear zone” samples from this study, and also places timing constraints on the early folding in the belt. This event most likely represents the timing of initial collision and compression during Neoproterozoic subduction.

The youngest episode(s) of deformation in greenstone belts in this part of the Superior Province are associated with movements along fault structures that are parallel to and similar in nature to the Savage Island shear zone, as well as deposition of “Timiskaming type” sedimentary groups (Thurston and Chivers 1990). Determining the timing of movement along these structures has been done indirectly in the northwestern Superior Province by assuming the movement is contemporaneous with the ages of deposition of these sedimentary groups. Deposition of these groups in the northwest Superior Province range from <2.713 Ga (at Stull Lake, Skulski et al. 2000) to 2.705 Ga (at Oxford Lake, Lin et al. 2006). Although these ages are indirect, they are within a few million years of the two direct ages of ca. 2.700 Ga for the syntectonic dykes dated in the Island Lake greenstone belt. Together these data and the age of ca. 2.700 Ga are interpreted as the age of final movement along shear zones and terminal collision in the northwestern Superior Province.

### **3.6 Tectonic synthesis**

Based on all of the evidence presented above, the following scenarios are proposed for the tectonic evolution along the northern margin of the North Caribou terrane in the northwestern Superior Province in the Meso – and Neoproterozoic.

#### **3.6.1 Mesoarchean Events**

The volcano-plutonic events in the Mesoarchean started at ca. 2.9 Ga, with south dipping subduction under the North Caribou terrane, along a trend that parallels the present day position of the north Kenyon fault (Figure 3.16). During the first stages of subduction, the 2.89 Ga Whiteway volcanic assemblage and related intrusive rocks were deposited onto and into the 3.0 Ga basement of the North Caribou terrane. The volcanic eruptions through the North Caribou terrane crust generated the TLT enriched basalts of the Whiteway assemblages, and the negative  $\epsilon_{\text{Nd}}$  values and >3.0 Ga model ages of the 2.894 Ga granodiorite and leucotonalite in the belt.

As subduction continued, the mafic and felsic volcanic rocks of the 2.85 Ga Jubilee assemblage were deposited unconformably on top of the Whiteway assemblage and North Caribou terrane basement (Figure 3.16). Contemporaneous plutons were emplaced in the Island Lake greenstone belt and in the Pierce Lake area to the east (Skulski et al. 2000), all of which have negative  $\epsilon_{\text{Nd}}$  values and ca. 3.0 Ga model ages (this study; Skulski et al. 2000). During the initial stages of volcanism at 2.85 Ga, the contaminated TLT basalts of the southern suite (Jubilee assemblage) were deposited. As volcanism continued, the crust either started to thin, or the magma conduits became chilled and/or depleted of Th and LREE. This resulted in the chemical signature of the basalts being erupted changing to the FPT basalts observed in the northern suite of the Jubilee assemblage, while the Nd isotopic evidence shows that the northern suite were still being influenced by the North Caribou

basement. Starting at ca. 2.83 Ga, the active volcanic front migrated northward, possibly due to waning subduction (Figure 3.16). This produced the ca. 2.834 Ga volcanic rocks observed in the Knee Lake area (Corkery et al. 2000). Post volcanic plutons were emplaced at 2.825 Ga (Corfu and Lin 2000) in the Island Lake greenstone belt. The youngest granitoid was emplaced at 2.813 Ga in Kasabonika Lake in the Oxford-Stull domain. The youngest Mesoarchean intrusive age is that of a 2.807 Ga gabbro in the Island Lake greenstone belt (Corfu and Lin 2000), and could reflect crustal thinning, extension, and/or local rifting. The Mesoarchean subduction event would have terminated before the emplacement of this gabbro.

### **3.6.2 Neoarchean Events**

The Neoarchean tectonic evolution starts at 2.75 Ga (Figure 3.16), when a southward dipping subduction was re-initiated along the north Kenyon fault on the northern margin of the North Caribou terrane. This subduction was eventually responsible for the final juxtaposition of the Northern Superior superterrane and the North Caribou terrane. At the beginning of this renewed subduction, the 2.75-2.74 Ga plutonic suite was emplaced and the volcanic rocks of the 2.744 Ga Loonfoot assemblage were deposited in the Island Lake greenstone belt. Nd isotope data suggests the Loonfoot assemblage and contemporaneous plutons were still being influenced by the North Caribou basement. The basalts were erupted on top of the Mesoarchean volcanic pile over a thinned continental crust, possibly using the same Th and LREE depleted magma conduits as previous eruptions, resulting in an FPT geochemical signature (Figure 3.16). The volcanic front moved northward into the OSD, producing the 2.737 to 2.721 Ga volcanic packages in the Knee Lake, Gods Lake and McFaulds Lake area. Minor porphyries were emplaced further inboard in the Island Lake greenstone belt (e.g. 2.729 Ga Pipe Point porphyry; Parks et al. 2006). As the volcanic front moved northward, an influx of a

depleted mantle underneath the Island Lake domain could explain the ~2.9 Ga Nd model ages and positive  $\epsilon\text{Nd}$  values seen in the youngest porphyries in the Island Lake greenstone belt.

Initial collision and compression during subduction resulted in folding and thrusting in the supracrustal rocks in the northwestern Superior Province, related to the pre 2.72 Ga event dated in the Island Lake greenstone belt and in the Gods Lake greenstone belt (this study; Lin et al. 2006). Plutons were emplaced throughout the Island Lake domain and Oxford-Stull domain from 2.72 to 2.70 Ga. “Timiskaming” type sediments were deposited, and a last episode of movement occurred on the major fault structures in the area at 2.700 Ga. At the end of this process the North Superior superterrane was terminally docked to the North Caribou terrane along the North Kenyon fault. Plutons continued to be emplaced in the northern margin of the North Caribou terrane until ~2.680 Ga due to post orogenic processes (such as orogenic collapse and the addition of heat from upwelling asthenosphere during slab break off).

Chapter 2 and Parks et al. (2006) defined a megasequence based on a commonality of ages across the southern margin, core region and parts of the northern margin of the North Caribou terrane. This package, however, cannot be a “megasequence” deposited by the same tectonic process given the tectonic synthesis presented above. The rocks in the northern margin were generated by a southward dipping subduction zone, while the rocks along the southern margin were generated by a northward dipping subduction zone (Sanborn-Barrie et al. 2001; Percival et al. 2006).

The Mesoarchean sequence of events suggested above represents the author’s first attempt to explain the generation of rocks of this age along the northern margin of the North Caribou terrane. The second stage of tectonic evolution in this model broadly follows the sequence of tectonic evolution suggested by Percival et al. 2006) for the western Superior Province (Figure 9A of Percival

et al. (2006)). A zone of high mantle resistivity defined by magnetotelluric studies (Figure 3 of Percival et al. 2006) extends to a depth of ~100 km directly under the North Caribou terrane and could be a relic of the Mesoarchean subduction slab. The existence of a Neoproterozoic subduction zone with a southward dipping polarity was also suggested by Lin et al. (2006) based on north-vergent structures and south dipping seismic reflectors near the north margin of the North Caribou terrane (White et al. 2003). As well, a second zone of high mantle resistivity defined by magnetotelluric studies (Figure 3 of Percival et al. 2006) dips to the south and extends to a depth of ~200 km which is most likely a relic of the Neoproterozoic subducting slab beneath the North Caribou terrane.

### **3.7 Conclusions**

Geochemical and  $\epsilon\text{Nd}$  isotopic data indicates that the Meso – and Neoproterozoic volcanic assemblages in the Island Lake greenstone belt are most likely part of an intact primary volcanic pile, and have been variably contaminated by an older crustal source. This ca. 3.0 Ga older crustal source acted as basement and contaminant in the Island Lake and Oxford-Stull domains, and is the crust of the core of the North Caribou terrane. U-Pb zircon TIMS geochronology identified two ages of deformation in the Island Lake greenstone belt. Two dykes that crosscut an older  $D_1$  foliation place a minimum age of ca. 2.722 Ga on the  $D_1$ , and two dykes in shear zones in the belt both date movement along the  $D_2$  structures to 2.700 Ga. It appears that Meso – and Neoproterozoic periods of southward dipping subduction were responsible for generating the rocks along the northern margin of the North Caribou terrane. At the end of Neoproterozoic subduction, terrane accretion was complete and the North Caribou terrane was terminally juxtaposed to the Northern Superior superterrane at 2.70 Ga.

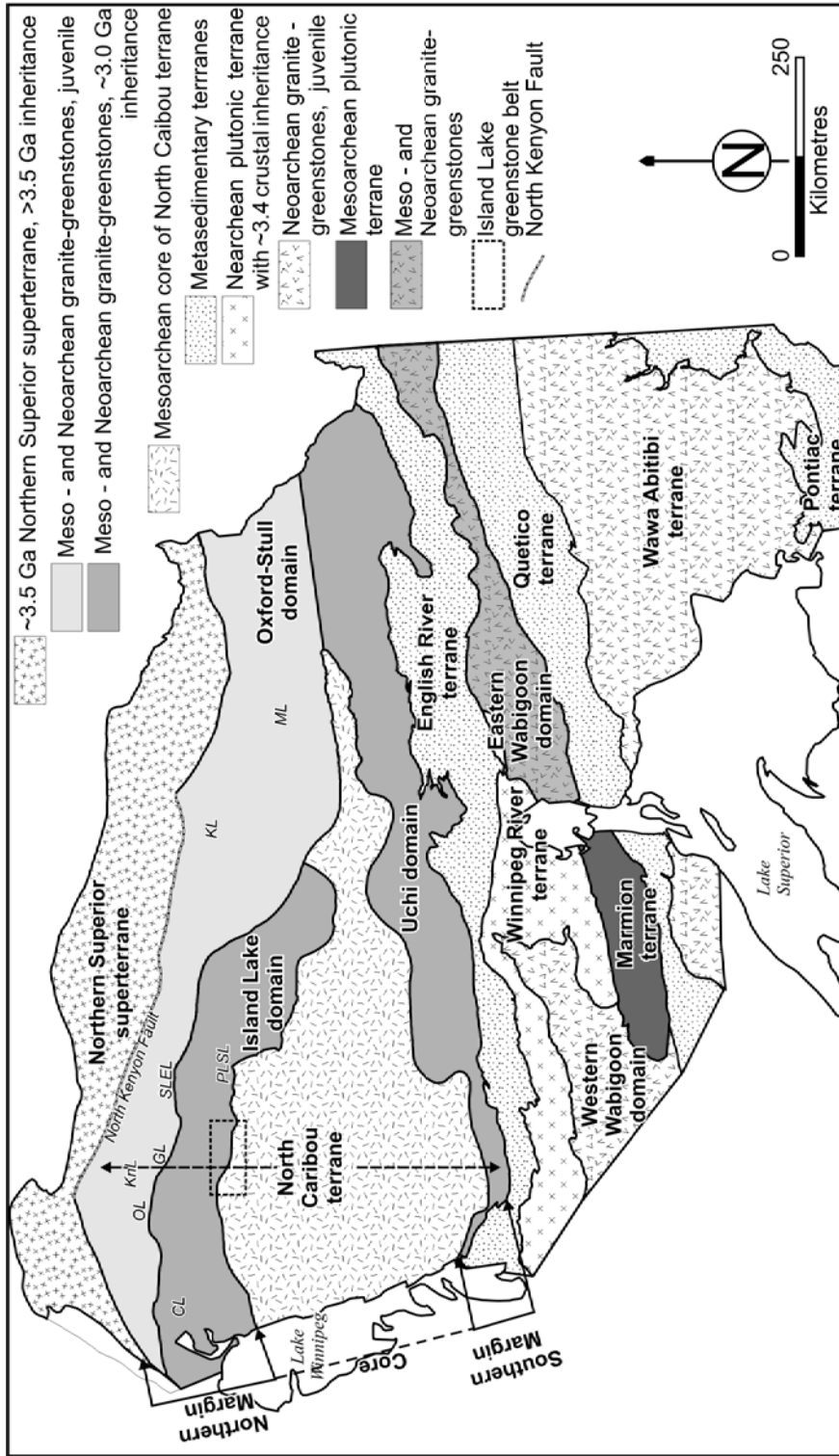


**Figure 3.1** Map of the Superior Province showing the location of basins, domains, terranes and superterranes. The location of the Island Lake greenstone belt and other belts mentioned in the text are indicated. Abbreviations for places names and greenstone belts mentioned in text: SLEL - Stull Lake-Edmund Lake greenstone belt; OL - Oxford Lake greenstone belt; KnL - Kneee Lake greenstone belt; GL - Gods Lake greenstone belt; KL - Kasabonika Lake; PLSL - Ponask Lake-Sachigo Lake greenstone belt; ML - McFaulds Lake; NC - North Caribou greenstone belt; CL - Cross Lake. Map modified from Stott (2009).

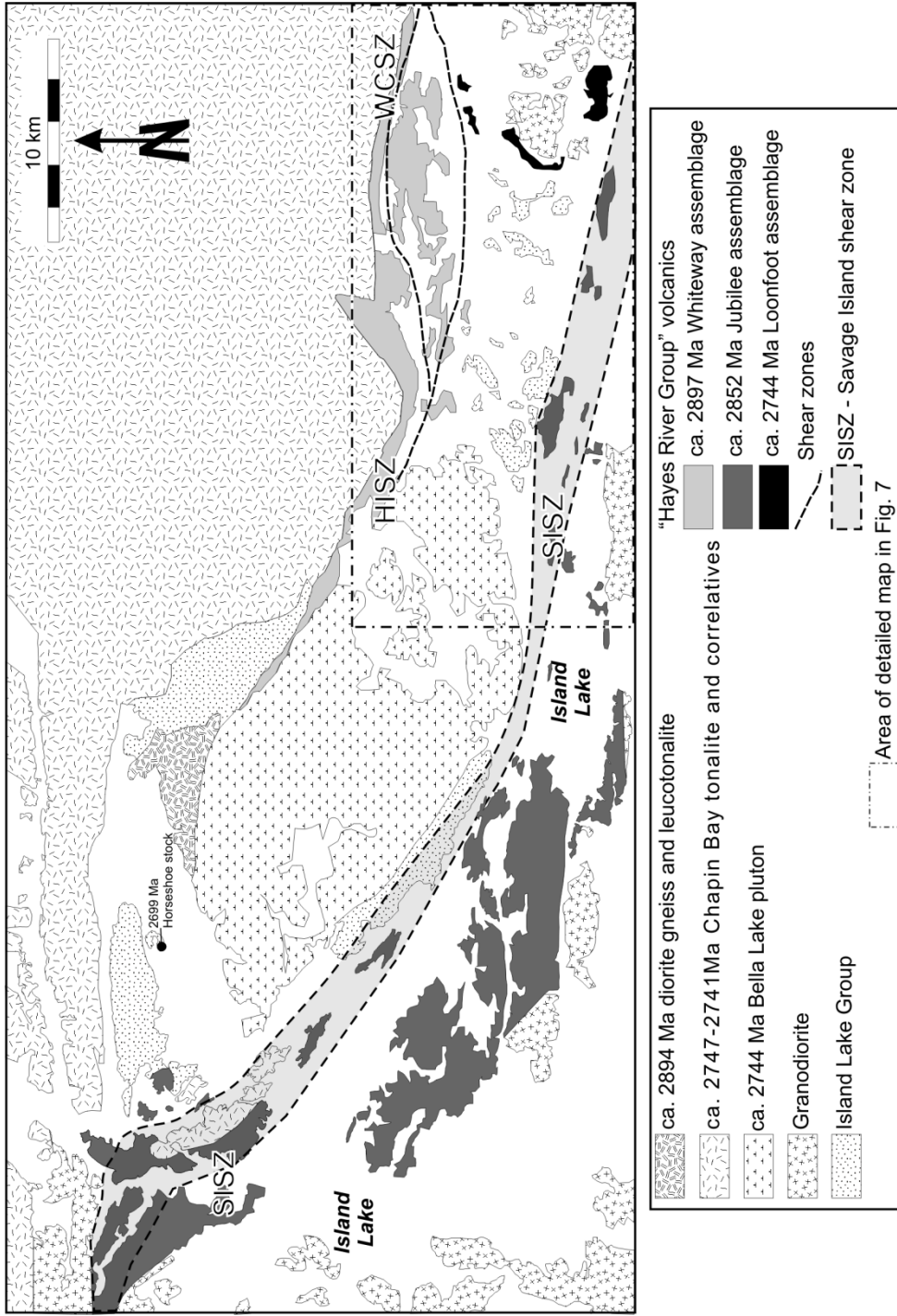


**Figure 3.2** Map of the Island Lake greenstone belt. Dashed rectangle indicates area shown in Figure 3.3. Abbreviations: HISZ - Harper Island shear zone; WCSZ - Whiteway Channel shear zone; SISZ - Savage Island shear zone.

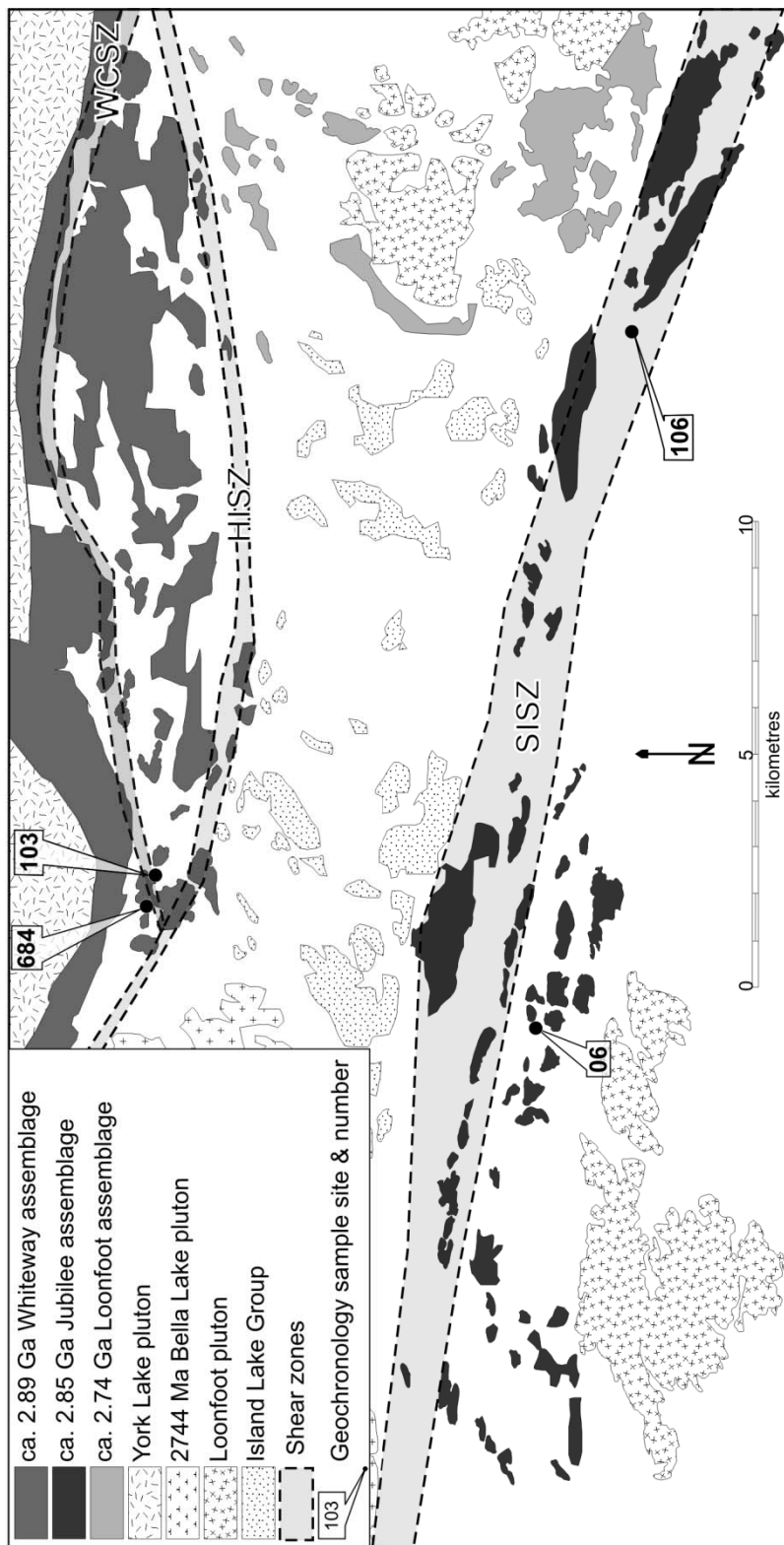


**Figure 3.3** Map of the eastern portion of the Island Lake greenstone belt. The location of shear zones and U-Pb samples are indicated. Abbreviations: HISZ - Harper Island shear zone; WCSZ - Whiteway Channel shear zone; SISZ - Savage Island shear zone.

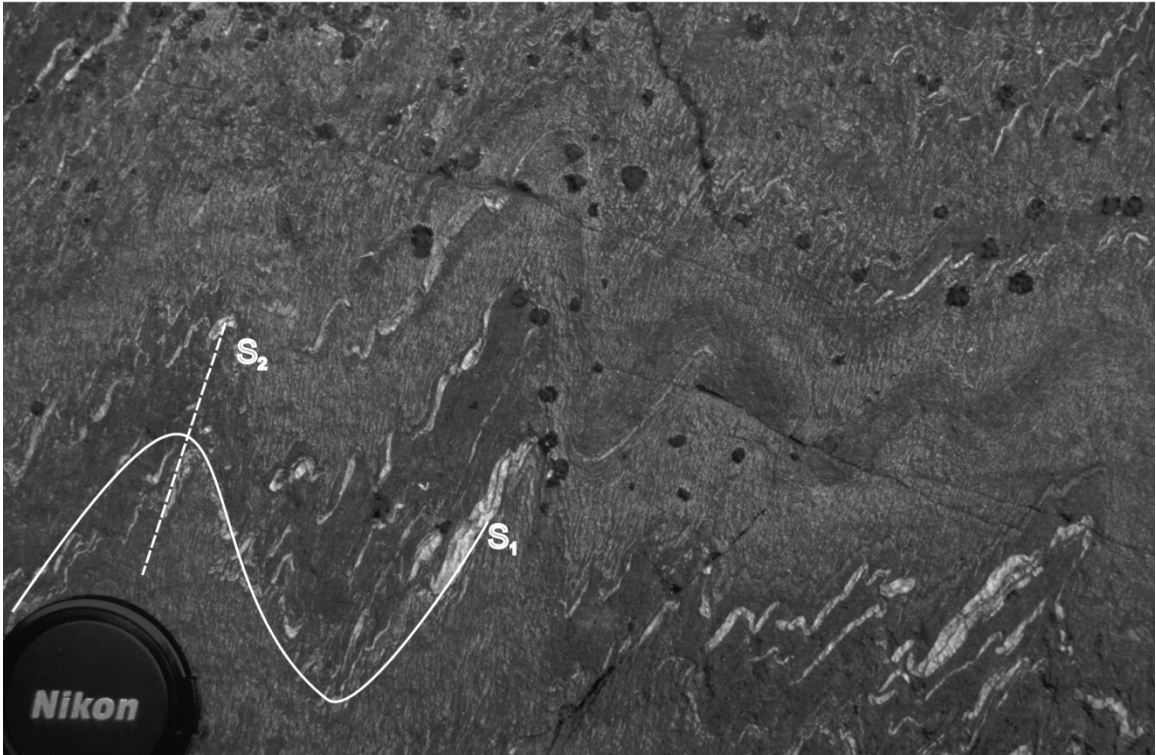


**Figure 3.4** Transposition of an older foliation ( $S_1$  – solid line) into the orientation of the foliation associated with the Savage Island shear zone ( $S_2$  – dashed line). Camera lens for scale.

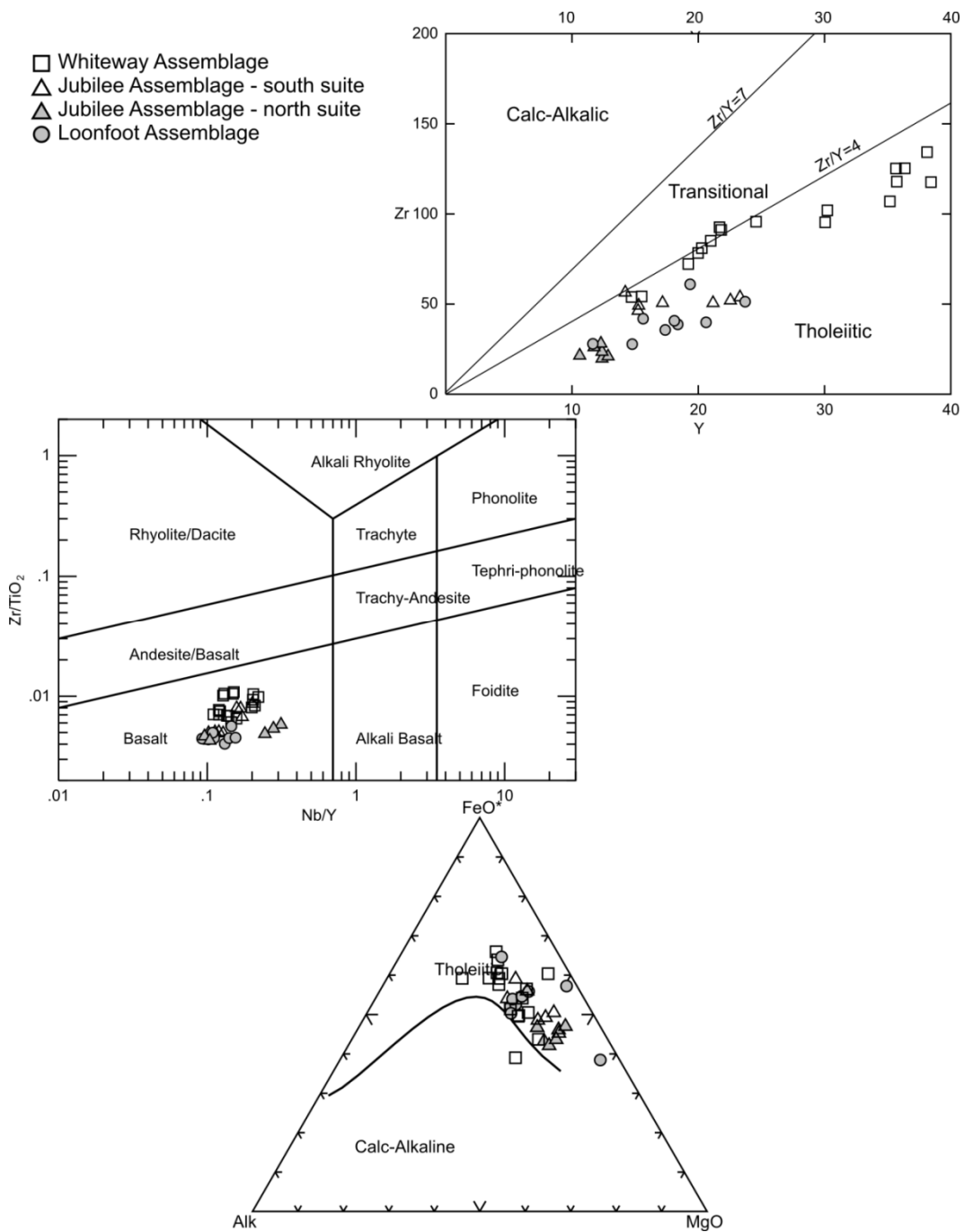


**Figure 3.5** Classification diagrams for the mafic volcanic rocks in the different assemblages in the Island Lake greenstone belt. Fields on the Zr/TiO<sub>2</sub> vs. Nb/Y plot after Pearce (1996) and AFM diagram after Irving and Baragar (1971). Fields on the Zr/Y plot are from Barrett and MacLean (1999).

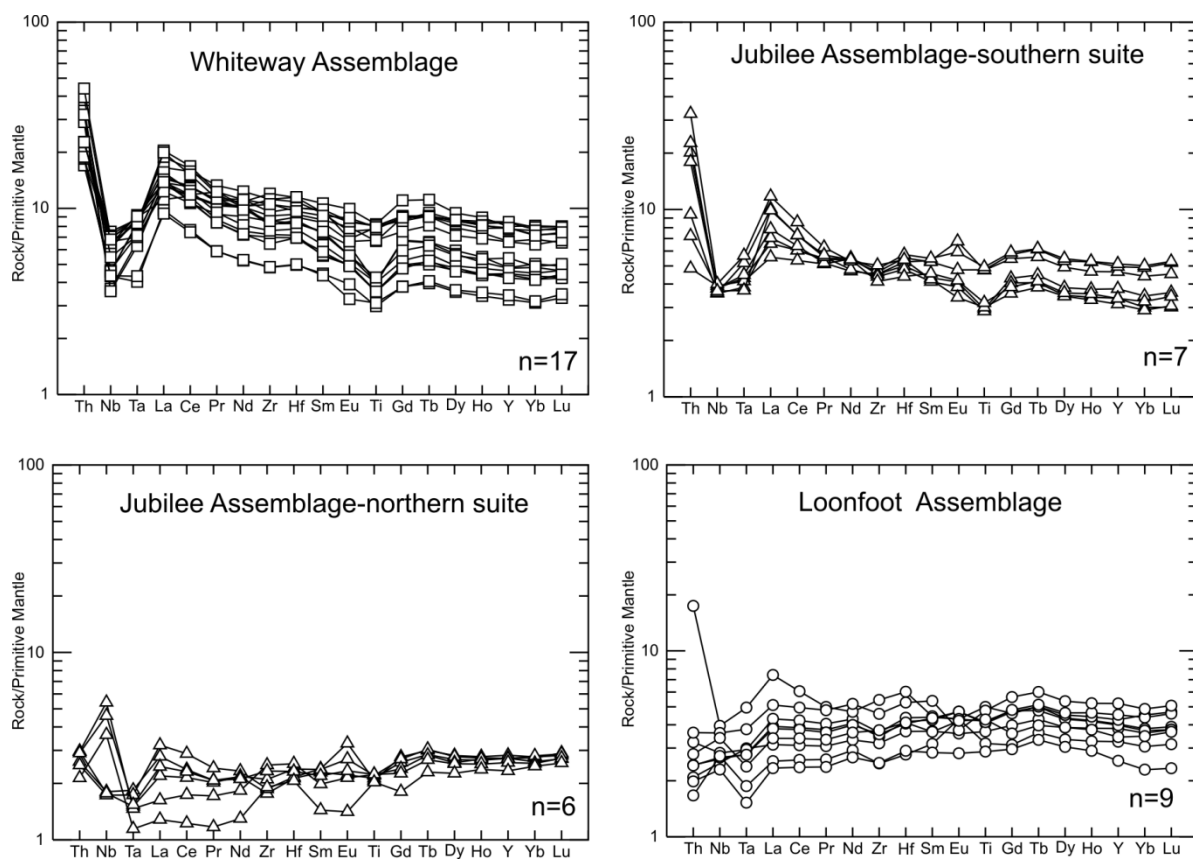


**Figure 3.6** Primitive mantle normalized multi element diagrams of mafic volcanic rocks in the Island Lake greenstone belt. Values from Sun and McDonough (1989).

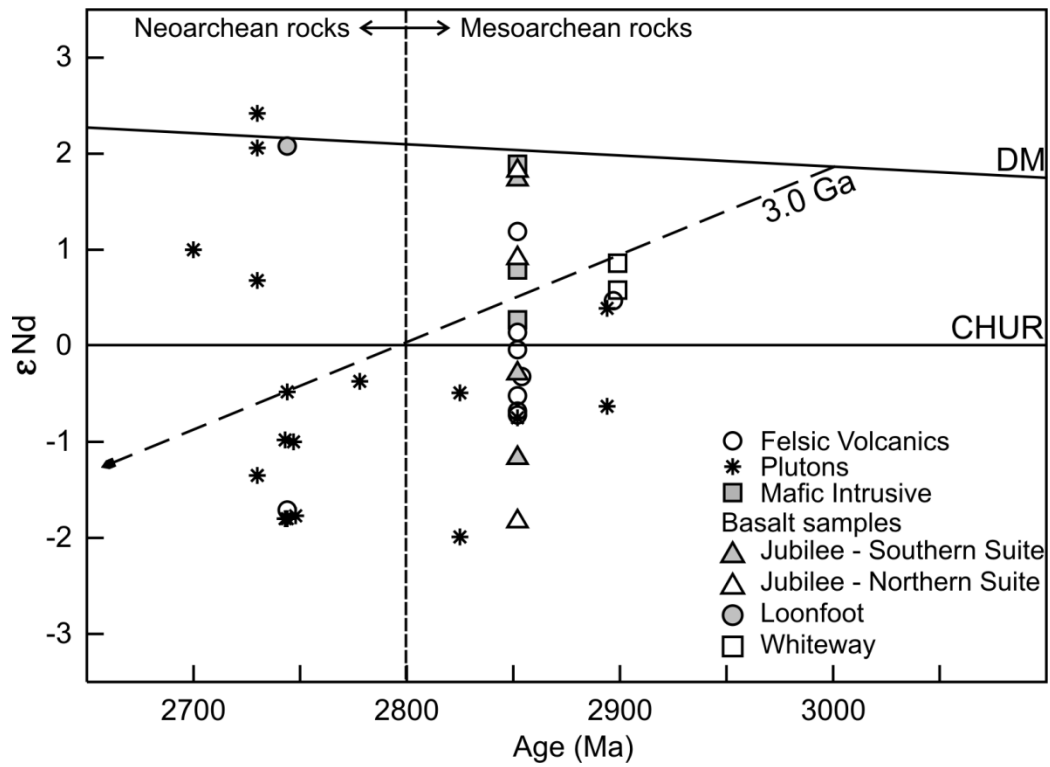


**Figure 3.7**  $\epsilon$ Nd diagram for rocks in the Island Lake greenstone belt. DM - depleted mantle curve from DePaolo (1981). CHUR – chondritic uniform reservoir.

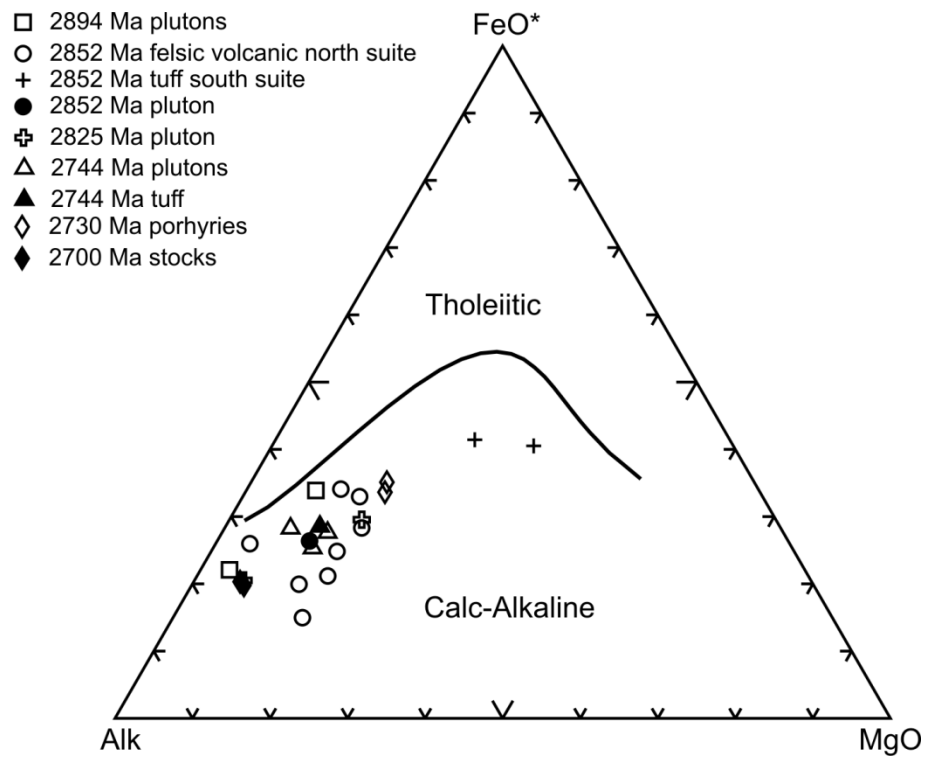


**Figure 3.8** Classification diagrams for the felsic intrusive and extrusive rocks in the Island Lake greenstone belt. Fields on the AFM diagram after Irving and Baragar (1971).

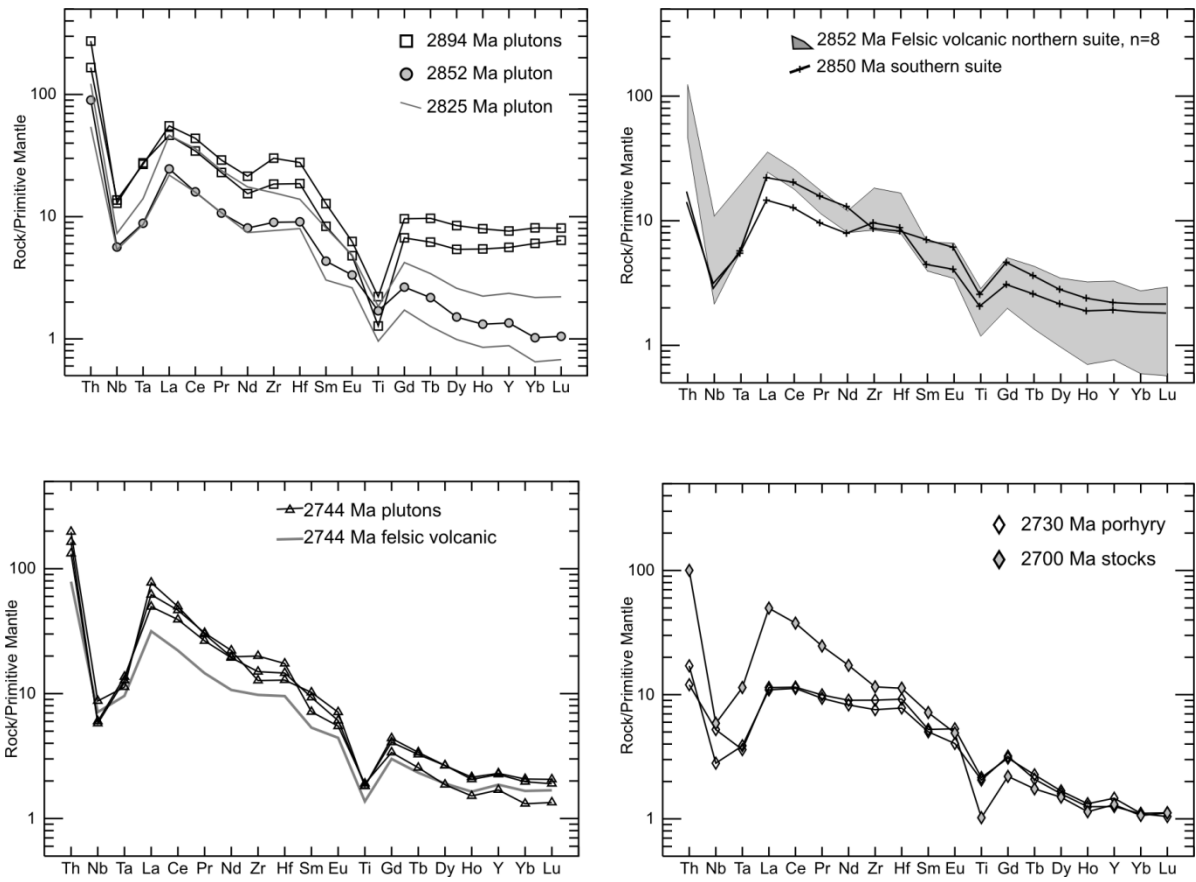


**Figure 3.9** Primitive mantle normalized multi element diagrams of felsic intrusive and extrusive rocks in the Island Lake greenstone belt. Values from Sun and McDonough (1989).

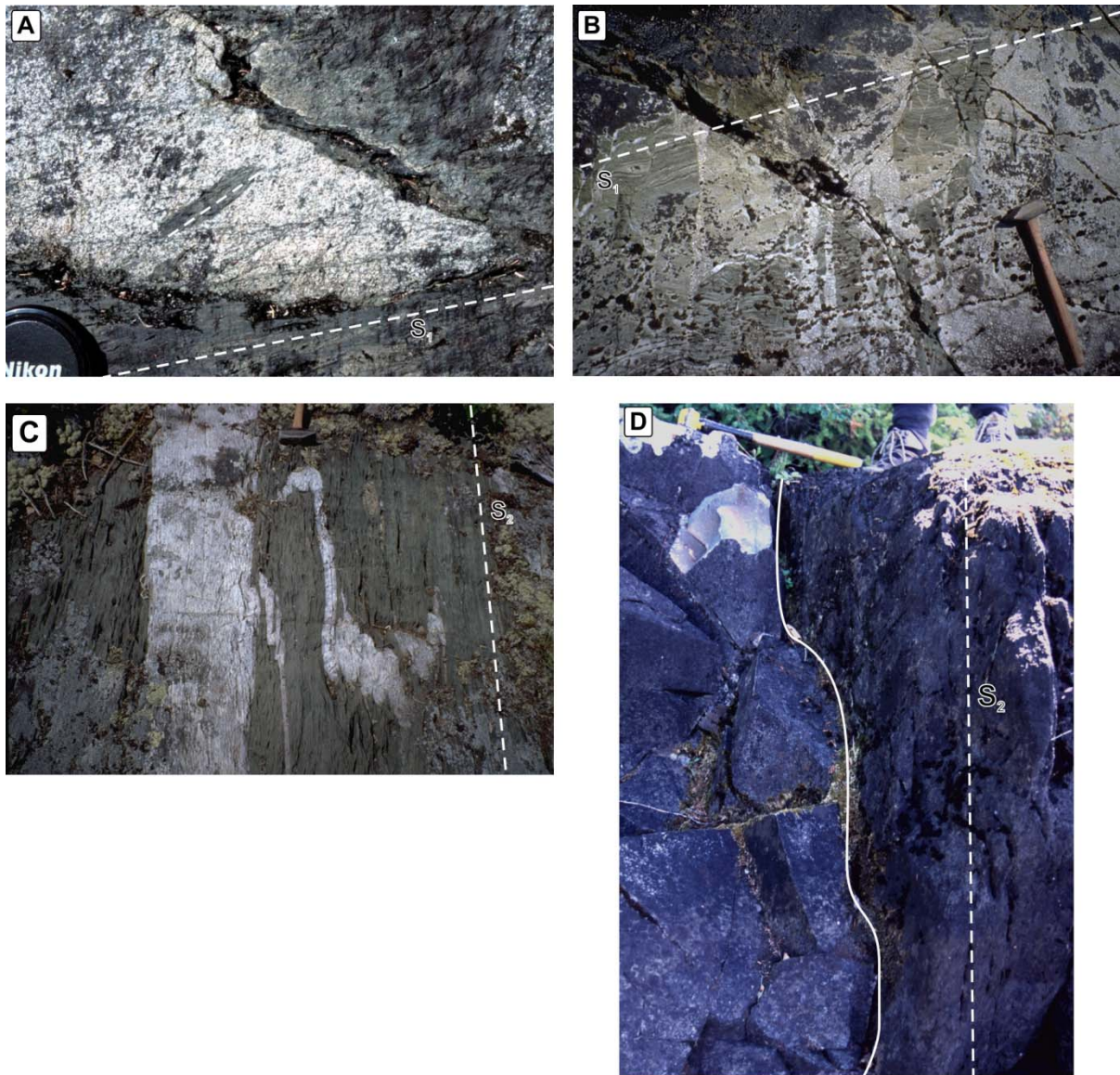


**Figure 3.10** Field photos showing field setting of U-Pb samples. A - Sample 684, a post kinematic dyke that cross cuts an early foliation ( $S_1$  indicated by dashed line) and contains a xenolith of foliated mafic country rock. Camera lens for scale. B - Sample 06 from the Savage Island shear zone, a post-tectonic quartz porphyry dyke running from the top to the bottom of the photo, cross cutting foliation in the mafic host rock ( $S_1$  indicated by dashed line). Hammer for scale. C - Sample 103, a pre-to early syn-kinematic quartz porphyry dike that is strongly internally sheared and folded with the sheared mafic country rock ( $S_2$  indicated by dashed line). D - Sample 106 from the Savage Island shear zone, a post- to late syn-kinematic quartz porphyry dyke that cuts  $S_2$ , indicated by dashed line. Contact between dyke and country rock indicated by solid line. Hammer and feet at top of photo for scale.

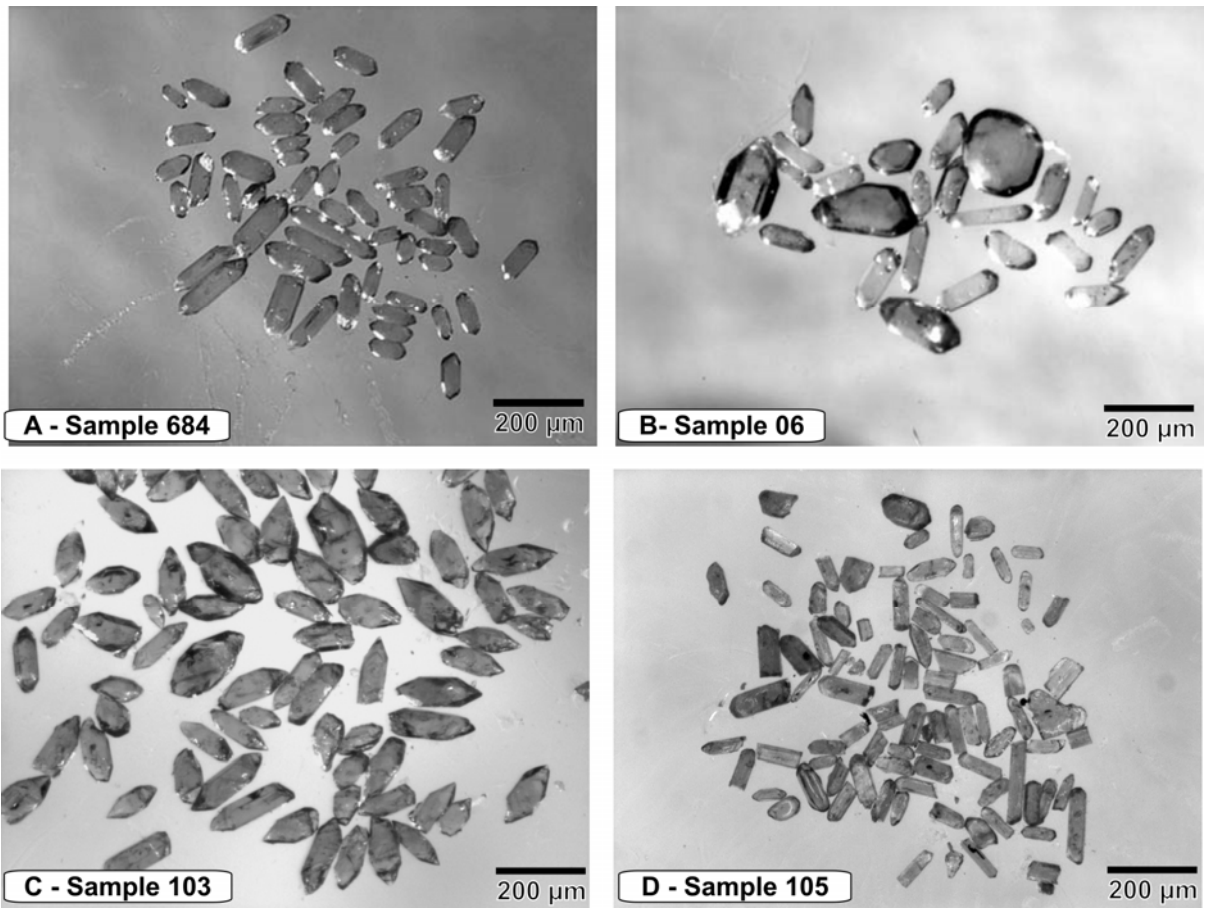


**Figure 3.11** Unabraded zircon populations from each dyke. 200μm scale bar on each photo.

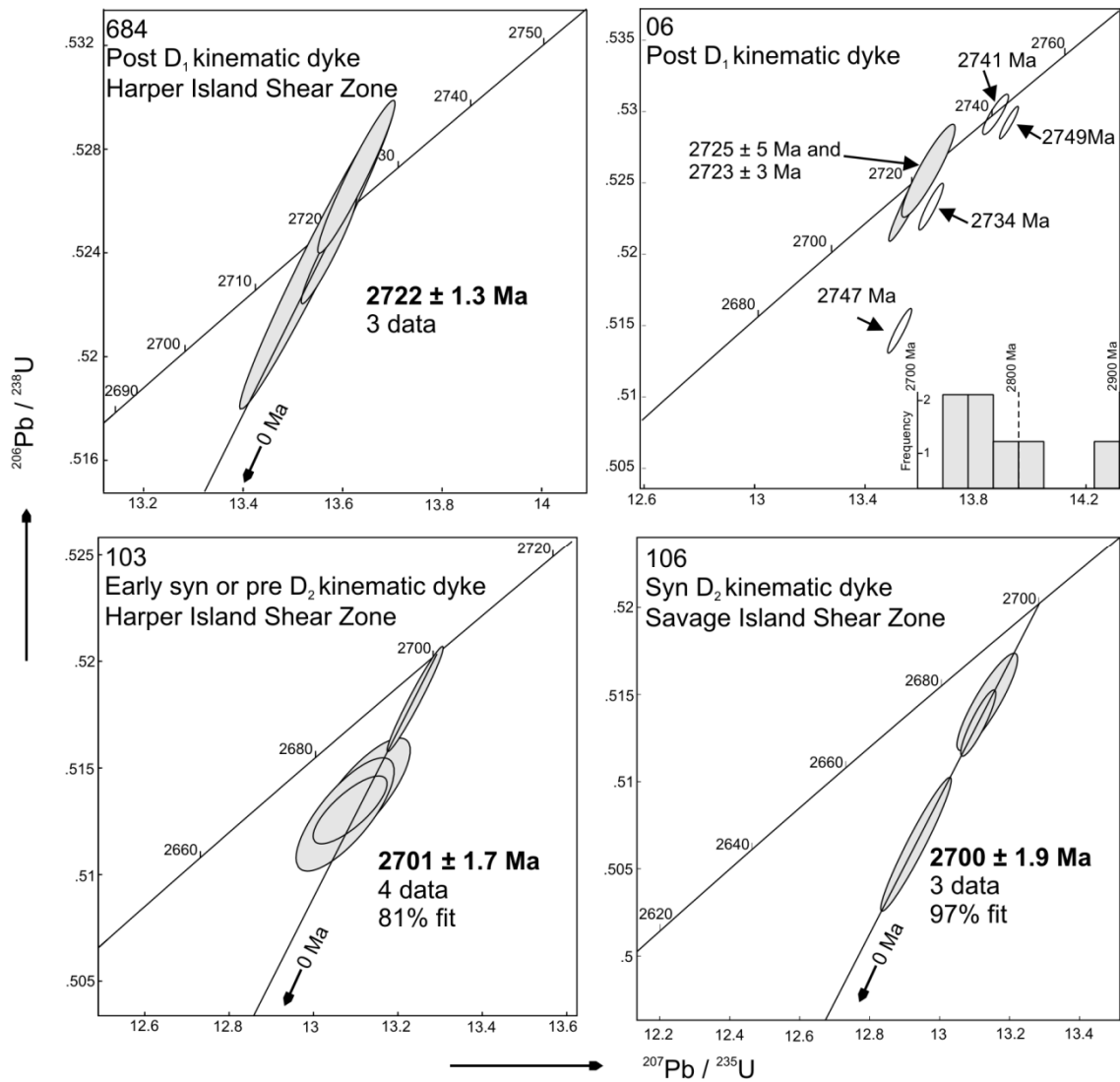


**Figure 3.12** Concordia diagrams showing zircon data for dyke samples in the Island Lake greenstone belt. Inset histogram on sample 06,  $^{206}/^{207}\text{Pb}$  Laser ablation ages.

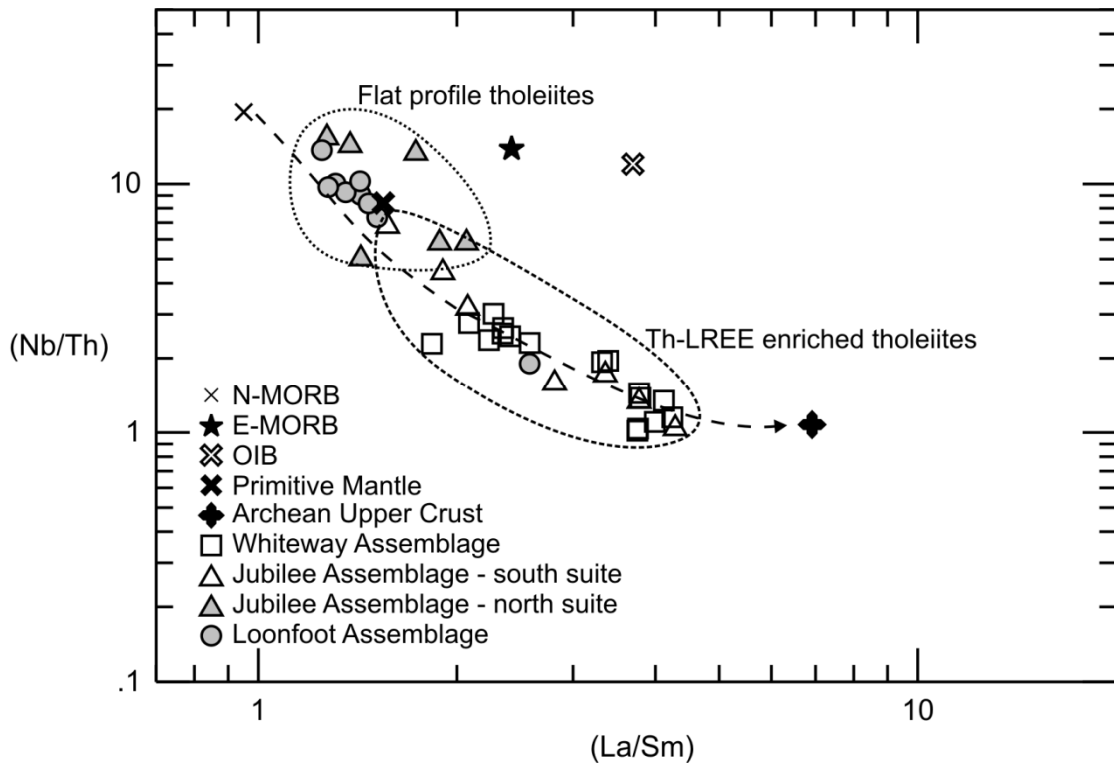


**Figure 3.13** Nb/Th vs. La/Sm plot for all of the mafic volcanic rocks in the Island Lake greenstone belt. The data falls on an array from N-MORB through Primitive mantle to a proposed composition of Archean upper crust, and falls below the E-MORB and OIB data points. Values for N-MORB, E-MORB, OIB, and primitive mantle from Sun and McDonough (1989). Value for Archean upper crust from Condie (1993).

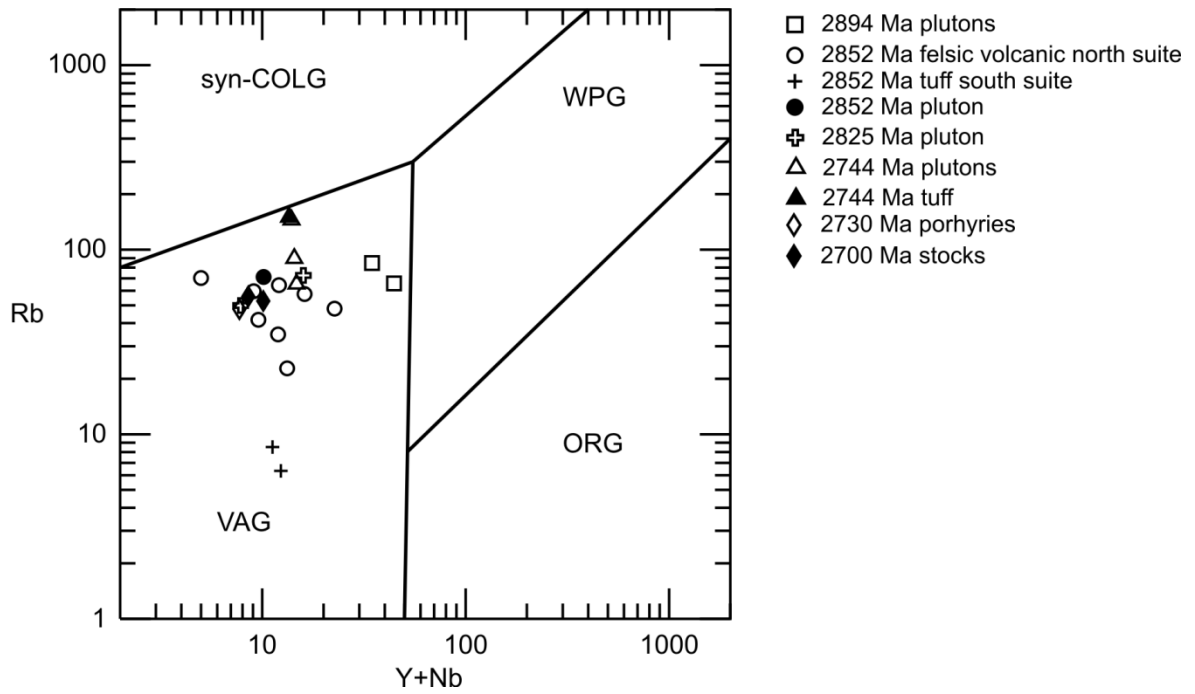


**Figure 3.14** Tectonic discrimination diagram for the felsic intrusive and extrusive rocks in the Island Lake greenstone belt. Fields on diagram after Pearce et al. 1984.

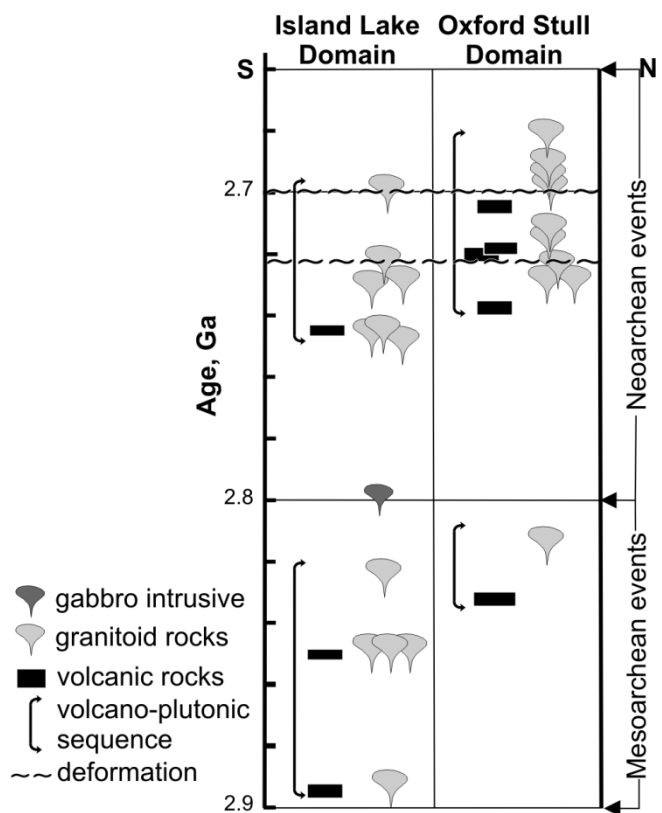


**Figure 3.15** A timeline showing age relationships of volcanic and plutonic rocks in the northern part of the northwestern Superior Province. Ages from Stevenson and Turek (1992); Corfu and Lin (2000); Corkery et al. (2000); Skulski et al. (2000); Rayner and Stott (2005); and Lin et al. (2006).

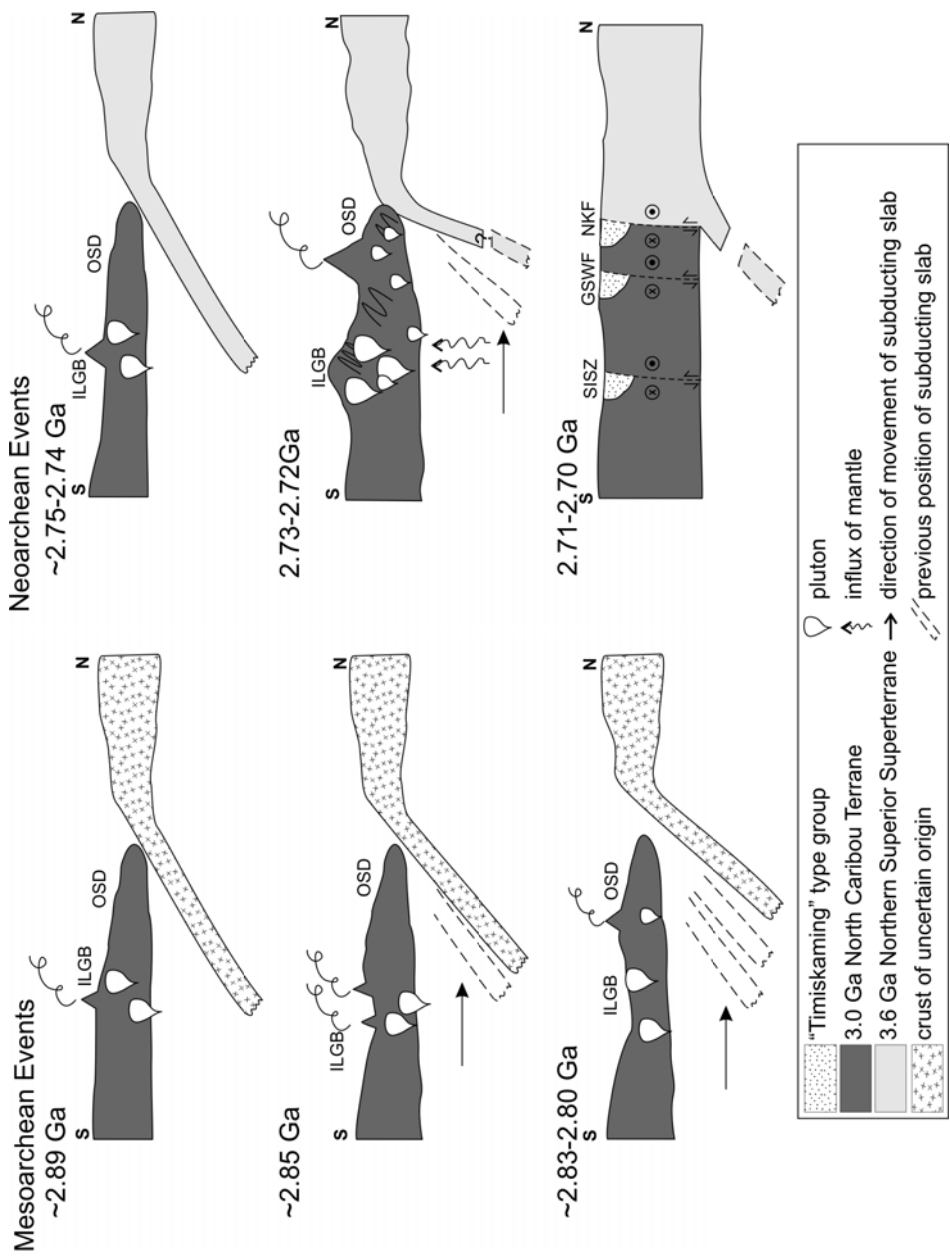


**Figure 3.16** A model for the tectonic evolution of the northwestern Superior Province in the Meso- and Neoproterozoic. Abbreviations: NCT - North Caribou terrane; NSS - Northern Superior superterrane; ILGB - Island Lake greenstone belt, OSD - Oxford Stull domain, SISZ - Savage Island shear zone; GSWF - Gods Lake Narrows-Stull Lake-Wunnummin Lake fault zone; NKF - North Kenyon fault.

**Table 3-1 Lithochemical results**

Assemblage/Rock name	Whiteway Assemblage					
	102-98-692	52-IL-98-30	52-IL-98-31	52-IL-98-32	52-IL-98-34	52-IL-98-36
Sample name						
Rock or Basalt type	TLT	TLT	TLT	TLT	TLT	TLT
age (Ma)	2897	2897	2897	2897	2897	2897
UTM easting	418350	415275	414800	414700	418525	424400
UTM northing	5965250	5966200	5966650	5966950	5968000	5968450
SiO <sub>2</sub> (wt %)	48.39	50.77	52.94	51.87	52.01	57.20
Al <sub>2</sub> O <sub>3</sub>	15.48	13.42	14.55	15.37	15.42	13.57
Fe <sub>2</sub> O <sub>3</sub>	14.25	14.89	13.83	11.90	11.87	10.67
MnO	0.23	0.33	0.23	0.21	0.20	0.20
MgO	4.02	5.07	3.48	7.25	7.26	5.80
CaO	13.43	9.45	8.06	8.99	9.03	8.33
Na <sub>2</sub> O	2.22	3.70	4.70	2.80	2.77	2.36
K <sub>2</sub> O	0.39	0.44	0.40	0.76	0.84	0.93
TiO <sub>2</sub>	1.45	1.75	1.67	0.77	0.78	0.87
P <sub>2</sub> O <sub>5</sub>	0.14	0.18	0.16	0.08	0.08	0.09
LOI	1.22	0.69	0.76	1.00	2.76	1.83
Total	99.33	99.87	99.99	99.00	99.40	100.16
Mg#	36	40	33	55	55	52
Cr (ppm)	172	77	97	120	113	28
Co	42	37	35	44	43	39
Ni	72	30	44	78	81	47
Rb	4.00	8.46	7.41	14.10	13.94	17.36
Sr	279.2	137.7	149.5	122.7	120.2	71.2
Cs	b.d.	0.52	b.d.	b.d.	b.d.	b.d.
Ba	117	178	278	352	348	201
Sc	40	44	42	39	38	36
V	287	289	275	179	176	221
Ta	0.29	0.38	0.37	0.27	0.26	0.34
Hf	2.87	3.53	3.35	2.21	2.14	2.66
Nb	3.33	4.57	4.35	2.64	2.56	3.25
Zr	101.97	134.25	125.20	81.00	78.33	91.11
Th	1.45	1.93	1.91	2.60	2.47	2.95
U	0.38	0.52	0.51	0.84	0.70	0.91
Y	30.23	38.12	35.66	20.28	19.99	21.82
Cu	13.6	35.5	20.2	99.6	95.1	62.3
Zn	68	130	111	77	73	93
Mo	b.d.	2.12	b.d.	4.01	3.00	3.03
Pb	8.30	b.d.	5.02	7.09	9.33	7.64
Bi	b.d.	b.d.	b.d.	b.d.	b.d.	b.d.
La	9.92	9.43	7.66	9.27	9.40	12.96
Ce	23.44	23.19	20.66	20.42	19.45	28.91
Pr	2.98	3.06	2.85	2.40	2.32	3.30
Nd	13.76	14.68	13.72	10.20	9.76	13.64
Sm	3.84	4.21	4.18	2.47	2.50	3.24
Eu	1.33	1.42	1.26	0.83	0.84	0.93
Gd	5.34	5.42	5.35	2.96	2.93	4.02

Assemblage/Rock name	Whiteway Assemblage					
	102-98-692	52-IL-98-30	52-IL-98-31	52-IL-98-32	52-IL-98-34	52-IL-98-36
Sample name	TLT	TLT	TLT	TLT	TLT	TLT
Rock or Basalt type	2897	2897	2897	2897	2897	2897
age (Ma)						
UTM easting	418350	415275	414800	414700	418525	424400
UTM northing	5965250	5966200	5966650	5966950	5968000	5968450
Tb	0.98	0.99	0.98	0.56	0.54	0.71
Dy	5.79	6.34	6.12	3.52	3.41	4.37
Ho	1.21	1.36	1.28	0.73	0.72	0.90
Er	3.51	3.78	3.65	2.12	2.07	2.61
Tm	0.55	0.57	0.54	0.32	0.32	0.38
Yb	3.36	3.79	3.56	2.13	2.05	2.48
Lu	0.48	0.57	0.54	0.32	0.31	0.36
(La/Sm)pm	1.67	1.45	1.19	2.43	2.43	2.58
(Th/La)pm	1.18	1.66	2.01	2.27	2.12	1.84
(Nb/La)pm	0.32	0.47	0.55	0.27	0.26	0.24
(Gd/Yb)pm	1.31	1.18	1.24	1.15	1.18	1.34
(Nb/Th)pm	0.27	0.28	0.27	0.12	0.12	0.13
(La/Yb)pm	2.12	1.79	1.54	3.12	3.29	3.75
eNd						
T						

notes: pm values are from Sun and McDonough, 1989

samples were recalculated to an anhydrous basis

b.d.=below detection limits

All UTM's are zone 15, NAD 27.

Assemblage/Rock name	Whiteway Assemblage						
	52-IL-98-38	52-IL-98-39	JP02-556	JP02-557	JP02-559	JP02-560	JP02-562
Sample name	TLT	TLT	TLT	TLT	TLT	TLT	TLT
Rock or Basalt type	2897	2897	2897	2897	2897	2897	2897
age (Ma)	428950	428850	415134	414057	414365	418052	422522
UTM easting	5967825	5966500	5966521	5967070	5966693	5965207	5967552
UTM northing							
SiO <sub>2</sub> (wt %)	58.05	51.50	48.60	49.27	52.06	51.55	51.45
Al <sub>2</sub> O <sub>3</sub>	13.62	13.68	15.09	15.37	13.74	14.23	13.70
Fe <sub>2</sub> O <sub>3</sub>	9.86	13.40	15.14	13.85	10.10	12.24	15.05
MnO	0.19	0.27	0.38	0.19	0.22	0.26	0.29
MgO	5.29	4.93	5.68	5.49	8.93	10.36	5.26
CaO	9.82	11.26	9.41	10.55	8.99	6.79	8.76
Na <sub>2</sub> O	1.96	2.88	2.61	2.52	2.36	3.37	3.32
K <sub>2</sub> O	0.27	0.11	1.12	1.16	2.91	0.47	0.24
TiO <sub>2</sub>	0.86	1.78	1.72	1.46	0.65	0.67	1.75
P <sub>2</sub> O <sub>5</sub>	0.09	0.18	0.25	0.13	0.05	0.06	0.18
LOI	1.74	3.38	1.60	1.65	4.09	2.70	2.84
Total	99.83	99.55	100.40	99.43	99.68	100.32	99.83
Mg#	52	42	43	44	64	63	41
Cr (ppm)	27	77	101	160	404	516	75
Co	40	44	31	45	42	50	42
Ni	50	37	67	70	108	146	37
Rb	4.39	2.06	24.12	33.97	103.73	8.43	5.66
Sr	71.7	149.9	111.8	235.3	176.9	123.9	106.2
Cs	b.d.	b.d.	0.92	0.46	1.75	0.54	0.25
Ba	91	103	487	325	816	144	89
Sc	36	42	42	41	36	38	44
V	228	334	287	269	175	185	306
Ta	0.34	0.36	0.36	0.29	0.17	0.18	0.37
Hf	2.56	3.55	3.11	2.77	1.54	1.54	3.10
Nb	3.27	4.37	5.34	4.73	3.08	3.10	5.10
Zr	92.60	125.30	117.63	95.34	53.93	54.21	106.93
Th	2.84	1.78	1.93	1.57	1.58	1.60	1.93
U	0.84	0.45	0.54	0.41	0.42	0.46	0.51
Y	21.69	36.37	38.43	30.05	14.71	15.53	35.18
Cu	88.7	149.6	41.0	66.0	114.0	33.0	106.0
Zn	85	130	89	77	65	98	109
Mo	4.45	2.96	6.00	b.d.	9.00	11.00	4.00
Pb	b.d.	b.d.	b.d.	7.00	b.d.	b.d.	b.d.
Bi	b.d.	b.d.	b.d.	b.d.	6.76	b.d.	b.d.
La	14.04	11.37	9.03	8.47	6.72	6.43	10.29
Ce	29.87	28.01	20.96	18.91	13.59	13.21	22.79
Pr	3.39	3.66	2.89	2.56	1.62	1.62	3.11
Nd	13.94	16.68	13.93	12.23	7.10	7.15	15.13
Sm	3.31	4.72	4.33	3.72	1.98	1.94	4.37
Eu	1.06	1.67	1.15	1.12	0.66	0.55	1.43
Gd	3.98	6.57	5.16	4.48	2.26	2.26	5.09

Assemblage/Rock name	Whiteway Assemblage						
	52-IL-98-38	52-IL-98-39	JP02-556	JP02-557	JP02-559	JP02-560	JP02-562
Sample name	TLT	TLT	TLT	TLT	TLT	TLT	TLT
Rock or Basalt type							
age (Ma)	2897	2897	2897	2897	2897	2897	2897
UTM easting	428950	428850	415134	414057	414365	418052	422522
UTM northing	5967825	5966500	5966521	5967070	5966693	5965207	5967552
Tb	0.70	1.20	1.02	0.87	0.43	0.44	0.98
Dy	4.19	6.95	6.38	5.26	2.62	2.68	6.29
Ho	0.84	1.46	1.40	1.13	0.55	0.58	1.33
Er	2.48	4.21	3.97	3.27	1.63	1.65	3.86
Tm	0.36	0.61	0.61	0.51	0.26	0.26	0.61
Yb	2.38	3.97	3.89	3.15	1.53	1.56	3.74
Lu	0.34	0.59	0.59	0.50	0.24	0.26	0.58
(La/Sm)pm	2.74	1.56	1.35	1.47	2.19	2.15	1.52
(Th/La)pm	1.64	1.27	1.73	1.50	1.90	2.02	1.51
(Nb/La)pm	0.22	0.37	0.57	0.54	0.44	0.46	0.48
(Gd/Yb)pm	1.39	1.37	1.10	1.18	1.22	1.20	1.13
(Nb/Th)pm	0.14	0.29	0.33	0.36	0.23	0.23	0.32
(La/Yb)pm	4.24	2.05	1.66	1.93	3.14	2.95	1.97
eNd				0.86	0.58		
T				N/A	N/A		

Assemblage/Rock name Sample name Rock or Basalt type age (Ma) UTM easting UTM northing	Whiteway Assemblage				Jubilee Assemblage - southern suite	
	JP02-563	JP02-564	JP02-565	JP02-566	52-IL-98-02	52-IL-98-10
	TLT	TLT	TLT	TLT	TLT	TLT
	2897	2897	2897	2897	2852	2852
	422916	423492	426889	429535	419050	426733
	5968000	5968530	5968308	5967658	5957550	5957828
SiO <sub>2</sub> (wt %)	57.48	53.23	55.01	50.88	49.91	50.59
Al <sub>2</sub> O <sub>3</sub>	13.35	14.76	14.11	13.70	15.46	14.92
Fe <sub>2</sub> O <sub>3</sub>	9.47	11.04	11.98	15.22	13.26	14.11
MnO	0.17	0.20	0.22	0.26	0.18	0.26
MgO	4.92	6.97	6.12	4.73	6.93	6.84
CaO	13.01	10.18	9.35	10.32	10.70	8.17
Na <sub>2</sub> O	0.46	2.15	1.85	2.86	2.29	3.95
K <sub>2</sub> O	0.21	0.62	0.34	0.16	0.19	0.03
TiO <sub>2</sub>	0.87	0.77	0.92	1.72	1.03	1.03
P <sub>2</sub> O <sub>5</sub>	0.09	0.08	0.09	0.16	0.08	0.09
LOI	2.28	2.08	2.39	3.54	5.30	2.56
Total	100.18	100.27	100.12	99.30	100.26	99.48
Mg#	51	56	50	38	51	49
Cr (ppm)	26	110	32	90	215	174
Co	34	42	40	43	49	55
Ni	42	62	46	37	131	129
Rb	4.62	13.79	8.30	5.48	5.40	b.d.
Sr	78.8	127.9	109.9	94.5	159.4	65.9
Cs	b.d.	b.d.	0.11	0.28	85.72	0.47
Ba	81	162	99	99	45	53
Sc	35	38	38	41	39	46
V	203	192	224	281	269	288
Ta	0.34	0.29	0.34	0.37	0.18	0.16
Hf	2.39	2.15	2.58	2.98	1.62	1.70
Nb	4.63	3.90	5.02	4.85	2.71	2.54
Zr	85.04	72.23	95.69	117.93	50.53	51.96
Th	3.36	2.71	3.74	1.93	0.61	0.80
U	0.93	0.80	1.04	0.51	0.13	0.20
Y	20.99	19.21	24.58	35.72	21.17	22.55
Cu	66.0	83.0	98.0	108.0	199.9	144.1
Zn	52	57	65	75	93	101
Mo	3.91	7.00	2.00	6.00	6.16	b.d.
Pb	b.d.	7.00	b.d.	b.d.	b.d.	8.72
Bi	b.d.	b.d.	b.d.	b.d.	b.d.	b.d.
La	10.72	9.81	13.70	9.50	4.51	4.85
Ce	22.04	19.26	26.92	21.01	10.77	10.73
Pr	2.62	2.32	3.11	3.38	1.51	1.49
Nd	10.98	9.85	13.31	15.06	7.45	7.29
Sm	2.82	2.59	3.32	4.05	2.37	2.33
Eu	0.85	0.82	0.94	1.49	1.14	0.80
Gd	3.12	2.83	3.53	5.32	3.25	3.43

Assemblage/Rock name	Whiteway Assemblage				Jubilee Assemblage - southern suite	
	JP02-563	JP02-564	JP02-565	JP02-566	52-IL-98-02	52-IL-98-10
Sample name	TLT	TLT	TLT	TLT	TLT	TLT
Rock or Basalt type	TLT	TLT	TLT	TLT	TLT	TLT
age (Ma)	2897	2897	2897	2897	2852	2852
UTM easting	422916	423492	426889	429535	419050	426733
UTM northing	5968000	5968530	5968308	5967658	5957550	5957828
Tb	0.61	0.56	0.68	0.97	0.60	0.66
Dy	3.62	3.38	4.11	6.38	3.62	3.92
Ho	0.78	0.74	0.88	1.33	0.77	0.86
Er	2.27	2.13	2.50	3.76	2.20	2.58
Tm	0.35	0.33	0.40	0.57	0.33	0.39
Yb	2.21	2.04	2.40	3.52	2.17	2.41
Lu	0.34	0.33	0.37	0.55	0.33	0.38
(La/Sm)pm	2.45	2.44	2.66	1.52	1.23	1.34
(Th/La)pm	2.54	2.23	2.21	1.64	1.10	1.34
(Nb/La)pm	0.42	0.38	0.35	0.49	0.58	0.51
(Gd/Yb)pm	1.17	1.15	1.22	1.25	1.24	1.17
(Nb/Th)pm	0.16	0.17	0.16	0.30	0.53	0.38
(La/Yb)pm	3.48	3.46	4.09	1.94	1.49	1.44
eNd						
T						

Assemblage/Rock name	Jubilee Assemblage - southern suite				
	52-IL-98-44	52-IL-98-46	JP01-82-G	JP02-463	JP02-549
Sample name	TLT	TLT	TLT	TLT	TLT
Rock or Basalt type	2852	2852	2852	2852	2852
age (Ma)	400350	397100	386468	383992	397856
UTM easting	5958100	5960550	5974061	5976927	5960896
UTM northing					
SiO <sub>2</sub> (wt %)	51.50	50.70	53.98	54.45	51.20
Al <sub>2</sub> O <sub>3</sub>	14.78	13.16	11.94	12.99	13.72
Fe <sub>2</sub> O <sub>3</sub>	13.10	11.20	10.86	11.49	11.56
MnO	0.19	0.18	0.21	0.30	0.33
MgO	5.68	9.99	7.92	8.21	8.48
CaO	11.06	11.85	12.23	9.11	12.21
Na <sub>2</sub> O	2.07	1.88	1.92	2.71	1.39
K <sub>2</sub> O	0.46	0.34	0.25	0.05	0.36
TiO <sub>2</sub>	1.07	0.64	0.62	0.65	0.69
P <sub>2</sub> O <sub>5</sub>	0.08	0.06	0.06	0.06	0.06
LOI	1.55	1.54	2.08	10.89	1.87
Total	100.25	100.10	99.39	99.06	100.39
Mg#	46	64	59	59	59
Cr (ppm)	233	965	594	341	425
Co	55	65	53	41	45
Ni	124	280	138	117	131
Rb	9.16	7.30	5.79	b.d.	10.18
Sr	141.5	106.7	247.8	119.7	142.8
Cs	0.25	0.41	1.16	0.30	0.30
Ba	78	85	98	6	97
Sc	43	35	38	36	36
V	312	210	217	184	199
Ta	0.17	0.18	0.21	0.23	0.15
Hf	1.78	1.54	1.48	1.67	1.36
Nb	2.79	2.71	2.56	2.86	2.62
Zr	53.77	50.62	49.11	56.40	46.25
Th	0.41	1.71	1.93	2.76	1.53
U	0.10	0.41	0.57	0.80	0.45
Y	23.31	17.17	15.28	14.22	15.24
Cu	152.3	107.1	102.9	71.0	84.0
Zn	105	83	75	59	49
Mo	b.d.	3.42	b.d.	3.00	5.00
Pb	8.70	7.13	b.d.	8.00	10.00
Bi	b.d.	b.d.	b.d.	b.d.	b.d.
La	3.82	5.40	6.92	8.07	6.80
Ce	9.49	11.33	12.95	15.18	12.96
Pr	1.41	1.43	1.54	1.73	1.58
Nd	7.39	6.34	6.48	7.16	7.33
Sm	2.43	1.92	1.83	1.88	2.03
Eu	1.00	0.69	0.65	0.57	0.70
Gd	3.52	2.56	2.42	2.12	2.30

Assemblage/Rock name	Jubilee Assemblage - southern suite				
	52-IL-98-44	52-IL-98-46	JP01-82-G	JP02-463	JP02-549
Sample name	44	46	G	463	549
Rock or Basalt type	TLT	TLT	TLT	TLT	TLT
age (Ma)	2852	2852	2852	2852	2852
UTM easting	400350	397100	386468	383992	397856
UTM northing	5958100	5960550	5974061	5976927	5960896
Tb	0.67	0.48	0.44	0.41	0.45
Dy	4.03	2.82	2.57	2.54	2.64
Ho	0.87	0.62	0.56	0.54	0.58
Er	2.57	1.82	1.58	1.52	1.66
Tm	0.39	0.27	0.24	0.24	0.26
Yb	2.47	1.70	1.48	1.43	1.59
Lu	0.39	0.27	0.22	0.23	0.25
(La/Sm)pm	1.02	1.82	2.44	2.77	2.17
(Th/La)pm	0.87	2.57	2.25	2.76	1.81
(Nb/La)pm	0.70	0.48	0.36	0.34	0.37
(Gd/Yb)pm	1.18	1.24	1.35	1.23	1.19
(Nb/Th)pm	0.81	0.19	0.16	0.12	0.20
(La/Yb)pm	1.11	2.27	3.35	4.05	3.07
eNd	-1.17			-0.29	
T	N/A			N/A	

Assemblage/Rock name	Jubilee Assemblage - northern suite					
	102-98-809	102-98-812	JP01-246-G	JP02-266	JP02-362	JP02-375
Sample name	FPT	FPT	FPT	FPT	FPT	FPT
Rock or Basalt type	FPT	FPT	FPT	FPT	FPT	FPT
age (Ma)	2852	2852	2852	2852	2852	2852
UTM easting	385495	385085	388341	381228	381490	390401
UTM northing	5967628	5966441	5966995	5969270	5968387	5965761
SiO <sub>2</sub> (wt %)	51.74	51.40	52.56	49.91	53.46	51.80
Al <sub>2</sub> O <sub>3</sub>	15.11	14.83	15.51	15.25	14.86	14.36
Fe <sub>2</sub> O <sub>3</sub>	9.14	10.76	8.73	11.16	8.87	9.61
MnO	0.21	0.13	0.10	0.18	0.17	0.18
MgO	7.91	8.16	7.74	9.71	8.39	8.93
CaO	13.63	11.33	12.23	11.63	11.11	12.40
Na <sub>2</sub> O	1.64	2.19	2.43	1.59	2.44	2.17
K <sub>2</sub> O	0.07	0.72	0.16	0.05	0.16	0.08
TiO <sub>2</sub>	0.46	0.45	0.48	0.48	0.48	0.44
P <sub>2</sub> O <sub>5</sub>	0.07	0.05	0.04	0.04	0.04	0.04
LOI	1.78	1.60	1.93	1.95	1.57	4.63
Total	99.71	99.93	100.20	99.61	99.99	99.17
Mg#	63	60	64	63	65	65
Cr (ppm)	416	407	433	435	412	403
Co	40	35	31	45	49	43
Ni	102	76	101	84	98	86
Rb	1.13	33.96	5.77	1.82	5.98	b.d.
Sr	87.3	112.9	120.8	79.7	78.6	157.2
Cs	b.d.	0.52	0.17	b.d.	0.30	b.d.
Ba	13	99	23	25	48	3
Sc	48	47	48	47	46	44
V	221	218	226	225	213	189
Ta	0.08	0.07	0.06	0.06	0.06	0.05
Hf	0.66	0.67	0.74	0.79	0.72	0.64
Nb	1.29	1.23	1.26	3.85	3.28	2.59
Zr	19.77	20.92	23.53	28.04	26.06	21.37
Th	0.22	0.21	0.25	0.25	0.25	0.18
U	0.06	0.14	0.21	0.06	0.09	0.06
Y	12.38	12.86	12.38	12.30	11.75	10.61
Cu	9.9	b.d.	b.d.	84.0	100.0	b.d.
Zn	73	50	60	49	42	42
Mo	3.90	4.98	3.15	b.d.	9.00	2.00
Pb	22.48	b.d.	b.d.	b.d.	b.d.	b.d.
Bi	0.22	0.32	0.20	b.d.	b.d.	0.47
La	1.91	2.20	1.51	1.12	1.69	0.88
Ce	4.21	5.12	3.81	3.09	4.10	2.17
Pr	0.57	0.67	0.56	0.47	0.57	0.32
Nd	2.94	3.15	2.95	2.48	2.86	1.76
Sm	1.02	1.06	1.05	0.88	0.97	0.64
Eu	0.37	0.55	0.45	0.36	0.39	0.24
Gd	1.54	1.65	1.61	1.43	1.35	1.08

Assemblage/Rock name	Jubilee Assemblage - northern suite					
	102-98-809	102-98-812	JP01-246-G	JP02-266	JP02-362	JP02-375
Sample name	FPT	FPT	FPT	FPT	FPT	FPT
Rock or Basalt type	FPT	FPT	FPT	FPT	FPT	FPT
age (Ma)	2852	2852	2852	2852	2852	2852
UTM easting	385495	385085	388341	381228	381490	390401
UTM northing	5967628	5966441	5966995	5969270	5968387	5965761
Tb	0.31	0.32	0.33	0.31	0.29	0.25
Dy	1.98	2.07	2.05	1.90	1.88	1.67
Ho	0.44	0.46	0.45	0.44	0.42	0.39
Er	1.33	1.38	1.33	1.31	1.25	1.18
Tm	0.21	0.22	0.20	0.22	0.20	0.19
Yb	1.35	1.37	1.29	1.38	1.26	1.22
Lu	0.22	0.21	0.20	0.21	0.20	0.19
(La/Sm)pm	1.22	1.34	0.92	0.82	1.12	0.89
(Th/La)pm	0.94	0.78	1.35	1.82	1.18	1.67
(Nb/La)pm	0.65	0.54	0.81	3.32	1.87	2.83
(Gd/Yb)pm	0.95	1.00	1.03	0.85	0.88	0.73
(Nb/Th)pm	0.69	0.69	0.60	1.83	1.58	1.70
(La/Yb)pm	1.02	1.16	0.84	0.58	0.96	0.52
eNd			0.91	-1.83		
T			N/A	N/A		

Assemblage/Rock name	Loonfoot Assemblage						
	52-IL-98-11	52-IL-98-12	52-IL-98-13	52-IL-98-24	52-IL-98-25	52-IL-98-26	JP02-569
Sample name	FPT	FPT	FPT	FPT	FPT	FPT	FPT
Rock or Basalt type	2744	2744	2744	2744	2744	2744	2744
age (Ma)							
UTM easting	426750	426950	427200	426750	428325	428075	427441
UTM northing	5958650	5958850	5959925	5963700	5964750	5964925	5965228
SiO <sub>2</sub> (wt %)	53.93	56.17	58.21	52.16	55.10	52.24	51.37
Al <sub>2</sub> O <sub>3</sub>	15.54	14.19	15.89	14.31	15.73	14.54	14.83
Fe <sub>2</sub> O <sub>3</sub>	8.82	11.53	8.34	15.00	11.66	13.20	13.45
MnO	0.19	0.23	0.16	0.21	0.19	0.21	0.20
MgO	4.69	6.26	4.74	4.70	5.90	6.96	8.56
CaO	13.30	7.65	9.04	9.74	7.39	8.85	10.36
Na <sub>2</sub> O	2.62	3.12	2.68	2.06	2.94	2.91	0.46
K <sub>2</sub> O	b.d.	b.d.	b.d.	0.63	0.14	b.d.	0.02
TiO <sub>2</sub>	0.88	0.80	0.91	1.08	0.90	1.03	0.69
P <sub>2</sub> O <sub>5</sub>	0.08	0.06	0.07	0.10	0.08	0.10	0.05
LOI	7.01	4.69	3.97	10.59	8.73	4.84	8.01
Total	100.19	99.80	100.21	99.77	99.64	98.87	99.10
Mg#	51	52	53	38	50	51	56
Cr (ppm)	189	173	193	28	190	153	288
Co	47	46	55	56	54	49	48
Ni	108	119	134	50	140	118	147
Rb	b.d.	b.d.	b.d.	20.46	3.94	b.d.	b.d.
Sr	136.5	69.8	114.5	66.6	78.9	126.1	238.1
Cs	0.26	0.30	0.21	1.00	0.78	0.19	0.36
Ba	33	30	26	192	44	16	5
Sc	44	39	44	37	44	43	39
V	284	248	282	272	291	323	221
Ta	0.11	0.12	0.12	0.20	0.11	0.16	0.08
Hf	1.29	1.14	1.35	1.86	1.25	1.63	0.85
Nb	1.87	1.78	2.01	2.82	1.90	2.58	1.94
Zr	38.70	35.63	40.74	60.97	39.83	51.31	27.73
Th	0.21	0.18	0.27	1.48	0.21	0.31	0.14
U	0.05	0.06	0.16	0.40	0.06	0.09	0.05
Y	18.38	17.39	18.11	19.36	20.62	23.71	14.77
Cu	159.4	135.7	160.3	166.5	164.7	109.9	141.0
Zn	66	114	96	102	105	102	58
Mo	b.d.	5.02	5.56	b.d.	4.35	3.01	7.00
Pb	b.d.	b.d.	b.d.	b.d.	b.d.	b.d.	b.d.
Bi	b.d.	b.d.	b.d.	b.d.	b.d.	b.d.	b.d.
La	2.70	2.15	2.96	5.09	2.62	3.51	1.75
Ce	6.84	5.51	7.49	10.76	6.69	8.79	4.60
Pr	1.04	0.85	1.12	1.38	1.00	1.32	0.72
Nd	5.51	4.49	5.82	6.36	5.40	7.02	3.95
Sm	1.89	1.64	1.95	1.97	1.93	2.39	1.40
Eu	0.79	0.60	0.72	0.72	0.79	0.63	0.72
Gd	2.80	2.37	2.84	2.75	2.86	3.36	1.86

Assemblage/Rock name	Loonfoot Assemblage						
	52-IL-98-11	52-IL-98-12	52-IL-98-13	52-IL-98-24	52-IL-98-25	52-IL-98-26	JP02-569
Sample name	FPT	FPT	FPT	FPT	FPT	FPT	FPT
Rock or Basalt type	2744	2744	2744	2744	2744	2744	2744
age (Ma)	426750	426950	427200	426750	428325	428075	427441
UTM easting	5958650	5958850	5959925	5963700	5964750	5964925	5965228
UTM northing							
Tb	0.54	0.46	0.52	0.54	0.55	0.65	0.39
Dy	3.20	2.85	3.16	3.33	3.42	3.95	2.46
Ho	0.69	0.63	0.68	0.73	0.76	0.86	0.54
Er	2.01	1.83	1.95	2.19	2.22	2.48	1.54
Tm	0.30	0.28	0.29	0.34	0.34	0.39	0.25
Yb	1.88	1.78	1.83	2.23	2.16	2.40	1.51
Lu	0.29	0.28	0.28	0.35	0.34	0.38	0.23
(La/Sm)pm	0.92	0.85	0.98	1.67	0.88	0.95	0.81
(Th/La)pm	0.62	0.67	0.75	2.35	0.63	0.71	0.65
(Nb/La)pm	0.67	0.80	0.66	0.53	0.70	0.71	1.07
(Gd/Yb)pm	1.23	1.10	1.28	1.02	1.10	1.16	1.02
(Nb/Th)pm	1.08	1.20	0.88	0.23	1.11	1.00	1.63
(La/Yb)pm	1.03	0.87	1.16	1.64	0.87	1.05	0.83
eNd		2.08					
T		N/A					

Assemblage/Rock name	Loonfoot Assemblage		Cochrane Bay		jubilee southern suite	
	Sample name	JP02-570	JP02-571	JP00-31	JP00-33-G	102-98-617G
Rock or Basalt type	FPT	FPT	diorite	leucotonalite	andesitic tuff	massive dacite
age (Ma)	2744	2744	2894	2894	2852	2852
UTM easting	426153	424720	394203	398318	430535	427002
UTM northing	5963553	5962919	5977216	5979790	5956498	5956774
SiO <sub>2</sub> (wt %)	50.12	52.98	75.72	72.21	62.73	64.88
Al <sub>2</sub> O <sub>3</sub>	8.67	14.27	12.72	13.34	15.53	15.40
Fe <sub>2</sub> O <sub>3</sub>	12.05	12.82	2.43	4.21	6.64	6.28
MnO	0.20	0.21	0.04	0.07	0.09	0.07
MgO	16.17	6.78	0.37	1.01	4.97	3.51
CaO	10.93	9.61	1.04	2.19	5.52	4.79
Na <sub>2</sub> O	1.11	2.26	3.84	3.77	3.16	4.18
K <sub>2</sub> O	0.08	0.08	3.51	2.62	0.64	0.31
TiO <sub>2</sub>	0.62	0.93	0.28	0.48	0.57	0.46
P <sub>2</sub> O <sub>5</sub>	0.04	0.07	0.06	0.11	0.17	0.12
LOI	3.13	10.18	1.1	0.82	2.74	1.98
Total	99.23	99.66	100.35	100.29	100.25	100.07
Mg#	73	51	23	32	60	53
Cr (ppm)	1590	128	b.d.	b.d.	166	112
Co	62	44	3	7	23	21
Ni	317	103	b.d.	b.d.	136	93
Rb	b.d.	3.42	84.59	65.65	6.33	8.52
Sr	104.0	99.3	90	135	419	467
Cs	0.35	1.16	2.16	4.56	b.d.	b.d.
Ba	27	24	591	677	132	143
Sc	52	44	5	8	15	12
V	220	259	13	41	106	78
Ta	0.06	0.10	1.13	1.10	0.24	0.23
Hf	0.90	1.27	5.76	8.58	2.61	2.78
Nb	1.64	2.42	9.18	9.76	2.09	2.29
Zr	27.94	41.88	207	337	99	110
Th	0.17	0.24	23.26	14.12	1.49	1.23
U	0.16	0.08	5.79	3.54	0.38	0.35
Y	11.65	15.64	25.49	34.68	10.26	8.94
Cu	68.0	193.0	b.d.	17.1	34.2	18.7
Zn	50	71	b.d.	50	80	34
Mo	b.d.	5.00	8.00	4.09	4.31	2.20
Pb	b.d.	b.d.	20.00	6.72	8.07	b.d.
Bi	b.d.	b.d.	b.d.	b.d.	b.d.	b.d.
La	1.61	2.32	31.83	38.04	15.58	10.27
Ce	4.19	6.00	61.17	77.69	37.01	23.13
Pr	0.65	0.92	6.34	8.02	4.45	2.71
Nd	3.62	4.92	20.89	28.98	18.02	10.98
Sm	1.26	1.63	3.70	5.68	3.20	2.02
Eu	0.47	0.71	0.80	1.05	1.05	0.70
Gd	1.76	2.14	4.00	5.73	2.82	1.88

Assemblage/Rock name	Loonfoot Assemblage		Cochrane Bay		jubilee southern suite	
	Sample name	JP02-570	JP02-571	JP00-31	JP00-33-G	102-98-617G
Rock or Basalt type	FPT	FPT	diorite	leucotonalite	andesitic tuff	massive dacite
age (Ma)	2744	2744	2894	2894	2852	2852
UTM easting	426153	424720	394203	398318	430535	427002
UTM northing	5963553	5962919	5977216	5979790	5956498	5956774
Tb	0.36	0.43	0.67	1.05	0.40	0.29
Dy	2.24	2.85	3.98	6.23	2.12	1.62
Ho	0.48	0.62	0.89	1.31	0.40	0.32
Er	1.31	1.77	2.95	3.96	1.16	0.91
Tm	0.20	0.28	0.47	0.63	0.16	0.14
Yb	1.13	1.71	2.98	3.99	1.08	0.93
Lu	0.17	0.27	0.47	0.60	0.16	0.14
(La/Sm)pm	0.83	0.92	5.56	4.33	3.15	3.28
(Th/La)pm	0.85	0.82	5.91	3.00	0.77	0.97
(Nb/La)pm	0.98	1.00	0.28	0.25	0.13	0.21
(Gd/Yb)pm	1.29	1.03	1.11	1.19	2.15	1.67
(Nb/Th)pm	1.16	1.22	0.05	0.08	0.17	0.22
(La/Yb)pm	1.02	0.97	7.68	6.84	10.31	7.91
eNd				-0.63		
T				3.14		

Assemblage/Rock name Sample name Rock or Basalt type age (Ma) UTM easting UTM northing	jubilee - northern suite				
	102-98-807	102-98-816	52-IL-98-50	52-IL-98-53	JP02-389
	tuff	tuff	dacite	tuff	tuff
	2852	2852	2852	2852	2852
	385156	385085	399858	396842	384198
	5968280	5966441	5963964	5964236	5966544
SiO <sub>2</sub> (wt %)	69.83	63.84	69.54	70.76	66.29
Al <sub>2</sub> O <sub>3</sub>	17.09	17.32	15.74	16.30	16.75
Fe <sub>2</sub> O <sub>3</sub>	1.68	4.51	3.13	2.81	4.90
MnO	0.08	0.09	0.02	0.05	0.06
MgO	1.69	1.44	2.25	0.43	2.02
CaO	2.35	5.71	0.65	2.33	2.29
Na <sub>2</sub> O	3.47	4.34	5.65	5.12	5.98
K <sub>2</sub> O	3.46	2.07	2.60	1.67	0.97
TiO <sub>2</sub>	0.26	0.54	0.35	0.42	0.62
P <sub>2</sub> O <sub>5</sub>	0.09	0.15	0.10	0.10	0.13
LOI	2.6	3.5	1.34	2.9	2.15
Total	100.05	99.92	99.77	100.25	100.3
Mg#	67	39	59	23	45
Cr (ppm)	b.d.	b.d.	b.d.	b.d.	26
Co	3	12	8	7	11
Ni	b.d.	b.d.	b.d.	b.d.	27
Rb	70.15	57.51	59.50	41.69	22.72
Sr	130	350	151	110	358
Cs	1.02	1.81	3.31	1.63	0.69
Ba	366	533	693	516	394
Sc	4	6	6	6	7
V	34	46	45	54	48
Ta	0.23	0.32	0.46	0.38	0.47
Hf	2.44	3.67	3.08	2.84	3.47
Nb	1.53	2.98	3.32	3.09	4.84
Zr	94	134	116	107	136
Th	5.31	3.96	5.80	6.14	7.57
U	1.94	1.43	1.83	1.27	1.99
Y	3.48	13.18	5.76	6.48	8.41
Cu	b.d.	26.7	23.3	33.9	46.0
Zn	62	76	37	39	78
Mo	2.52	2.23	b.d.	b.d.	4.00
Pb	16.46	14.38	b.d.	7.12	11.00
Bi	b.d.	b.d.	b.d.	b.d.	b.d.
La	16.84	16.86	20.10	20.23	18.17
Ce	31.77	34.17	37.10	37.68	36.32
Pr	3.14	3.67	3.57	3.73	3.64
Nd	10.88	14.09	12.20	13.19	12.41
Sm	1.75	3.00	2.09	2.24	2.31
Eu	0.58	1.03	0.68	0.72	0.87
Gd	1.18	3.00	1.68	1.79	2.07

Assemblage/Rock name	jubilee - northern suite				
	102-98-807	102-98-816	52-IL-98-50	52-IL-98-53	JP02-389
Sample name	tuff	tuff	dacite	tuff	tuff
Rock or Basalt type	tuff	tuff	dacite	tuff	tuff
age (Ma)	2852	2852	2852	2852	2852
UTM easting	385156	385085	399858	396842	384198
UTM northing	5968280	5966441	5963964	5964236	5966544
Tb	0.15	0.47	0.24	0.26	0.29
Dy	0.71	2.55	1.19	1.35	1.57
Ho	0.12	0.49	0.21	0.23	0.31
Er	0.33	1.42	0.62	0.67	0.81
Tm	b.d.	0.21	0.08	0.09	0.11
Yb	0.29	1.30	0.52	0.57	0.71
Lu	0.04	0.18	0.07	0.08	0.11
(La/Sm)pm	6.21	3.63	6.22	5.83	5.07
(Th/La)pm	2.55	1.90	2.33	2.45	3.37
(Nb/La)pm	0.09	0.17	0.16	0.15	0.26
(Gd/Yb)pm	3.34	1.91	2.68	2.60	2.41
(Nb/Th)pm	0.03	0.09	0.07	0.06	0.08
(La/Yb)pm	41.37	9.33	27.79	25.47	18.32
eNd					
T					

Assemblage/Rock name Sample name	Jubilee - northern suite			Jubilee JP02-289 granodiorite
	JP02-425	JP02-807	JP02-839	
Rock or Basalt type	tuff	felsic extrusive	tuff	
age (Ma)	2852	2852	2852	2852
UTM easting	383881	385023	379818	385602
UTM northing	5977554	5968322	5978878	5967142
SiO <sub>2</sub> (wt %)	74.27	68.32	71.37	68.98
Al <sub>2</sub> O <sub>3</sub>	16.18	15.94	16.04	16.02
Fe <sub>2</sub> O <sub>3</sub>	1.77	3.89	2.27	3.29
MnO	0.02	0.09	0.06	0.04
MgO	1.04	2.18	1.42	1.34
CaO	2.34	2.39	1.48	2.95
Na <sub>2</sub> O	1.86	5.28	2.26	4.84
K <sub>2</sub> O	1.92	1.40	4.55	2.09
TiO <sub>2</sub>	0.49	0.40	0.46	0.37
P <sub>2</sub> O <sub>5</sub>	0.10	0.10	0.11	0.08
LOI	2.01	2.05	3.55	1.67
Total	99.75	99.54	100.26	100.25
Mg#	54	53	55	45
Cr (ppm)	b.d.	35	26	b.d.
Co	3	10	12	8
Ni	b.d.	22	22	b.d.
Rb	47.88	34.70	64.26	71.16
Sr	109	351	33	337
Cs	5.31	1.11	1.69	3.01
Ba	232	455	638	645
Sc	8	6	7	5
V	29	51	59	45
Ta	0.81	0.49	0.33	0.36
Hf	5.15	3.22	3.26	2.80
Nb	7.80	4.52	3.70	4.02
Zr	205	124	136	101
Th	10.49	7.29	7.06	7.65
U	3.15	2.04	1.93	1.88
Y	14.89	7.45	8.39	6.14
Cu	b.d.	15.0	20.0	86.0
Zn	b.d.	182	37	46
Mo	6.00	4.00	4.00	6.00
Pb	b.d.	20.00	b.d.	15.00
Bi	b.d.	b.d.	b.d.	b.d.
La	24.46	23.44	22.88	16.89
Ce	46.25	40.10	40.29	28.29
Pr	4.80	3.82	3.87	2.95
Nd	16.20	13.27	13.15	10.93
Sm	2.71	2.39	2.44	1.92
Eu	1.11	0.73	0.76	0.56
Gd	2.74	1.76	2.05	1.58

Assemblage/Rock name Sample name	Jubilee - northern suite			Jubilee
	JP02-425	JP02-807	JP02-839	JP02-289
Rock or Basalt type	tuff	felsic extrusive	tuff	granodiorite
age (Ma)	2852	2852	2852	2852
UTM easting	383881	385023	379818	385602
UTM northing	5977554	5968322	5978878	5967142
Tb	0.44	0.27	0.30	0.23
Dy	2.42	1.45	1.54	1.11
Ho	0.53	0.25	0.30	0.22
Er	1.55	0.68	0.82	0.55
Tm	0.22	0.10	0.11	0.08
Yb	1.35	0.61	0.74	0.50
Lu	0.22	0.09	0.11	0.08
(La/Sm)pm	5.82	6.34	6.05	5.69
(Th/La)pm	3.47	2.52	2.49	3.66
(Nb/La)pm	0.31	0.19	0.16	0.23
(Gd/Yb)pm	1.68	2.40	2.30	2.59
(Nb/Th)pm	0.09	0.07	0.06	0.06
(La/Yb)pm	13.03	27.76	22.29	24.08
eNd	-0.32		0.14	-0.75
T	3.17		3.13	3.19

Assemblage/Rock name	southern pluton		Loonfoot JP01-105	Bella Lake	
	52-IL-98-01	JP02-419		JP01-176- G	JP01-67- G
Sample name	tonalite	tonalite	tuff	tonalite	tonalite
Rock or Basalt type	gneiss	gneiss			
age (Ma)	2825	2825	2744	2744	2744
UTM easting	417463	417458	425563	387261	390580
UTM northing	5956678	5956678	5961134	5982855	5975736
SiO <sub>2</sub> (wt %)	75.00	73.41	70.97	68.40	69.22
Al <sub>2</sub> O <sub>3</sub>	13.08	14.65	15.12	15.37	15.13
Fe <sub>2</sub> O <sub>3</sub>	3.30	2.02	2.98	3.51	3.70
MnO	0.04	0.04	0.07	0.06	0.06
MgO	1.72	0.56	1.15	1.61	1.65
CaO	1.00	2.55	3.73	2.76	2.59
Na <sub>2</sub> O	3.00	4.81	1.36	4.26	4.27
K <sub>2</sub> O	2.37	1.69	4.22	3.47	2.83
TiO <sub>2</sub>	0.40	0.21	0.30	0.39	0.40
P <sub>2</sub> O <sub>5</sub>	0.09	0.07	0.11	0.16	0.14
LOI	1.2	0.57	4.91	0.83	1.99
Total	100.19	99.89	99.17	99.64	100.28
Mg#	51	36	43	48	47
Cr (ppm)	82	b.d.	44	b.d.	b.d.
Co	12	3	4	7	8
Ni	45	b.d.	b.d.	b.d.	b.d.
Rb	72.47	49.84	149.84	89.43	65.11
Sr	167	397	95	503	535
Cs	3.86	2.14	16.27	3.54	4.73
Ba	489	578	934	1170	1110
Sc	7	4	5	6	7
V	43	15	38	49	57
Ta	0.58	0.35	0.39	0.52	0.56
Hf	4.29	2.47	2.95	3.96	4.52
Nb	5.19	3.83	5.07	4.12	4.28
Zr	176	86	109	143	168
Th	10.40	4.63	6.71	13.92	11.25
U	3.38	1.08	2.06	1.96	2.54
Y	10.74	4.00	8.49	10.26	10.47
Cu	40.6	0.0	17.0	38.1	11.1
Zn	81	52	94	48	56
Mo	3.46	5.00	11.00	38.31	3.08
Pb	25.60	18.00	169.00	15.40	16.93
Bi	0.47	b.d.	b.d.	0.70	0.41
La	31.76	15.05	21.73	42.53	34.11
Ce	64.02	28.13	39.37	82.58	69.52
Pr	6.59	2.98	4.03	8.45	7.30
Nd	23.70	10.03	14.49	30.00	26.21
Sm	3.59	1.35	2.37	4.53	4.14
Eu	0.82	0.44	0.74	1.19	1.02
Gd	2.51	1.03	1.79	2.61	2.43

Rock or Basalt type	tonalite gneiss	tonalite gneiss	tuff	tonalie	tonalite
age (Ma)	2825	2825	2744	2744	2744
UTM easting	417463	417458	425563	387261	390580
UTM northing	5956678	5956678	5961134	5982855	5975736
Tb	0.37	0.14	0.25	0.37	0.35
Dy	1.91	0.73	1.40	1.96	1.96
Ho	0.37	0.14	0.27	0.34	0.35
Er	1.07	0.39	0.80	0.98	0.99
Tm	0.17	0.05	0.13	0.14	0.15
Yb	1.07	0.32	0.82	0.97	1.02
Lu	0.16	0.05	0.12	0.14	0.15
(La/Sm)pm	5.72	7.23	5.93	6.06	5.32
(Th/La)pm	2.65	2.48	2.49	2.65	2.66
(Nb/La)pm	0.16	0.24	0.22	0.09	0.12
(Gd/Yb)pm	1.93	2.65	1.81	2.23	1.97
(Nb/Th)pm	0.06	0.10	0.09	0.04	0.05
(La/Yb)pm	21.21	33.79	19.03	31.45	23.97
eNd		-0.49	-1.71		-1.80
T		3.11	3.19		3.14

Assemblage/Rock name Sample name Rock or Basalt type age (Ma) UTM easting UTM northing	Bella Lake JP02-420 tonalite 2744 427592 5960965	Pipe Point JP01-45 quartz-feldspar porphyry 2730 383615 5979444	Linklater and hoseshoe stock JP01-116-G JP01-217-G quartz-feldspar porphyry    quartz-feldspar porphyry 2700                                  2700 385763                                391571 5974486                               5978687	
	SiO <sub>2</sub> (wt %)	70.82	65.83	71.67
Al <sub>2</sub> O <sub>3</sub>	15.28	16.36	15.22	14.72
Fe <sub>2</sub> O <sub>3</sub>	3.30	4.76	2.17	2.29
MnO	0.05	0.07	0.04	0.04
MgO	0.90	2.30	0.67	0.61
CaO	2.47	3.92	2.65	2.20
Na <sub>2</sub> O	3.18	4.18	4.68	4.60
K <sub>2</sub> O	3.48	1.99	2.58	2.86
TiO <sub>2</sub>	0.41	0.47	0.24	0.22
P <sub>2</sub> O <sub>5</sub>	0.12	0.12	0.08	0.12
LOI	3.29	2.62	2.81	1.41
Total	99.96	100.06	99.93	100.28
Mg#	35	49	38	34
Cr (ppm)	b.d.	20	b.d.	b.d.
Co	3	9	3	2
Ni	b.d.	b.d.	b.d.	b.d.
Rb	144.58	41.78	55.76	52.64
Sr	199	615	387	526
Cs	12.33	6.07	2.34	1.41
Ba	1010	363	745	1160
Sc	3	8	4	3
V	31	74	25	16
Ta	0.46	0.15	0.33	0.47
Hf	5.38	2.84	2.66	3.48
Nb	6.23	3.73	2.69	4.19
Zr	224	101	101	130
Th	16.80	1.02	30.06	8.52
U	1.32	0.29	3.63	1.75
Y	7.71	6.67	5.86	5.93
Cu	46.0	b.d.	11.0	b.d.
Zn	64	51	38	41
Mo	5.00	3.00	2.43	b.d.
Pb	6.00	13.00	8.42	15.58
Bi	b.d.	b.d.	b.d.	b.d.
La	53.13	7.83	20.79	34.13
Ce	88.39	20.39	39.46	66.85
Pr	8.25	2.75	3.97	6.80
Nd	26.68	12.20	13.90	23.29
Sm	3.17	2.33	2.09	3.18
Eu	0.92	0.89	0.63	0.83
Gd	2.01	1.84	1.29	1.31

Assemblage/Rock name Sample name Rock or Basalt type age (Ma) UTM easting UTM northing	Bella Lake JP02-420 tonalite 2744 427592 5960965	Pipe Point JP01-45 quartz-feldspar porphyry 2730 383615 5979444	Linklater and hoseshoe stock JP01-116-G      JP01-217-G quartz-feldspar porphyry      quartz-feldspar porphyry 2700      2700 385763      391571 5974486      5978687	
	Tb	0.28	0.24	0.19
Dy	1.38	1.24	1.02	1.10
Ho	0.25	0.22	0.18	0.19
Er	0.75	0.61	0.53	0.53
Tm	0.10	0.09	0.07	0.08
Yb	0.65	0.55	0.51	0.52
Lu	0.10	0.08	0.08	0.08
(La/Sm)pm	10.82	2.17	6.43	6.93
(Th/La)pm	2.55	1.05	11.69	2.02
(Nb/La)pm	0.11	0.46	0.12	0.12
(Gd/Yb)pm	2.57	2.79	2.11	2.07
(Nb/Th)pm	0.04	0.44	0.01	0.06
(La/Yb)pm	58.90	10.30	29.45	46.72
eNd		0.68		1.00
T		3.03		2.91

**Table 3-2 Nd isotope data summary**

Sample	Rock type/Unit	Age (Ma)	$\epsilon$ Nd	TDM
Italic sample names - recalculated data from Stevenson and Turek, 1992				
<i>Felsic rocks</i>				
102-98-859	Volcanogenic sediments	2897	0.47	3.27
999	<i>Cochrane Bay tonalite</i>	2894	0.39	3.16
JP00-33	Cochrane Bay diorite	2894	-0.63	3.14
JP02-425	Jubilee assemblage tuff	2854	-0.32	3.17
110	<i>Knight Lake tuff (Jubilee assemblage)</i>	2852	-0.04	3.17
158	<i>Bigstone Lake tuff (Jubilee assemblage)</i>	2852	-0.72	N/A
3114	<i>Jubilee assemblage dacite</i>	2852	-0.52	3.18
3115	<i>Jubilee assemblage crystal tuff</i>	2852	-0.68	3.16
3140	<i>Nickel Island tuff (Jubilee assemblage?)</i>	2852	1.19	N/A
JP02-289	Jubilee assemblage granodiorite	2852	-0.75	3.19
JP02-839	Jubilee assemblage tuff	2852	0.14	3.13
JP02-419	Southern tonalite gneiss	2825	-0.49	3.11
JP02-424	York Lake pluton	2825	-1.99	3.27
3116	<i>Wassagomach tonalite</i>	2778	-0.37	3.05
3141	<i>Chapin Bay tonalite</i>	2748	-1.77	3.17
372	<i>Cochrane Bay (Bella Lake) tonalite</i>	2747	-1.00	3.09
35	<i>Bella Lake pluton</i>	2744	-0.48	3.01
JP01-105	Loonfoot assemblage tuff	2744	-1.71	3.19
JP01-67	Cochrane Bay (Bella Lake) pluton	2744	-1.80	3.14
815	<i>Beemingi porphyry</i>	2743	-0.98	3.08
983	<i>Linklater porphyry</i>	2743	-1.80	3.16
44	<i>Pipe Point porphyry</i>	2730	2.06	2.93
140	<i>Pipe Point tonalite</i>	2730	-1.35	3.09
143	<i>Pipe Point quartz diorite</i>	2730	2.42	2.91
JP01-45	Pipe Point porphyry	2730	0.68	3.03
217G	Horeschoe Island porphyry	2700	1.00	2.91
<b>Basalts</b>				
JP02-559	Whiteway assemblage basalt	2897	0.58	N/A
JP02-557	Whiteway assemblage basalt	2897	0.86	N/A
349	<i>Bigstone Lake basalt (Jubilee assemblage)</i>	2852	1.73	N/A
3117	<i>Gabbro (Jubilee assemblage)</i>	2852	0.79	N/A
860	<i>Gabbro (Jubilee assemblage)</i>	2852	1.89	N/A
1	<i>Stevenson Lake amphibolite (Jubilee assemblage)</i>	2852	0.27	3.17
JP01-246G	Jubilee assemblage – northern suite basalt	2852	0.91	N/A
JP02-266	Jubilee assemblage – northern suite basalt	2852	-1.83	N/A
52-IL-98-44	Jubilee assemblage – southern suite basalt	2852	-1.17	N/A
JP02-463	Jubilee assemblage – southern suite basalt	2852	-0.29	N/A
52-IL-98-12	Loonfoot assemblage basalt	2744	2.08	N/A



**LA-MC-ICP-MS U-Pb results**

Analysis number	$^{206}\text{Pb}/^{238}\text{U}$	$\pm 2\sigma$	$^{207}\text{Pb}/^{235}\text{U}$	$\pm 2\sigma$	$^{207}\text{Pb}/^{206}\text{Pb}$	$\pm 2\sigma$	Age (Ma)	$\pm 2\sigma$
<b>006: Post kinematic dyke south of Savage Island Shear Zone (UTM coordinates: 5957872N, 425494E)</b>								
JP00-06-5	0.5129	0.0098	13.527	0.010	0.1907	0.0007	2748	17
JP00-06-3	0.5038	0.0100	13.002	0.010	0.1883	0.0006	2728	17
JP00-06-2	0.5246	0.0126	14.417	0.013	0.1992	0.0011	2819	19
JP00-06-6	0.5060	0.0109	13.341	0.011	0.1912	0.0007	2752	18
JP00-06-10	0.5025	0.0115	13.467	0.011	0.1941	0.0009	2778	18
JP00-06-11	0.4593	0.0133	12.262	0.013	0.1933	0.0011	2771	19
JP00-06-8	0.4807	0.0324	13.713	0.033	0.2084	0.0029	2893	28

**FOOTNOTES TO ID-TIMS DATA**

**TABLE**

zr - zircon grain; ab - abraded; eq - equant; euh - euhedral; rnd - rounded; incl - inclusions, brn - brownish, pnk - pink, clr - clear

Pbcom is total measured common Pb assuming the isotopic composition of laboratory blank:  
206/204 - 18.221; 207/204 - 15.612; 208/204 - 39.360 (1 sigma errors of 2%).

Th/U calculated from radiogenic 208Pb/206Pb ratio and 207Pb/206Pb age assuming concordance.

Disc - per cent discordance for the given 207Pb/206Pb age

Uranium decay constants are from Jaffey et al. (1971).

## Chapter 4

# Archean tectonics and basin formation: Constraints from U- Pb detrital zircon dating by LA-MC-ICP-MS in a “Timiskaming-type” sedimentary group in the Superior craton

### 4.1 Introduction

Vertical tectonics has been revisited as an important tectonic process in Archean terranes and recent papers have focused on the structural, geometric, geophysical and metamorphic aspects of vertical tectonics in Archean terranes (Dhawar craton – Choukroune et al. 1997; Pilbara craton- Van Kranendonk et al. 2007 and references therein; Superior Province – Bedard et al. 2003; Bedard 2006; Lin 2005; Parmenter et al. 2006; Robin 2009). In “modern-style” or horizontal tectonics, tectonism involves the organized movement of plates, and the motion of these plates is driven by slab pull and/or push. In vertical tectonics, tectonism involves movement via the diapiric ascent of underlying buoyant felsic material into domes, and the sagging, or “sagduction,” of volcanic and volcanoclastic supracrustal material into the flanks or synclines between the domes. This style of tectonism is driven by heat and/or density contrast in the crust. Upwelling heat is generated by mantle plumes or by delamination of the lower crust, and density contrasts occur when mafic rocks overlie felsic rocks in thickened crustal sections (Van Kranendonk et al. 2007; Lin 2005; Parmenter et al. 2006; Robin and Bailey 2009).

Most authors see vertical and horizontal tectonism as separate processes that would have operated exclusively from each other (e.g. De Wit 1998 vs. Hamilton 1998), although recent work has indicated that these two processes could be contemporaneous (Lin 2005). The Superior Province is the largest piece of exposed Archean crust in the world, and has long been referred to as the best example of horizontal tectonics in the Archean. Recent studies show that vertical tectonics may have played an important (but overlooked) part in the geological evolution of greenstone belts built on

smaller, cratonic blocks in the province (Bedard 2003; Lin 2005; Parmenter et al. 2006), which are closer in size to other Archean cratons (i.e. the Pilbara and Dhawar cratons). As such, greenstone belts in the Superior province offer good opportunities to look for evidence of vertical tectonism, and the possible interaction of vertical and horizontal tectonic processes.

One approach to investigating the tectonic processes operating in the Archean is to investigate the formation of what are thought to be tectonically controlled basins. This study investigates “Timiskaming” type sediments; young, clastic, sedimentary packages characteristic of Neoproterozoic greenstone belts that are traditionally interpreted to have been deposited in strike-slip related basins (Thurston and Chivers 1990). We suggest these sediments can be explained as being deposited in inter-diapiric basins created by diapirism and sagduction processes. During the diapiric ascent of the felsic material, inter-diapiric basins are formed in the synclines between adjacent domes, into which sediments are deposited (Van Kranendonk et al. 2004; Lin 2005; Parmenter et al. 2006). This study was accomplished by examining the distribution of U-Pb detrital zircon ages at different stratigraphic levels in a “Timiskaming type” sedimentary succession located in the Island Lake greenstone belt, Superior Province, Manitoba, Canada (Figure 4.1).

## **4.2 Geological Setting**

### **4.2.1 The Superior Province and Timiskaming-type sedimentary sequences**

The Superior Province is subdivided into east-west trending domains, terranes, and superterranes that all have distinct tectonic histories prior to amalgamation of the province. The Island Lake greenstone belt is part of the northern margin of the North Caribou terrane, a granite-greenstone terrane which is juxtaposed to the Northern Superior superterrane to the north along the North Kenyon Fault (Figure 4.1, Card and Ciesielski, 1980, Percival et al. 2006; Stott 2009). In the North Caribou terrane, as with other granite greenstone terranes in the Archean, a dome and keel pattern is

seen on the regional scale (Figure 4.1), with greenstones representing a keel structure between surrounding granitoid domes (e.g. in the Pilbara, Van Kranendonk et al. 2004). Greenstone belts in the Superior Province consist of two different types of supracrustal packages: older volcanogenic assemblages and a young clastic fluvial-alluvial sedimentary group. The older volcanic assemblages typically consist of Archean style bimodal volcanic units and volcanogenic sedimentary rocks, and belts in the northwestern Superior Province typically contain two or more volcanic assemblages that represent chronologically distinct episodes of volcanism (Figure 4.1; Corfu and Lin 2000; Corkery et al. 2000; Parks et al. 2006; Lin et al. 2006).

Young, clastic, fluvial-alluvial sedimentary units are common and characteristic of Archean greenstone belts. In the Superior Province these units are referred to as “Timiskaming-type” groups after the type locality of this group in the Abitibi greenstone belt (Thurston and Chivers 1990). These groups are the youngest in the greenstone belt stratigraphy and are composed of clastic fluvial-alluvial sedimentary rocks and typically include “Archean style” turbidites (mixed sandstone/shales), arenites, conglomerates, and sandstones. In some belts they also contain subordinate alkaline volcanic rocks (Thurston and Chivers 1990). When observed, the contacts between these groups and the older plutons and volcanic sequences in the belt are unconformable. The groups show a synformal geometry and are situated in the “middle” of the keel structures formed by the greenstone belts they occur in (see Figure 4.2 and Figure 2 of Lin 2005). In the Abitibi greenstone belt, these groups are commonly spatially associated with late strike-slip or transpressional shear zones as well as gold mineralization (Thurston and Chivers 1990). The timing of the deposition of these sediments is constrained by either the age of the youngest detrital zircon in the group, or the age of co-eval alkalic volcanism. In the northwest Superior province these ages range from <2713 Ma (at Stull Lake, Skulski et al. 2000) to 2705 Ma (at Oxford Lake, Lin et al. 2006) (Figure 4.1).

#### 4.2.2 Geology of the Island Lake greenstone belt

The Island Lake greenstone belt of Northern Manitoba can be divided into three distinct volcanic assemblages; the 2.897 Ga Whiteway assemblage, the 2.852 Ga Jubilee assemblage and the 2.744 Ga Loonfoot assemblage, as well as the unconformably overlying younger clastic rocks of the Island Lake Group (Lin et al. 1998; Parks et al. 2006). The primary contact relationships between the volcanic assemblages are not clear in the field; previous work had proposed that the shear zones in the belt represented the primary contacts between the different assemblages (e.g. the Savage Island shear zone, Lin et al. 1998). Recent field work and new geochronological results that are part of this study have shown that the volcanic assemblages cross the shear zones in the belt, and as such cannot be the primary contacts between assemblages (Parks et al. 2006). These data as well as evidence of contamination by older crustal material in the bulk rock composition and Nd isotopes of the volcanic assemblages suggest the volcanic packages have autochthonous relationships with each other and were built on older 3.0 Ga crust (Stevenson and Turek 1992; Parks et al. 2006; Chapter 2; Chapter 3). It is very likely that the volcanic assemblages are in conformable contact with each other, represent an intact primary volcanic stratigraphy, and that the assemblages were deposited on a Mesoarchean basement that has been pervasively reworked by Neoproterozoic plutonism and deformation (Chapter 3). This leads to a schematic stratigraphic column presented here for the supracrustal rocks in the Island Lake greenstone belt (Figure 4.3).

Plutonic rocks in the belt range in age from 2894 Ma to 2699 Ma, with a concentration of Neoproterozoic magmatic activity at 2.75-2.74 Ga (Turek et al. 1986; Stevenson and Turek 1992; Corfu and Lin 2000; Parks et al. 2006). All of the rocks in the belt are metamorphosed from lower greenschist to lower amphibolite facies and have experienced multiple deformation events. At least two episodes of deformation have been identified in the belt, a D<sub>1</sub> event related to folding in the older volcanic assemblages dated at 2.723 Ga (Chapter 2 and Chapter 3) and a D<sub>2</sub> event related to final movement along

the Savage Island shear zone and Harper Island shear zone (see Figure 3.2), and terminal collision in the NW Superior Province dated at 2.70 Ga (Chapter 3).

#### 4.2.2.1 Sedimentary Rocks of the Island Lake Group

The Timiskaming-type sequence in the Island Lake greenstone belt is called the Island Lake Group (ILG) (Lin et al. 2006; Parks et al. 2006). The ILG is observed to have an unconformable relationship (see Figure 2.6) with older plutonic and supracrustal rocks in the belt. The group has a synformal geometry, with facing directions consistently point away from the contacts with the older plutonic and supracrustal rocks (Figure 4.2). It has been metamorphosed to greenschist facies and is only weakly deformed. Well preserved primary features such as graded bedding, cross bedding, and flame structures define younging directions and provide excellent control on the stratigraphic sequence within the group (Figure 4.2 and Figure 4.3). Sedimentation in this group is bracketed between 2712 Ma (the age of the youngest detrital zircon dated by thermal ionization mass spectrometry (Corfu and Lin 2000) and ca. 2699 Ma (the age of a crosscutting intrusion, Turek et al. 1986).

The lowest unit at the base of the ILG is the lower mixed sandstone/shale unit (sample I, Figure 4.4A). The base of this unit consists of a layer of black shale that grades into a repeating sequence of 5 to 10 cm thick layers of graded sediment. These layers consist of blue-quartz-rich very coarse to coarse sand at the base that grades up to a thin (<5cm) silty dark pelitic layer at the top that is similar in lithology to the “black shale” layer at the base of the unit (Figure 4.4A). Identifiable grains at the base of each layer include bluish quartz, feldspar, felsic and mafic volcanic grains. The layers are internally well sorted and the grains are moderately well rounded. The sandy layer becomes more conglomeratic in discrete lenses, and the clasts in this conglomerate exhibit poor rounding and sorting. The clasts are the same composition as the grains in the base of the sandy layers. This unit grades into a layer of blue quartz sandstone, which in turn grades into the next unit up sequence (Lin et al. 1998).

The next unit is the interbedded sandstone-polymictic conglomerate unit (sample II, Figure 4.4B). This unit is interbedded on the decimeter to meter scale. The conglomerate layers are well sorted, dominantly clast supported, and heterolithic. The clasts range in size from pebbles to boulders and are subangular to rounded. The clast size is consistent within each layer, and differs from layer to layer. The clast population includes mafic and felsic volcanic rocks, mylonite, gneiss, tonalite, quartz and chert. The sandstone layers are medium to coarse grained, and the grains are very well sorted and rounded. Primary structures in this unit include graded bedding and cross bedding in the sandstone layers.

This unit grades into a massive sandstone unit (sample III, Figure 4.4C), which is medium to coarse grained, massive and lithic in composition. The grains are very well sorted and well rounded. Primary structures in this bed include load structures and well-developed cross-beds with local concentrations of heavy minerals such as sulphides at the base of each cross-bed.

This grades into the upper mixed sandstone/shale unit (sample IV, Figure 4.4D). This unit is greenish in colour and is bedded on the centimeter scale. The grains in each bed range in size from silt to medium sand sized. The smaller grain sizes are dominantly mafic in composition, while the larger are dominantly felsic in composition. Primary features include graded bedding and load structures such as flame and ball and pillow structures (Lin et al. 1998; Parks et al. 2006).

### **4.3 Results**

Photographs of zircons for each sample are presented in Figure 4.5. Details on the analytical methods used for this can be found in Appendix D. To examine how the detrital zircon population changes from unit to unit, the  $^{207}\text{Pb}/^{206}\text{Pb}$  age was calculated for each grain using *Isoplot 3.0*. (Ludwig 2003), and the  $^{207}\text{Pb}/^{206}\text{Pb}$  age histograms were constructed for each of the four samples using *AgeDisplay* (Sircombe 2004) (Table 4.1 and Figure 4.6). In the lower mixed sandstone/shale (sample I, Figure 4.6), a few ages (n=6) are observed at 2.76-2.70 Ga, and a large peak (n=80) is observed in the data between 2.78-2.86 Ga. No detrital zircon ages older than 2.90 Ga is observed in these data. In the conglomerate (sample II,

Figure 4.6), a larger spread of ages are observed. A small population of zircons have  $^{207}\text{Pb}/^{206}\text{Pb}$  ages between 2.76 and 2.70 Ga (n=17), as well as a larger peak at 2.90-2.98 Ga (n=56). This sample also shows input from a ca. 3.0 Ga source (n=11). In the massive sandstone (sample III, Figure 4.6), a large peak is observed at 2.70-2.78 Ga (n=65), as well as a small contribution of material that is older than 2.80 Ga (n= 17). In the upper mixed sandstone/shale (sample IV, Figure 4.6), a large peak is observed around 2.74-2.72 Ga (n=42), which itself is set in a broader peak that ranges from 2.70-2.80 Ga (n=89). Only a very small amount of older material (n=5) is present in this sample.

Very distinct detrital zircon ages or strong "age signatures" are recorded in each of the four samples and these vary from sample to sample. Two such signatures are the 2.78-2.86 Ga ages seen in sample I and the 2.90-2.98 Ga signature seen in sample II (Figure 4.6). Another trend in the data is the steady increase in the size of a ca. 2.70-2.76 Ga signature coupled with a decrease in size of a signature older than 2.80 Ga. This trend is seen from the lowermost sample to the upper most sample in the stratigraphy.

These dominant age signatures correspond well with known volcanic and plutonic ages in the Island Lake greenstone belt and surrounding terranes. The detrital zircon ages in the two lowermost units correlate to the age of the two oldest volcanic assemblages in the belt. The largest age signature in sample I, correlates well with the 2.85 Ga Jubilee assemblage in this greenstone belt (Parks et al. 2006; Corfu and Lin 2000), and similar younger ages of the 2.83 Ga "Hayes River" Group in greenstone belts to the north (Lin et al. 2006 and references within). The next sample up stratigraphy, sample II, has a distinctively older age signature which correlates well with the 2.89 Ga Whiteway Assemblage and older components in the Island Lake greenstone belt (Corfu and Lin 2000; Parks et al. 2006). The 2.70 to 2.76 Ga signature seen to increase up-stratigraphy corresponds to the age of youngest porphyry intrusions and the voluminous ca. 2.75-2.74 Ga plutons in the belt (Corfu and Lin 2000; Parks et al. 2006).

## 4.4 Discussion

A few detrital zircon in this study (n=17/360) have  $^{207}\text{Pb}/^{206}\text{Pb}$  ages that overlap within error of, or are just younger (within 1 to 2 Ma) than the age of the youngest detrital zircon analyzed by Corfu and Lin (2000) that provides a maximum age constraint for the deposition of the Island Lake group. The analysis of Corfu and Lin is a concordant datum obtained by TIMS, whereas the ages in this study are discordant (-2.26 to 0.57). It is unclear if these ages provide a more accurate but less precise, younger, maximum age for the deposition of the Island Lake group. Regardless, these ages support interpretation of Corfu and Lin (2000) that the Island Lake greenstone belt was deposited over a relatively short period of time.

The sediment being deposited in a basin at any given time is a reflection of what rocks are available for erosion, which is related to the pre-basin geometry and the processes that are responsible for the opening of the basin. As such, if the original geometry is known, and there is good control on the ages of the rocks in the area, the provenance of the sediments can be traced back to their source by determining the age of the detrital zircons in the sediment. This can be done for each stratigraphic level within a sedimentary group, and then used to constrain what tectonic processes were responsible for opening the basin. Using detrital zircons to track provenance in a sedimentary sequence biases the data towards whatever zircon bearing rocks are available to be eroded in the source region. In the Island Lake greenstone belt, the potential zircon bearing rocks being sourced for the detritus are the felsic volcanic and volcanogenic sedimentary rocks which have been used to successfully date each assemblage, and the voluminous plutons in the belt which are contemporaneous with the volcanic assemblages (Chapter 2; Parks et al. 2006).

The original pre-basin geometry in the Island Lake greenstone belt is presented in Figure 4.7 A, and is identical to the geometry of the older volcanic assemblages presented in Figure 4.3 with the exception that the 2.744 Ga Loonfoot assemblage is not included. This is because this assemblage consists

dominantly of mafic volcanics with limited present day extent, and as such is not expected to be a source of detrital zircon for the Island Lake group. It is also possible that if there was a detrital zircon contribution from the Loonfoot assemblage, it would have fed the detritus at the bottom of the Island Lake group that is not observed on surface and not sampled in this study.

One model proposed to explain how the basins form into which these Timiskaming-type sediments are deposited is the inter-diapiric basin model. This model invokes the opening of basins during the diapiric ascent of the buoyant felsic material into domes, and the sagduction of the denser volcanic and volcanoclastic supracrustal material into the keels in between adjacent domes (stages B-D in Figure 4.7; Bleeker 2000; Van Kranendonk et al. 2004; Lin 2005; Parmenter et al. 2006). In the inter-diapiric basin model, the material that is available for erosion during the different stages of basin development is dictated by what material is above the “erosional surface” (controlled by what is on the surface of the earth, dashed line in Figure 4.7). In the first stage of basin development, the supracrustal assemblages at surface are the major source of detritus (stages B-C in Figure 4.7). As sagduction/diapirism continues the supracrustal rocks either become completely eroded away, or are suffocated below the erosional surface. At this point in the evolution of the basin, the younger felsic domes are unroofed and become the major source of detritus to the basin (Stage D in Figure 4.7). Thus, two important criteria for sediments deposited in different stages of a basin formed by this model are 1) evidence of detritus from “at surface” supracrustal assemblages lowest in the stratigraphy (i.e. deposited in the first stages of sedimentation into the basin), and 2) evidence of detritus from unroofing felsic domes towards the top of the stratigraphy (i.e. deposited in the latter stages of sedimentation into the basin).

The two lowermost samples from this study clearly show a pattern of downward erosion through two distinct supracrustal units. The first material available for erosion and deposition in the lowest unit in the stratigraphy (sample I) is the younger of the two volcanic assemblages, the ca. 2.85 Ga Jubilee assemblage and related volcanic rocks (corresponding to stage B in Figure 4.7). This material is then

eroded away or buried beneath the erosional surface during unroofing. The next material available for erosion and deposition in the subsequent unit up sequence (sample II) is the underlying ca. 2.89 Ga Whiteway assemblage and older equivalents of the belt (corresponding to stage C in Figure 4.7). As diapiric movement continues, the volcanic rocks are either completely eroded away or are suffocated below the erosional surface, and the younger plutonic rocks are unroofed and then become the main source of detritus (corresponding to stage D in Figure 4.7). This is reflected in the strong 2.70 to 2.76 Ga signature that is only observed in the two uppermost samples (III and IV) of the stratigraphy.

The detrital zircon data from this study fulfills the two criteria listed above and are consistent with the development of an inter-diapiric basin and related sedimentation. A striking signature which fits the model presented above is the presence of the oldest volcanic assemblage, the 2.89 Ga Whiteway assemblage, and older components in sample II, and an almost complete absence of this age signature in samples stratigraphically above or below it. Such a distribution of this age signature reflects that it was only available for erosion during a very short and specific period of time within the stages of basin development, and represents the transition from stages C to D (Figure 4.7). The data from this study agrees well with the predicted pattern of downward erosion through a supracrustal pile in the early stages of basin formation and sedimentation, and an unroofing of underlying plutons in the later stages. We suggest therefore that the Island Lake group was deposited in an inter-diapiric basin.

#### **4.5 Synchronous Vertical and Horizontal Processes in the Neoproterozoic**

In the western Superior Province, there is much evidence for horizontal tectonism being responsible for producing deformation events on the belt and regional scale (e.g. the development of large D<sub>2</sub> transpressional shear zones and the amalgamation of terranes in the area via a series of subduction zones; Percival et al. 2006 and references within; Chapter 3). The diapiric structures in the northwestern Superior Provinces, although related to vertical tectonic processes, are also thought to be related to the same late

regional shear zones (Lin 2005 and Parmenter et al. 2006). Detailed kinematic work on the D<sub>2</sub> structures in the Carrot River and Cross Lake greenstone belts (locations in Figure 4.1 ) have been completed by Lin (2005) and Parmenter et al. (2006). These studies have shown that the strike-slip component of these structures are related regional horizontal shearing as a result of horizontal tectonism, while the dip-slip component is related to diapirism/sagduction processes (vertical tectonism). Both Lin (2005) and Parmenter et al. (2006) use this data to suggest that vertical and horizontal tectonism occurred synchronously in the northwestern Superior Province.

In the Island Lake greenstone belt the D<sub>2</sub> event is expressed as the last episode of movement along the Savage Island shear zone (SISZ, Chapter 3). Shear sense indicators in the SISZ show evidence for south-over-north dip slip and dextral strike slip movement (This study, Lin et al. 1998), and has similar geometric and kinematic characteristics as shear zones in the Carrot River and Cross Lake greenstone belts (locations in Figure 4.1; Lin 2005; Parmenter et al. 2006). Given the similarities in the shear zones between these belts in the northwestern Superior Province, it is likely that the diapiric structures in the Island Lake greenstone belt are also related to D<sub>2</sub> dip-slip movement on the SISZ due to vertical tectonic processes.

The synchronous development of horizontal and vertical tectonics is also suggested by U-Pb ages in the Island Lake greenstone belt. U-Pb zircon dating of cross cutting dykes (Chapter 3) and detrital zircons (from this contribution) show that movement on spatially related D<sub>2</sub> 2.70 Ga strike-slip shear zones and formation of inter-diapiric basins are contemporaneous events at ca. 2.70 Ga. These age data agree with the work of Lin (2005) and Parmenter et al. (2006) detailed above that conclude that both vertical and horizontal tectonic processes were operating synchronously in the same geodynamic setting in the Superior Province.

A summary of age/space (craton)/tectonic regime is presented in Figure 4.8. It is clear that the Archean is a time of evolution in tectonic regimes, and both vertical and horizontal tectonism operated in both the Mesoarchean and Neoarchean. It is evident from this diagram that vertical tectonism is still an active tectonic regime at the end of the Neoarchean, and it is active in at least two cratons (Figure 4.8, the Superior and Dharwar). Perhaps the transition between vertical to horizontal tectonic regimes as proposed by Lin (2005) in fact occurred at different times in different cratons. When this transition occurred in a craton could be dependent on the amount of heat available underneath each craton, and the presence and thickness of continental crust (influencing the ductility of felsic crust via diapirs and density contrasts within the crust, respectively). It is clear that horizontal or “modern style” plate tectonics did not become the dominant tectonic process until sometime during the Proterozoic.

#### **4.6 Conclusions**

Data from this study indicates that the ages of detritus change from unit to unit up sequence in this sedimentary group, and are easily correlated to ages of volcanism and plutonism in the belt. The age pattern of detritus revealed by detrital zircons best fits a scenario that involves vertical tectonic processes being active during basin evolution and sedimentation. We suggest that vertical tectonic processes played an important, but overlooked, role in the development of these sedimentary basins and in the tectonic evolution of Archean cratons. Furthermore, vertical and horizontal tectonic processes were synchronous and both operated in the Neoarchean, and the timing of transition between the two tectonic regimes might have taken place at different times and rates in different Archean cratons. Horizontal or “modern style” tectonics did not become the dominant tectonic process until sometime during the Proterozoic.

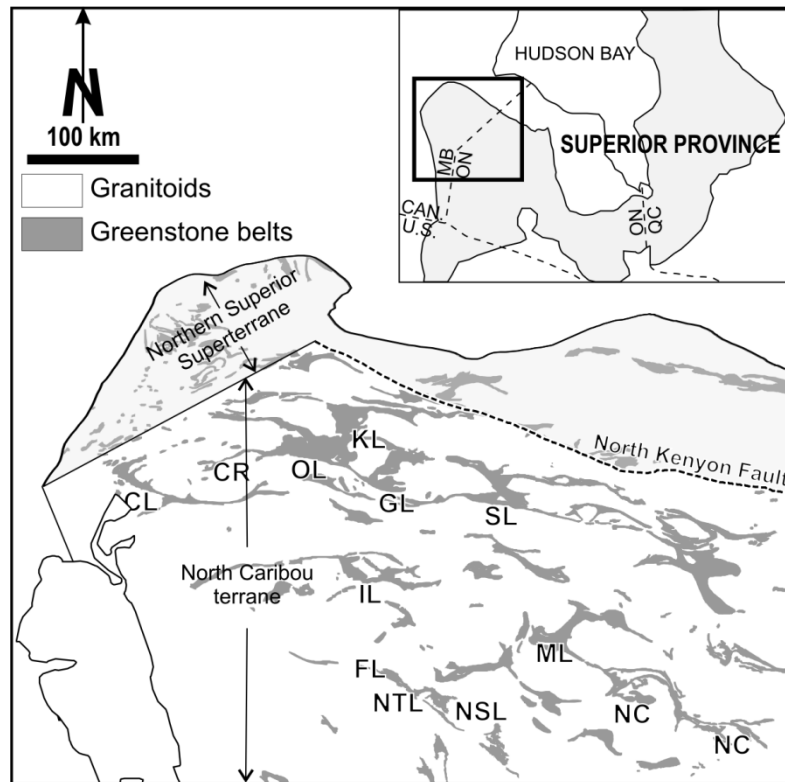


**Figure 4-1** Location of the Island Lake greenstone belt and distribution of “Timiskaming” type groups in the northwestern Superior Province. All of the greenstone belts in the that have a “Timiskaming” type group are shown. Box in inset map shows location within the larger Superior Province. The relative positions of the Northern Superior superterrane, the North Caribou terrane, and the location of the North Kenyon Fault (dashed line) are shown. The dome and keel structure is evident across the whole North Caribou terrane, and is particularly well developed in the Oxford and Gods Lake area as well as the Muskrat Dam and North Caribou lake area. Abbreviations of greenstone belts: IL - Island Lake; CL - Cross Lake; CR - Carrot River; OL - Oxford Lake, KL - Knee Lake; GL - God's Lake; ST - Stull Lake; ML - Muskrat Dam Lake; NC - North Caribou Lake; FL - Favourable Lake; NST - North Spirit Lake; NTL - North Trout Lake. Ages from Corkery et al. 1992; Corfu et al. 1998; Skulski et al. 2000; Corkery et al. 2000; Corfu and Lin 2000; Lin et al. 2006. Modified after Stott (2009).

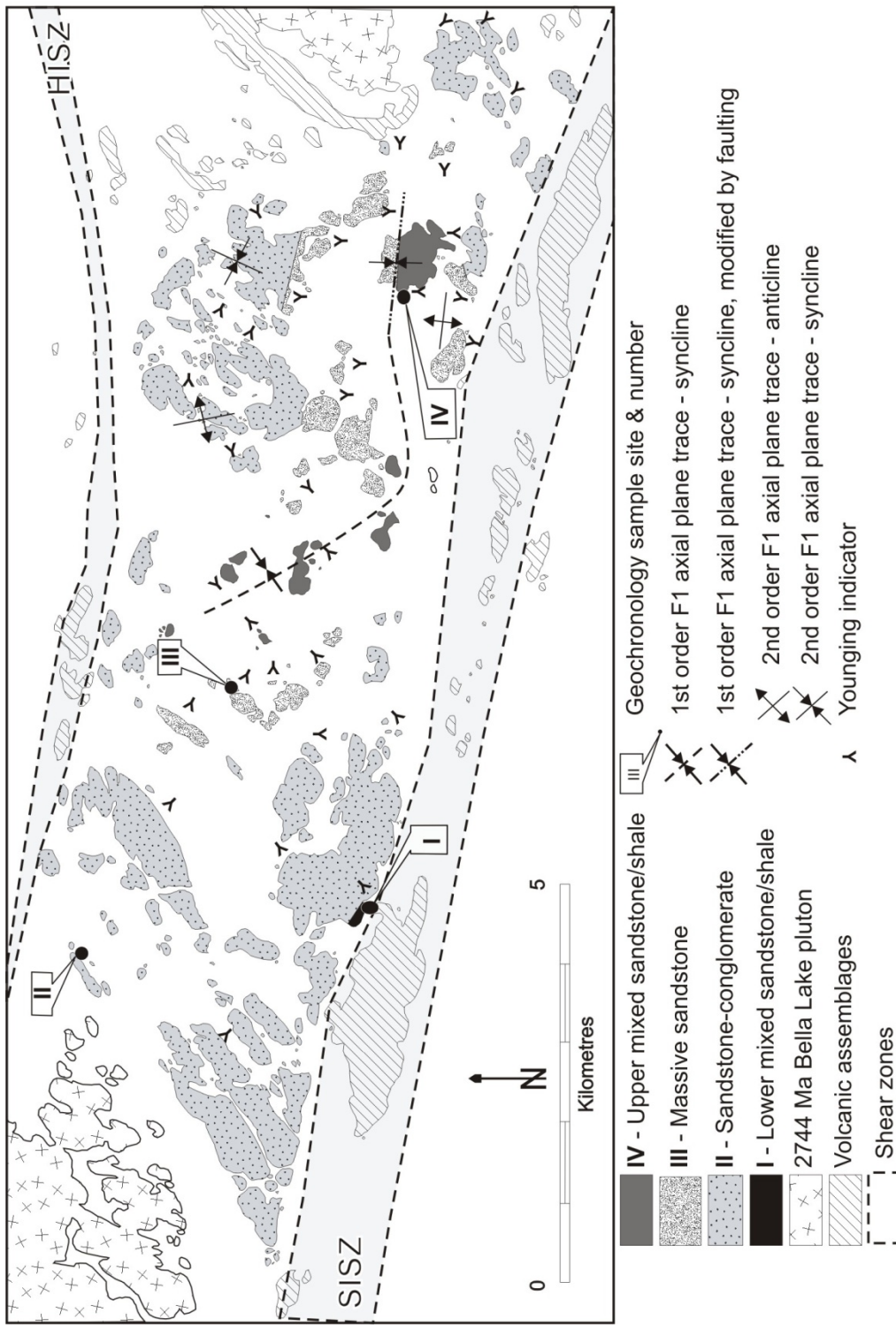


**Figure 4.2.** Detailed map of the Island Lake Group with reversals in younging directions that show an overall synclinal fold geometry. Data from this study and Lin et al. (1998).

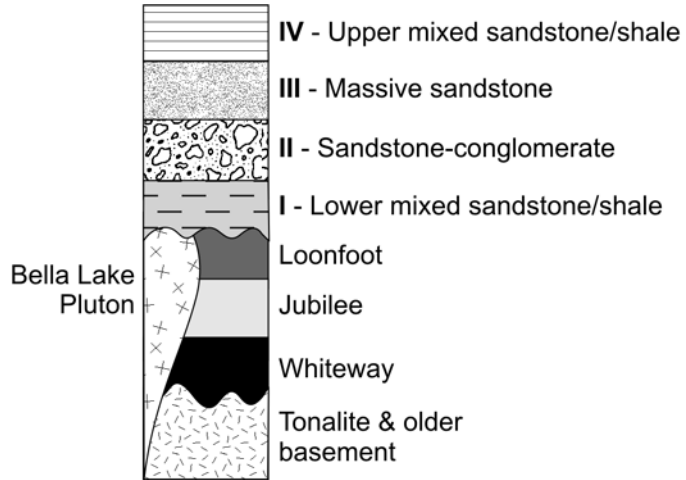


**Figure 4.3** Schematic stratigraphic column for the Island Lake greenstone belt. The sample locations within the Island Lake Group are noted.

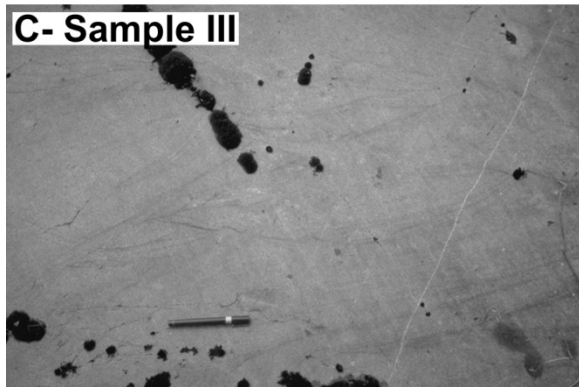
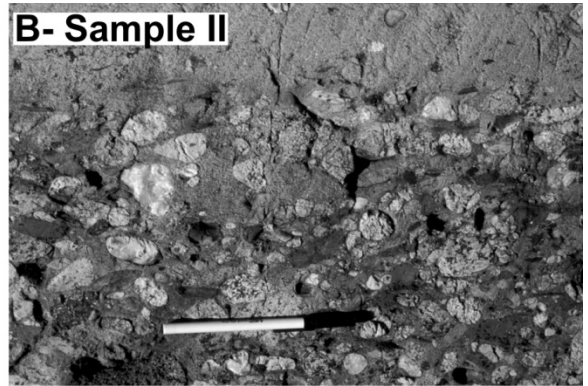
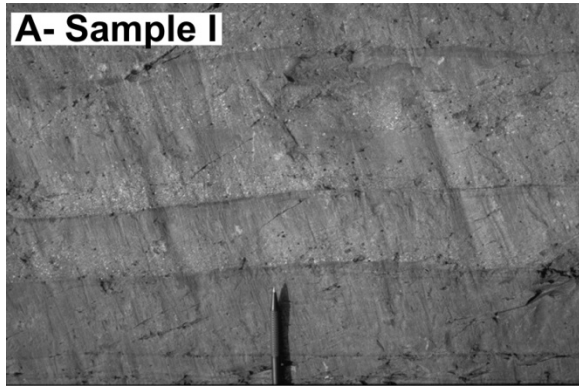


**Figure 4.4** Photographs of units in the Island Lake Group. A - Lower mixed sandstone/shale unit (sample I), pen at bottom of picture for scale. B- Interbedded sandstone-polymictic conglomerate unit (sample II), pen at bottom of picture for scale. C- Massive sandstone unit (sample III), pen at bottom of picture for scale. D- Upper mixed sandstone/shale unit (sample IV), pen at top right of picture for scale.

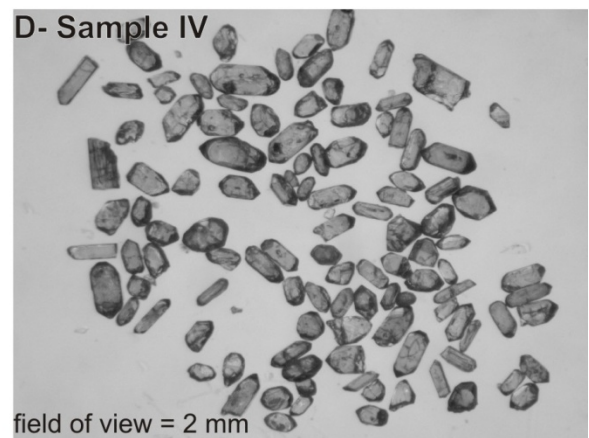
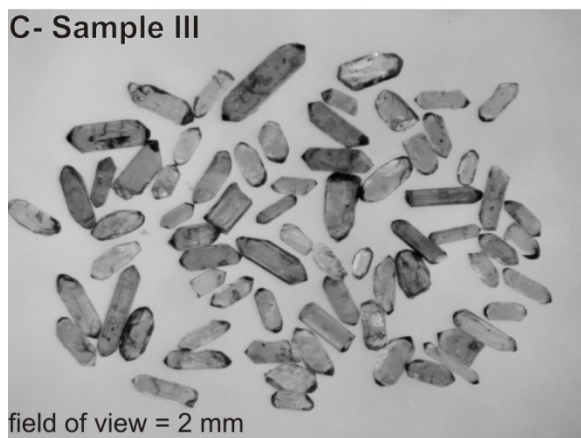
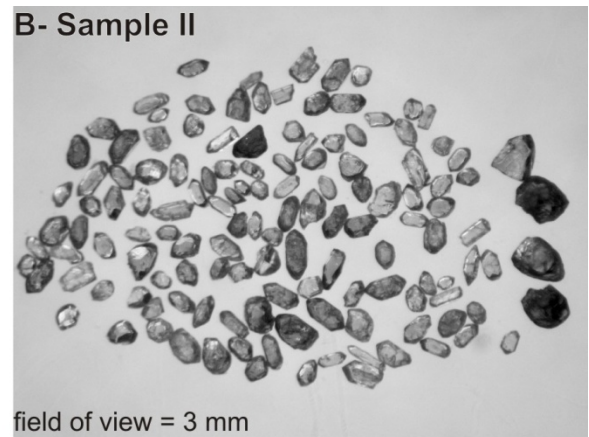
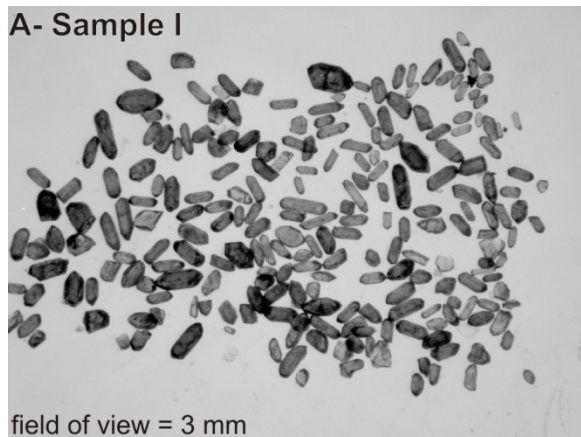


**Figure 4.5** Photographs of representative zircon populations from each sample.

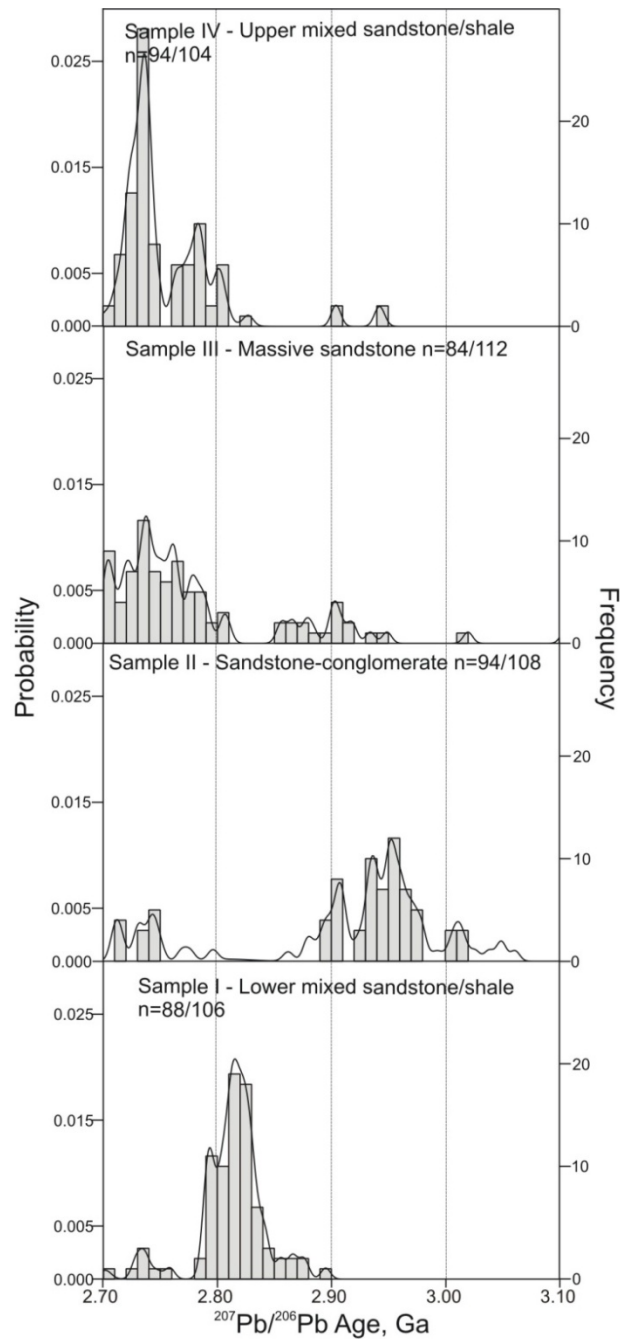


**Figure 4.6**  $^{207}\text{Pb}/^{206}\text{Pb}$  age frequency- probability histograms for four samples from the Island Lake Group. “n” indicates the number of analysis used to construct each histogram. Analysis that were more than +/-10% discordant, showed evidence of “mixed ages” during runs, or had anomalously high  $^{204}\text{Pb}$  counts during analysis are not included in the final data.

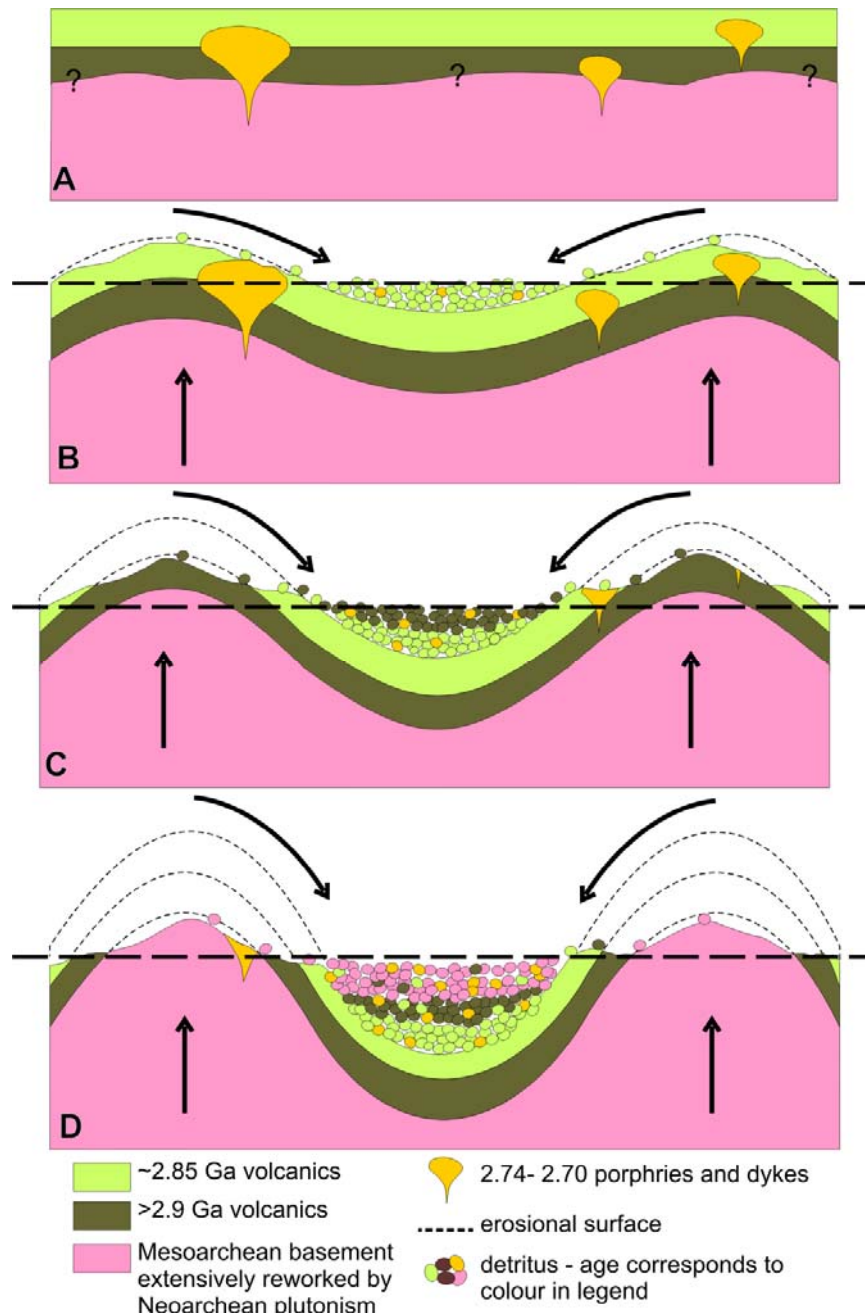


**Figure 4.7** Cartoon diagrams of the stages of evolution of an inter-diapiric basin. Stage A - original stratigraphy of greenstone belt, stage B through D - progressive stages of basin development. In stages B and C, the supracrustal pile is eroded from top to bottom, and is the major supply of detritus to the basin until a time at which they are either completely eroded away, or they lie below the “erosional surface”, represented by the dashed line. In stage D, the underlying plutons and youngest porphyries and dykes are eroded and supply detritus to the basin.

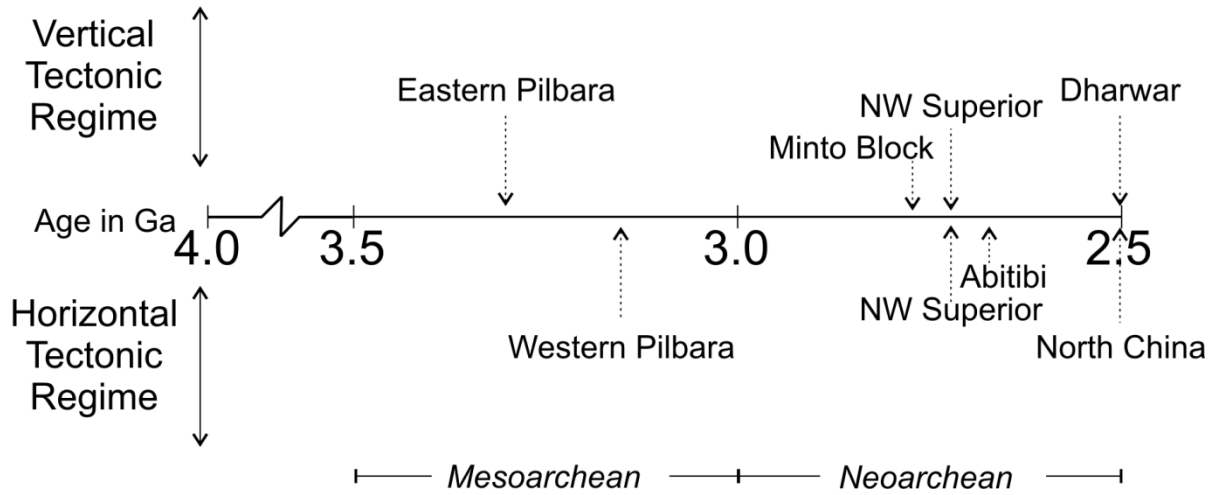


**Figure 4.8** A summary of age/space (craton)/tectonic regime operating in the Archean. Position of dashed arrow on time line indicates when evidence for regime being active has been documented. Data from this study; Calvert et al. 1995; Choukroune et al. 1997; Bedard et al. 2003; Van Kranendonk et al. 2004; Wang et al. 2004; Lin 2005; Percival et al. 2006; Van Kranendonk et al. 2007.

**Table 4-1 LA-ICP-MS U-Pb data**

\* radiogenic, adjusted for common

grain ID	spot size (µm)	<sup>206</sup> Pb* cps	<sup>204</sup> Pb cps	<sup>206</sup> Pb/ <sup>238</sup> U ±1σ	<sup>207</sup> Pb/ <sup>235</sup> U ±1σ	<sup>207</sup> Pb/ <sup>206</sup> Pb ±1σ	rho	<sup>207</sup> Pb/ <sup>206</sup> Pb ±2σ	Age (Ma)	Disc.			
<b>Sample IV: Turbidite (UTM coordinates: 5961284N, 422926E)</b>													
<b>n=94</b>													
102-97-481-1	40	1937439	10933	0.5286	0.0072	14.005	0.008	0.1935	0.0031	0.59	2772	27	1.62
102-97-481-2	40	407432	10	0.5192	0.0054	13.902	0.005	0.1943	0.0003	0.97	2779	8	3.65
102-97-481-3	40	423186	37	0.5117	0.0048	13.729	0.005	0.1946	0.0001	0.97	2782	8	5.18
102-97-481-4	40	245094	751	0.5338	0.0074	14.594	0.008	0.1973	0.0035	0.48	2804	30	2.06
102-97-481-5	40	453516	69	0.5199	0.0055	13.947	0.006	0.1947	0.0002	0.97	2782	8	3.66
102-97-481-6	40	394071	2	0.5144	0.0032	13.837	0.003	0.1952	0.0002	0.95	2786	8	4.85
102-97-481-7	40	1125832	53	0.5707	0.0041	16.496	0.004	0.2097	0.0001	0.95	2903	8	-0.31
102-97-481-8	40	182131	0	0.5145	0.0044	13.966	0.004	0.1969	0.0002	0.96	2801	8	5.45
102-97-481-9	40	377028	5	0.5156	0.0046	13.896	0.005	0.1955	0.0002	0.96	2789	8	4.77
102-97-481-10	40	786938	27	0.5399	0.0041	14.501	0.004	0.1948	0.0001	0.96	2783	8	0.02
102-97-481-11	40	911560	27	0.5290	0.0028	13.839	0.003	0.1971	0.0001	0.95	2802	8	2.84
102-97-481-12	40	704809	88	0.5215	0.0042	13.846	0.004	0.1926	0.0002	0.96	2765	8	2.62
102-97-481-13	40	980668	177	0.5169	0.0046	13.901	0.005	0.1951	0.0001	0.96	2785	8	4.35
102-97-481-15	40	664282	20	0.5280	0.0034	14.091	0.004	0.1936	0.0001	0.95	2773	8	1.78
102-97-481-16	40	376052	0	0.5486	0.0038	15.879	0.004	0.2100	0.0002	0.95	2905	8	3.65
102-97-481-17	40	374465	3	0.5172	0.0039	13.807	0.004	0.1937	0.0001	0.96	2774	8	3.80
102-97-481-18	40	1130156	50	0.5271	0.0031	14.097	0.003	0.1940	0.0001	0.95	2777	8	2.09
102-97-481-19	40	931538	9	0.5174	0.0037	13.739	0.004	0.1927	0.0001	0.95	2765	8	3.40
102-97-481-20	40	551083	77	0.5117	0.0049	13.759	0.005	0.1951	0.0001	0.97	2786	8	5.34
102-97-481-21	40	896367	0	0.5196	0.0041	13.956	0.004	0.1949	0.0002	0.96	2784	8	3.79
102-97-481-22	40	836242	534	0.5115	0.0074	13.801	0.008	0.1932	0.0013	0.94	2769	14	4.69
102-97-481-24	40	211456	0	0.5189	0.0037	13.796	0.004	0.1930	0.0004	0.95	2768	9	3.23

grain ID	spot size (μm)	<sup>206</sup> Pb* cps	<sup>204</sup> Pb cps	<sup>206</sup> Pb/ <sup>238</sup> U ±1σ	<sup>207</sup> Pb/ <sup>235</sup> U ±1σ	<sup>207</sup> Pb/ <sup>206</sup> Pb ±1σ	rho	Age (Ma)	±2σ	Disc.			
102-97-481-25	40	413259	0	0.5070	0.0035	13.533	0.004	0.1937	0.0002	0.95	2773	8	5.70
102-97-481-26	40	135542	64	0.5251	0.0021	14.292	0.002	0.1975	0.0009	0.90	2805	11	3.69
102-97-481-27	40	409665	16	0.5259	0.0045	14.254	0.005	0.1966	0.0002	0.96	2798	8	3.25
102-97-481-28	40	343971	69	0.5319	0.0038	14.492	0.004	0.1977	0.0003	0.95	2807	8	2.52
102-97-481-29	40	579018	17	0.5287	0.0054	14.311	0.005	0.1963	0.0001	0.97	2796	8	2.61
102-97-481-30	40	515345	106	0.5101	0.0036	13.680	0.004	0.1945	0.0001	0.95	2781	8	5.44
102-97-481-31	40	203247	17	0.5139	0.0052	14.176	0.005	0.2001	0.0004	0.96	2827	9	6.65
102-97-481-32	40	387365	0	0.5147	0.0045	13.863	0.005	0.1954	0.0002	0.96	2788	8	4.87
102-97-481-33	40	122030	0	0.5234	0.0042	13.920	0.004	0.1924	0.0005	0.95	2763	9	2.18
102-97-481-34	40	412424	0	0.5463	0.0057	14.261	0.006	0.1893	0.0001	0.97	2736	8	-3.32
102-97-481-35	40	242810	0	0.5205	0.0053	13.626	0.005	0.1899	0.0002	0.97	2741	8	1.77
102-97-481-36	40	485291	25	0.5536	0.0067	14.420	0.007	0.1887	0.0002	0.99	2731	8	-4.95
102-97-481-37	40	137269	0	0.4961	0.0043	12.824	0.004	0.1874	0.0002	0.96	2720	8	5.47
102-97-481-38	40	224966	0	0.5168	0.0033	13.463	0.003	0.1889	0.0002	0.95	2732	9	2.10
102-97-481-40	40	202484	11	0.4974	0.0052	12.993	0.005	0.1895	0.0004	0.97	2737	9	5.99
102-97-481-41	40	176864	0	0.5122	0.0054	13.342	0.006	0.1889	0.0002	0.97	2733	8	2.97
102-97-481-42	40	307053	0	0.4989	0.0037	13.037	0.004	0.1895	0.0002	0.95	2738	8	5.70
102-97-481-43	40	275780	96	0.4989	0.0048	13.025	0.005	0.1894	0.0003	0.96	2737	9	5.68
102-97-481-44	40	131204	0	0.5116	0.0027	13.276	0.003	0.1882	0.0003	0.95	2726	9	2.82
102-97-481-45	40	236485	191	0.5144	0.0033	13.631	0.003	0.1922	0.0004	0.94	2761	9	3.78
102-97-481-46	40	42001	5	0.5123	0.0044	13.201	0.005	0.1869	0.0008	0.93	2715	11	2.19
102-97-481-47	40	308853	0	0.5054	0.0042	13.178	0.004	0.1891	0.0002	0.96	2734	8	4.32
102-97-481-48	40	197867	45	0.5091	0.0042	13.274	0.004	0.1892	0.0003	0.96	2735	9	3.66
102-97-481-49	40	486864	0	0.5132	0.0030	13.388	0.003	0.1891	0.0002	0.95	2735	8	2.88
102-97-481-50	40	342031	292	0.4925	0.0085	12.955	0.009	0.1905	0.0007	0.66	2746	10	7.29
102-97-481-51	40	246963	0	0.5002	0.0043	13.036	0.004	0.1890	0.0002	0.96	2733	8	5.26
102-97-481-52	40	217151	0	0.5092	0.0040	13.285	0.004	0.1893	0.0002	0.96	2736	8	3.69
102-97-481-53	40	154636	0	0.5013	0.0048	12.992	0.005	0.1880	0.0003	0.96	2725	9	4.70
102-97-481-54	40	155538	0	0.5050	0.0039	13.263	0.004	0.1904	0.0004	0.95	2745	9	4.88
102-97-481-55	40	203388	0	0.5051	0.0041	13.027	0.004	0.1871	0.0003	0.95	2717	9	3.65
102-97-481-56	40	201308	83	0.5190	0.0036	13.576	0.004	0.1897	0.0003	0.95	2739	9	1.99

grain ID	spot size ( $\mu\text{m}$ )	$^{206}\text{Pb}^*$ cps	$^{204}\text{Pb}$ cps	$^{206}\text{Pb}/^{238}\text{U}$ $\pm 1\sigma$	$^{207}\text{Pb}/^{235}\text{U}$ $\pm 1\sigma$	$^{207}\text{Pb}/^{206}\text{Pb}$ $\pm 1\sigma$	rho	Age (Ma)	$\pm 2\sigma$	Disc.
102-97-481-59	40	208450	0	0.5044	0.0038	0.1882	0.95	2727	9	4.21
102-97-481-60	40	136561	0	0.4980	0.0038	0.1887	0.95	2731	9	5.58
102-97-481-61	40	306652	0	0.5195	0.0022	0.1881	0.95	2725	8	1.26
102-97-481-62	40	156983	0	0.4963	0.0044	0.1877	0.96	2722	8	5.54
102-97-481-63	40	260062	0	0.5063	0.0038	0.1877	0.95	2723	9	3.65
102-97-481-64	40	229444	0	0.5250	0.0050	0.1896	0.96	2739	9	0.82
102-97-481-65	40	190070	0	0.5012	0.0053	0.1874	0.97	2719	8	4.48
102-97-481-66	40	490895	0	0.5161	0.0026	0.1866	0.95	2712	8	1.33
102-97-481-68	40	201898	0	0.5072	0.0033	0.1882	0.95	2726	9	3.64
102-97-481-70	40	220887	0	0.5188	0.0035	0.1879	0.95	2724	8	1.34
102-97-481-71	40	636409	22	0.5498	0.0059	0.1971	0.98	2803	8	-0.94
102-97-481-72	40	283281	2	0.5203	0.0028	0.1879	0.95	2724	8	1.05
102-97-481-73	40	137739	0	0.5090	0.0054	0.1878	0.97	2723	9	3.16
102-97-481-74	40	112627	0	0.5235	0.0043	0.1861	0.95	2708	9	-0.26
102-97-481-75	40	369087	9	0.5157	0.0046	0.1885	0.96	2729	8	2.14
102-97-481-76	40	285874	25	0.5479	0.0046	0.2150	0.95	2944	9	5.34
102-97-481-77	40	224211	0	0.5038	0.0042	0.1888	0.96	2732	8	4.51
102-97-481-78	40	329271	0	0.4958	0.0059	0.1889	0.98	2732	9	6.08
102-97-481-80	40	201723	7	0.5001	0.0056	0.1893	0.97	2736	9	5.42
102-97-481-81	40	218132	0	0.5111	0.0039	0.1892	0.95	2735	8	3.30
102-97-481-82	40	613896	87	0.5171	0.0062	0.1907	0.99	2748	8	2.73
102-97-481-83	40	233266	0	0.5194	0.0031	0.1895	0.95	2738	8	1.84
102-97-481-84	40	341226	0	0.5176	0.0030	0.1896	0.95	2738	8	2.20
102-97-481-85	40	151824	0	0.5332	0.0061	0.1893	0.98	2736	9	-0.84
102-97-481-86	40	459138	10	0.5364	0.0163	0.1897	0.44	2740	8	-1.28
102-97-481-87	40	250395	0	0.5270	0.0087	0.1900	0.67	2743	8	0.62
102-97-481-88	40	212475	0	0.5247	0.0035	0.1853	0.95	2701	8	-0.85
102-97-481-89	40	307672	0	0.5177	0.0037	0.1897	0.95	2740	8	2.25

grain ID	spot size (µm)	<sup>206</sup> Pb* cps	<sup>204</sup> Pb cps	<sup>206</sup> Pb/ <sup>238</sup> U ±1σ	<sup>207</sup> Pb/ <sup>235</sup> U ±1σ	<sup>207</sup> Pb/ <sup>206</sup> Pb ±1σ	rho	<sup>207</sup> Pb/ <sup>206</sup> Pb Age (Ma)	±2σ	Disc.
102-97-481-90	40	159185	0	0.5710	0.0075	0.008	1.00	2941	8	1.23
102-97-481-91	40	127213	0	0.5247	0.0033	0.004	0.95	2727	9	0.34
102-97-481-93	40	188680	0	0.5223	0.0047	0.005	0.96	2724	9	0.69
102-97-481-94	40	203103	1	0.5100	0.0051	0.005	0.97	2748	9	4.07
102-97-481-95	40	701742	0	0.5106	0.0036	0.004	0.95	2737	8	3.48
102-97-481-96	40	185080	0	0.5189	0.0049	0.005	0.96	2720	9	1.14
102-97-481-97	40	230960	0	0.5133	0.0037	0.004	0.95	2739	8	3.07
102-97-481-99	40	247081	0	0.4989	0.0033	0.003	0.95	2731	8	5.43
102-97-481-100	40	263720	1	0.5090	0.0047	0.005	0.96	2744	8	4.06
102-97-481-101	40	242028	3	0.5245	0.0043	0.004	0.96	2736	8	0.77
102-97-481-102	40	505157	3	0.5395	0.0027	0.003	0.95	2740	9	-1.86
102-97-481-103	40	388679	6	0.5161	0.0049	0.005	0.97	2741	8	2.61
102-97-481-104	40	250719	0	0.5129	0.0042	0.004	0.96	2712	9	1.95

Sample III: Cross bedded sandstone (UTM coordinates: 5956405N, 421768E)										
n=83										
JP00-03-1	40	599110	856	0.5108	0.0065	0.007	0.99	2792	9	5.77
JP00-03-2	40	906607	708	0.5478	0.0048	0.005	0.96	2857	8	1.76
JP00-03-3	40	721287	404	0.5212	0.0126	0.013	0.53	2878	9	7.37
JP00-03-7	40	378082	40	0.5174	0.0053	0.005	0.97	2878	8	8.05
JP00-03-8	40	510414	242	0.5367	0.0063	0.006	0.98	2866	8	4.12
JP00-03-9	40	773299	228	0.5366	0.0082	0.008	0.70	2920	8	6.32
JP00-03-10	40	2509736	0	0.5361	0.0058	0.006	0.98	2909	8	6.00
JP00-03-12	40	915459	217	0.5442	0.0053	0.005	0.97	2899	8	4.16
JP00-03-14	40	358662	0	0.5109	0.0076	0.008	0.71	2806	8	6.33
JP00-03-16	40	624128	520	0.5113	0.0049	0.005	0.97	2720	8	2.61
JP00-03-17	40	1004566	498	0.5318	0.0162	0.016	0.44	2776	8	1.19
JP00-03-18	40	1293110	1314	0.5454	0.0059	0.006	0.98	2787	8	-0.84
JP00-03-19	40	900102	363	0.5297	0.0041	0.004	0.96	2766	8	1.17

grain ID	spot size (µm)	<sup>206</sup> Pb* cps	<sup>204</sup> Pb cps	<sup>206</sup> Pb/ <sup>238</sup> U ±1σ	<sup>207</sup> Pb/ <sup>235</sup> U ±1σ	<sup>207</sup> Pb/ <sup>206</sup> Pb ±1σ	<sup>207</sup> Pb/ <sup>206</sup> Pb ±1σ	rho	Age (Ma)	±2σ	Disc.		
JP00-03-20	40	1005280	0	0.5510	0.0044	14.830	0.005	0.1953	0.0002	0.96	2787	8	-1.86
JP00-03-21	40	614765	0	0.5866	0.0080	18.230	0.008	0.2254	0.0002	0.74	3020	8	1.84
JP00-03-22	40	427293	0	0.5383	0.0060	14.443	0.006	0.1947	0.0005	0.97	2782	9	0.27
JP00-03-23	40	817526	0	0.5423	0.0040	14.755	0.004	0.1974	0.0003	0.95	2805	8	0.50
JP00-03-24	40	372017	0	0.5209	0.0058	13.614	0.006	0.1896	0.0003	0.98	2739	9	1.59
JP00-03-25	40	404678	0	0.5495	0.0044	14.548	0.005	0.1919	0.0003	0.96	2759	9	-2.87
JP00-03-26	40	335948	0	0.5261	0.0067	13.509	0.007	0.1862	0.0003	0.99	2709	9	-0.72
JP00-03-27	40	1011304	59	0.5407	0.0032	14.244	0.003	0.1910	0.0001	0.95	2751	8	-1.61
JP00-03-29	40	457905	0	0.5354	0.0040	13.948	0.004	0.1889	0.0001	0.96	2732	8	-1.44
JP00-03-30	40	550299	0	0.4968	0.0043	13.051	0.004	0.1904	0.0002	0.96	2746	8	6.46
JP00-03-31	40	570074	0	0.5142	0.0076	13.575	0.008	0.1914	0.0001	0.71	2754	8	3.53
JP00-03-34	40	380660	224	0.5173	0.0054	13.221	0.005	0.1853	0.0002	0.97	2700	8	0.57
JP00-03-35	40	422787	0	0.5095	0.0053	13.451	0.005	0.1914	0.0002	0.97	2754	8	4.42
JP00-03-36	40	551313	0	0.5393	0.0049	14.174	0.005	0.1906	0.0002	0.96	2747	8	-1.48
JP00-03-37	40	438642	0	0.5338	0.0056	15.516	0.006	0.2114	0.0001	0.97	2916	8	6.69
JP00-03-38	40	307870	0	0.5236	0.0056	15.106	0.006	0.2098	0.0002	0.97	2904	8	8.00
JP00-03-39	40	275892	0	0.5309	0.0040	15.295	0.004	0.2095	0.0002	0.96	2902	8	6.61
JP00-03-40	40	211074	0	0.5204	0.0045	14.668	0.005	0.2050	0.0003	0.96	2867	8	7.07
JP00-03-41	40	268416	164	0.5741	0.0063	18.768	0.006	0.2377	0.0002	0.98	3105	8	7.21
JP00-03-42	40	185070	0	0.5161	0.0049	14.448	0.005	0.2036	0.0005	0.96	2856	9	7.39
JP00-03-44	40	616765	0	0.5354	0.0059	15.737	0.006	0.2137	0.0001	0.98	2934	8	7.11
JP00-03-47	40	321286	36	0.5165	0.0060	14.899	0.006	0.2098	0.0002	0.98	2904	8	9.24
JP00-03-49	40	235162	90	0.4928	0.0034	12.750	0.004	0.1877	0.0002	0.95	2722	8	6.21
JP00-03-50	40	257657	40	0.4961	0.0037	12.862	0.004	0.1881	0.0003	0.95	2726	9	5.74
JP00-03-51	40	3656805	22	0.5290	0.0027	13.558	0.003	0.1858	0.0001	0.95	2705	8	-1.45
JP00-03-52	40	398606	113	0.5560	0.0042	14.340	0.004	0.1871	0.0002	0.95	2717	9	-6.09
JP00-03-57	40	381744	8	0.5133	0.0045	13.492	0.005	0.1907	0.0001	0.96	2749	8	3.47
JP00-03-58	40	307209	3	0.5359	0.0178	14.213	0.018	0.1923	0.0003	0.41	2762	8	-0.19
JP00-03-59	40	770430	141	0.5331	0.0045	13.659	0.005	0.1853	0.0003	0.96	2701	9	-2.41

grain ID	spot size (µm)	<sup>206</sup> Pb* cps	<sup>204</sup> Pb cps	<sup>206</sup> Pb/ <sup>238</sup> U ±1σ	<sup>206</sup> Pb/ <sup>235</sup> U ±1σ	<sup>207</sup> Pb/ <sup>235</sup> U ±1σ	<sup>207</sup> Pb/ <sup>206</sup> Pb ±1σ	rho	<sup>207</sup> Pb/ <sup>206</sup> Pb Age (Ma)	±2σ	Disc.	
JP00-03-61	40	322051	16	0.5168	0.0027	13.944	0.003	0.1957	0.95	2791	8	4.61
JP00-03-62	40	998008	67	0.5725	0.0157	14.992	0.016	0.1895	0.48	2738	9	-8.18
JP00-03-63	40	394309	18	0.5799	0.0139	15.516	0.014	0.1939	0.53	2776	8	-7.77
JP00-03-64	40	107792	23	0.5507	0.0040	14.411	0.004	0.1898	0.96	2741	8	-3.94
JP00-03-65	40	646476	4	0.4880	0.0028	12.931	0.003	0.1922	0.95	2761	8	8.71
JP00-03-66	40	371276	1	0.5250	0.0040	14.049	0.004	0.1942	0.96	2778	8	2.53
JP00-03-67	40	283845	140	0.5008	0.0041	13.367	0.004	0.1936	0.94	2773	9	6.83
JP00-03-68	40	560904	251	0.5328	0.0100	13.886	0.010	0.1891	0.63	2734	9	-0.86
JP00-03-69	40	383072	142	0.5120	0.0041	13.316	0.004	0.1887	0.96	2731	8	2.94
JP00-03-70	40	899829	160	0.5166	0.0022	13.474	0.002	0.1892	0.95	2735	8	2.25
JP00-03-71	40	879365	110	0.5279	0.0029	15.081	0.003	0.2073	0.95	2884	8	6.46
JP00-03-72	40	702976	1	0.5324	0.0027	15.831	0.003	0.2157	0.95	2949	8	8.20
JP00-03-73	40	841860	71	0.5210	0.0030	13.596	0.003	0.1892	0.95	2736	8	1.43
JP00-03-74	40	459805	133	0.5287	0.0070	13.715	0.007	0.1881	1.00	2726	8	-0.45
JP00-03-75	40	621784	23	0.5032	0.0025	13.241	0.003	0.1907	0.95	2749	8	5.35
JP00-03-76	40	415786	9	0.5089	0.0043	13.505	0.004	0.1924	0.96	2763	8	4.90
JP00-03-77	40	145878	97	0.4881	0.0032	13.065	0.003	0.1941	0.94	2777	9	9.37
JP00-03-78	40	443223	17	0.5004	0.0027	13.270	0.003	0.1924	0.95	2762	8	6.47
JP00-03-79	40	257972	4	0.5187	0.0028	13.910	0.003	0.1945	0.95	2780	8	3.80
JP00-03-80	40	695817	7	0.5467	0.0081	14.293	0.008	0.1896	0.71	2739	8	-3.28
JP00-03-82	40	531639	112	0.5169	0.0039	13.329	0.004	0.1870	0.96	2716	8	1.35
JP00-03-83	40	172411	114	0.5073	0.0031	13.256	0.003	0.1893	0.94	2736	9	4.07
JP00-03-84	40	594937	19	0.5128	0.0033	13.387	0.003	0.1893	0.95	2736	8	3.00
JP00-03-85	40	553895	15	0.5084	0.0034	13.317	0.004	0.1900	0.95	2742	8	4.11
JP00-03-86	40	531056	156	0.5147	0.0042	13.317	0.004	0.1876	0.96	2722	9	2.02
JP00-03-87	40	172742	116	0.5065	0.0035	13.217	0.004	0.1892	0.95	2735	9	4.18
JP00-03-88	40	1717263	177	0.5373	0.0031	13.778	0.003	0.1860	0.95	2707	8	-2.97
JP00-03-89	40	895600	37	0.5330	0.0051	14.049	0.005	0.1911	0.97	2752	8	-0.09
JP00-03-90	40	673615	365	0.5171	0.0028	13.373	0.003	0.1876	0.95	2721	8	1.54

grain ID	spot size (µm)	<sup>206</sup> Pb* cps	<sup>204</sup> Pb cps	<sup>206</sup> Pb/ <sup>238</sup> U ±1σ	<sup>207</sup> Pb/ <sup>235</sup> U ±1σ	<sup>207</sup> Pb/ <sup>206</sup> Pb ±1σ	rho	<sup>207</sup> Pb/ <sup>206</sup> Pb ±2σ	Age (Ma)	Disc.
JP00-03-91	40	311565	353	0.4987	0.0041	0.1897	0.96	2740	9	5.83
JP00-03-93	40	790106	31	0.5020	0.0022	0.1926	0.95	2765	8	6.26
JP00-03-94	40	510460	305	0.5106	0.0036	0.1880	0.94	2725	9	2.95
JP00-03-95	40	633428	90	0.5333	0.0098	0.1921	0.63	2760	8	0.22
JP00-03-96	40	59232	368	0.5019	0.0054	0.1917	0.96	2757	10	5.95
JP00-03-98	40	591778	22	0.5354	0.0028	0.1922	0.95	2761	8	-0.15
JP00-03-99	40	526976	362	0.5182	0.0042	0.1857	0.96	2704	8	0.57
JP00-03-100	40	347396	391	0.5194	0.0032	0.1865	0.95	2711	8	0.66
JP00-03-101	40	743232	582	0.5236	0.0032	0.1857	0.95	2704	8	-0.46
JP00-03-102	40	314020	405	0.5116	0.0049	0.1856	0.97	2704	8	1.81
JP00-03-103	40	596449	372	0.5237	0.0047	0.1852	0.96	2700	8	-0.67
JP00-03-104	40	345774	39	0.5104	0.0050	0.1980	0.97	2809	8	6.56
JP00-03-106	40	862364	30	0.4930	0.0021	0.1901	0.95	2743	8	7.06
JP00-03-107	40	385353	373	0.5040	0.0031	0.1872	0.95	2718	8	3.89
JP00-03-109	40	469688	14	0.5026	0.0035	0.1948	0.95	2783	8	6.92
<b>Sample II: Polymictic conglomerate/sandstone (UTM coordinates: 5957463N, 419032E)</b>										
<b>n=92</b>										
JP00-02-1	40	207303	0	0.5351	0.0056	0.2093	0.97	2900	8	5.81
JP00-02-2	40	263765	0	0.5419	0.0042	0.2181	0.95	2966	9	7.25
JP00-02-3	40	215194	0	0.5527	0.0029	0.2104	0.94	2908	8	3.06
JP00-02-4	40	182543	17	0.5490	0.0048	0.2142	0.96	2937	8	4.88
JP00-02-5	40	1003212	0	0.5191	0.0038	0.1910	0.95	2751	8	2.47
JP00-02-6	40	211941	0	0.5610	0.0033	0.2135	0.95	2932	8	2.58
JP00-02-7	40	329658	0	0.4994	0.0030	0.1890	0.95	2734	9	5.45
JP00-02-8	40	250765	0	0.5525	0.0040	0.2250	0.95	3017	8	7.41
JP00-02-9	40	231479	0	0.5365	0.0046	0.2240	0.95	3009	9	9.82
JP00-02-10	40	320133	0	0.5519	0.0046	0.2167	0.96	2956	8	5.16
JP00-02-11	40	140075	0	0.5371	0.0040	0.2102	0.95	2907	9	5.74
JP00-02-13	40	202818	0	0.5466	0.0038	0.2134	0.95	2932	8	5.08

grain ID	spot size (µm)	<sup>206</sup> Pb* cps	<sup>204</sup> Pb cps	<sup>206</sup> Pb/ <sup>238</sup> U ±1σ	<sup>207</sup> Pb/ <sup>235</sup> U ±1σ	<sup>207</sup> Pb/ <sup>206</sup> Pb ±1σ	<sup>207</sup> Pb/ <sup>206</sup> Pb ±1σ	rho	Age (Ma)	±2σ	Disc.		
JP00-02-14	40	208302	97	0.5563	0.0028	16.094	0.003	0.2100	0.0005	0.94	2905	9	2.30
JP00-02-15	40	264148	0	0.5437	0.0041	16.305	0.004	0.2174	0.0002	0.96	2961	8	6.77
JP00-02-16	40	467071	498	0.5422	0.0035	16.378	0.004	0.2189	0.0005	0.94	2973	9	7.45
JP00-02-17	40	301348	0	0.5464	0.0038	16.181	0.004	0.2147	0.0003	0.95	2942	8	5.51
JP00-02-18	40	450901	1545	0.5751	0.0194	16.836	0.020	0.2158	0.0031	0.41	2950	25	0.88
JP00-02-19	40	318640	0	0.5563	0.0029	16.581	0.003	0.2160	0.0002	0.95	2951	8	4.18
JP00-02-20	40	472746	4	0.5516	0.0040	16.628	0.004	0.2185	0.0002	0.95	2970	8	5.74
JP00-02-21	40	157783	0	0.5396	0.0055	15.206	0.006	0.2045	0.0005	0.96	2862	9	3.45
JP00-02-23	40	181382	0	0.5347	0.0043	15.659	0.004	0.2124	0.0004	0.95	2924	9	6.82
JP00-02-24	40	175240	0	0.5392	0.0035	15.636	0.004	0.2104	0.0004	0.95	2909	9	5.43
JP00-02-25	40	207903	0	0.5475	0.0038	16.185	0.004	0.2143	0.0003	0.95	2938	8	5.19
JP00-02-26	40	118385	0	0.5322	0.0042	15.343	0.004	0.2091	0.0006	0.94	2899	9	6.27
JP00-02-27	40	240104	0	0.5289	0.0032	15.655	0.003	0.2147	0.0003	0.95	2941	8	8.53
JP00-02-28	40	543886	0	0.5103	0.0047	13.396	0.005	0.1903	0.0001	0.96	2745	8	3.85
JP00-02-29	40	384303	0	0.5682	0.0048	17.874	0.005	0.2280	0.0002	0.96	3038	8	5.63
JP00-02-31	40	121957	0	0.5348	0.0060	15.505	0.006	0.2102	0.0003	0.98	2907	9	6.16
JP00-02-32	40	636105	48	0.5840	0.0030	17.996	0.003	0.2234	0.0003	0.95	3005	8	1.65
JP00-02-33	40	327631	154	0.5447	0.0036	15.865	0.004	0.2111	0.0002	0.95	2914	8	4.69
JP00-02-34	40	159581	0	0.5367	0.0046	15.436	0.005	0.2086	0.0004	0.96	2895	9	5.31
JP00-02-35	40	274650	35	0.5438	0.0041	16.284	0.004	0.2171	0.0003	0.95	2959	8	6.65
JP00-02-36	40	327091	0	0.5539	0.0044	16.489	0.005	0.2159	0.0003	0.95	2950	8	4.55
JP00-02-37	40	460912	0	0.5173	0.0021	13.559	0.002	0.1901	0.0002	0.94	2743	8	2.49
JP00-02-38	40	1000676	0	0.5984	0.0031	18.963	0.003	0.2297	0.0002	0.95	3050	8	1.09
JP00-02-39	40	327789	0	0.5174	0.0037	13.461	0.004	0.1887	0.0002	0.95	2731	8	1.91
JP00-02-40	40	435244	0	0.5567	0.0043	16.696	0.004	0.2174	0.0002	0.96	2962	8	4.54
JP00-02-41	40	420846	0	0.5118	0.0036	13.392	0.004	0.1899	0.0002	0.95	2741	8	3.41
JP00-02-42	40	204553	0	0.4919	0.0034	13.316	0.004	0.1964	0.0003	0.95	2796	9	9.41
JP00-02-44	40	188196	0	0.4941	0.0051	13.214	0.005	0.1940	0.0003	0.97	2776	9	8.21
JP00-02-45	40	304085	205	0.5537	0.0023	16.920	0.003	0.2216	0.0007	0.92	2992	10	6.27
JP00-02-46	40	1254174	12826	0.5176	0.0048	14.143	0.007	0.1979	0.0050	0.23	2809	42	5.23

grain ID	spot size (µm)	<sup>206</sup> Pb* cps	<sup>204</sup> Pb cps	<sup>206</sup> Pb/ <sup>238</sup> U ±1σ	<sup>207</sup> Pb/ <sup>235</sup> U ±1σ	<sup>207</sup> Pb/ <sup>206</sup> Pb ±1σ	rho	<sup>207</sup> Pb/ <sup>206</sup> Pb ±2σ	Disc.
Age (Ma)									
JP00-02-47	40	203120	0	0.5505	0.0057	0.2164	0.97	2954	8
JP00-02-48	40	180803	22	0.5509	0.0049	0.2170	0.96	2959	9
JP00-02-49	40	429710	0	0.5583	0.0033	0.2176	0.95	2963	8
JP00-02-52	40	367438	131	0.5497	0.0039	0.2163	0.95	2954	8
JP00-02-54	40	151576	0	0.5074	0.0041	0.1864	0.95	2711	9
JP00-02-55	40	172707	0	0.5489	0.0050	0.2152	0.96	2945	9
JP00-02-56	40	282965	0	0.5562	0.0035	0.2160	0.95	2951	8
JP00-02-57	40	352626	0	0.5761	0.0032	0.2161	0.95	2952	8
JP00-02-58	40	200332	0	0.5571	0.0036	0.2151	0.95	2945	9
JP00-02-60	40	190089	0	0.5539	0.0042	0.2158	0.95	2950	8
JP00-02-61	40	213466	1	0.5615	0.0046	0.2294	0.96	3048	8
JP00-02-62	40	488302	0	0.5582	0.0029	0.2197	0.95	2978	8
JP00-02-63	40	128958	0	0.5468	0.0032	0.2138	0.94	2934	9
JP00-02-65	40	185515	0	0.5486	0.0019	0.2123	0.93	2923	9
JP00-02-67	40	412449	0	0.5078	0.0040	0.1931	0.96	2769	8
JP00-02-68	40	500876	0	0.5484	0.0036	0.2074	0.95	2885	8
JP00-02-69	40	381510	34	0.5556	0.0048	0.2198	0.96	2979	8
JP00-02-70	40	263536	0	0.5373	0.0041	0.2082	0.96	2892	8
JP00-02-71	40	132256	0	0.5003	0.0046	0.1888	0.96	2732	9
JP00-02-72	40	344482	178	0.5427	0.0034	0.2140	0.95	2936	8
JP00-02-73	40	243622	0	0.5105	0.0029	0.1862	0.94	2709	9
JP00-02-74	40	202465	0	0.5539	0.0031	0.2139	0.95	2935	8
JP00-02-75	40	182951	0	0.5913	0.0034	0.2243	0.93	3012	10
JP00-02-76	40	258865	0	0.5663	0.0040	0.2243	0.95	3012	8
JP00-02-77	40	177033	0	0.5532	0.0036	0.2132	0.94	2930	9
JP00-02-78	40	111120	0	0.5596	0.0036	0.2200	0.95	2981	9
JP00-02-79	40	203448	0	0.5307	0.0043	0.2142	0.96	2938	8
JP00-02-82	40	236518	3	0.5508	0.0043	0.2186	0.95	2970	8
JP00-02-83	40	244849	0	0.5571	0.0039	0.2161	0.95	2952	8
JP00-02-84	40	194204	0	0.5572	0.0042	0.2141	0.96	2937	8

grain ID	spot size (µm)	<sup>206</sup> Pb* cps	<sup>204</sup> Pb cps	<sup>206</sup> Pb/ <sup>238</sup> U ±1σ	<sup>207</sup> Pb/ <sup>235</sup> U ±1σ	<sup>207</sup> Pb/ <sup>206</sup> Pb ±1σ	rho	<sup>207</sup> Pb/ <sup>206</sup> Pb ±2σ	Age (Ma)	Disc.	
JP00-02-85	40	355329	187	0.5569	0.0034	0.2107	0.95	0.0002	2911	8	2.42
JP00-02-86	40	448515	289	0.5489	0.0047	0.2184	0.96	0.0004	2969	9	6.15
JP00-02-87	40	175301	0	0.5550	0.0035	0.2098	0.95	0.0003	2904	8	2.47
JP00-02-88	40	940135	23	0.5661	0.0036	0.2066	0.95	0.0001	2879	8	-0.54
JP00-02-89	40	279523	0	0.5043	0.0033	0.1871	0.95	0.0003	2717	9	3.78
JP00-02-90	40	260417	0	0.5173	0.0024	0.1868	0.94	0.0002	2714	9	1.20
JP00-02-91	40	269830	0	0.5495	0.0035	0.2263	0.95	0.0003	3026	8	8.28
JP00-02-93	40	241729	39	0.5467	0.0040	0.2192	0.95	0.0003	2975	8	6.75
JP00-02-94	40	405596	0	0.5139	0.0034	0.1898	0.95	0.0003	2740	9	2.98
JP00-02-95	40	156189	0	0.5593	0.0021	0.2103	0.94	0.0004	2908	9	1.89
JP00-02-97	40	480363	0	0.5204	0.0026	0.1905	0.95	0.0002	2746	8	2.02
JP00-02-98	40	290914	0	0.5644	0.0025	0.2066	0.94	0.0002	2879	8	-0.25
JP00-02-99	40	274708	0	0.5104	0.0019	0.1884	0.94	0.0003	2728	9	3.11
JP00-02-101	40	217418	0	0.5721	0.0029	0.2162	0.95	0.0002	2953	8	1.53
JP00-02-102	40	250356	0	0.5736	0.0043	0.2175	0.95	0.0003	2962	8	1.66
JP00-02-103	40	111233	0	0.5507	0.0034	0.2155	0.94	0.0004	2947	9	4.98
JP00-02-105	40	296002	506	0.5711	0.0047	0.2236	0.76	0.0022	3007	18	3.90
JP00-02-106	40	272240	0	0.5733	0.0038	0.2168	0.95	0.0002	2957	8	1.50
JP00-02-107	40	177062	2	0.5643	0.0037	0.2313	0.95	0.0003	3061	8	7.15
JP00-02-108	40	210812	0	0.5736	0.0032	0.2137	0.95	0.0003	2934	8	0.47
<b>Sample I: Basal turbidite (UTM coordinates: 5961722N, 415110E)</b>											
<b>n=84</b>											
102-98-744-1	40	163494	2	0.5385	0.0042	0.2035	0.95	0.0003	2855	8	3.34
102-98-744-2	40	1074571	1	0.5432	0.0036	0.1983	0.95	0.0002	2812	8	0.66
102-98-744-3	40	1319886	257	0.5791	0.0061	0.1958	0.97	0.0002	2792	8	-6.86
102-98-744-4	40	250026	2	0.5486	0.0051	0.2050	0.96	0.0002	2866	8	2.02
102-98-744-6	40	2121614	19	0.5753	0.0061	0.1962	0.97	0.0001	2795	8	-5.99
102-98-744-7	40	1023993	213	0.5776	0.0037	0.1963	0.95	0.0001	2796	8	-6.37
102-98-744-8	40	1369574	343	0.5924	0.0076	0.1973	0.99	0.0004	2804	9	-8.70

grain ID	spot size ( $\mu\text{m}$ )	$^{206}\text{Pb}^*$ cps	$^{204}\text{Pb}$ cps	$^{206}\text{Pb}/^{238}\text{U}$ $\pm 1\sigma$	$^{207}\text{Pb}/^{235}\text{U}$ $\pm 1\sigma$	$^{207}\text{Pb}/^{206}\text{Pb}$ $\pm 1\sigma$	rho	Age (Ma)	$\pm 2\sigma$	Disc.
102-98-744-9	40	1179996	420	0.5908	0.0019	0.1958	0.95	2791	8	-9.03
102-98-744-11	40	1173776	602	0.5907	0.0031	0.1962	0.95	2795	8	-8.85
102-98-744-12	40	1005670	6	0.5867	0.0056	0.2005	0.97	2830	8	-6.46
102-98-744-13	40	2099430	198	0.5669	0.0037	0.1989	0.95	2817	8	-3.42
102-98-744-14	40	1566686	156	0.5763	0.0050	0.2004	0.96	2829	8	-4.60
102-98-744-15	40	327065	573	0.5285	0.0047	0.1955	0.94	2789	10	2.37
102-98-744-16	40	1083109	95	0.5714	0.0046	0.2004	0.96	2830	8	-3.69
102-98-744-17	40	3255716	217	0.5807	0.0046	0.1987	0.96	2815	8	-6.03
102-98-744-18	40	280672	5	0.5467	0.0064	0.2064	0.98	2877	8	2.81
102-98-744-19	40	1884519	136	0.5825	0.0057	0.1997	0.97	2823	8	-5.99
102-98-744-20	40	1229906	1	0.5786	0.0046	0.2049	0.96	2866	8	-3.35
102-98-744-22	40	1429082	281	0.5363	0.0053	0.2003	0.97	2828	8	2.63
102-98-744-23	40	1500952	529	0.5608	0.0050	0.1999	0.96	2825	8	-1.98
102-98-744-25	40	1466855	411	0.5815	0.0041	0.1960	0.95	2793	8	-7.22
102-98-744-26	40	1045202	11	0.5794	0.0037	0.1995	0.95	2822	8	-5.50
102-98-744-27	40	1855074	592	0.5918	0.0048	0.1980	0.96	2810	8	-8.31
102-98-744-29	40	1714534	0	0.5885	0.0050	0.1981	0.96	2811	8	-7.66
102-98-744-30	40	1011960	65	0.5808	0.0050	0.1999	0.96	2826	8	-5.57
102-98-744-31	40	2708146	72	0.5950	0.0036	0.1975	0.95	2806	8	-9.09
102-98-744-33	40	2455531	1	0.5971	0.0030	0.1989	0.95	2817	8	-8.95
102-98-744-34	40	1549989	233	0.5733	0.0026	0.1974	0.95	2805	8	-5.18
102-98-744-40	40	376008	58	0.5453	0.0042	0.2019	0.96	2841	8	1.56
102-98-744-41	40	2483035	170	0.5720	0.0046	0.1982	0.96	2811	8	-4.65
102-98-744-42	40	3321243	296	0.5896	0.0043	0.1993	0.96	2821	8	-7.40
102-98-744-43	40	2403295	6	0.5748	0.0044	0.1996	0.96	2823	8	-4.62
102-98-744-44	40	2692813	1894	0.5759	0.0051	0.1984	0.96	2813	8	-5.24
102-98-744-45	40	1629029	160	0.5637	0.0044	0.1976	0.96	2807	8	-3.32
102-98-744-46	40	1684294	535	0.5666	0.0057	0.1998	0.97	2824	8	-3.06
102-98-744-49	40	527798	526	0.5425	0.0057	0.1999	0.97	2826	8	1.37
102-98-744-51	40	1712604	792	0.5632	0.0034	0.1972	0.94	2803	9	-3.40

grain ID	spot size (µm)	<sup>206</sup> Pb* cps	<sup>204</sup> Pb cps	<sup>206</sup> Pb/ <sup>238</sup> U ±1σ	<sup>207</sup> Pb/ <sup>235</sup> U ±1σ	<sup>207</sup> Pb/ <sup>206</sup> Pb ±1σ	rho	Age (Ma)	±2σ	Disc.
102-98-744-53	30	665583	168	0.5438	0.0064	0.1968	0.98	2800	8	0.04
102-98-744-54	30	602282	1	0.5477	0.0058	0.1997	0.97	2824	8	0.35
102-98-744-55	30	371853	112	0.5285	0.0058	0.1982	0.98	2812	8	3.34
102-98-744-56	30	174764	135	0.5228	0.0073	0.1995	0.73	2822	8	4.82
102-98-744-57	30	639957	371	0.5304	0.0037	0.1957	0.95	2791	8	2.09
102-98-744-58	30	402190	23	0.5357	0.0047	0.2015	0.96	2839	8	3.17
102-98-744-59	30	311833	118	0.5399	0.0064	0.1988	0.98	2816	8	1.47
102-98-744-61	30	369867	56	0.5268	0.0045	0.1994	0.96	2821	8	4.03
102-98-744-62	30	932997	868	0.5473	0.0040	0.1972	0.94	2803	9	-0.45
102-98-744-63	30	362135	106	0.5391	0.0042	0.1977	0.95	2807	8	1.19
102-98-744-64	30	668722	475	0.5374	0.0049	0.1970	0.96	2802	8	1.29
102-98-744-65	30	703577	205	0.5525	0.0066	0.1919	0.99	2758	8	-3.46
102-98-744-66	30	268479	188	0.5868	0.0068	0.1989	0.98	2817	9	-7.07
102-98-744-67	30	793540	18	0.5621	0.0063	0.1984	0.98	2813	8	-2.73
102-98-744-68	30	384551	193	0.5659	0.0074	0.1955	1.00	2789	8	-4.54
102-98-744-69	30	408064	1	0.5771	0.0046	0.1994	0.96	2821	8	-5.12
102-98-744-70	30	725077	222	0.5760	0.0071	0.1961	0.99	2794	8	-6.16
102-98-744-71	30	230548	96	0.5483	0.0059	0.1980	0.97	2810	8	-0.36
102-98-744-72	30	222147	129	0.5440	0.0056	0.2005	0.97	2831	9	1.32
102-98-744-73	30	834866	219	0.5647	0.0061	0.1961	0.98	2794	8	-4.08
102-98-744-74	30	176959	7	0.5439	0.0051	0.2037	0.96	2856	9	2.45
102-98-744-76	30	713692	162	0.5689	0.0047	0.1957	0.96	2790	8	-5.02
102-98-744-77	30	1202259	141	0.5582	0.0051	0.2002	0.96	2828	8	-1.37
102-98-744-78	30	514312	136	0.5658	0.0055	0.2007	0.97	2832	8	-2.56
102-98-744-79	30	621514	13	0.5700	0.0059	0.2021	0.97	2844	8	-2.82
102-98-744-80	30	2042668	193	0.5704	0.0054	0.1988	0.97	2817	8	-4.09
102-98-744-81	30	563962	130	0.5897	0.0052	0.2014	0.96	2838	9	-6.62
102-98-744-82	30	529861	451	0.5749	0.0080	0.2009	0.73	2834	8	-4.13
102-98-744-83	30	505725	230	0.5683	0.0077	0.2012	0.74	2836	8	-2.86

grain ID	spot size (μm)	<sup>206</sup> Pb* cps	<sup>204</sup> Pb cps	<sup>206</sup> Pb/ <sup>238</sup> U ±1σ	<sup>207</sup> Pb/ <sup>235</sup> U ±1σ	<sup>207</sup> Pb/ <sup>206</sup> Pb ±1σ	rho	<sup>207</sup> Pb/ <sup>206</sup> Pb Age (Ma)	±2σ	Disc.
102-98-744-84	30	932068	171	0.5827	0.0066	0.1999	0.98	2825	8	-5.94
102-98-744-85	30	1885539	171	0.5820	0.0027	0.2006	0.95	2831	8	-5.55
102-98-744-86	30	962521	168	0.5655	0.0060	0.2021	0.97	2843	8	-2.02
102-98-744-87	30	1274961	220	0.4953	0.0055	0.1894	0.98	2737	8	6.36
102-98-744-88	30	1413563	168	0.5606	0.0055	0.1991	0.97	2819	8	-2.23
102-98-744-89	30	812918	186	0.5797	0.0048	0.1958	0.96	2791	8	-6.98
102-98-744-90	30	388430	19	0.5768	0.0047	0.2086	0.96	2895	8	-1.75
102-98-744-91	30	673378	131	0.5815	0.0049	0.1983	0.96	2812	8	-6.33
102-98-744-92	30	447688	109	0.5634	0.0046	0.1974	0.96	2805	8	-3.35
102-98-744-93	30	814816	143	0.5779	0.0052	0.1968	0.96	2800	8	-6.26
102-98-744-94	30	958743	89	0.5741	0.0052	0.1982	0.96	2812	8	-5.01
102-98-744-95	30	826738	220	0.5599	0.0061	0.1985	0.97	2814	9	-2.31
102-98-744-96	30	1105737	14	0.5853	0.0045	0.1986	0.96	2815	8	-6.90
102-98-744-97	30	799025	126	0.5766	0.0045	0.1990	0.96	2818	8	-5.18
102-98-744-98	30	164220	27	0.5382	0.0049	0.2060	0.96	2874	9	4.21
102-98-744-99	30	336721	477	0.5624	0.0051	0.1996	0.86	2823	14	-2.34
102-98-744-100	30	628742	140	0.5741	0.0054	0.1986	0.97	2815	8	-4.85
102-98-744-103	30	49970	163	0.5324	0.0056	0.1854	0.95	2702	10	-2.26
102-98-744-105	30	500168	130	0.5700	0.0050	0.1884	0.96	2728	8	-8.21

## **Chapter 5**

### **Summary of Conclusions**

#### **5.1 Summary of Findings**

U-Pb TIMS zircon geochronology data presented in the second chapter address the age of the different volcanic assemblages, as well as key intrusive rocks. The data shows that the Island Lake greenstone belt experienced a long and complex geological history. Three distinct ages of volcanism are observed at ca. 2897 Ma, 2852 Ma, and 2744 Ma. These ages occur in what was previously considered as one supracrustal group, the Hayes River Group. This study and others (Lin et al. 2006), indicate that the term “Hayes River Group” should no longer be used for all volcanic rocks in the northwestern Superior Province. The Savage Island shear zone, a regional fault structure that transects the Island Lake greenstone belt, is not a terrane-bounding feature, as correlative supracrustal assemblages are observed on both sides of it. The volcanic sequences at Island Lake can be correlated on the basis of age with rocks in other areas within the Island Lake domain (and possibly the Oxford-Stull domain) to the north and within the North Caribou terrane to the south. Similar ages of volcanism are reported in the Favourable Lake, McInnes Lake, Hornby Lake, and Red Lake greenstone belts. Based on these data the Island Lake domain and North Caribou terrane, and possibly the Oxford-Stull domain, are suggested to be part of a larger reworked Mesoarchean crustal block.

Chapter three builds on the ideas presented in the second chapter. The first part of the chapter presents lithochemical and Nd isotope data from the volcanic assemblages and associated plutonic rocks to investigate the tectonic affinity of the assemblages, and the second part of the chapter presents U-Pb ages for syn- and post tectonic dykes in order to place age constraints on the tectonic amalgamation in the northwestern Superior Province. The mafic volcanic rocks have two distinct

geochemical signatures, and show a pattern of decreasing crustal contamination with decreasing age. The Nd isotope data shows that the volcanic assemblages have been variably contaminated by an older crustal source. Together these data suggests that the Meso – and Neoproterozoic volcanic assemblages are part of an intact primary volcanic pile that was built on the same basement and has autochthonous relationships with each other. U-Pb zircon TIMS geochronology identified two ages of deformation in the Island Lake greenstone belt. Two dykes that crosscut an older, D<sub>1</sub> foliation place a minimum age of ca. 2723 Ma on the D<sub>1</sub> deformation, and two syn-kinematic dykes date movement along two different structures to 2700 Ma. Regional age correlations in the northwestern Superior Province and data from this study indicate that Meso – and Neoproterozoic periods of southward dipping subduction with a northward moving volcanic front were responsible for generating the rocks in the northern margin of the North Caribou terrane. At the end of Neoproterozoic subduction, terrane accretion was complete and the North Caribou terrane was terminally juxtaposed to the Northern Superior superterrane at 2.70 Ga.

Chapter four presents U-Pb detrital zircon data from the youngest sedimentary group in the greenstone belt, the Island Lake group. The Island Lake group consists of “Timiskaming” type sediments, which are the youngest clastic sedimentary packages present in many Neoproterozoic greenstone belts. These sediments are traditionally interpreted to have been deposited in strike-slip basins (Thurston and Chivers 1990), however new work suggests that these sediments can be explained as being deposited in inter-diapiric basins created by diapirism and sagduction processes. During the diapiric ascent of the felsic material, inter-diapiric basins are formed in the synclines between adjacent domes, into which sediments are deposited (Parmenter et al. 2006; Lin 2005; Van Kranendonk et al. 2004). About ~100 detrital zircons were dated using in situ laser ablation multi collector ICP-MS for each of the four units from the stratigraphic bottom to the top of the Island Lake

group. Data from this study indicates that the ages of detritus change from unit to unit up sequence in this sedimentary group, and are easily correlated to ages of volcanism and plutonism in the belt. The age pattern is most consistent with a scenario in which vertical tectonic processes were active during basin evolution and sedimentation. It is clear that vertical tectonic processes played an important, but overlooked, role in the development of these sedimentary basins and in the tectonic evolution of Archean cratons. Furthermore, vertical and horizontal tectonic processes were synchronous and both operated in the Neoproterozoic, and the timing of transition between the two tectonic regimes might have taken place at different times and rates in different Archean cratons. Horizontal or “modern style” plate tectonics did not become the dominant tectonic process until sometime during the Proterozoic.

## **5.2 Tectonic evolution of the northwestern Superior Province**

The tectonic evolution in the Island Lake greenstone belt and along the northern margin of the North Caribou terrane involved two periods of southward dipping subduction underneath the ca. 3.0 Ga stable cratonic core of the North Caribou terrane. This evolution occurred in three main stages. The first two stages involved the generation of Meso – and Neoproterozoic volcanic assemblages and contemporaneous plutonic rocks due to southward dipping subduction (details in Chapter 2 and 3). The third stage involved the deposition of late clastic sediments during vertical tectonic processes in conjunction with horizontal tectonic movement along the late shear zones at ca. 2.70 Ga. (details in Chapter 4). Plutons continued to be emplaced in the northern margin until ~2.680 Ga (Rayner and Stott 2005). At the end of this process the North Superior superterrane was terminally docked to the North Caribou terrane along the North Kenyon fault.

### **5.3 Scientific Contributions**

This thesis made the following main contributions to the understanding of the geology and geochronology of the Island Lake greenstone belt, the tectonic evolution of northwestern Superior Province, and Archean tectonics:

1. Subdividing the volcanic rocks in the Island Lake greenstone belt, previously considered part of the “Hayes River Group”, into three chronologically and geochemically distinct assemblages that have conformable relationships with each other;
2. Refining the domains, terranes and superterranes in the northwestern Superior Province, and contributing to defining the extent and composition of the northern margin of the North Caribou terrane;
3. Proposing a model for the generation of Timiskaming type basins that suggests vertical tectonic processes were operating in the Neoproterozoic, and with evidence from U-Pb dating of syn - tectonic dykes suggesting the interplay of vertical and horizontal tectonics in the Neoproterozoic;
4. Proposing a detailed model for the Meso – and Neoproterozoic tectonic evolution of the northwestern Superior Province that involves two episodes of southward dipping subduction underneath the North Caribou terrane.

### **5.4 Future Studies**

1. In the second chapter, the age of detrital zircons in the Whiteway assemblage is interpreted to be the age of volcanism in the assemblage, which is ca. 40 M.y. older than the Jubilee assemblage. In the third chapter, the trace element chemistry of the Whiteway assemblage and the Jubilee assemblage – southern basaltic suite are very similar. It cannot be ruled out that the interpretation of the age of the Whiteway assemblage is incorrect. It is possible that the two

assemblages are correlative and form opposite limbs of a synclinal structure in the eastern portion of the Island Lake greenstone belt. Such a structure would have interesting implications to the vertical tectonic model presented for the deposition of the Island Lake group in Chapter 4. Focused structural mapping and more detailed isotopic and geochemical studies of the Whiteway and Jubilee assemblage would help to test this possibility.

2. It would be interesting to use the geochemistry and  $\epsilon\text{Nd}$  data from the Th-LREE enriched basalts to determine if the chemical signature is truly the result of crustal contamination, or a product of arc enrichment. In either case, it would also be instructive to quantify the extent to which each processes has influenced the geochemistry.
3. It would be interesting to quantify the diapiric rise of the plutons and/or sagduction of the volcanic assemblage. One approach would be to take samples across one of the dome structures and use geobarometry techniques to investigate any differential uplift along the structure.
4. Based on the tectonic model presented here and in Percival et al. (2006) the North Kenyon fault is a significant structure and is a major suture between the North Caribou terrane and northern Superior superterrane. Little detailed work has been conducted on this structure, partially due to its lack of exposure. This structure needs to be investigated.

## References

- Ashton, K. E., Heaman, L.M., Lewry, J.F., Hartaub, R.P., and Shi, R. 1999. Age and origin of the Jan Lake complex: a glimpse at the buried Arcehan craton fo the Trans-Hudson Orogen. *Canadian Journal of Earth Sceinces*, 36: 185-208.
- Ayer, J., Amelin, Y., Corfu, C., Kamo, K., Ketchum, J., Kwok, K., Trowell, N. 2002. Evolution of the southern Abitibi greenstone belt based on U-Pb geochronology: autochthonous volcanic construction followed by plutonism, regional deformation and sedimentation. *Precambrian Research*, 115: 63-95.
- Beaumont-Smith, C.J., Anderson, S.D., Bailes, A.H., and Corkery, M.T. 2003. Preliminary results and economic significance of geological mapping and structural analysis at Sharpe Lake, northern Superior Province, Manitoba. (parts of NTS 53K5 and 6). In Report of Activities 2003, Manitoba Industry, Trade and Mines, Manitoba Geological Survey, pp. 140–158.
- Bedard, J.H. 2006: A catalytic delamination-driven model for coupled genesis of Archaean crust and sub-continental lithospheric mantle. *Geochimica et Cosmochimica Acta*. 70: 118-1214.
- Bedard, J.H., Brouillette, P., Mador, L., and Berclaz, A. 2003: Archaean cratonization and deformation in the northern Superior Province, Canada: an evaluation of plate tectonic versus vertical tectonic models. *Precambrian Research*, 127: 61-87.
- Bleeker, W. 2000: Archaean tectonics; a review, with illustrations from the Slave Craton; in *The early Earth; physical, chemical and biological development*. Fowler, C.M.R., Ebinger, C.J., Hawkesworth, C. J. (eds) Geological Society Special Publications, v. 199 p. 151-181.

- Böhm, C.O., Heaman, L.M., Stern, R.A., Corkery, M.T., and Creaser, R.A. 2003. Nature of Assean Lake ancient crust, Manitoba: a combined SHRIMP-ID-TIMS U-Pb geochronology and Sm-Nd isotope study. *Precambrian Research*, 126: 55-94.
- Böhm, C.O., Heaman, L.M., Creaser, R.A., and Corkery, M.T. 2000. Discovery of pre-3.5 Ga exotic crust at the northwestern Superior Province margin, Manitoba. *Geology*, 28: 75-78.
- Calvert, A.J., and Ludden, J.N. 1999. Archean continental assembly in the southeastern Superior Province of Canada. *Tectonics*, 18: 412-429.
- Calvert, A.J., Sawyer, E.W., Davis, W.J., and Ludden, J.N. 1995. Archean subduction inferred from seismic images of a mantle suture in the Superior province. *Nature*, 375: 670-674.
- Card, K.D. 1990. A review of the Superior Craton of the Canadian Shield, a product of Archean accretion. *Precambrian Research*, 48: 99-156.
- Card, K.D., and Ciesielski, A., 1986. DNAG #1. Subdivisions of the Superior Province of the Canadian shield. *Geoscience Canada*, 13: 5-13.
- Choukroune, P, Ludden, J.N., Chardon, D., Calvert, A.J. and Bouhallier, H. 1997. Archaean crustal growth and tectonic processes: a comparison of the Superior Province, Canada and the Dharwar Craton, India; in *Orogeny Through Time*. Burg, J.P and Ford, M. (eds) Geological Society Special Publications, v. 121, p. 63-98.
- Condie, K.C. 2005. *Earth as an Evolving Planetary System*. Elsevier Academic Press, Oxford, England. 447p.
- Condie, K.C. 2005. High field strength element ratios in Archean basalts: a window to evolving sources of mantle plumes? *Lithos*, 79: 491-504

- Condie, K.C. 1993. Chemical composition and evolution of the upper continental crust: Contrasting results from surface samples and shales. *Chemical Geology*, 104: 1-37.
- Corfu, F., and Andrews, A.J. 1987. Geochronological constraints on the timing of magmatism, deformation and gold mineralization in the Red Lake greenstone belt, northwestern Ontario. *Canadian Journal of Earth Sciences*, 24: 1302-1320.
- Corfu, F., and Ayers, L.D. 1991. Unscrambling the stratigraphy of an Archean greenstone belt: a U-Pb geochronological study of the Favourable Lake belt, northwestern Ontario. *Canada. Precambrian Research*, 50: 201-220.
- Corfu, F. and Lin, S. 2000: Geology and U-Pb geochronology of the Island Lake greenstone belt, northwestern Superior Province, Manitoba; *Canadian Journal of Earth Sciences*, 37: 1275–1286.
- Corfu, F., and Stone, D. 1998. Age structure and orogenic significance of the Berens River composite batholiths, western Superior Province. *Canadian Journal of Earth Sciences*, 35: 1089-1109.
- Corfu, F., and Wallace, H. 1986. U-Pb zircon ages for magmatism in the Red Lake greenstone belt, northwestern Ontario. *Rocks. Canadian Journal of Earth Sciences*, 23: 27-42.
- Corfu, F., Jackson, S.L., and Sutcliffe, R.H. 1991. U-Pb ages and tectonic significance of late alkalic magmatism and nonmarine sedimentation: Timiskaming Group, southern Abitibi belt. *Canadian Journal of Earth Sciences*, 28: 489-503.
- Corfu, F., Davis, D.W., Stone, D., and Moore, M. 1998. Chronostratigraphic constraints on the genesis of Archean greenstone belts, northwestern Superior Province, Ontario, Canada; *Precambrian Research*, 92: 277–295.

- Corkery, M.T., Cameron, H.D.M., Lin, S., Skulski, T., Whalen, J.B. and Stern, R.A. 2000. Geological investigations in the Knee Lake belt (parts of NTS 53L). In Report of Activities 2000, Manitoba Industry, Trade and Mines, Manitoba Geological Survey, pp. 129-136.
- Corkery, M.T., Davis, D.W., and Lenton P.G. 1992. Geochronological constraints on the development of the Cross Lake greenstone belt, northwest Superior Province, Manitoba. *Canadian Journal of Earth Sciences*, 29: 2171-2185.
- Creaser, R.A., Erdmer, P., Stevens, R.A., and Grant, S.L. 1997. Tectonic affinity of Nisutlin and Anvil assemblage strata from the Teslin tectonic zone, northern Canadian Cordillera: Constraints from neodymium isotope and geochemical evidence. *Tectonics*, 16: 107-121.1286.
- Davis, D.W. 2002. U-Pb geochronology of Archean metasediments in the Pontiac and Abitibi subprovinces, Quebec, constraints on timing, provenance and regional tectonics. *Precambrian Research*, 115: 97-117.
- Davis, D.W. 1982. Optimum linear regression and error estimation applied to U-Pb data. *Canadian Journal of Earth Sciences*, 19: 2141–2149.
- Davis, D.W., Blackburn, C.E., and Krogh, T.E. 1982. Zircon U-Pb ages from the Wabigoon - Manitou Lakes region, Wabigoon subprovince, northwest Ontario. *Canadian Journal of Earth Sciences*, 19: 254-266.
- Depaolo, D.J. 1981. Nd isotopic studies; some new perspectives on Earth structure and evolution. *Eos, Transactions, American Geophysical Union*, 62: 137-140
- de Wit, M.J., 1998. On Archean granites, greenstones, cratons and tectonics: does the evidence demand a verdict? *Precambrian Research* 91, 181-226.

- Gilbert, H.P. 1985a: Loonfoot Island; Manitoba Energy and Mines, Preliminary map 1985I-3, 1:20 000.
- Gilbert, H.P. 1985b: Island Lake; Manitoba Energy and Mines, Preliminary map 1985I-3, 1:20 000.
- Gilbert, H.P. 1984a: Loonfoot Island; Manitoba Energy and Mines, Preliminary map 1984I-1, 1:20 000.
- Gilbert, H.P. 1984b: Island Lake project; in Report of Activities 1984, Manitoba Energy and Mines, p. 120-125.
- Gilbert, H.P., Neale, K.L., Weber, W., Corkery, M.T. and McGregor, C.R. 1983: Island Lake; Manitoba Energy and Mines, Preliminary map 1983I-1, 1:20 000.
- Gilbert, H.P., Neale, K.L., Weber, W., Corkery, M.T. and McGregor, C.R. 1982: Island Lake; Manitoba Energy and Mines, Preliminary map 1982I-4, 1:20 000.
- Godard, J.D. 1963a: Island Lake: Manitoba Mines and Natural Resources, Mines Branch, Map 59-3A, 1: 63,360.
- Godard, J.D. 1963b: Island Lake: Manitoba Mines and Natural Resources, Mines Branch, Map 59-3B, 1: 63,360.
- Goodwin, A.M., 1991. Precambrian Geology, The dynamic evolution of the Continental Crust. Academic Press, London.
- Hamilton, W.B. 1998. Archean magmatism and deformation were not products of plate tectonics. Precambrian Research, 91: 143-179.

- Heaman, L.M., Erdermer, P. and Owen, J.V. 2002. U-Pb geochronologic constraints on the crustal evolution of the Long Range Inlier, Newfoundland. *Canadian Journal of Earth Sciences*, 39:845-865.
- Hickman, A.H. 2004. Two contrasting granite-greenstone terranes in the Pilbara Craton, Australia: evidence for vertical and horizontal tectonic regimes prior to 2900Ma. *Precambrian Research*, 131: 153-172.
- Hoffman, P.F. 1989, Precambrian geology and tectonic history of North America, in Bally, A.W. and Palmer, A.R., eds., *The geology of North America-an overview: Geological Society of America, The Geology of North America, A*, p. 447-512.
- Hollings, P. and Kerrich, R. 1999. Trace element systematic of ultramafic and mafic volcanic rocks from the 3 Ga North Caribou greenstone belt, northwestern Superior Province. *Precambrian Research*, 93. Pp 257-279.
- Irvine, T.N., and Baragar, W.R.A., 1971. A guide to the chemical classification of the common volcanic rocks. *Can. J. Earth Sci.*, 8:523-548.
- Krogh, T.E. 1982. Improved accuracy of U-Pb zircon ages by the creation of more concordant systems using an air abrasion technique. *Geochimica et Cosmochimica Acta*, 46: 637-649.
- Krogh, T.E. 1973. A low contamination method for hydrothermal decomposition of zircon and extraction of U and Pg for isotopic age determinations. *Geochimica et Cosmochimica Acta*, 37: 485-494
- Kusky, T.M. 1989. Accretion of the Archean Slave Province ,*Geology*, 17: 63-67

- Kusky, T.M., and Polat, A. 1999. Growth of granite-greenstone terranes at convergent margins, and stabilization of Archean cratons. *Tectonophysics*, 305: 43-73.
- Langford, F.F. and Morin, J.A. 1976. The development of the Superior Province of northwestern Ontario by merging island arcs. *American Journal of Science*, 276: 1023-1034.
- Lin, S., Davis, D.W., Rotenberg, E., Corkery, M.T., and Bailes, A.H. 2006. Geological evolution of the northwestern Superior Province: Clues from geology, kinematics and geochronology in the Gods Lake Narrows area, Gods Lake greenstone belt, Manitoba. *Canadian Journal of Earth Sciences*, 43: 749-765.
- Lin, S. 2005. Synchronous vertical and horizontal tectonism in the Neoproterozoic: Kinematic evidence from a synclinal keel in the northwestern Superior craton, Canada. *Precambrian Research* v. 139 p. 181–194.
- Lin, S. and Cameron, H.D.M. 1997: Structural setting of the Au-bearing quartz veins at the Henderson Island gold deposit (Ministik Mine), Island Lake, Manitoba; in *Manitoba Energy and Mines, Mineral Division, Report of Activities, 1997*, p. 6-12.
- Lin, S., and Corfu, F. 2002. Structural setting and geochronology of auriferous quartz veins at the High Rock Island gold deposit, northwestern Superior Province. *Economic Geology*. 97:p. 43-57.
- Lin, S., Cameron, H.D.M., Syme, E.C., and Corfu, F. 1998: Geological investigation in the Island Lake greenstone belt, northwestern Superior Province (parts of NTS 53E/15 & 16): in *Manitoba Energy and Mines, Geological Services, Report of Activities, 1998*, p. 78-87.
- Ludwig, K. R. 2003. *Isoplot 3.0; A Geochronological Toolkit for Microsoft EXCEL*. Berkeley Geochronology Center, Special Publication No. 4. 71 pgs. Mueller, W., and Donaldson, J.A.,

1992. Development of sedimentary basins in the Archean Abitibi belt, Canada: an overview. *Canadian Journal of Earth Sciences*, 29: 2249-2265.
- MacDonald, P.J., Piercey, S.J. and Hamilton, M.A. 2005. An integrated study of intrusive rocks spatially associated with gold and base metal mineralization in Abitibi greenstone belt, Timmins area and Clifford Township: Discover Abitibi Initiative; Ontario Geological Survey, Open File Report 6160, 190p.
- Maurice, C., David, J., Bedard, J.H., Franics, D. 2009. Evidence for a widespread mafic cover sequence and its implications for continental growth in the Northeastern Superior Province. *Precambrian Research*, 168, 45-65.
- McGregor, C.R. and Weber, W. 1982: St. Theresa Point: Manitoba Energy and Mines, Preliminary map 1982I-3, 1: 20 000.
- Mueller, W., and Donaldson, J.A. 1992. Development of sedimentary basins in the Archean Abitibi belt, Canada: an overview. *Canadian Journal of Earth Sciences*, 29: 2249-2265.
- Neale, K.L. 1981: Island Lake-Sinclair-Savage Islands; Manitoba Energy and Mines, Preliminary map 1981I-2, 1:20 000.
- Neale, K.L. and Weber, W. 1981: Island Lake-Cochrane Bay; Manitoba Energy and Mines, Preliminary map 1981I-1, 1:20 000.
- Neale, K.L., Weber, W., and McGregor C.R. 1982: Garden Hill; Manitoba Energy and Mines, Preliminary map 1982I-2, 1:20 000.

- Parks, J., Lin, S., Davis, D., and Corkery, M.T., 2006: New high-precision U-Pb ages for the Island Lake greenstone belt, northwestern Superior Province: implications for regional stratigraphy and the extent of the North Caribou Terrane. *Canadian Journal of Earth Sciences*. v 43, p.789-803.
- Parks, J., Lin, S., Corkery, M.T., and Davis, D.W. 2003. New insights into supracrustal assemblages and regional correlations for the Island Lake greenstone belt, northwest Superior Province, Manitoba. In *Report of Activities 2003, Manitoba Industry, Trade and Mines, Manitoba Geological Survey*, pp. 159–164.
- Parks, J., Lin, S., Corkery, M.T., and Davis, D.W. 2001. Geology and geochronology of the Island Lake greenstone belt, northwest Superior Province. In *Report of Activities 2001, Manitoba Industry, Trade and Mines, Manitoba Geological Survey*, pp. 133–137.
- Parks, J., Lin, S., Corkery, M.T., Tomlinson, K.Y., and Davis, D.W. 2002. Tectonostratigraphic panels and early deformation in the Island Lake Greenstone Belt, northwest Superior Province. In *Report of Activities 2002, Manitoba Industry, Trade and Mines, Manitoba Geological Survey*, pp. 216–225.
- Parmenter, A.C., Lin, S., and Corkery, M.T. 2006. Structural Evolution of the Cross Lake Greenstone Belt in the Northwestern Superior Province, Manitoba: Implications for Relationship between Vertical and Horizontal Tectonism. *Canadian Journal of Earth Sciences*, 43: 767-787.
- Pearce, J.A. and Peate, D.W. 1995 Tectonic implications of the composition of volcanic arc magmas. *Annual Review in Earth and Planetary Science*. v 23, p 251-285.
- Pearce, J.A., Harris, B.W., and Tindle, A.G., 1984. Trace element discrimination diagrams for the tectonic interpretation of granitic rocks. *J. Petrol.* 25:956-983.

- Percival, J.A., Stern, R.A., and Skulski, T. 2001. Crustal growth through successive arc magmatism: reconnaissance U-Pb SHRIMP data from the northeastern Superior Province, Canada. *Precambrian Research*, 109: 203-238.
- Percival, J.A., Sanborn-Barrie, M., Skulski, T., Stott, G.M., and Helmstaedt, H. 2006. Tectonic evolution of the Western Superior Province from NATMAP and Lithoprobe studies. *Canadian Journal of Earth Sciences*, 43: 1085-111.
- Percival, J., Bleeker, W., Cook, F., Rivers, T., Ross, G., and van Staal, C. 2004. PanLITHOPROBE Workshop IV: Intra-Orogen Correlations and Comparative Orogenic Anatomy. *Geoscience Canada*, 31: 23-39
- Piercey, S.J., Mortensen, J.K., Murphy, D.C., Paradis, S. and Creaser, R.A. 2002. Geochemistry and tectonic significance of alkali mafic magmatism in the Yukon-Tanana terrane, Finlayson Lake region, Yukon. *Canadian Journal of Earth Sciences* v. 39, p. 1729-1744.
- Rayner, N. and Stott, G. 2005. Ontario Geological Survey, Open File Report, 6172, p.10-1 to 10-21.
- Robin, C.M.I and Bailey, R.C. 2009. Simultaneous generation of Archean crust and subcratonic roots by vertical tectonics. *Geology*. 37, pp 523-526.
- Sanborn-Barrie, M., Skulski, T. and Parker, J., 2001. Three hundred million years of tectonic history recorded by the Red Lake greenstone belt, Ontario; Geological Survey of Canada, Current Research 2001-C19.
- Simonetti, A, Heaman, L.M, Hartlaub, R.P., Creaser, R.A., MacHattie, T.G., and Bohm, C. 2005: U-Pb zircons dating by laser ablation-MC-ICP-MS using a new multiple ion counting-faraday collector array. *Journal of Analytical Atomic Spectrometry*, 20, 677-686.

- Sircombe, K.N., 2004. AgeDisplay: an EXCEL workbook to evaluate and display univariate geochronological data using binned frequency histograms and probability density distributions. *Computers & Geosciences*, 20, p.21-31.
- Skulski, T., Corkery, M.T., Stone, D., Whalen, J.B., and Stern, R.A. 2000. Geological and geochronological investigations in the Stull Lake–Edmund Lake greenstone belt and granitoid rocks of the northwestern Superior Province. In Report of Activities 2000, Manitoba Industry, Trade and Mines, Manitoba Geological Survey, pp. 117–128.
- Stevenson, R.K., and Turek, A. 1992: An isotope study of the Island Lake Greenstone Belt, Manitoba: crustal evolution and progressive cratonization in the late Archean; *Canadian Journal of Earth Sciences*, 29: 2200-2210.
- Stockwell, C.H. 1982. Proposals for time classification and correlation of Precambrian rocks and events in Canada and adjacent areas of the Canadian Shield, Part 1: A time classification of Precambrian rocks and events: Geological Survey of Canada, Paper 80-19, 135 p.
- Stott G.M. 2009. Precambrian Geology of Ontario's Far North. Ontario Geological Survey, poster. Northwestern Ontario Mines and Minerals Symposium, Thunder Bay, Ontario.
- Stott, G.M. 1997. The Superior Province, Canada; In *Greenstone Belts*. Edited by M. DeWit and L.D. Ashwol. Oxford Monographs on Geology and Geophysics no. 35, pp. 480–507.
- Stott, G.M., and Corfu, F. 1991. Uchi Subprovince. In *Geology of Ontario*. Edited by P.C. Thurston, H.R. Williams, R.H. Sutcliffe, and G.M. Stott. Ontario Geological Survey Special Volume 4, pp. 145-236.
- Syme, E.C, Corkery, M.T., Bailes, A.H., Lin, S., Skulski, T., and Stern, R.A. 1999. Towards a New Tectonostratigraphy for the Knee Lake Greenstone Belt, Sachigo Subprovince, Manitoba. In

- Western Superior Transect. Fifth Annual Workshop. Edited by R.M. Harrap, and H.H. Helmstaedt. Lithoprobe Report #70, Lithoprobe Secretariat, University of British Columbia. p. 124-131.
- Sun, S.S and McDonough, W.F., 1989. Chemical and isotopic systematics of ocean basalts: implications for mantle composition and processes, in *Magmatism in the Ocean Basins*, Saunders, A.D., and Norry, M.J. (ed.) Geological Society Special Publication No. 42, pp.313-345.
- Theyer, P. 1998: Mineral Deposits and Occurrences in the Island Lake Area, NTS 53E/15, 53E/16, 53F/13, 53E/10, 53E/9, 53E/12; Manitoba Energy and Mines Mineral Deposits Series Report No.32.
- Thurston, P.C. 2002. Autochthonous development of Superior Province greenstone belts?. *Precambrian Research*, 115: 11-36.
- Thurston, P.C., and Chivers, K.M. 1990. Secular Variation in Greenstone Sequence Development Emphasizing Superior Province, Canada. *Precambrian Research*, 26, 21-58.
- Thurston, P.C., Osmani, I.A. and Stone, D. 1991a. Northwestern Superior Province: review and terrane analysis; in *Geology of Ontario*, P.C. Thurston, H.R. Williams, R.H. Sutcliffe and G.M. Stott (ed.), Ontario Geological Survey, Special Volume 4, pt. 1, p. 81–142.
- Thurston, P.C., Williams, H.R., Sutcliffe R.H., and Stott, G.M. (Editors) .1991b. *Geology of Ontario*, Ontario Geological Survey, Special Volume 4, pt. 1 and 2.
- Tomlinson, K.Y., and Percival, J. A. 2000. Geochemistry and Nd isotopes of granitoid rocks in the Shika-Garden lakes area, Ontario: Mesoarchean crust in the central Wabigoon Subprovince. In *Geological Survey of Canada, Current Research 2000-E12*, 11pp.

- Turek, A., Carson, T.M., Smith, P.E., van Schmus, W.R. and Weber, W. 1986: U-Pb zircon ages from the Island Lake greenstone belt, Manitoba; *Canadian Journal of Earth Sciences*, 23: 92–101.
- Van Kranendonk, M.J., Collins, W.J., Hickman, A., and Pawley, M.J. 2004. Critical test of vertical vs. horizontal tectonic models for the Archaean East Pilbara Granite-Greenstone terrane, Pilbara Craton, Western Australia. *Precambrian Research*, 131: 173-211.
- Wang, Z., Wilde, S.A., Wang, K., Yu, L. 2004. *Precambrian Research*, 131:323-343 . 2004. *Precambrian Research*, 131:323-343
- Weber, W., McGregor, C.R., and Neale, K.L. 1982a: Waasagomach Bay; Manitoba Energy and Mines, Preliminary Map 1982I-1, 1:20 000.
- Weber, W., Gilbert, H.P., McGregor, C.R., and Neale, K.L. 1982b: Island Lake Project; in Manitoba Energy and Mines, Mineral Resources Division, Report of Activities, 1982, p. 34-43
- White, D.J., Musacchio, G., Helmstaedt, H.H., Thurston, P.C., van der Velden, A., and Hall, K. 2003. Images of a lower-crustal oceanic slab: Direct evidence from tectonic accretion in the Archean western Superior province. *Geology*, 31: 997-1000.
- Wood, 1980. The application of a Th-Hf-Ta diagram to problems of tectonomagmatic classification and to establishing the nature of crustal contamination of basaltic lavas of the British Tertiary volcanic province. *Earth and Planetary Science Letters*, v 50,11-30.
- Wright, J.F. 1928. Island Lake area, Manitoba. In Summary report 1927, part B. Geological Survey of Canada, pp.54-80.

Wyman, D.A., Kerrich, R. and Polat, A. 2002. Assembly of Archean cratonic mantle lithosphere and crust: plum-arc interaction in the Abitibi-Wawa subduction-accretion complex. *Precambrian Research*, 115; 37-62.

Young, M.D., McNicoll, V., Helmstedt, H., Skulski, T., and Percival, J.A. 2006. Pickle Lake revisited: New structural, geochronological and geochemical constraints on greenstone belt assembly, western Superior Province, Canada. *Canadian Journal of Earth Sciences*, 43: 821-847-111



## **Appendix B**

### **Analytical Methods - Chapter 2**

#### **U/Pb Geochronology**

Single grain zircon U-Pb analysis was done at the Jack Satterly Laboratory, Royal Ontario Museum (now at the University of Toronto) using standard methods (Krogh, 1973, 1982; Davis et al., 1982). Samples were crushed and separated using standard methods and the zircon grains were examined and selected under a binocular microscope. Selected grains were air abraded (Krogh, 1982) for 8 to 40 hours before chemical dissolution. The dissolution and isotope dilution methods of Krogh (1973) were followed with reduced bomb and column sizes. Ion exchange chromatography to separate U and Pb was only carried out on grains larger than 4  $\mu\text{g}$ . Common lead blanks are essentially equivalent to total common Pb measured in the samples (Table 2.1). All analyses were carried out using a VG354 equipped with a Daly pulse counting detector at the Jack Satterly Laboratory, with the exception of lab numbers JP01-067-A and JP01-067-B. These analyses were carried out using the sample type of mass spectrometer at the Radiogenic Isotope Facility at the University of Alberta (see Heaman et al. 2002 for analytical techniques). Data were calculated, regressed and plotted using ROMAGE software with the regression program of Davis (1982). Sample locations are shown on Figure 2.2. Analytical data are given in Table 2.1 and Concordia diagrams are shown on Figures 2.4 and 2.7.

## **Appendix C**

### **Analytical Techniques – Chapter 3**

#### **Lithochemical analysis**

Lithochemical analysis was completed on selected samples in the belt to better understand the nature and tectonic affinity of the rocks in the belt. Samples were taken from the basaltic units in the different volcanic assemblages and from each of the plutonic suites and felsic volcanic units that were dated by U-Pb ID-TIMS in Chapter 2. Clean (i.e. no weathered surfaces or xenocrystic material) samples were crushed by a jaw crusher and powdered by a disk mill at the Manitoba Geological Survey in Winnipeg, Manitoba. The powders were sent to ACTLABS in Hamilton, Ontario where analysis for major and trace element were completed under accordance with their “4E-Research” package of analysis. The analytical methods used at ACTLABS are detailed below<sup>1</sup>. Data is presented in Table 3.1 and Figure 3.5; Figure 3.6 Figure 3.8; and Figure 3.9. Standard reproducibility data is listed in Table A.1

#### **Major Elements**

*A 0.2 g sample is mixed with a mixture of lithium metaborate/lithium tetraborate and fused in a graphite crucible. The molten mixture is poured into a 5% nitric acid solution and shaken until dissolved (~ 30 minutes). The samples are run for major oxides and selected traces on a combination simultaneous/sequential Thermo Jarrell-Ash Enviro II ICP. Calibration is achieved using a variety of international reference materials. Independent control standards are also analyzed.*

#### **Base Metals and Selected Trace Elements**

---

<sup>1</sup> From <http://www.actlabs.com/page.aspx?page=518&app=226&cat1=549&tp=12&lk=no&menu=64>

*A 0.25 g sample is digested with four acids beginning with hydrofluoric, followed by a mixture of nitric and perchloric acids, heated using precise programmer controlled heating in several ramping and holding cycles which takes the samples to dryness. After dryness is attained, samples are brought back into solution using hydrochloric acid. With this digestion certain phases may be only partially solubilized. These phases include zircon, monazite, sphene, gahnite, chromite, cassiterite, rutile and barite. Ag greater than 100 ppm and Pb greater than 5,000 ppm should be assayed as high levels may not be solubilized. Only sulphide sulfur will be solubilized. An in-lab standard (traceable to certified reference materials) or certified reference materials are used for quality control. Samples are analyzed using a Perkin Elmer Optima 3000 ICP.*

### **Trace Elements**

*For each sample, a 1 g aliquot is encapsulated in a polyethylene vial and irradiated with flux wires and an internal standard (1 for 11 samples) at a thermal neutron flux of  $7 \times 10^{12} \text{ n cm}^{-2} \text{ s}^{-1}$ . After a 7-day decay to allow Na-24 to decay the samples are counted on a high purity Ge detector with resolution of better than 1.7 KeV for the 1332 KeV Co-60 photopeak. Using the flux wires, the decay-corrected activities are compared to a calibration developed from multiple certified international reference materials. The standard present is only a check on accuracy and is not used for calibration purposes. From 10-30% of the samples are rechecked by re-measurement. One standard is run for every 11 samples. One blank is analyzed per work order. Duplicates are analyzed when samples are provided. Gamma-ray energies are listed in Hoffman, E.L., 1992. Instrumental Neutron Activation in Geoanalysis. Journal of Geochemical Exploration, volume 44, pp. 297-319.*

## **Nd isotopic analysis**

Nineteen new samples were analyzed as part of this study, and were added to the existing Nd isotope data set of Stevenson and Turek, (1992, 20 samples). The new samples were analyzed at the Radiogenic Isotope Facility at the University of Alberta were run on the samples powdered at the Manitoba Geological Survey that the geochemical analyses was performed on, and in some cases were re-powdered to ensure the grain size was small enough for proper sample dissolution. See Creaser et al. (1997) for details on the analytical protocols. Model ages based on DePolo's depleted mantle evolution curve (1981) and  $\epsilon\text{Nd}$  values were calculated for 19 new samples analyzed, as well as for the Nd isotopic results from Stevenson and Turek (1992) using the new geochronology results present in Chapter 2. The data is found in Table A.2, and a summary is presented in Table 3.2 and Figure 3.7.

## **U-Pb geochronology**

Single grain zircon U-Pb analysis for the four samplers was done at the Jack Satterly Laboratory, Royal Ontario Museum (now at the University of Toronto) using standard methods (Krogh, 1973, 1982; Davis et al., 1982). Samples were crushed and separated using standard methods and the zircon grains were examined and selected under a binocular microscope. Selected grains were air abraded (Krogh, 1982) for 8 to 24 hours before chemical dissolution. The dissolution and isotope dilution methods of Krogh (1973) were followed with reduced bomb and column sizes. Ion exchange chromatography to separate U and Pb was only carried out on grains larger than 4  $\mu\text{g}$ . Common lead blanks are essentially equivalent to total common Pb measured in the samples (Table 3). Analyses were carried out using a VG354 equipped with a Daly pulse counting detector. Data were calculated, regressed and plotted using ROMAGE software with the regression program of Davis (1982). Analytical data are given in Table 3.3, and Concordia diagrams are shown in Figure 3.12.

Additional MC-ICP-MS analysis was completed on 12 zircon grains from sample JP00-06 in order to resolve the age of the sample after conflicting TIMS ages were obtained. This analysis was done using the laser ablation multi collector-ICP-MS at the Radiogenic Isotope Facility at the University of Alberta. The instrument configuration employed consisted of a UP213 laser ablation system coupled to a multicollector- ICP-MS equipped with a cup collector array that includes three ion counters and 12 Faraday buckets (Simonetti et al., 2005). This set up allows for the simultaneous detection of ion signals from  $^{238}\text{U}$  to  $^{203}\text{Tl}$ , permitting for highly precise and reproducible Pb-Pb and Pb/U ratio, as well as being able to measure low Pb signals resulting from the ablation of small sample volumes (single ablation spots  $<40\mu\text{m}$ , Simonetti et al., 2005; See Simonetti et al., 2005 for more details on analytical protocol). Spot sizes of analysis ranged from 30-40  $\mu\text{m}$ , and were dependent on the size and Pb content of the zircon (i.e. low Pb content zircons usually require larger spot sizes). The data were reduced and common Pb corrections were carried out following Simonetti et al. (2005). U/Pb normalization was monitored by repeat measurements of an internal zircon standard LH94-15 (with an age of 1830 Ma, Ashton et al., 1999). Analyses that were more than  $\pm 10\%$  discordant, had “mixed ages” during runs (i.e. a core and an overgrowth of different ages were both sampled during the analysis), or had anomalously high  $^{204}\text{Pb}$  counts during analysis were not included in the final data set. The data was then plotted using AgeDisplay, and is presented in Figure 3.12. External reproducibility during analyses time was:  $^{207}\text{Pb}/^{206}\text{Pb} = 0.5\%$ ;  $^{206}\text{Pb}/^{238}\text{U} = 1.5\%$ ; and  $^{207}\text{Pb}/^{235}\text{U} = 1.5\%$ .

**Table A.2 Geochemistry standard reproducibility during analyses**

underlined, bracked or starred value = recommended value for standard  
 negative values = below detection limit

SAMPLE	SiO <sub>2</sub> %	Al <sub>2</sub> O <sub>3</sub> %	Fe <sub>2</sub> O <sub>3</sub> %	MnO %	MgO %	CaO %
<b>SY3 CERT (syenite - known)</b>	<u>59.62</u>	<u>11.75</u>	<u>6.49</u>	<u>0.32</u>	<u>2.67</u>	<u>8.26</u>
SY-3/20 (measured)	59.57	11.66	6.41	0.326	2.64	8.30
<b>NIST 694 CERT (western phosphate rock - known)</b>	<u>11.20</u>	<u>1.80</u>	<u>0.79</u>	<u>0.01</u>	<u>0.33</u>	<u>43.60</u>
NIST 694/B98 (measured)	10.98	1.87	0.72	0.011	0.33	43.57
<b>W-2 CERT (diabase - known)</b>	<u>52.44</u>	<u>15.35</u>	<u>10.74</u>	<u>0.163</u>	<u>6.37</u>	<u>10.87</u>
W-2/162 (measured)	52.47	15.20	10.69	0.164	6.46	10.92
<b>DNC-1 CERT (dolerite - known)</b>	<u>47.04</u>	<u>18.30</u>	<u>9.93</u>	<u>0.149</u>	<u>10.05</u>	<u>11.27</u>
DNC-1/12 (measured)	46.88	18.37	9.72	0.144	10.21	11.23
<b>BIR-1 CERT (basalt - known)</b>	<u>47.77</u>	<u>15.35</u>	<u>11.26</u>	<u>0.171</u>	<u>9.68</u>	<u>13.24</u>
BIR-1/B34 (measured)	47.55	15.41	11.16	0.169	9.65	13.08
<b>GBW 07113 CERT (rhyolite - known)</b>	<u>72.78</u>	<u>12.96</u>	<u>3.21</u>	<u>0.140</u>	<u>0.16</u>	<u>0.59</u>
GBW 07113/152 (measured)	72.47	12.88	3.16	0.143	0.16	0.59
<b>NBS 1633b CERT (fly ash - known)</b>	<u>49.24</u>	<u>28.43</u>	<u>11.13</u>	<u>0.020</u>	<u>0.799</u>	<u>2.11</u>
NBS 1633b/180 (measured)	49.37	28.57	11.42	0.018	0.78	2.12
<b>STM-1 CERT (syenite - known)</b>	<u>59.64</u>	<u>18.39</u>	<u>5.22</u>	<u>0.22</u>	<u>0.101</u>	<u>1.09</u>
STM-1/108 (measured)	59.63	18.35	5.16	0.219	0.10	1.13
<b>IF-G CERT (iron from sample - known)</b>	<u>41.20</u>	<u>0.15</u>	<u>55.85</u>	<u>0.042</u>	<u>1.89</u>	<u>1.55</u>
IF-G/B28 (measured)	40.88	0.14	56.12	0.038	1.87	1.50
<b>MICA-Fe CERT (Biotite - known)</b>	<u>34.40</u>	<u>19.50</u>	<u>25.65</u>	<u>0.350</u>	<u>4.55</u>	<u>0.43</u>
MICA-Fe/224 (measured)	34.14	19.28	25.69	0.344	4.58	0.41

SAMPLE	Na <sub>2</sub> O %	K <sub>2</sub> O %	TiO <sub>2</sub> %	P <sub>2</sub> O <sub>5</sub> %	Sc ppm	Be ppm
<b>SY3 CERT (syenite - known)</b>	<u>4.12</u>	<u>4.23</u>	<u>0.15</u>	<u>0.54</u>	6.8	20
SY-3/20 (measured)	4.11	4.23	0.146	0.54	8	20
<b>NIST 694 CERT (western phosphate rock - known)</b>	<u>0.86</u>	<u>0.51</u>	<u>0.11</u>	<u>30.20</u>		
NIST 694/B98 (measured)	0.90	0.50	0.115	28.06	3	2
<b>W-2 CERT (diabase - known)</b>	<u>2.14</u>	<u>0.627</u>	<u>1.06</u>	<u>0.131</u>	<u>35</u>	1.3
W-2/162 (measured)	2.29	0.64	1.073	0.14	36	1
<b>DNC-1 CERT (dolerite - known)</b>	<u>1.87</u>	<u>0.229</u>	<u>0.48</u>	<u>0.085</u>	<u>31</u>	1
DNC-1/12 (measured)	1.98	0.25	0.488	0.08	31	-1
<b>BIR-1 CERT (basalt - known)</b>	<u>1.75</u>	0.027	0.96	0.05	<u>44</u>	0.58
BIR-1/B34 (measured)	1.85	-0.01	0.968	0.03	44	-1
<b>GBW 07113 CERT (rhyolite - known)</b>	<u>2.57</u>	<u>5.43</u>	<u>0.30</u>	<u>0.05</u>	<u>5.2</u>	<u>4.09</u>
GBW 07113/152 (measured)	2.57	5.43	0.283	0.05	5	4
<b>NBS 1633b CERT (fly ash - known)</b>	<u>0.271</u>	2.26	<u>1.32</u>	0.53	41	
NBS 1633b/180 (measured)	0.28	2.33	1.300	0.53	41	12
<b>STM-1 CERT (syenite - known)</b>	<u>8.94</u>	<u>4.28</u>	<u>0.135</u>	<u>0.158</u>	<u>0.61</u>	9.6
STM-1/108 (measured)	8.87	4.28	0.137	0.16	-1	9
<b>IF-G CERT (iron from sample - known)</b>	<u>0.032</u>	<u>0.012</u>	<u>0.014</u>	<u>0.063</u>	0.38	4.7
IF-G/B28 (measured)	0.04	0.02	0.005	0.06	-1	4
<b>MICA-Fe CERT (Biotite - known)</b>	<u>0.300</u>	<u>8.750</u>	<u>2.500</u>	<u>0.450</u>	<u>14.8</u>	<u>4.5</u>
MICA-Fe/224 (measured)	0.25	8.92	2.513	0.39	15	4

Sample	Ge ppm	As ppm	Rb ppm	Sr ppm	Y ppm	Zr ppm	Ba ppm	La ppm
Blank	-0.5	-5	-1	-2	-0.5	-1	-3	-0.05
Control Material W2 (measured)	1.8	-5	21	197	21.9	87	181	11.1
<b>Certified W2 (known)</b>	<b>(1.0)</b>	<b>1.2</b>	<b>20*</b>	<b>194*</b>	<b>24*</b>	<b>94*</b>	<b>182*</b>	<b>11.4*</b>
Control Material WMG-1 (measured)	1.8	10	3	41	13.6	50	114	8.11
<b>Certified WMG-1 (known)</b>		<b>(7)</b>	<b>(4)</b>	<b>(41)</b>	<b>(12)</b>	<b>(43)</b>	<b>(114)</b>	<b>(8.2)</b>
Calibration Standard MAG1 (measured)	1.8	13	152	145	27.1	111	509	43.3
<b>Certified MAG1 (known)</b>		<b>9.2</b>	<b>149*</b>	<b>146*</b>	<b>28*</b>	<b>126*</b>	<b>479*</b>	<b>43*</b>
Calibration Standard BIR1 (measured)	1.8	-5	-1	112	15.9	15	7	0.72
<b>Certified BIR1 (known)</b>	<b>1.5</b>	<b>(0.4)</b>	<b>0.25*</b>	<b>108*</b>	<b>16*</b>	<b>15.5</b>	<b>7</b>	<b>0.62*</b>
Calibration Standard DNC1 (measured)	1.3	-5	4	142	17.0	32	104	3.88
<b>Certified DNC1 (known)</b>	<b>(1.3)</b>	<b>(0.2)</b>	<b>(4.5)</b>	<b>145*</b>	<b>18*</b>	<b>41*</b>	<b>114*</b>	<b>3.8*</b>
Calibration Standard GXR-2 (measured)	1.1	33	77	154	16.9	226	2,240	25.6
<b>Certified GXR-2 (known)</b>		<b>25</b>	<b>78</b>	<b>160</b>	<b>17</b>	<b>269</b>	<b>2,240</b>	<b>25.6</b>
Calibration Standard LKSD-3 (measured)	1.2	32	78	253	29.6	165	683	50.8
<b>Certified LKSD-3 (known)</b>		<b>27</b>	<b>78</b>	<b>240</b>	<b>30</b>	<b>178</b>	<b>680</b>	<b>52</b>
Calibration Standard MICA Fe (measured)	3.2	-5	2,380	4	47.0	837	150	201
<b>Certified MICA Fe (known)</b>	<b>3.2</b>	<b>3</b>	<b>2200*</b>	<b>5*</b>	<b>48*</b>	<b>800*</b>	<b>150*</b>	<b>200*</b>
Calibration Standard GXR1 (measured)	3	425	3	306	32	26	691	7.8
<b>Certified GXR1 (known)</b>		<b>427</b>	<b>(14)</b>	<b>275</b>	<b>32</b>	<b>(38)</b>	<b>750</b>	<b>7.5</b>
Calibration Standard SY3 (measured)	3	20	210	301	719	355	435	1,330
<b>Certified SY3 (known)</b>	<b>1.4</b>	<b>18.8</b>	<b>206*</b>	<b>302*</b>	<b>718*</b>	<b>320</b>	<b>450</b>	<b>1340*</b>
Calibration Standard STM1 (measured)	1.4	-5	117	708	45.0	1,210	589	150
<b>Certified STM1 (known)</b>	<b>(1.4)</b>	<b>4.6</b>	<b>118*</b>	<b>700*</b>	<b>46*</b>	<b>1210*</b>	<b>560*</b>	<b>150*</b>
Calibration Standard IFG1 (measured)	24.8	-5	-1	4	9.3	2	-3	3.01
<b>Certified IFG1 (known)</b>	<b>24</b>	<b>1.5</b>	<b>0.4</b>	<b>3</b>	<b>9*</b>	<b>1</b>	<b>1.5</b>	<b>2.8*</b>

Sample	Nb ppm	Mo ppm	Ag ppm	In ppm	Sn ppm	Sb ppm	Cs ppm	Ce ppm
Blank	-0.2	-2	-0.5	-0.1	-1	-0.2	-0.1	-0.05
Control Material W2 (measured)	7.9	-2	-0.3	-0.1	2	0.8	1.0	22.8
<b>Certified W2 (known)</b>	<b>7.9</b>	<b>(0.6)</b>	<b>(0.046)</b>			<b>0.79</b>	<b>0.99*</b>	<b>24*</b>
Control Material WMG-1 (measured)	5.7	-2	12.7	-0.1	2	2.3	0.4	15.9
<b>Certified WMG-1 (known)</b>	<b>(6)</b>	<b>(1.4)</b>	<b>(2.7)</b>		<b>(2.2)</b>	<b>(1.8)</b>	<b>(0.48)</b>	<b>(16)</b>
Calibration Standard MAG1 (measured)	14.4	-2	-0.5	-0.1	3	1.0	9.0	84.1
<b>Certified MAG1 (known)</b>	<b>12</b>	<b>1.6</b>	<b>0.08</b>	<b>(0.18)</b>	<b>3.6</b>	<b>0.96*</b>	<b>8.6*</b>	<b>88*</b>
Calibration Standard BIR1 (measured)	0.5	-2	-0.5	-0.1	-1	0.5	-0.1	1.96
<b>Certified BIR1 (known)</b>	<b>0.6</b>	<b>(0.5)</b>	<b>(0.036)</b>		<b>0.65</b>	<b>0.58</b>	<b>0.005</b>	<b>1.95*</b>
Calibration Standard DNC1 (measured)	1.3	-2	-0.5	-0.1	-1	0.7	0.2	8.48
<b>Certified DNC1 (known)</b>	<b>3</b>	<b>(0.7)</b>	<b>(0.027)</b>			<b>0.96*</b>	<b>(0.34)</b>	<b>10.6</b>
Calibration Standard GXR-2 (measured)	10.0	-2	16.5	-0.1	2	36.7	5.2	50.2
<b>Certified GXR-2 (known)</b>	<b>11</b>	<b>(2.1)</b>	<b>17</b>	<b>(0.252)</b>	<b>1.7</b>	<b>49</b>	<b>5.2</b>	<b>51.4</b>
Calibration Standard LKSD-3 (measured)	8.4	-2	6.0	-0.1	2	1.1	2.3	91.0
<b>Certified LKSD-3 (known)</b>	<b>8</b>	<b>(&lt;5)</b>	<b>2.7</b>		<b>3</b>	<b>1.3</b>	<b>2.3</b>	<b>90</b>
Calibration Standard MICA Fe (measured)	286	-2	-0.5	0.6	70	-0.2	180	440
<b>Certified MICA Fe (known)</b>	<b>270*</b>	<b>1.2</b>		<b>0.60</b>	<b>70*</b>		<b>180*</b>	<b>420*</b>
Calibration Standard GXR1 (measured)	1.1	18	363	0.8	55	122	3.1	14.5
<b>Certified GXR1 (known)</b>	<b>(0.8)</b>	<b>18</b>	<b>31</b>	<b>0.77</b>	<b>54</b>	<b>122</b>	<b>3</b>	<b>17</b>
Calibration Standard SY3 (measured)	157	-4	2	-0.2	6	0.4	2.8	2240
<b>Certified SY3 (known)</b>	<b>148</b>	<b>(1.0)</b>	<b>(1.5)</b>		<b>(6.5)</b>	<b>0.31</b>	<b>2.5</b>	<b>2230*</b>
Calibration Standard STM1 (measured)	250	6	6.9	-0.1	7	1.2	1.6	243
<b>Certified STM1 (known)</b>	<b>268*</b>	<b>5.2</b>	<b>0.079*</b>	<b>(0.12)</b>	<b>6.8</b>	<b>1.66*</b>	<b>1.54*</b>	<b>259*</b>
Calibration Standard IFG1 (measured)	-0.2	-2	-0.5	-0.1	-1	0.7	-0.1	3.99
<b>Certified IFG1 (known)</b>	<b>0.1*</b>	<b>0.7</b>		<b>0.2</b>	<b>0.3</b>	<b>0.63</b>	<b>0.06</b>	<b>4*</b>

Sample	Ta ppm	W ppm	Tl ppm	Pb ppm	Bi ppm	Th ppm	U ppm	Pr ppm
Blank	-0.01	-0.5	-0.05	-5	-0.1	-0.05	-0.01	-0.01
Control Material W2 (measured)	0.50	-0.5	0.14	8	-0.1	2.21	0.53	2.87
<b>Certified W2 (known)</b>	<b>0.5</b>	<b>(0.3)</b>	<b>(0.2)</b>	<b>9</b>	<b>(0.03)</b>	<b>2.2*</b>	<b>0.53</b>	<b>(5.9)</b>
Control Material WMG-1 (measured)	0.35	4.7	0.05	14	0.4	1.14	0.64	2.00
<b>Certified WMG-1 (known)</b>	<b>(0.5)</b>	<b>(1.3)</b>		<b>(15)</b>		<b>(1.1)</b>	<b>(0.65)</b>	
Calibration Standard MAG1 (measured)	1.17	1.5	0.22	8	-0.1	11.6	2.87	9.36
<b>Certified MAG1 (known)</b>	<b>1.1</b>	<b>1.4</b>	<b>(0.59)</b>	<b>24*</b>	<b>0.34</b>	<b>11.9*</b>	<b>2.7*</b>	<b>9.3</b>
Calibration Standard BIR1 (measured)	0.04	-0.5	-0.05	-5	-0.1	-0.02	0.02	0.38
<b>Certified BIR1 (known)</b>	<b>0.04</b>	<b>0.07</b>	<b>(0.01)</b>	<b>3</b>	<b>(0.02)</b>	<b>0.03</b>	<b>0.01</b>	<b>0.38*</b>
Calibration Standard DNC1 (measured)	0.07	-0.5	-0.05	-5	-0.1	0.25	0.06	1.09
<b>Certified DNC1 (known)</b>	<b>0.098*</b>	<b>(0.2)</b>	<b>(0.026)</b>	<b>6.3</b>	<b>(0.02)</b>	<b>(0.2)</b>	<b>(0.1)</b>	<b>1.3</b>
Calibration Standard GXR-2 (measured)	0.83	1.4	0.21	28	-0.1	8.36	2.90	5.15
<b>Certified GXR-2 (known)</b>	<b>0.9</b>	<b>1.9</b>	<b>1.03</b>	<b>690</b>	<b>(0.69)</b>	<b>8.8</b>	<b>2.9</b>	
Calibration Standard LKSD-3 (measured)	0.67	1.1	0.24	-5	-0.1	10.8	4.59	11.5
<b>Certified LKSD-3 (known)</b>	<b>0.7</b>	<b>(&lt;4)</b>		<b>29</b>		<b>11.4</b>	<b>4.6</b>	
Calibration Standard MICA Fe (measured)	34.6	7.9	16.0	12	0.4	166	86.3	49.0
<b>Certified MICA Fe (known)</b>	<b>35*</b>	<b>15</b>	<b>16</b>	<b>13*</b>	<b>2</b>	<b>150*</b>	<b>80*</b>	<b>49*</b>
Calibration Standard GXR1 (measured)	0.06	166	0.5	731	1380	2.6	34.9	1.84
<b>Certified GXR1 (known)</b>	<b>0.175</b>	<b>164</b>	<b>(0.39)</b>	<b>730</b>	<b>1,380</b>	<b>2.44</b>	<b>34.9</b>	
Calibration Standard SY3 (measured)	20.9	1	1.6	76	-0.2	1,000	650	210
<b>Certified SY3 (known)</b>	<b>30*</b>	<b>1.1*</b>	<b>1.50</b>	<b>133*</b>	<b>(0.8)</b>	<b>1003*</b>	<b>650*</b>	<b>223*</b>
Calibration Standard STM1 (measured)	19.7	3.3	0.23	11	-0.1	31.1	9.0	24.3
<b>Certified STM1 (known)</b>	<b>18.6*</b>	<b>3.6*</b>	<b>0.26</b>	<b>17.7*</b>	<b>0.13</b>	<b>31*</b>	<b>9.06*</b>	<b>19*</b>
Calibration Standard IFG1 (measured)	0.19	220	-0.05	-5	-0.1	0.03	0.03	0.44
<b>Certified IFG1 (known)</b>	<b>0.2</b>	<b>220</b>	<b>0.02</b>	<b>4</b>		<b>0.1</b>	<b>0.02</b>	<b>0.4*</b>

Sample	Gd ppm	Tb ppm	Dy ppm	Ho ppm	Er ppm	Tm ppm	Yb ppm	Nd ppm
Blank	-0.01	-0.01	-0.01	-0.01	-0.01	-0.005	-0.01	-0.05
Control Material W2 (measured)	3.49	0.67	3.89	0.81	2.27	0.358	2.07	12.6
<b>Certified W2 (known)</b>	<b>3.6*</b>	<b>0.63</b>	<b>3.8*</b>	<b>0.76*</b>	<b>2.5</b>	<b>0.4</b>	<b>2.05*</b>	<b>14.0</b>
Control Material WMG-1 (measured)	2.37	0.43	2.45	0.50	1.40	0.220	1.30	9.08
<b>Certified WMG-1 (known)</b>		<b>(0.4)</b>	<b>(2.8)</b>	<b>(0.5)</b>		<b>(0.2)</b>	<b>(1.3)</b>	<b>(9)</b>
Calibration Standard MAG1 (measured)	5.77	0.97	5.20	1.02	2.81	0.432	2.60	36.9
<b>Certified MAG1 (known)</b>	<b>5.8*</b>	<b>0.96*</b>	<b>5.2*</b>	<b>1.02*</b>	<b>3</b>	<b>0.43*</b>	<b>2.6*</b>	<b>38*</b>
Calibration Standard BIR1 (measured)	1.82	0.41	2.68	0.62	1.74	0.286	1.71	2.49
<b>Certified BIR1 (known)</b>	<b>1.85*</b>	<b>0.36*</b>	<b>2.5*</b>	<b>0.57*</b>	<b>1.7*</b>	<b>0.26*</b>	<b>1.65</b>	<b>2.5*</b>
Calibration Standard DNC1 (measured)	1.99	0.42	2.81	0.65	1.94	0.329	1.97	4.91
<b>Certified DNC1 (known)</b>	<b>2</b>	<b>0.41*</b>	<b>2.7</b>	<b>0.62</b>	<b>2*</b>	<b>(0.33)</b>	<b>2.01*</b>	<b>4.9*</b>
Calibration Standard GXR-2 (measured)	2.94	0.50	2.87	0.60	1.75	0.285	1.76	19.1
<b>Certified GXR-2 (known)</b>	<b>(3.3)</b>	<b>0.48</b>	<b>3.3</b>			<b>(0.3)</b>	<b>2.04</b>	<b>(19)</b>
Calibration Standard LKSD-3 (measured)	6.29	0.97	5.19	1.06	2.99	0.468	2.76	44.3
<b>Certified LKSD-3 (known)</b>		<b>1.0</b>	<b>4.9</b>				<b>2.7</b>	<b>44</b>
Calibration Standard MICA Fe (measured)	21.1	2.71	10.9	1.53	3.81	0.563	3.43	180
<b>Certified MICA Fe (known)</b>	<b>21*</b>	<b>2.7*</b>	<b>11*</b>	<b>1.6*</b>	<b>3.8*</b>	<b>0.48*</b>	<b>3.5*</b>	<b>180*</b>
Calibration Standard GXR1 (measured)	3.91	0.85	5.06	1.03	2.82	0.44	2.31	8.4
<b>Certified GXR1 (known)</b>	<b>4.2</b>	<b>0.83</b>	<b>4.3</b>			<b>(0.43)</b>	<b>1.9</b>	<b>(18)</b>
Calibration Standard SY3 (measured)	113	22.0	133	29.7	86.2	13.2	67.8	701
<b>Certified SY3 (known)</b>	<b>105*</b>	<b>18</b>	<b>118</b>	<b>29.5*</b>	<b>68</b>	<b>11.6*</b>	<b>(62)</b>	<b>670</b>
Calibration Standard STM1 (measured)	8.8	1.51	8.12	1.60	4.43	0.713	4.40	78.4
<b>Certified STM1 (known)</b>	<b>9.5*</b>	<b>1.55*</b>	<b>8.1*</b>	<b>1.9</b>	<b>4.2*</b>	<b>0.69</b>	<b>4.4*</b>	<b>79*</b>
Calibration Standard IFG1 (measured)	0.66	0.12	0.81	0.21	0.63	0.097	0.57	1.76
<b>Certified IFG1 (known)</b>	<b>0.74*</b>	<b>0.11*</b>	<b>0.8*</b>	<b>0.2*</b>	<b>0.63*</b>	<b>0.09*</b>	<b>0.6*</b>	<b>0.2</b>

Sample	Lu ppm	Hf ppm	Sm ppm	Eu ppm	V ppm	Cr ppm	Co ppm	Ni ppm
Blank	-0.002	-0.1	-0.01	-0.005	-5	-20	-1	-20
Control Material W2 (measured)	0.318	2.4	3.33	1.15	263	93	44	120
<b>Certified W2 (known)</b>	<b>0.33*</b>	<b>2.56*</b>	<b>3.25*</b>	<b>1.1*</b>	<b>262*</b>	<b>93*</b>	<b>44*</b>	<b>70*</b>
Control Material WMG-1 (measured)	0.202	1.5	2.33	0.757	158	765	201	2,490
<b>Certified WMG-1 (known)</b>	<b>(0.21)</b>	<b>(1.3)</b>	<b>(2.3)</b>	<b>(0.8)</b>	<b>(149)</b>	<b>(770)</b>	<b>(200)</b>	<b>(2700)</b>
Calibration Standard MAG1 (measured)	0.391	3.3	7.43	1.54	134	96	21	49
<b>Certified MAG1 (known)</b>	<b>0.40*</b>	<b>3.7*</b>	<b>7.5*</b>	<b>1.55*</b>	<b>140*</b>	<b>97*</b>	<b>20.4*</b>	<b>53*</b>
Calibration Standard BIR1 (measured)	0.262	0.6	1.16	0.561	313	403	53	167
<b>Certified BIR1 (known)</b>	<b>0.26*</b>	<b>0.6*</b>	<b>1.1*</b>	<b>0.54*</b>	<b>313*</b>	<b>382*</b>	<b>51.4*</b>	<b>166*</b>
Calibration Standard DNC1 (measured)	0.302	1.0	1.44	0.614	140	284	55	247
<b>Certified DNC1 (known)</b>	<b>0.32*</b>	<b>1.01*</b>	<b>1.38*</b>	<b>0.59*</b>	<b>148*</b>	<b>285*</b>	<b>54.7*</b>	<b>247*</b>
Calibration Standard GXR-2 (measured)	0.277	6.3	3.71	0.754	46	36	8	-20
<b>Certified GXR-2 (known)</b>	<b>(0.27)</b>	<b>8.3</b>	<b>3.5</b>	<b>0.81</b>	<b>52</b>	<b>36</b>	<b>8.6</b>	<b>21</b>
Calibration Standard LKSD-3 (measured)	0.439	4.5	8.53	1.55	75	82	30	46
<b>Certified LKSD-3 (known)</b>	<b>0.4</b>	<b>4.8</b>	<b>8.0</b>	<b>1.50</b>	<b>82</b>	<b>87</b>	<b>30</b>	<b>47</b>
Calibration Standard MICA Fe (measured)	0.502	26.7	35.3	0.650	131	93	26	38
<b>Certified MICA Fe (known)</b>	<b>0.5*</b>	<b>26*</b>	<b>33*</b>	<b>0.7*</b>	<b>135*</b>	<b>90*</b>	<b>23*</b>	<b>35*</b>
Calibration Standard GXR1 (measured)	0.322	0.7	2.99	0.67	77	-40	8	83
<b>Certified GXR1 (known)</b>	<b>0.28</b>	<b>0.96</b>	<b>2.7</b>	<b>0.69</b>	<b>80</b>	<b>12</b>	<b>8.2</b>	<b>41</b>
Calibration Standard SY3 (measured)	8.62	10.5	127	19.0	51	-40	7	-40
<b>Certified SY3 (known)</b>	<b>7.90</b>	<b>9.70</b>	<b>109</b>	<b>17*</b>	<b>50</b>	<b>(11)</b>	<b>8.8</b>	<b>11</b>
Calibration Standard STM1 (measured)	0.649	27.4	12.6	3.62	-5	-20	-1	-20
<b>Certified STM1 (known)</b>	<b>0.60</b>	<b>28*</b>	<b>12.6*</b>	<b>3.6*</b>	<b>(8.7)</b>	<b>(4.3)</b>	<b>0.9</b>	<b>(3)</b>
Calibration Standard IFG1 (measured)	0.093	-0.1	0.42	0.383	9	-20	29	26
<b>Certified IFG1 (known)</b>	<b>0.09*</b>	<b>0.04</b>	<b>0.4*</b>	<b>0.39*</b>	<b>2</b>	<b>4</b>	<b>29*</b>	<b>23</b>

Sample	Cu ppm	Zn ppm	Ga ppm
Blank	-10	-30	-1
Control Material W2 (measured)	107	85	19
<b>Certified W2 (known)</b>	<b>103*</b>	<b>77*</b>	<b>20*</b>
Control Material WMG-1 (measured)	5,480	125	10
<b>Certified WMG-1 (known)</b>	<b>(5900)</b>	<b>(110)</b>	<b>(10.3)</b>
Calibration Standard MAG1 (measured)	28	75	21
<b>Certified MAG1 (known)</b>	<b>30*</b>	<b>130*</b>	<b>20.4*</b>
Calibration Standard BIR1 (measured)	126	80	16
<b>Certified BIR1 (known)</b>	<b>126*</b>	<b>71*</b>	<b>16</b>
Calibration Standard DNC1 (measured)	91	58	14
<b>Certified DNC1 (known)</b>	<b>96*</b>	<b>66*</b>	<b>15</b>
Calibration Standard GXR-2 (measured)	64	52	36
<b>Certified GXR-2 (known)</b>	<b>76</b>	<b>52</b>	<b>37</b>
Calibration Standard LKSD-3 (measured)	31	55	15
<b>Certified LKSD-3 (known)</b>	<b>35</b>	<b>152</b>	<b>15</b>
Calibration Standard MICA Fe (measured)	-10	1,260	98
<b>Certified MICA Fe (known)</b>	<b>5*</b>	<b>1300*</b>	<b>95*</b>
Calibration Standard GXR1 (measured)	1,110	812	13
<b>Certified GXR1 (known)</b>	<b>1,110</b>	<b>760</b>	<b>13.8</b>
Calibration Standard SY3 (measured)	-20	246	34
<b>Certified SY3 (known)</b>	<b>17</b>	<b>244*</b>	<b>27*</b>
Calibration Standard STM1 (measured)	78	234	36
<b>Certified STM1 (known)</b>	<b>(4.6)</b>	<b>235*</b>	<b>36*</b>
Calibration Standard IFG1 (measured)	11	-30	-1
<b>Certified IFG1 (known)</b>	<b>13*</b>	<b>20*</b>	<b>0.7</b>

Table A.2 All Sm-Nd Data

Sample number	Sm ppm	Nd ppm	$^{147}\text{Sm}/^{144}\text{Nd}$	$^{143}\text{Nd}/^{144}\text{Nd}$	uncert. 2sm +/-	TDM	Age (Ma)	$\epsilon\text{NdT at t=Age}$	Nd Correction	$^{145}\text{Nd}/^{144}\text{Nd}$
<i>New data from this study</i>										
JP02 559	1.83	7.02	0.1579	0.511924	0.000005	N/A	2899	0.6	Nu Alpha=0.512249	0.348414
JP02 557	3.67	12.69	0.1748	0.512263	0.000005	N/A	2899	0.9	Nu Alpha=0.512249	0.348414
102-98-859	2.68	13.17	0.1232	0.511254	0.000007	3.19	2899	0.5	Nu Alpha=0.512285	0.348422
52-IL 98-37	0.99	2.89	0.2078	0.512939	0.000008	N/A	2897	1.8	Nu Alpha=0.512250	0.348416
00-33	5.69	28.71	0.1199	0.511138	0.000006	3.27	2894	-0.6	Nu Alpha=0.512285	0.348409
02-425	3.60	19.97	0.1090	0.510969	0.000005	3.17	2854	-0.3	Nu Alpha=0.512285	0.348413
52-IL-98-44	2.58	7.82	0.1994	0.512629	0.000021	N/A	2852	-1.2	Nu Alpha=0.512254	0.348407
JP01-246G	1.13	3.18	0.2158	0.513043	0.000012	N/A	2852	0.9	Nu Alpha=0.512254	0.348421
JP02-266	1.45	3.81	0.2296	0.513164	0.000011	N/A	2852	-1.8	Nu Alpha=0.512254	0.348425
JP02-463	1.57	5.90	0.1606	0.511943	0.000006	N/A	2852	-0.3	Nu Alpha=0.512250	0.348411
02-839	2.39	13.52	0.1069	0.510954	0.000004	3.13	2852	0.1	Nu Alpha=0.512285	0.348418
02-289	1.93	11.14	0.1048	0.510869	0.000006	3.19	2852	-0.7	Nu Alpha=0.512285	0.348416
02-419	1.53	10.28	0.0901	0.510625	0.000007	3.11	2825	-0.5	Nu Alpha=0.512285	0.348413
02-424	3.75	24.46	0.0927	0.510545	0.000005	3.27	2825	-3.0	Nu Alpha=0.512285	0.348414
52-IL-98-12	1.26	3.74	0.2039	0.512875	0.000018	N/A	2744	2.1	Nu Alpha=0.512254	0.348421
01-105	2.19	13.51	0.0982	0.510767	0.000007	3.14	2744	-1.7	Nu Alpha=0.512285	0.348414
jp01-67	4.02	25.48	0.0955	0.510714	0.000005	3.14	2744	-1.8	Nu Alpha=0.512285	0.348406
jp01-45	2.14	10.58	0.1222	0.511330	0.000004	3.03	2730	0.7	Nu Alpha=0.512285	0.348404
<i>Recalculated data from Stevenson and Turek, 1992</i>										
999	4.58	24.3	0.1138	0.511074		3.16	2894	0.39		
158	1.26	3.69	0.2062	0.51278		N/A	2852	-0.72		
3115	2.22	13.7	0.09779	0.510741		3.16	2852	-0.68		
3140	2.23	8.95	0.1504	0.511827		N/A	2852	1.19		
110	3.3	17.2	0.1158	0.511113		3.17	2852	-0.04		
3114	1.68	9.44	0.1076	0.510934		3.18	2852	-0.52		
349	0.56	1.93	0.1744	0.512306		N/A	2852	1.73		
3117	2.4	7.57	0.1917	0.512584		N/A	2852	0.79		
860	2.38	10	0.1439	0.511174		N/A	2852	1.89		
1	1.99	9.77	0.123	0.511264		3.17	2852	0.27		
3116	1.4	9.95	0.08526	0.510576		3.05	2778	-0.37		
3141	3.07	17.6	0.1056	0.510896		3.17	2748	-1.77		
372	3.16	19.7	0.09684	0.510777		3.09	2747	-1.00		
35	2.49	19.4	0.07771	0.510459		3.01	2744	-0.48		
983	1.73	10.3	0.1015	0.510823		3.16	2743	-1.80		
815	1.76	11.1	0.09538	0.510754		3.08	2743	-0.98		
44	2.35	11	0.1282	0.511509		2.93	2730	2.06		
143	1.58	7.07	0.1354	0.511657		2.91	2730	2.42		
140	3.84	25.4	0.09232	0.510689		3.09	2730	-1.35		
217G	3.02	20.2	0.0904	0.510796		2.91	2699	1.00		

## Appendix D

### Analytical Techniques – Chapter 4

#### U-Pb LA-MC-ICP-MS

A sample was taken from each of the four lithological units in the Island Lake group to examine the detrital zircon population up-sequence in the group. This study was completed using a laser ablation multi collector-ICP-MS at the Radiogenic Isotope Facility at the University of Alberta. This method is a fast, efficient, and reliable method to date a large number of detrital zircons. Rock samples were crushed using a jaw crusher and disc mill and the heavy minerals were then concentrated using a Wilfley table. Initial passes through a Franz magnetic separator concentrated the least magnetically susceptible heavy minerals. The sample was passed through methyl iodine which further separated the sample based on specific gravity. Minerals with a specific gravity > 3.3 were collected and passed through the Frantz to further concentrate high quality zircon from the sample. In order not to age bias the zircon population, zircon grains of various visual and magnetic qualities, morphologies, and grain size were chosen for analysis. Grains were mounted in epoxy prior to ablation.

The instrument configuration employed consisted of a UP213 laser ablation system coupled to a multicollector- ICP-MS equipped with a cup collector array that includes three ion counters and 12 Faraday buckets (Simonetti et al., 2005). This set up allows for the simultaneous detection of ion signals from  $^{238}\text{U}$  to  $^{203}\text{Tl}$ , permitting for highly precise and reproducible Pb-Pb and Pb/U ratio, as well as being able to measure low Pb signals resulting from the ablation of small sample volumes (single ablation spots <40 $\mu\text{m}$ , Simonetti et al., 2005; See Simonetti et al., 2005 for more details on analytical protocol). Spot sizes of analysis ranged from 30-40  $\mu\text{m}$ , and were dependent on the size and Pb content of the zircon (i.e. low Pb content zircons usually require larger spot sizes). The data

were reduced and common Pb corrections were carried out following Simonetti et al. (2005). U/Pb normalization was monitored by repeat measurements of an internal zircon standard LH94-15 (with an age of 1830 Ma, Ashton et al., 1999). Over 100 detrital zircons were analysed from each of the four samples. Analyses that were more than +/-10% discordant, had “mixed ages” during runs (i.e. a core and an overgrowth of different ages were both sampled during the analysis), or had anomalously high  $^{204}\text{Pb}$  counts during analysis were not included in the final data set. The data is presented in Table 4.1 and Figure 4.4.